

**Syntheses of Functionalized Benzylic Compounds:
Development of Palladium-catalyzed Decarboxylative Benzylations Reactions**

by

Robert Ryan Pangilinan Torregrosa

B.S. Chemistry, University of Santo Tomas, Manila Philippines, 2005

Submitted to the Department of Chemistry and the Faculty of the Graduate School of
The University of Kansas in partial fulfillment of the requirements for the degree of
Doctor of Philosophy

Jon A. Tunge, chairperson

Paul R. Hanson

Richard S. Givens

David R. Benson

Apurba Dutta

Date Defended: July 24, 2012

The Dissertation Committee for Robert Ryan Pangilinan Torregrosa certifies that
this is the approved version of the following dissertation:

**Syntheses of Functionalized Benzylic Compounds:
Development of Palladium-catalyzed Decarboxylative Benzylation Reactions**

Jon A. Tunge, chairperson

Paul R. Hanson

Richard S. Givens

David R. Benson

Apurba Dutta

Date Defended: July 24, 2012

Abstract

Robert R. P. Torregrosa

Department of Chemistry, July 2012

The University of Kansas

Carbon-carbon bond formation between the benzyl carbon and a functional group is important in organic synthesis because majority of the compounds in the chemical literature contain aromatic cores appended with different functionalities in the benzyl carbon. These compounds are utilized in pharmaceuticals and medicinal chemistry. While current literature in Pd-catalyzed benzylations is increasingly becoming recognized, conventional methodologies require the use of toxic benzyl halides, stoichiometric bases and/or preformed organometallics which not only generate benzyl compounds but also give side products and toxic metal wastes. Our research group has a long-standing interest using decarboxylation as a tool in constructing diverse compounds without the need of base and preformed organometallics. Previously applied in the synthesis of functionalized allylic compounds from allyl esters, we envisioned to utilize this tool towards the synthesis of functionalized benzylic compounds from benzyl esters. We thought that it would be feasible and ideal to perform decarboxylative benzylation (DcB) based from well-explored decarboxylative allylation (DcA) methodology. Indeed, we were able to show that Pd-catalyzed DcB was an indispensable tool in synthesizing functionalized benzylic compounds in good to high yields. This was shown in the syntheses of benzyl ketones and benzyl alkynes. In the DcB of ketones, simple and benzo-fused β -ketoesters underwent

decarboxylation affording benzyl ketones in good to high yields. DcB was also regioselective, the kinetically preferred enolate did not undergo thermodynamic isomerization resulting in direct functionalization to the carbon next to the carboxylate group where it was once located. In addition to naphthyl and simple benzyls, heteroaromatics were also used as coupling partners with enolate. The nature of substituents in the ring and its position from the benzyl moiety affected benzylation. Depending on the nature of heterocycle, regioselective benzylation occurred resulting in formation of C-benzylation ketone, C-arylation ketone, or O-benzylation enol ether. The utility of DcB methodology was also used towards the synthesis of Nabumetone. In the DcB of alkynes, simple and benzo-fused propiolates underwent decarboxylation to generate benzyl alkynes in good to high yields. The use of biphenyl derived ligand was crucial in the synthesis of simple benzyl alkynes. The benzylic carbon in diaryls and heterocycles can also be used as coupling partners with alkynes.

Acknowledgements

I am very grateful that I was able to work and get in touch with a lot of people and friends that made my stay in KU very enjoyable. I am blessed that I was given the opportunity to be part of the institution and have wonderful and incredible experiences. I have so many people to thank which I think have helped me to become a well-rounded person whether I was a professional student, a social entertainer, or influential brother.

To Jon, my boss, my research advisor, my guidance counselor, and my mentor. Your dedication in chemistry as showed in classroom teaching, group meeting discussions, or just the one-on-one talks is truly amazing. Thank you for all the advices and teachings. I'm glad that I picked the right (and best) mentor. I hope I would be the last person from the group, who would call you in the middle of the night.

To my committee members, Paul, Dr. Givens, Dr. Benson, Dr. Dutta, Dr. Carlson, and Helena. Thank you all for the support and contribution to my learning experience. It was my greatest pleasure to be able to work and chat with all of you whether classroom teaching, discussions, or leisure talking.

To the past members of the Tunge group, thank you for making my life in the lab truly enjoyable as I become an independent senior graduate student. Erin and Shelli, thanks for all the help with my chemistry and guidance in the lab during my early years. Both of you were like sisters to me. And as sisters, you really inspired me to become an effective leader in lab responsibilities and still do incredibly awesome chemistry. I will miss both of you. To my early lab mates, Chao, thanks for the help and fun conversations during those years. To Jimmie, thanks for everything, as in everything – from lab setup, advices, to the apartment bed, to the lift in

parties, to the free breads and pastries, and to the stimulating lab conversations. We sometimes butt heads in terms of lab matters but it was great and I learned a lot from it. To all postdocs, especially to Kali, who worked with me in benzyl ketone chemistry. I will miss all the chats regarding languages, cultures, and anything under the sun.

To the current members of the Tunge group, thank you for making my life in the lab and office even more enjoyable. To Yamuna, it's been a pleasure to work with you. I hope I was able to assist you in your chemistry. It was fun talking and interrupting you in the middle of your column chromatography, working in the glovebox, rotovaping, or even interpreting NMR spectra. To Shehani, I hope I was able to lead you in your chemistry. You will do very well in your chemistry. I hope I can visit Sri Lanka someday and meet both of you. To James, a very interesting guy in the group – working with chemistry by day, running by early night, and still doing more chemistry by late night. To Tapan, Ramu, Simon, Nathan, Theresa, and Mary, I wish you all the very best in your research. I can guarantee that you all made the best decision to join our research group!

To my dear friend Aileen, thanks for the fun and all the never-ending happenings we had. The sight seeings, joy rides, and food tripping were awesome. Thanks for the help during the times when I need it so much from simple favors to even bigger “demanding” favors. The best four years I experienced with you. With all the hustle and bustle of chemistry, you always keep reminding me that it takes not one day to relax and think outside chemistry, but seven days! I will miss you.

To the Filipino graduate students who I had the opportunity to interact with, to Rose – a very smart woman with a funny sense of humor and loves watching Tagalog movies. Thanks for

the laughter and making me somewhat “addicted” in watching movies. To Father Jojo, thanks for the assistance you provided to me when I first came to KU. To Lynn, thanks for the Sunday lunches, group gatherings, and introducing me to your Biology friends. To Joseph and Nette, my golly... as much as I am serious with my work, it’s just hard to keep up the demands of my career because I am having the best times of my life with these guys. Thanks for keeping my professional life “balanced”.

To my former research advisor in UST, Dr. Aristeo Bayquen, thanks for convincing me to pursue graduate studies after I did chemistry research with you during my undergraduate years. To Doc Sev and Ma’m Alice, thanks a lot for the guidance and inspiration.

To my aunt, Norma Pangilinan, thank you for all the assistance you’ve provided to me the moment I planned to study in KU. I don’t think I will survive American education, culture, and other else without your help. To my parents, Remy and Pete Torregrosa, and to my brother and sisters Raymond, Rachelle, and Rosalyn, a very big and heart warming thanks to all of you. The pictures, support, cheer, and motivation, even when we are thousands of miles apart, made me succeed and survived graduate school. Thank you. I think my doggies at home also deserve thanks too (arf, arf). I Love You All!

Thank you very much all and Maraming Salamat Po!

**Syntheses of Functionalized Benzylic Compounds:
Development of Palladium-catalyzed Decarboxylative Benzylations Reactions**

Table of Contents

Title Page	
Acceptance Page	ii
Abstract	iii
Acknowledgements	v
Table of Contents	viii
Abbreviations	xi
Chapter 1: Background of Palladium-catalyzed Benzylations Reactions	1
1.1 Introduction	2
1.2 Nucleophilic partners of η^3 -Pd-benzyl	10
1.2.1 Olefins	10
1.2.2 Alkylidene	14
1.2.2 Aromatics	14
1.2.3 Heteroatoms: phenols, amines, sulfinates, and phosphanates	18
1.2.4 Preformed organometallics	22
1.3 The Decarboxylative benzylation (DcB) reaction	29
1.3.1 Fundamental approach of DcB	29
1.3.2 Applications of DcB	30
1.4 Conclusion	34
1.5 References	35

Chapter 2: Palladium-Catalyzed Decarboxylative Benzylolation of Ketones	40
2.1 Introduction	41
2.2 Pd-catalyzed decarboxylative allylations (DcA): Prelude to DcB	61
2.3 Development of DcB of benzo-fused ketones	75
2.3.1 DcB of unsubstituted benzo-fused β -ketoesters	75
2.3.2 DcB of α -monosubstituted benzo-fused- β -ketoesters	81
2.3.3 DcB of α -disubstituted benzo-fused- β -ketoesters	86
2.3.4 Regioselective benzylolation	91
2.4 Development of DcB of simple benzyl ketones	95
2.4.1 DcB of unsubstituted β -ketoesters	95
2.4.2 DcB of α -substituted β -ketoesters	97
2.4.3 Efforts towards elucidating the source of protonation	100
2.5 Efforts towards asymmetric benzylolation	101
2.6 Mechanistic insights	106
2.7 Conclusion	107
2.8 References	108
2.9 Methodology and compound characterizations	113
Chapter 3: Palladium-Catalyzed Decarboxylative Benzylolation of Alkynes	173
3.1 Introduction	174
3.2 Prelude to DcB of alkynes: Decarboxylative allylation of alkynes	183
3.3 Development of DcB of benzo-fused alkynes	185
3.3.1 Substrate scope	185
3.3.2 Inevitable isomerizations	190
3.3.3 Diaryl alkyne synthesis	192
3.4 Development of DcB of simple benzyl alkynes	193
3.4.1 Background	193

3.4.2 Substrate scope	196
3.5 Mechanistic insights	200
3.6 Conclusion	201
3.7 References	202
3.8 Methodology and compound characterizations	204

Abbreviations

Ac	acetyl
AHP	accelerated hydrogen peroxide
AmOH	amyl alcohol
APT	attached proton test
Ar	aryl
BEt ₃	triethylborane
BF ₄	tetrafluoroborate
BHE	β-hydride elimination
Bn	benzyl
BSA	<i>N,O</i> -bis(trimethylsilyl)acetamide
Bu ₃ Sn	tributyltin
cat	catalytic
CF ₃	trifluoromethyl
CO	carbon monoxide
CO ₂	carbon dioxide
COD	1,5-cyclooctadiene
COX	cyclooxygenase
Cp	cyclopentadienyl
Cs ₂ CO ₃	cesium carbonate
Cy	cyclohexyl
dba	dibenzylideneacetone
DcA	decarboxylative allylation

DcB	decarboxylative benzylation
DCC	<i>N,N</i> -dicyclohexylcarbodiimide
DCM	dichloromethane
DEPT	distortionless enhancement by polarization transfer
DMAP	4-dimethylaminopyridine
DME	dimethyl ether
DMF	dimethyl formamide
DMSO	dimethyl sulfoxide
dppb	1,4-bis(diphenylphosphino)butane
dppe	1,2-bis(diphenylphosphino)ethane
dppf	1,1'-bis(diphenylphosphino)ferrocene
dppp	1,3-bis(diphenylphosphino)propane
dpppent	1,5-bis(diphenylphosphino)pentane
EDCI	1-ethyl-3-(3-dimethylaminopropyl)carbodiimide
EDG	electron donating group
ee	enantiomeric excess
ESI	electrospray ionization
Et	ethyl
Et ₂ O	diethyl ether
EWG	electron withdrawing group
FTIR	Fourier transform infrared
GC	gas chromatography
Het	heteroaromatic

HMBC	heteronuclear multiple bond correlation
HMPA	hexamethylphosphoramide
HPLC	high performance liquid chromatography
HSQC	heteronuclear single quantum coherence
K ₂ CO ₃	potassium carbonate
L _n	ligand
LAH	lithium aluminum hydride
LG	leaving group
Me	methyl
MeCN	acetonitrile
NaH	sodium hydride
NBD	norbornadiene
<i>n</i> -BuLi	<i>n</i> -butyllithium
NMP	<i>N</i> -methyl-2-pyrrolidone
NMR	nuclear magnetic resonance
NOESY	nuclear overhauser effect spectroscopy
NR	no reaction
NSAID	non-steroidal anti-inflammatory drug
Nu	nucleophile
OMe	methoxy
PBu ₃	tributylphosphine
Pd	palladium
PHOX	phosphinooxazoline

PivOH	pivalic acid
PPh ₃	triphenylphosphine
Ph	phenyl
Pr	propyl
QUINAP	1-(2-diphenylphosphino-1-naphthyl)isoquinoline
<i>rac</i> -BINAP	racemic 2,2'-bis(diphenylphosphino)-1,1'-binaphthyl
SeO ₂	selenium dioxide
S _N 2	bimolecular nucleophilic substitution
<i>t</i> -Bu	<i>tert</i> -butyl
<i>t</i> -BuOK	potassium <i>tert</i> -butoxide
TfOH	trifluoromethanesulfonic acid
TFP	trifurylphosphine
THF	tetrahydrofuran
TOF	time of flight
tol	toluene
TPO	triphenylphosphine oxide

Chapter 1

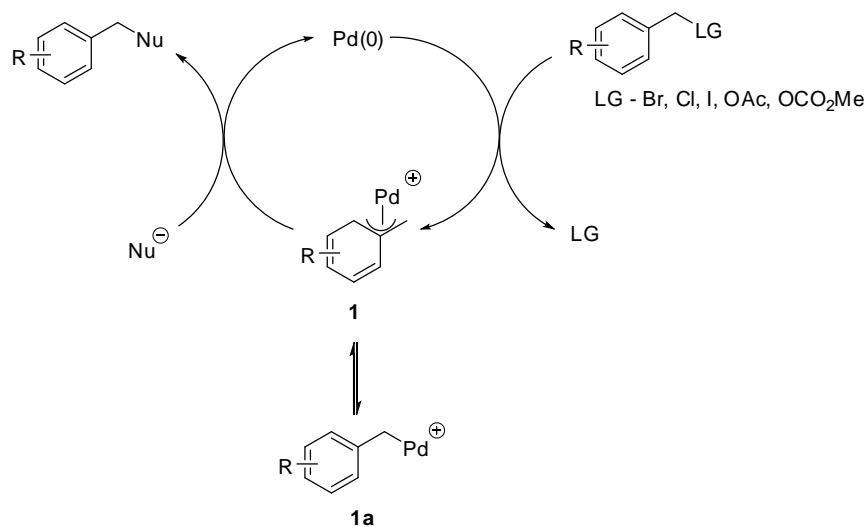
Background of Palladium-Catalyzed Benzylations Reactions

1.1 Introduction

Benzylic functionalization using palladium catalysis

The formation of carbon-carbon bonds in organic synthesis is important because it plays a vital role in creating molecules or targets for study in many scientific fields. More specifically, the construction of C-C bonds *via* benzylic functionalization is desirable given that many natural products and biologically active chemical compounds contain aromatic rings in which the benzylic carbon is functionalized. Current methodologies that utilize metal-catalyzed benzylations to generate benzylic compounds are superior to classical S_N2 alkylation because the latter requires use of stoichiometric bases to deprotonate nucleophiles, which attack benzyl electrophiles, often resulting in generation of mixtures of benzylation products. Among the metals used in metal-catalyzed benzylation reactions, Pd is typically the metal of choice because it has been shown to have remarkable reactivity to various benzyl moieties such as benzyl halides, acetates, carbonates, and other derivatives.¹ In the simplest sense, the catalytic cycle of Pd-catalyzed benzylation involves activation of benzyl-LG (LG = leaving group) with Pd *via* oxidative addition to generate η^3 -benzyl-Pd intermediate **1**, which is then attacked by a nucleophile to release the functionalized benzyl product and regenerate the Pd catalyst (Scheme 1). The formation of functionalized benzyl product depends on several variables present in the catalytic cycle: Pd choice, electronics of the R substituents on the benzyl reactant, the LG in benzyl-LG that will undergo oxidative addition to generate **1**, and the nature of nucleophile and how its method of generation.

Scheme 1.



The nature of Pd intermediate: η^3 -Pd-benzyl complex

As shown in Scheme 1, the most accepted structure of the Pd-benzyl complex is **1** in which it exists in η^3 fashion where the metal binds into three carbons. Another possibility is the same Pd-benzyl complex **1a** exists in η^1 fashion where the metal binds only to the benzylic carbon. It was reported that formation of **1a** is believed to be more thermodynamically favorable than **1** due to the loss of aromatic stabilization.² While **1b** (fig. 1) was the initial sole product generated from oxidative addition of Pd to benzyl trifluoroacetate or halide as reported by Yamamoto^{3a-b} and Turco,^{3c} the formation of **1c** (fig. 2) was only observed when sodium, potassium, or silver salt was added to the preformed η^1 -benzyl-Pd complex^{3a,c,5b} (eq 1). Mechanistic studies pertaining to the interconversion of **1** and **1a** in different solvents and varied temperatures indicated that the two equilibrate presumably through η^3 - η^1 - η^3 isomerization.⁴

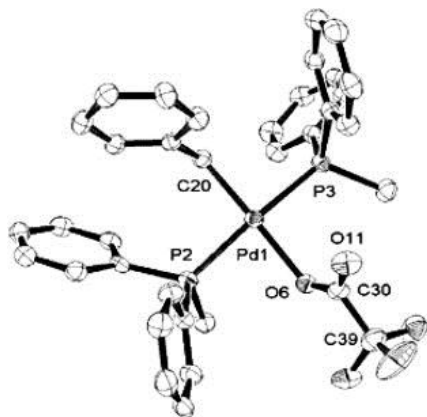
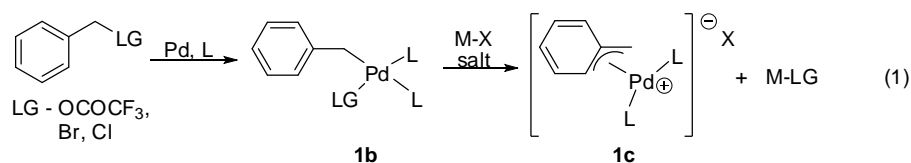


Figure 1. X-ray crystal structure of η^1 -benzyl-Pd **1b** (L = PPh₂Me₂, LG = OCOCF₃). Figure taken from ref. 3a.

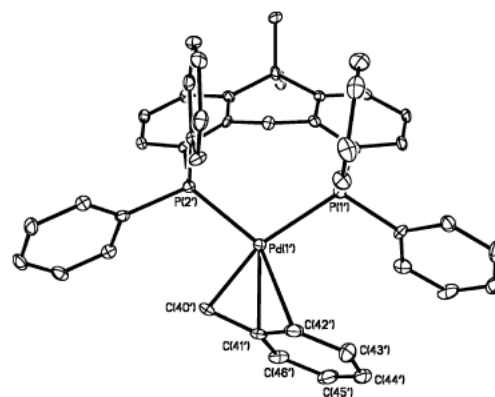
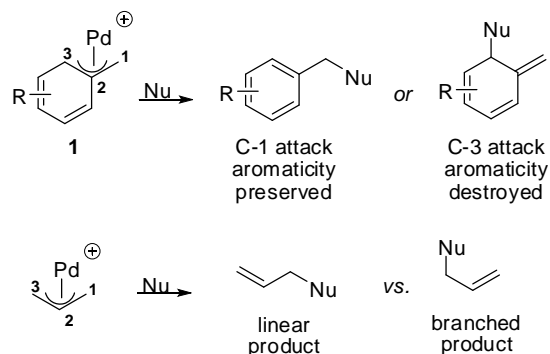


Figure 2. X-ray crystal structure of η^3 -benzyl-Pd **1c** (L = Xantphos, X = OTf). Figure taken from ref 5b.

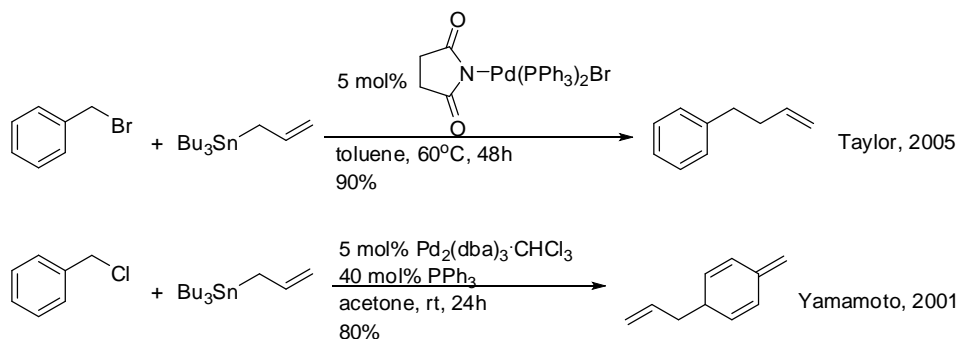
As shown from the catalytic cycle in Scheme 1, **1** is attacked by nucleophiles to release the functionalized benzylic product. The chemical nature of **1** as an electrophile has been established based on the reactivity of isolated η^3 -benzyl-Pd complexes from addition of Pd to benzyl halides, benzyl trifluoroacetates, or styrene to certain nucleophiles (Chapter 1.2). While the electrophilicity of **1** is known, the regioselectivity of C-C bond formation from the nucleophilic attack merits discussion. In **1**, the delocalization of positive charge is spread across three carbons similar to η^3 -allyl-Pd complex, and from these three carbons, nucleophiles only attack at positions 1 and 3. If the nucleophile attacks at C-1, benzyl (linear-type) product is obtained, whereas if the nucleophile attacks at C-3, a cyclohexadiene (branched-type) product is obtained (Scheme 2).

Scheme 2.



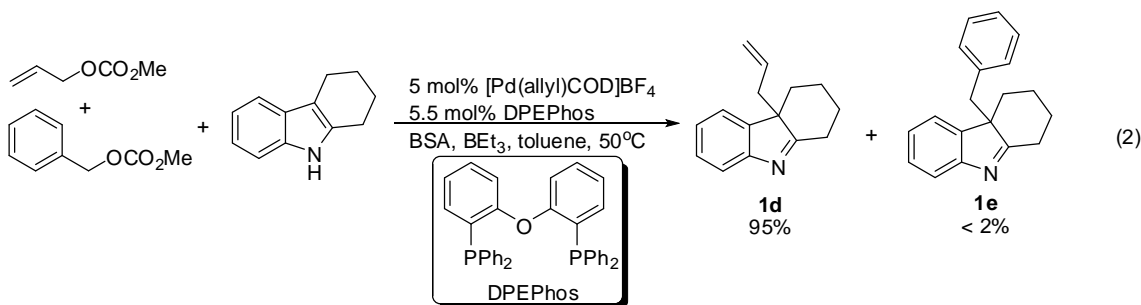
Based on several Pd-catalyzed benzylations reported, it was shown that nucleophiles regioselectively attack at C-1 to generate **1b** for two reasons. First, the formation of **1b** has the aromatic ring preserved from the reactant to the product in contrast with **1c** in which the aromaticity was destroyed. Second, the Pd-C₁ has been reported to contain higher degree of electrophilicity than the Pd-C₂ and -C₃ bonds.^{2,4a,5} This remarkable electrophilic character is possibly the consequence of its shorter bond length compared to other Pd-C bonds.^{4,5} While nucleophiles would prefer to attack at C-1 than C-3 of the complex giving benzyl compounds, it has been shown that by simply altering the conditions required for Pd-catalyzed benzylation such as in the Stille coupling of benzyl halide with allylstannane, dearomatized compound can also be accessed (Scheme 3).⁶

Scheme 3.



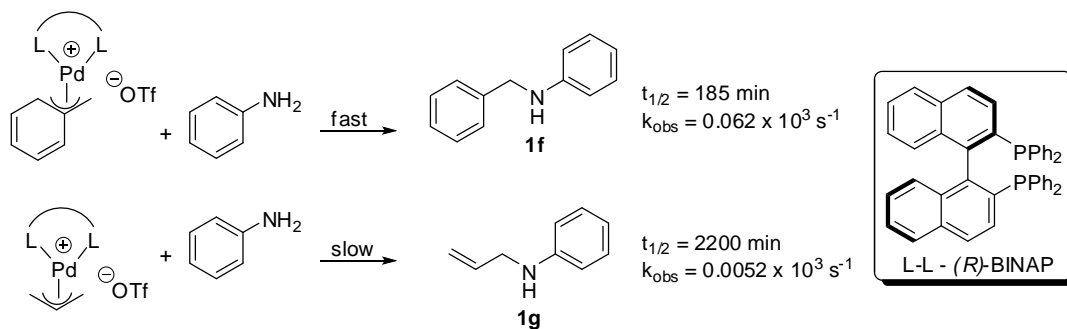
Reactivity of Pd-catalyzed benzylations versus allylations

Pd-catalyzed benzylations have similarities with Pd-catalyzed allylations because both generate Pd complexes which are coupled with nucleophiles giving linear or branched products. However, there are certain differences between the two analogous Pd-catalyzed reactions. Though both Pd complexes are electrophilic, the formation of η^3 -benzyl-Pd is kinetically less facile than formation of η^3 -allyl-Pd electrophile due to fact that the β,γ π -bond in the Pd-benzyl complex is part of the aromatic ring.^{1a,7} The reactivity of Pd-benzyl vs. Pd-allyl with nucleophiles is also slower due to lower stability of the preformed Pd π -complex. As shown by Rawal and Zhu, when an equimolar mixture of allyl carbonate and benzyl carbonate was reacted with indole, none of benzyl indole **1e** was observed but only allyl indole **1d** (eq 2).⁸ This result explains the faster generation of η^3 -Pd-allyl complex than **1** resulting in faster reactivity to the indole nucleophile.



While η^3 -allyl-Pd complexes react with nucleophiles faster than **1**, there are certain cases in which the reverse occurs such that **1** was more favorable to be attacked by nucleophiles than η^3 -allyl-Pd. Hartwig and coworkers have shown that the addition of aniline to η^3 -Pd-benzyl triflate decayed the Pd-complex and generated benzyl amine **1f** 12-times faster than formation of allyl amine **1g** from η^3 -Pd-allyl triflate complex (Scheme 4). Further evidence of their differences was shown by the calculated APT charges of the two model Pd complexes in which the degree of positive charge at the site of nucleophilic attack in η^3 -benzyl-Pd was greater than that of the η^3 -allyl-Pd.^{5a} The reactions in eq. 2 and Scheme 4 suggest that formation of Pd- π -benzyl is slower but the reaction with nucleophiles is faster. In these reactions, the high temperature requirement (50°C) is presumably one of the important conditions to consider in performing Pd-catalyzed benzylation reactions.

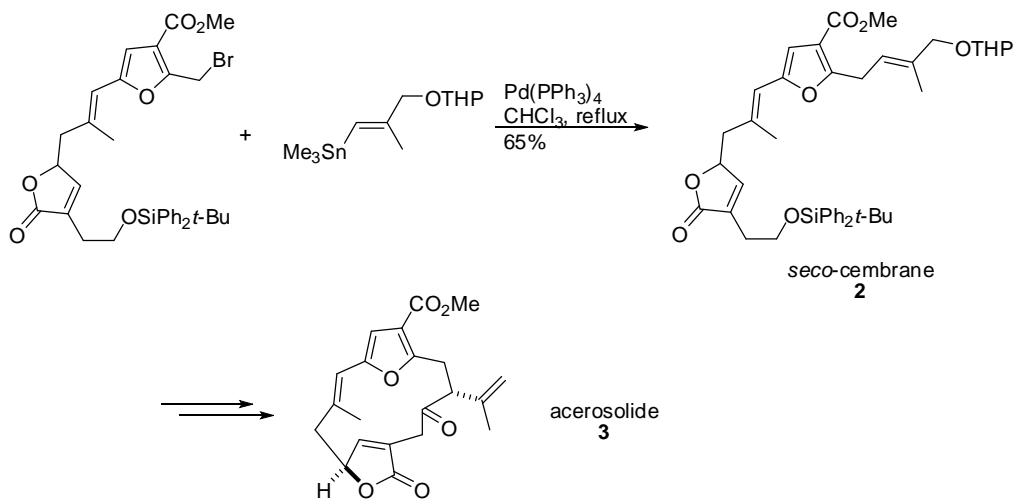
Scheme 4.



Applications of Pd-catalyzed benzylations in natural product synthesis

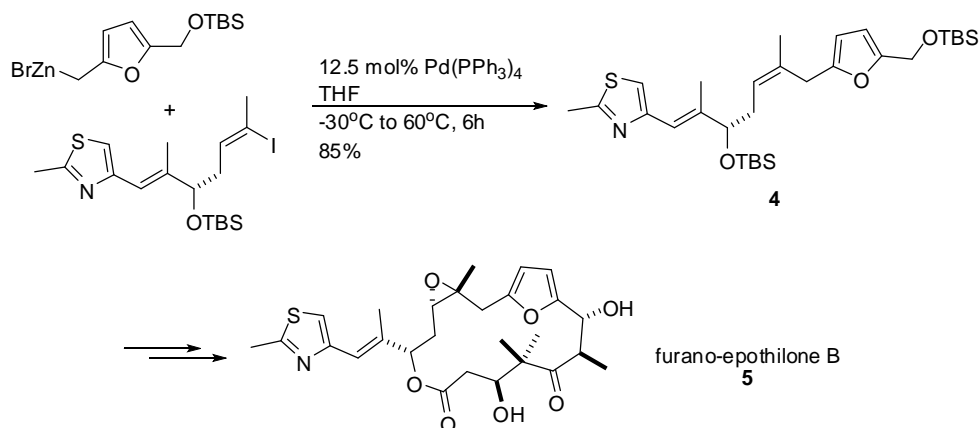
It is important for organic chemists to be able to synthesize small compounds using the developed methodology and to be able to apply it towards the synthesis of large molecules such as natural products. This is important because it allows scientists to produce greater quantities of these biologically active products that can be used in different scientific applications, which cannot feasibly be produced by direct isolation of the same compounds from natural resources. Despite advances of Pd-catalyzed benzylations reported in the chemical literature towards the construction of small-sized benzyl compounds (Chapter 1.2), application towards large molecule natural products and other biologically active compounds of interest remains limited. In 1993, Paquette and Astles utilized a Pd-catalyzed aryl methylation strategy towards the synthesis of *seco*-cembrane **2** through Stille cross-coupling of 2-furyl bromide derivative with vinyl stannane (Scheme 5).⁹ The formation of **2** depends on the solvent in which non-polar solvents such as benzene and DME gave poorer yields in contrast to chloroform. Their synthesis of **2** was only five steps towards the total synthesis of acerosolide **3**, a natural product that is a part of 14-membered marine furanocembranolide diterpenes.¹⁰ The synthesis of **2** is important because it allows construction of sp^3 - sp^2 C-C bonds directly without the need for additional steps which can be beneficial in large-scale applications.

Scheme 5.



After the acerosolide total synthesis, the utility of Pd-catalyzed benzylation in natural product synthesis was also reported in the synthesis of an important intermediate component of the macrocyclic epothilone. In 2004, Schinzer and coworkers reported the benzylation of a vinyl iodide through Negishi cross-coupling conditions to generate furan **4** (Scheme 6).¹¹ The formation of **4** is necessary towards the total synthesis of furano-epothilone D **5**, a derivative of epothilone macrolide that possesses antitubercular activity.¹² Based on these two examples, it is clear that Pd-catalyzed benzylation reactions typically used in small-molecule synthesis can be transferred and applied towards large-molecule synthesis. In order to adapt this methodology to other natural product synthesis, newer methods of constructing other small-sized functionalized benzylic compounds must be developed.

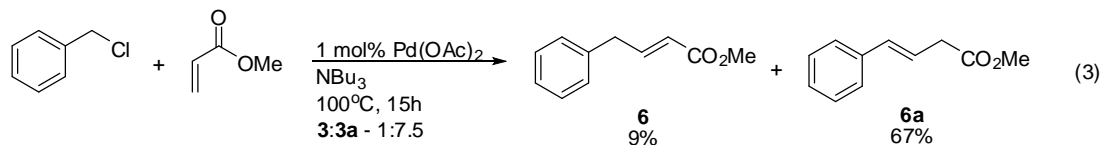
Scheme 6.



1.2 Nucleophilic partners of η^3 -Pd-benzyl

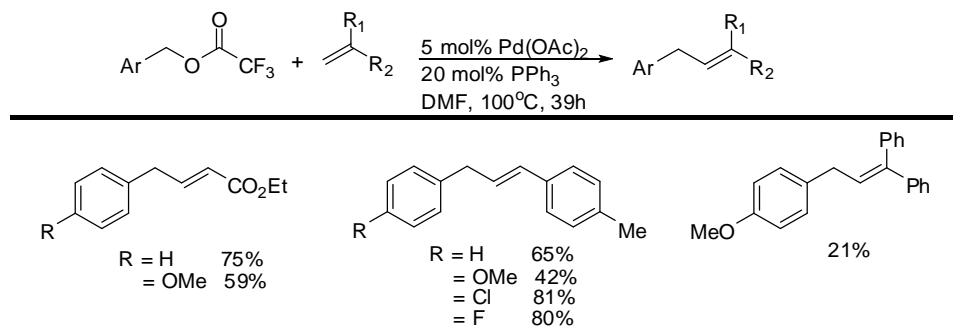
1.2.1 Olefins

Based on the catalytic cycle shown in Scheme 1, it has been shown that certain nucleophiles attack Pd- π -benzyl complexes to give functionalized benzyl derivatives. An example is the olefin which was reported as the first coupling partner of η^3 -benzyl-Pd complex through a Heck reaction in 1972. Heck and Nolley showed that treatment of benzyl bromide with Pd(OAc)₂ under basic conditions gave a mixture consisting of the desired benzyl product **6** in a very low yield and undesired aryl isomer **6a** in high yield (eq 3).¹³ The preferential formation of **6a** rather than **6** was the result of its higher thermodynamic stability due to the conjugation between the double bond and aromatic ring. Despite the low benzylation yield, its formation *via* sp³-sp² coupling between benzyl halide and olefin is possible since typical coupling partners used in Heck reactions form products through sp²-sp² coupling.



The low selectivity of **6** in the Heck reaction using benzyl chloride prompted Shimizu and coworkers to use other benzyl substrates that would also generate η^3 -benzyl-Pd complex. In 2004, they reported an improved formation of analog **6** and minimized the generation of isomerized product **6a** by Heck coupling of acrylates with benzyl trifluoroacetate using the same Pd catalyst but in the presence of monodentate phosphine ligand PPh₃ in DMF at 100°C.¹⁴ Under these conditions, a variety of olefins can be coupled in good yields without the need of benzyl chlorides and bases (Scheme 7). This is important because benzyl chloride is toxic in nature. The use of benzyl trifluoroacetate which generated the complex through cleavage of the benzyl-oxygen bond was thought to be more facile than cleavage of benzyl-chlorine bond in benzyl halide. While Heck benzylations occurred, the formation of these products requires higher temperatures and longer reaction times. Nevertheless, these reactions demonstrate the inherent power of benzylic sp³ coupling with olefinic sp² substrates without the need of strong bases.

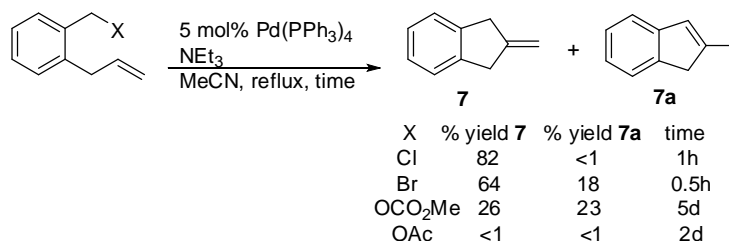
Scheme 7.



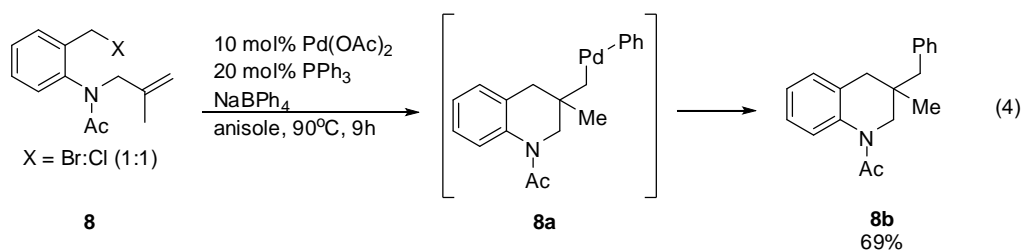
In addition to intermolecular benzylations, intramolecular Heck benzylations have also been realized. This was first demonstrated by Negishi and coworkers in the benzylation of *o*-

allylbenzyl chloride to generate 2-methyleneindane **7** exclusively without the formation of isomeric 2-methylindene **7a** (Scheme 8).¹⁵ The formation of **7** and **7a** significantly depends on the nature of the benzyl leaving group. While benzyl acetate does not undergo benzylation because acetates are not very good leaving groups in benzylation reactions, it is surprising that benzyl substrates which contain good leaving groups such as bromide and carbonate gave lower yields of **7** yet significant formation of undesired **7a**. Among these, it is intriguing that the formation of **7** from Heck cyclization of benzyl carbonate was slower (five days) in contrast to the Heck benzylation with benzyl trifluoroacetate in Scheme 7 though both benzyl substrates contain good leaving groups.

Scheme 8.

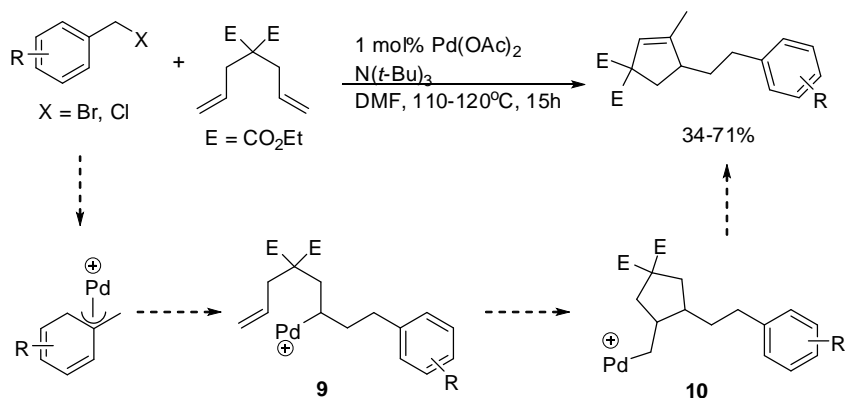


A similar intramolecular Heck benzylation was reported by Grigg and coworkers in 1991.¹⁶ They showed that an external phenyl source coming from NaBPh₄ can act as the second nucleophile to intermediate **8a** to generate dihydroquinoline **8b** in good yield (eq 4). While this reaction involves intramolecular Heck benzylic cyclization similar to Scheme 11, what makes this reaction important in developing newer benzylation methods is that the presence of an external nucleophile can be used to functionalize the initially preformed η^3 -Pd-benzyl complex. In this case, the Ph from anionic phenylborate adds to Pd to form **8a** *via* anion capture to generate the desired product.



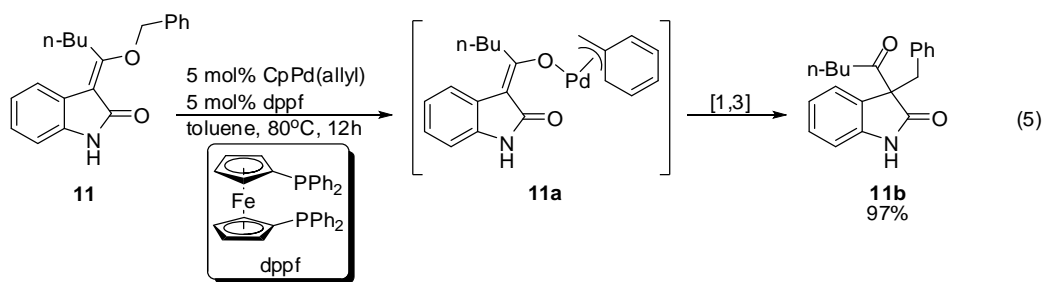
In some cases, instead of an external nucleophile, an internal nucleophile can be used to functionalize the preformed η^3 -benzyl-Pd complex. As shown by Pan and coworkers in the cascade cyclization of benzyl halides with diethyl-diallylmalonate, after the initial Heck benzylation generated **9**, the presence of the second double bond allowed a second Heck coupling *via* carbopalladation to occur, generating a Pd-cyclized intermediate **10** which forms cyclopentene (Scheme 9). In **9**, there is the possibility that BHE (β -hydride elimination) could occur because of the presence of nearby hydrogens. However, the proximity of a second nucleophilic source prevented BHE, which aided the overall Heck reaction.¹⁷ This suggests that while benzylation reactions are slow and require high temperatures, certain nucleophiles can take advantage of coupling with Pd- π -benzyl before completing the actual catalytic cycle, resulting in formation of functionalized and more complex benzyl compounds.

Scheme 9.



1.2.2 Alkylidene

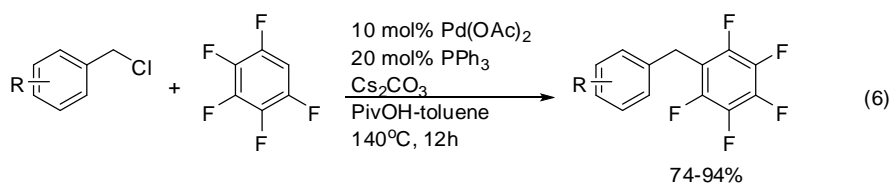
As of this writing, only one example of benzylation with a benzyl enol ether has been reported. In 2010, Murakami and coworkers reported the benzylation of 3-(alkoxyalkylidene oxindole) **11** with CpPd(allyl) and bidentate dppf ligand through an intramolecular process to generate 3,3-disubstituted oxindole **11b** in a high yield (eq 5). The formation of **11b** occurred via [1,3] rearrangement after generation of the η^3 -benzyl-Pd intermediate **11a**.¹⁸ This reaction is important because it highlights the *in situ* formation of a very reactive nucleophile concomitant with Pd- π -benzyl formation. The importance of Pd-catalyzed benzylation in the generation of reactive species *in situ* such as **5a** will be discussed in subsequent chapters.



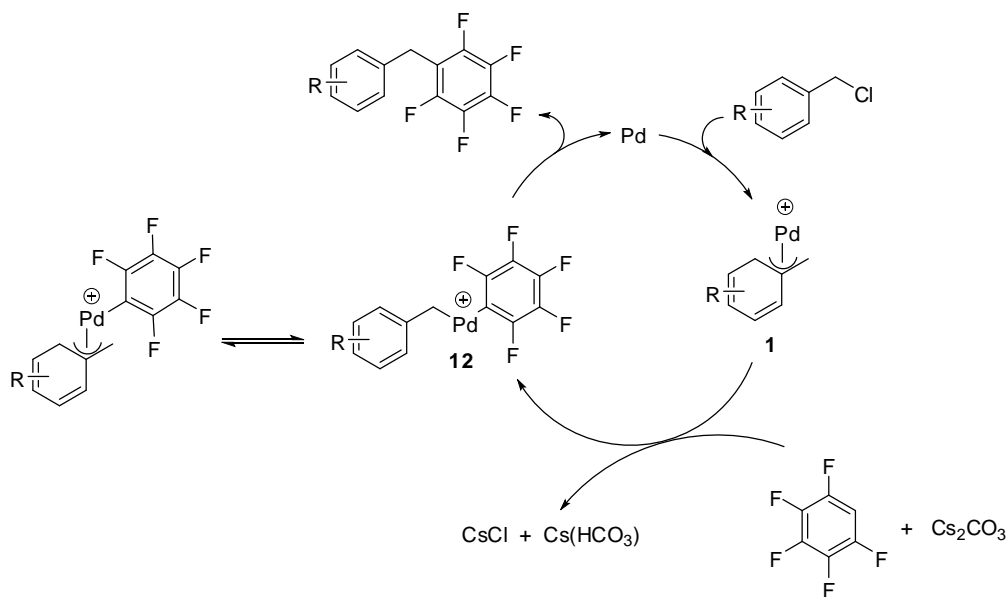
1.2.3 Aromatics

The cross-coupling of η^3 -benzyl-Pd with C-H bond of aromatic rings generate diarylmethanes. Diarylmethanes are an important class of compounds because there are many biologically active natural products in the chemical literature that contain this skeletal framework. Their synthesis merits paramount and practical importance in other applications such as medicine, biology, and nanotechnology.¹⁹ The earliest known Pd-catalyzed benzylation of arenes was reported by Zhang and coworkers in 2010.²⁰ Various benzyl chlorides undergo coupling with fluoroarenes in the presence of Pd(OAc)₂, PPh₃ and Cs₂CO₃ to generate fluoroaryl-phenylmethanes in good to high yields (eq 6). The proposed mechanism for this

reaction was thought to proceed through a concerted metallation-deprotonation step generating σ -benzyl-Pd-aryl intermediate **12**, which then undergoes reductive elimination to release diarylmethane and Pd is regenerated back in the catalytic cycle (Scheme 10).²⁰ Based on this mechanism, it appears that the C-H bond of the arene can be activated when appropriate reaction conditions such as base, Pd and ligand catalysts, and other additives are used. Once activated, it can couple to η^3 -benzyl-Pd **1** thus expanding the scope of Pd-catalyzed benzylation reactions in the synthesis of diverse diaryl compounds using substituted arenes and heteroarenes.

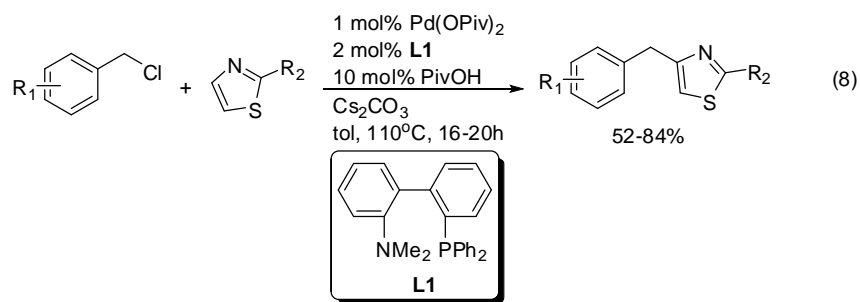
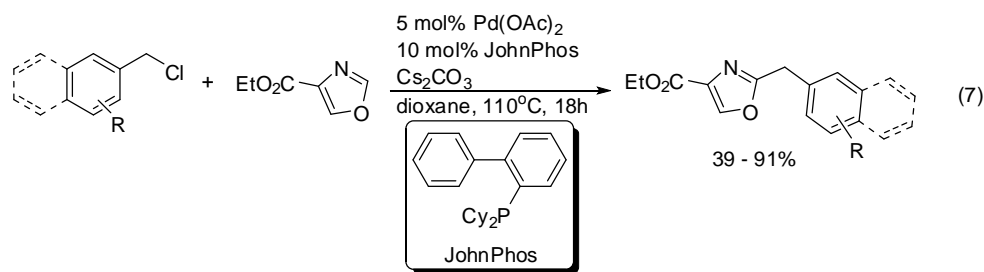


Scheme 10.



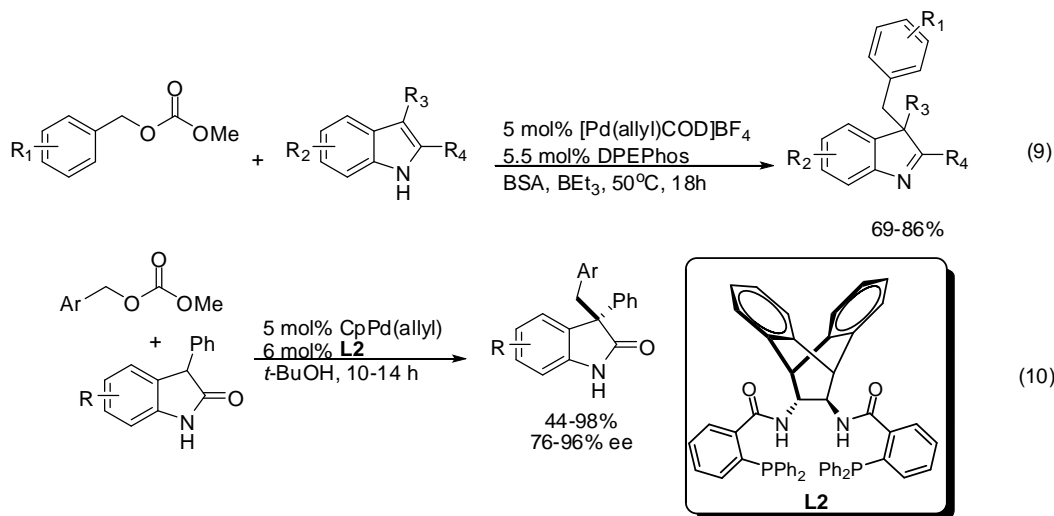
In addition to fluoroarenes, heteroarenes have also been used as coupling partners with benzyl halide. Hoarau and coworkers reported the benzylation of ethyl-4-oxazole carboxylate

using a biphenyl JohnPhos ligand and conditions identical to those used by Zhang (eq 7).²¹ Similarly, Fagnou and coworkers reported the benzylation of benzyl chlorides with thiazole and other heteroarenes using Pd(OPiv)₂, an amino-biphenyl phosphine ligand, Cs₂CO₃, and PivOH (eq. 8).²² In both cases, a variety of hetero-diarylmethanes were synthesized in good to high yields. Similar to the conditions of Zhang, a monodentate ligand is necessary to generate heterodiarylmethanes. It has been shown that bidentate ligands were ineffective presumably due to sterics and the inability to access an open coordination site from the Pd-benzyl complex with the activated arene.



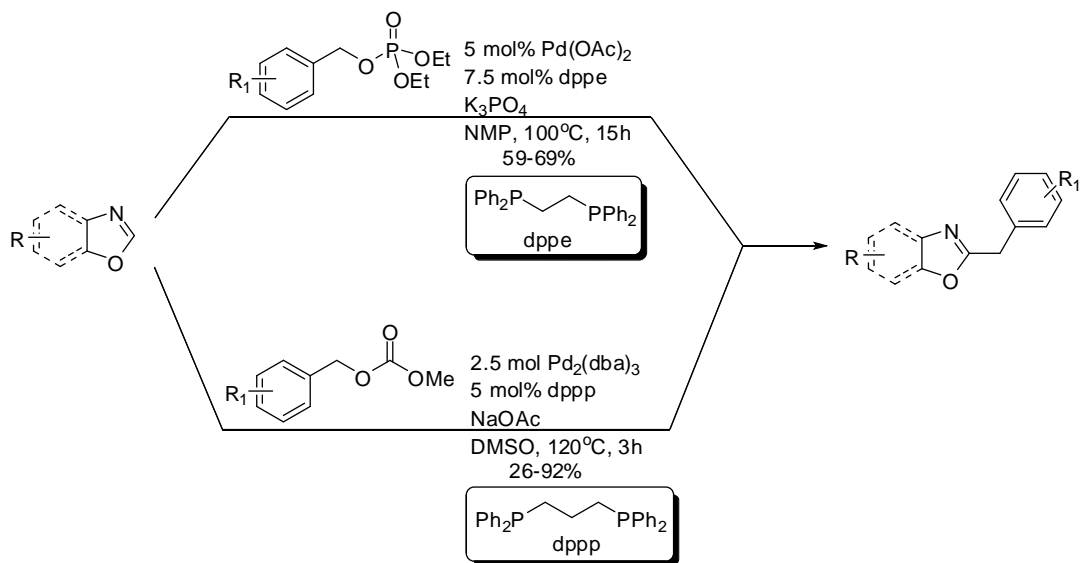
Other researchers recently reported benzylic alkylations with indole using Pd and bidentate ligands. Rawal and Zhu reported that the combination of cationic Pd, DPEPhos, BSA and BEt₃ allowed benzylic alkylation of benzyl carbonates to the C-3 position of indole to occur in high yields (eq 9). Here, the BEt₃ facilitates the formation of η³-benzyl-Pd complex by binding to the carbonyl group of the benzyl carbonate, while the BSA activates benzyl carbonate by forming a silyl enol ether nucleophile.⁸ Earlier, Trost and coworkers used a pre-activated

Pd(0)/bidentate ligand catalyst, and *t*-BuOH to benzylate aryl oxindoles (eq. 10). The use of a bulky chiral ligand **L2**, induced the asymmetric benzylic alkylation in good to high yields and ee's.²³ The importance of using very bulky bidentate ligands in Pd-catalyzed benzylations will be discussed in Chapter 2.



Aside from benzyl chloride, other leaving groups can be used to couple with heteroarenes (Scheme 11). Ackermann and coworkers have shown that benzyl phosphates can be used to couple with benzoxazoles in the presence of Pd(OAc)₂, dppe, and K₂CO₃ whereas Miura and coworkers used benzyl carbonates, similar to Rawal and Trost, in cross-coupling with identical heteroarenes under different Pd basic conditions.^{24,25} Overall, these reactions highlight the use of other benzyl substrates derived from benzyl alcohol in contrast with benzyl halides. It is important in developing new methods of Pd-catalyzed benzylations under milder conditions that occur and use benzyl-derived starting materials that are non-toxic.

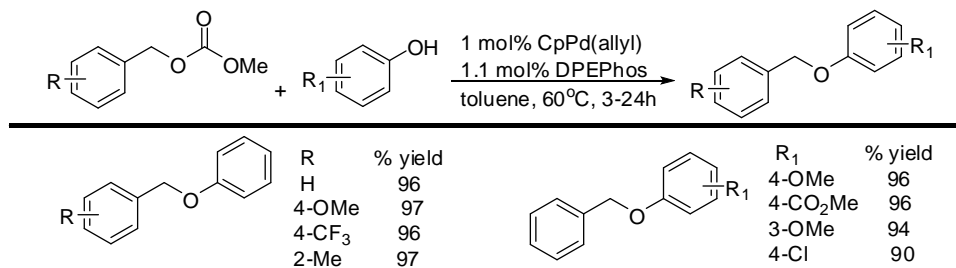
Scheme 11.



1.2.4 Heteroatom from phenols, amines, sulfinates, and phosphonates

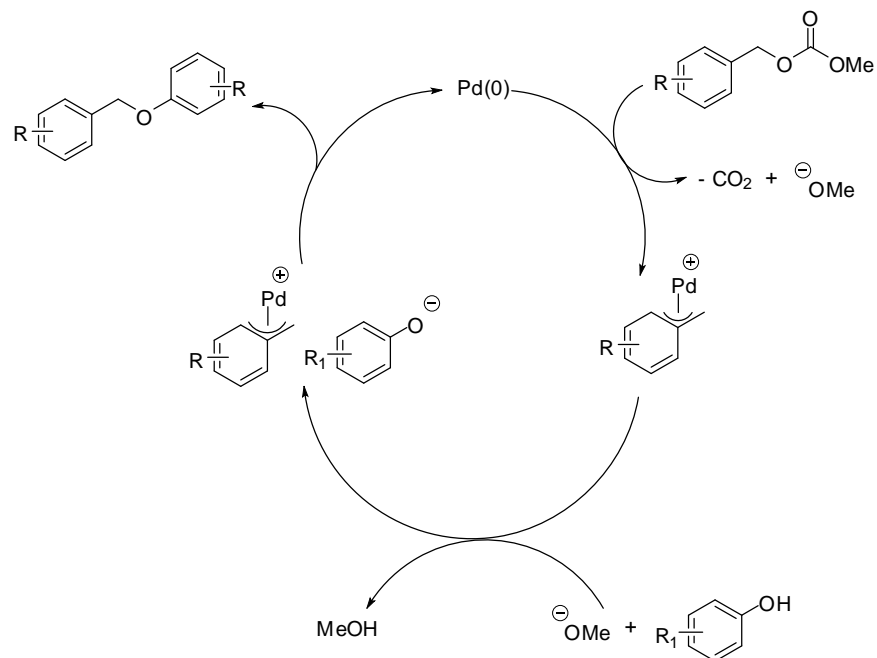
Other important classes of nucleophiles that have been used in coupling with η^3 -benzyl-Pd in Pd-catalyzed benzylations are from heteroatom-containing compounds derived from phenols, amines, sulfinates, and phosphonates in which the heteroatom is the nucleophile. These compounds have been used in a variety of cross-coupling reactions as nucleophiles because they have low pK_a 's (5-20) which can be easily deprotonated with mild bases to generate reactive heteroanions. While prevalent in the literature, their applications in Pd-catalyzed benzylation reactions are currently limited. Kuwano and Kusano reported the use of phenols in substitution of benzyl carbonates in the presence of CpPd(allyl) and DPEPhos ligand to generate benzyl phenyl ethers in high yields (Scheme 12). A variety of substituted phenols and benzyl carbonates showed that EDG and EWG are tolerable under the reaction conditions to give functionalized benzyl ethers.²⁶

Scheme 12.

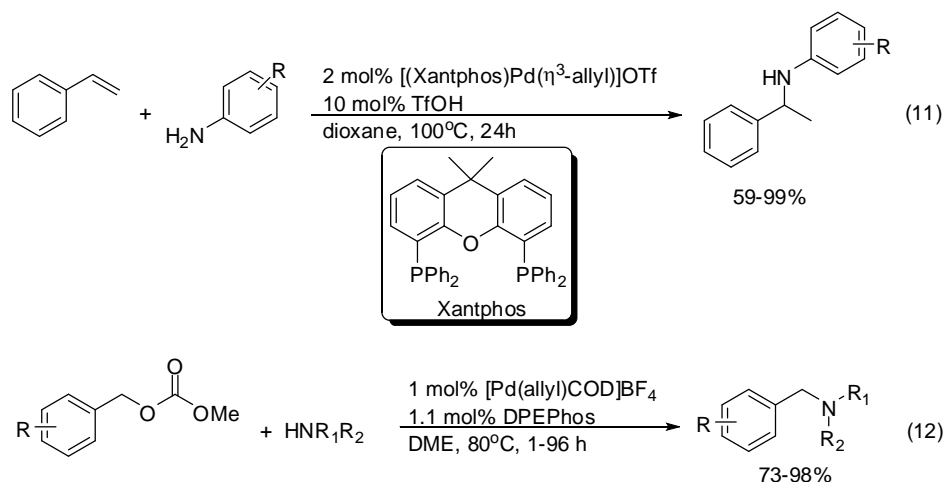


It has been proposed that the mechanism of the benzylic-etherification reaction is similar to the mechanism of Tsuji-Trost allylation. The Tsuji-Trost allylation reaction is well-known cross-coupling reaction between an allyl-LG and a nucleophile in the presence of Pd and base.²⁷ Its relation to benzylation reactions is analogous in which all components are identical with the exception of the type of Pd electrophile. The benzylation mechanism in particular begins by oxidative addition of Pd to benzyl carbonate which generates Pd- π -benzyl, CO₂ and methoxide anion (Scheme 13). While a base is needed in Tsuji-Trost reaction to deprotonate a pronucleophile, the methoxide anion generated from decarboxylation of benzyl carbonate acts as a base instead, to deprotonate phenol (pK_a – 10 in H₂O, 18 in DMSO) generating a more nucleophilic phenoxide anion. The anion undergoes nucleophilic substitution with Pd- π -benzyl to form benzyl phenyl ether. It is important to realize that this mechanism is operating for most types of intermolecular cross-coupling benzylation reactions in which Pd- π -benzyl is generated and the nucleophile is formed by base or an alkoxide deprotonation.

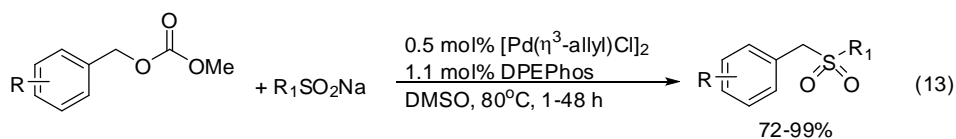
Scheme 13.



Amines have also been used to couple with Pd- π -benzyl complexes. Hartwig and coworkers reported the benzylation of bifunctional anilines with styrene to give benzyl amines in high yields in the presence of cationic Pd and Xantphos ligand (eq. 11).^{5b} Kuwano and coworkers on the other hand used secondary amines to couple with benzyl carbonates using a different cationic Pd catalyst and DPEPhos ligand (eq. 12).²⁸ The formation of C-N bonds in both cases depended significantly on the use of bulky bidentate phosphine ligands since no reactivity was observed when monodentate ligands were used.

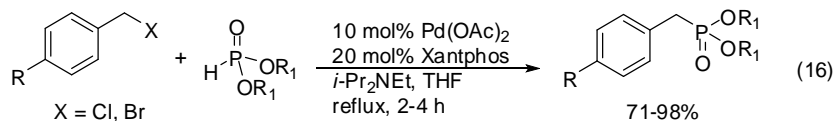
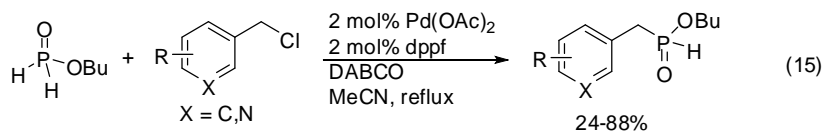


In addition to phenols and amines, sulfur-containing compounds such as sulfinates have also been utilized in Pd-catalyzed benzylation reactions. This was shown by Kuwano and coworkers in which arene sulfinates (pKa – 20 in DMSO) can couple with benzyl carbonates in the presence of [Pd(allyl)Cl]₂ and DPEPhos to form benzyl sulfones in high yields (eq. 13).²⁹ While the use of a base is not required in the reaction, the arene sulfinate from the salt is nucleophilic enough to react with Pd- π -benzyl generated from oxidative addition of benzyl carbonate. Similar to benzylation of amines and phenols, the use of bulky bidentate ligand gave the best results.



Aside from oxygen, nitrogen, and sulfur-containing compounds, phosphorus-containing compounds have also been used as nucleophiles in coupling with Pd- π -benzyl electrophiles. Currently, there are only two reports that showcased benzylic C-P bond formation to generate benzyl phosphine derivatives. The first application was reported in 2005 by Montchamp and coworkers in which they showed that benzylation of alkyl hypophosphite with benzyl chloride in

the presence of Pd(OAc)₂, dppf ligand, and DABCO generated benzyl phosphinates in good yields (eq. 14).³⁰ The second application was reported in 2009 by Stawinski and Lavén in which they have shown that benzylation of dialkyl phosphonate ester with benzyl halide in the presence of Pd(OAc)₂ and Xantphos under basic conditions form benzylphosphonates in good to high yields (eq. 15).³¹ Similar to the benzylation of phenols, amines, and arene sulfinates, the judicious choice of base and bulky bidentate ligands gave the best results.

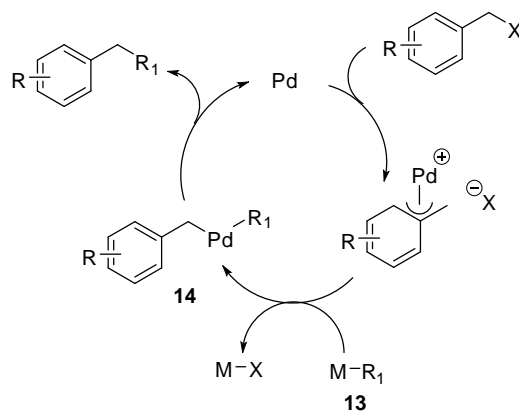


1.2.5 Preformed organometallics

Aside from olefins, aromatics, alkylidene, and heteroatom containing compounds, certain carbon nucleophiles have also been used as nucleophilic partners in Pd-catalyzed benzylation reactions. While carbon nucleophiles derived from enolates (Chapter 2) and alkynes (Chapter 3) will be discussed in succeeding chapters, other carbon nucleophile sources from preformed organometallics will be discussed here. Carbon nucleophiles derived from preformed organometallics are perhaps the most common and frequently used coupling partners in Pd-catalyzed benzylations. These are frequently used because they can be prepared easily by treating any coupling substrate (alkyl or aryl halide, for example) with an external metal similar to preparation of Grignard reagent in the presence of external additives. The preformed organometallics are very reactive towards any electrophiles. Their remarkable reactivity lies in

contrast with other anionic nucleophiles that have to be generated using base. In principle, these organometallic compounds react with Pd- π -benzyl complexes through transmetallation of **13** where a variety of metals have been used in the formation of M-R₁ organometallic reagent (Scheme 14). This results in the formation of **14** which undergoes reductive elimination to give the functionalized benzyl product. Certain organometallic reagents have been utilized in cross-coupling with Pd electrophile. As shown in Scheme 14, it is important that the generation of **13** must occur before it undergoes transmetallation with Pd- π -benzyl complex.

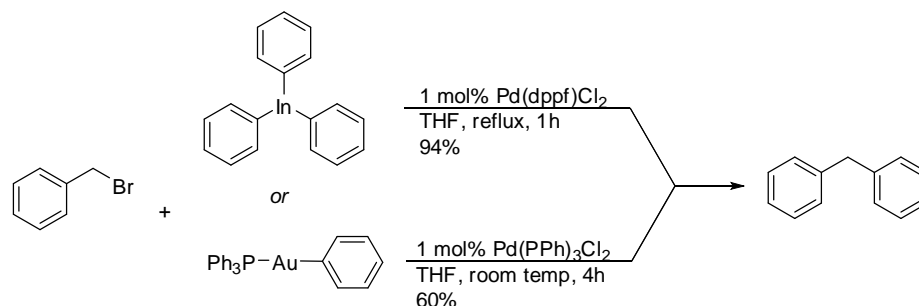
Scheme 14.



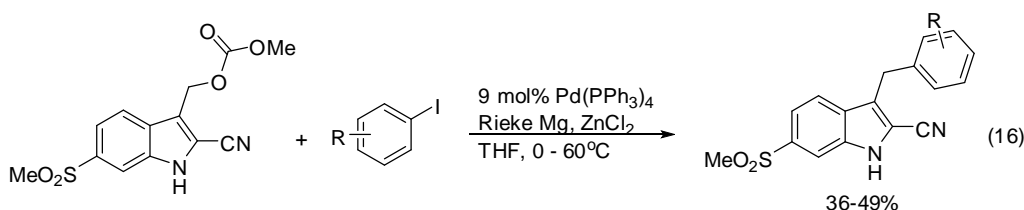
The following metals have been used in the formation of preformed organometallic M-R₁. One source of metal used to prepare the transmetallating reagent was In. Sarandeses and coworkers have shown that triphenylindium can be used to couple with benzyl chloride to form diphenylmethane in the presence of Pd(II) in high yield.³² Also, the same compound can be made using phenyl triphenylphosphine gold, where Au is another source of transmetallating reagent, to couple with the same benzyl halide in moderate yield using a slightly different Pd (II) catalyst.³³ For both reactions, the reaction of benzyl bromide with triphenyl-In occurred in one hour reflux

whereas with phenyl-Au, the reaction occurred at room temperature in four hours (Scheme 15).

Scheme 15.

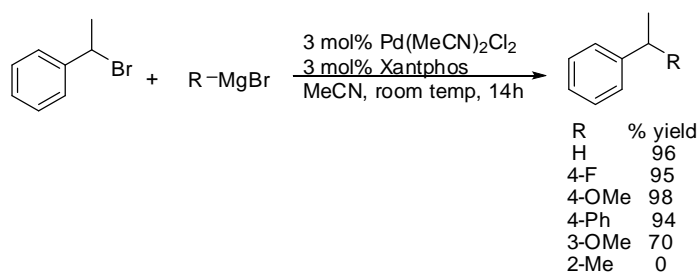


Another source of metal used as a transmetallating reagent for Pd-catalyzed benzylation was Zn. Campbell and coworkers have reported the utility of Zn in the coupling of indole carbonates with aryl iodides to form indole-arylmethanes.³⁴ Zn reacts to aryl iodide in the presence of Mg to form the reactive aryl-Zn which undergoes transmetallation with η^3 -Pd-indolyl complex from indole carbonate *via* Negishi cross-coupling to generate indolyl-aryl compounds that were used as target substrates for potential COX-2 inhibitors (eq 16). COX-2 is a type of enzyme in prostaglandin G/H synthesis induced by mitogens or cytokines in inflammatory sites where inflammation and other immunoreactions occur.³⁵ While the formation of aryl-Zn is high yielding, the low yield of the isolated products was presumably due to the presence of *ortho*-cyano and methylsulfone EWG's that destabilize the Pd complex. Also, the N-H proton of the indole could have been abstracted easily by the preformed transmetallating reagent.



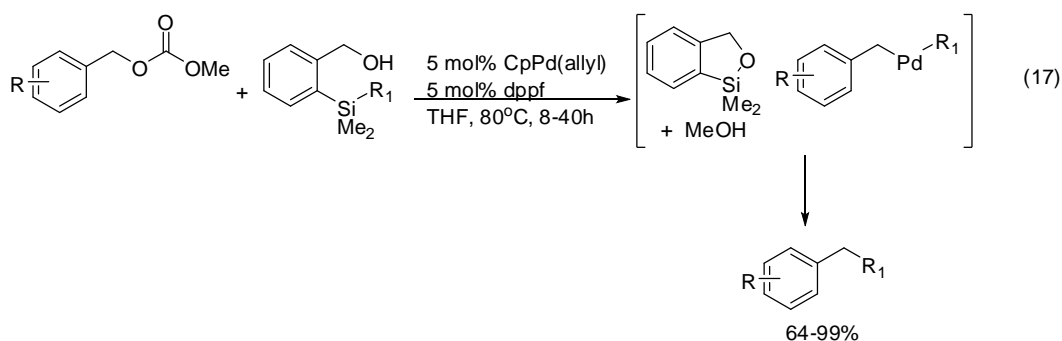
Another source of metal used as a transmetallating reagent in Pd-catalyzed benzylation reactions was Mg. It was shown by Carretero and coworkers that organomagnesium, or Grignard reagents, can couple with benzylic bromides through Kumada cross-coupling to generate functionalized benzylic products (Scheme 16).³⁶ The different electronic substituents at the *para* position of PhMgBr did not affect the overall benzylation. Benzylation only decreased when a *meta* substituent was used and no reaction was observed with an *ortho* substituent. This suggests that steric bulk in the ortho position of the benzyl ring significantly affects the benzylation process. More importantly, the use of bulky Xantphos ligand is desirable especially for α -substituted methyl benzyl bromide substrates ($R_1 = \text{Me}$) because its steric bulk presumably prevented the formation of undesired styrene derivatives *via* BHE.

Scheme 16.



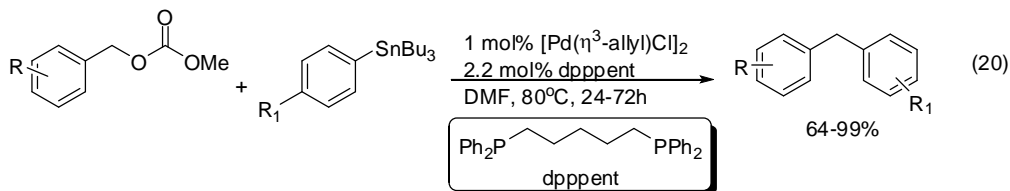
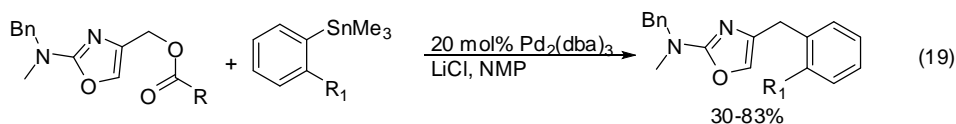
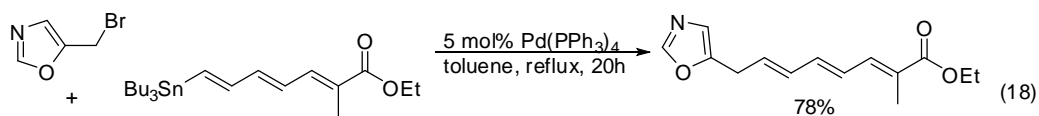
Another metal source used as a transmetallating reagent in Pd-catalyzed benzylation reactions is Si. This was shown by Hiyama and coworkers in 2007 in the benzylation of benzyl carbonates with *o*-silyl alcohols (eq. 18).³⁷ A variety of R-silyl alcohols underwent cross-coupling in which the R of the silyl group was transferred to the benzylic moiety. The presence of pendant alcohol near the silicon group was important because its role was to generate a five membered silacycle, coming from deprotonation of the alcohol by the alkoxide generated from decarboxylation of benzyl carboxylate. The reactive R_1 was expelled as the result of cyclization

which ultimately reacts with the Pd- π -benzyl intermediate to generate Bn-Pd-R₁ which undergoes reductive elimination to form the substituted benzyl product. Similar to previous benzylation reactions, the use of bidentate ligands such as dppf gave the best yields in contrast with monodentate ligands.

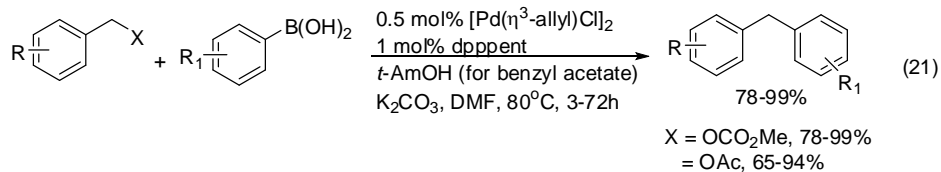


The use of Sn in Pd-catalyzed benzylation reactions as a transmetallating reagent was perhaps the oldest and most direct method in constructing functionalized benzyl compounds. Introduced in 1979, its utility was applied towards constructing benzylic compounds from small molecules to large molecule intermediates, such as in the total synthesis of acerosolide in Scheme 5. While Stille and Milstein first reported the use of SnMe₄ in coupling with benzyl bromide to give ethylbenzene in low yield,³⁸ significant improvement in benzylation was realized by changing the nature of benzyl moiety and the stannane coupling partner. This was demonstrated by Fairlamb and coworkers in which an oxazole benzyl bromide was used to couple with an olefin ester stannane to form an oxazole polyene (eq. 18).^{6b} In another case, Pettus and coworkers reported the Stille coupling of oxazole benzyl esters with aryl stananes using Pd₂(dba)₃ and LiCl to generate oxazole diarylmethanes in moderate to good yields (eq. 19).³⁹ Lastly, Kuwano and coworkers utilized benzyl carbonates instead of benzyl halides in the Stille coupling with aryl stannanes using Pd allyl dimer to form diarymethanes in good to high yields (eq. 20). In their approach, the use of base or salt additive is eliminated in contrast to the

benzylation reported by Pettus.⁴⁰ In these three reactions, Stille benzylation required higher temperatures and longer reaction times in order to achieve the desired formation of functionalized benzyl compounds.



The use of boron as an organometallic reagent in Pd-catalyzed benzylation reactions was also utilized. Kuwano and Yokogi have shown that benzyl acetate and benzyl carbonates can undergo Suzuki coupling with arylboronic acids in the presence of Pd and dppent (diphenylphosphinopentane) bidentate ligand to generate diarylmethanes in high yields (eq. 21).⁴¹ In the benzylation of benzyl acetate, the incorporation of *t*-AmOH and base in the reaction medium was necessary in order to allow ligand exchange between the acetate and alkoxide on the Pd catalyst to occur prior to transmetalation with arylboronic acid. In the benzylation of benzyl carbonates however, *t*-AmOH is not required to achieve the same benzylation, presumably because carbonates are better leaving groups than acetates in generating Pd- π -benzyl such that an external alcohol is not necessary.



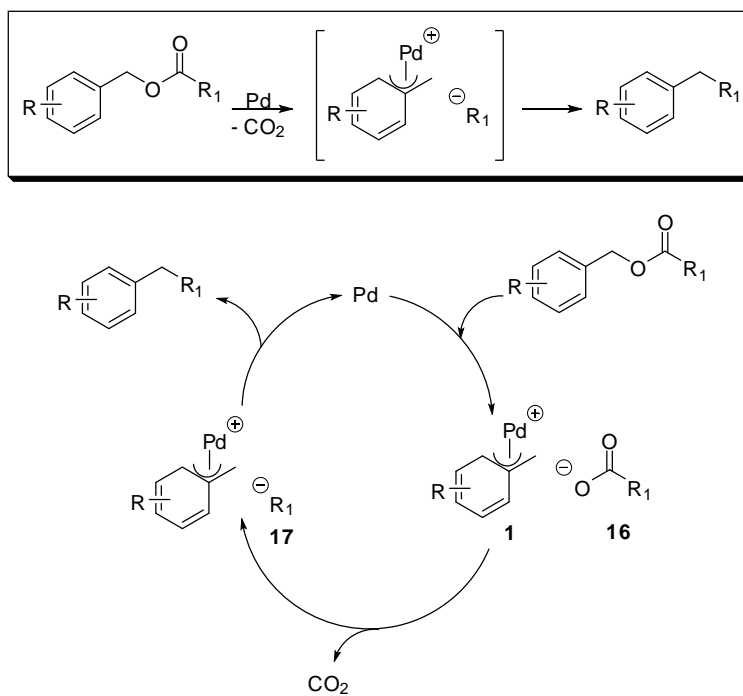
While these nucleophilic sources demonstrate their ability to couple with Pd- π -benzyl intermediates, these reactions also have limitations. First, the majority of these methodologies relies on the use of toxic benzyl halides and preformed organometallics. While preformed organometallics generate the desired benzyl compound in high yields, these additives also create metallic wastes which can lead to tedious workup and purification of the benzylic compound. Second, these additives are added stoichiometric or in excess to generate the reactive nucleophile prior to coupling with Pd- π -benzyl. While the fate of benzylation rests on the type of Pd, ligand, and the coupling partner to be used in reacting with benzyl-LG, the use of excess additives overrides the catalytic role of the reaction. While it is understood that benzyl-LG will generate Pd- π -benzyl from the catalytic cycle (Scheme 1), it is the nucleophile that will determine what functional group or unit can couple with the Pd complex. If the nucleophile is not reactive to attack the Pd- π -benzyl complex, then benzylation will not occur. As such, it is truly advantageous to look for other alternative methods and reaction conditions in constructing functionalized benzylic compounds that will not require the use of additives or incorporate hazardous reagents, yet will still generate the reactive intermediates that will couple to form the desired products.

1.3 The Decarboxylative Benzylation (DcB) reaction

1.3.1 Fundamentals of DcB

An alternative approach in constructing functionalized benzylic compounds through Pd catalysis is by decarboxylation, or loss of CO₂. In this approach, a benzyl ester, upon reaction with Pd, undergoes oxidative addition to generate Pd- π -benzyl **1** and carboxylate **16** (Scheme 17). Loss of CO₂ from **16** forms an anion **17**. This anion acts as a nucleophile that couples with **1** to generate the functionalized benzylic product. In this catalytic cycle, it is noteworthy that after decarboxylation, both electrophilic **1** and nucleophilic species are generated *in situ*.⁴² Thus, they can react immediately. Finally, since gaseous CO₂ is the only byproduct in the reaction, the generation of large toxic metal wastes is avoided.

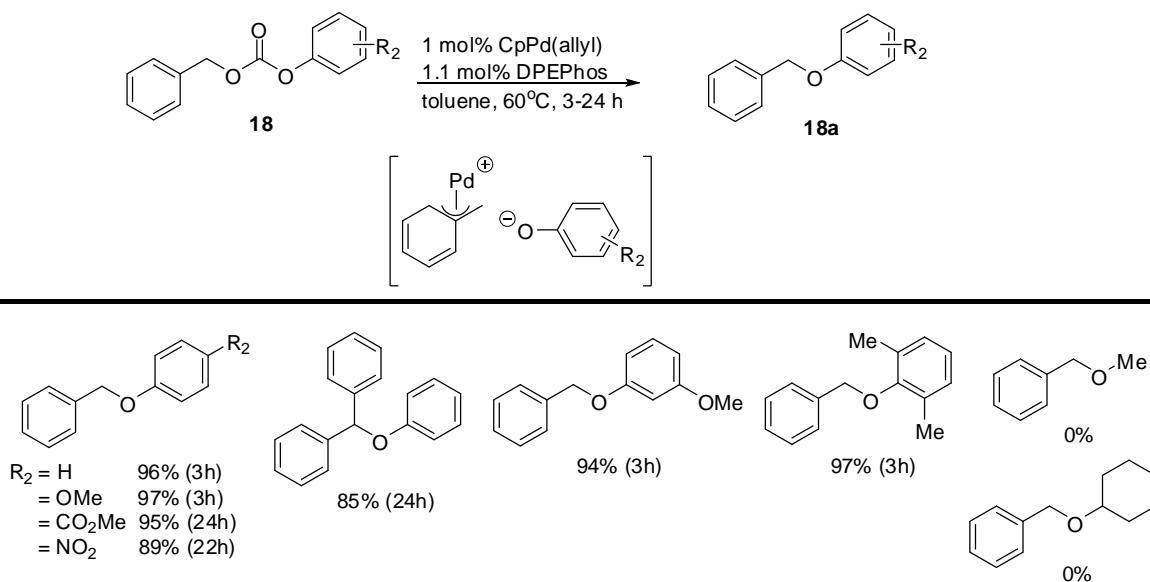
Scheme 17.



1.3.2 Applications of DcB

The earliest application of Pd-catalyzed decarboxylative benzylation (DcB) was reported by Kuwano and Kusano in 2008. They showed that benzyl aryl carbonates **18** undergo DcB in the presence of CpPd(allyl) and DPEPhos ligand to generate benzyl aryl ethers **18a** in high yields (Scheme 18).²⁶ In this reaction, the nucleophilic partner of Pd- π -benzyl complex **1** generated *in situ* was phenoxide anion. The choice of Pd and ligand catalyst was crucial. While **18** underwent DcB, a benzyl alkyl carbonate was unreactive to DcB, presumably due to the hardness or high pK_a of the alkoxide anion. Both EWGs and EDGs on the phenyl ring gave benzylations in high yields. Finally, a diaryl carbonate also underwent DcB to generate diaryl phenyl ether in high yield albeit with longer reaction time.

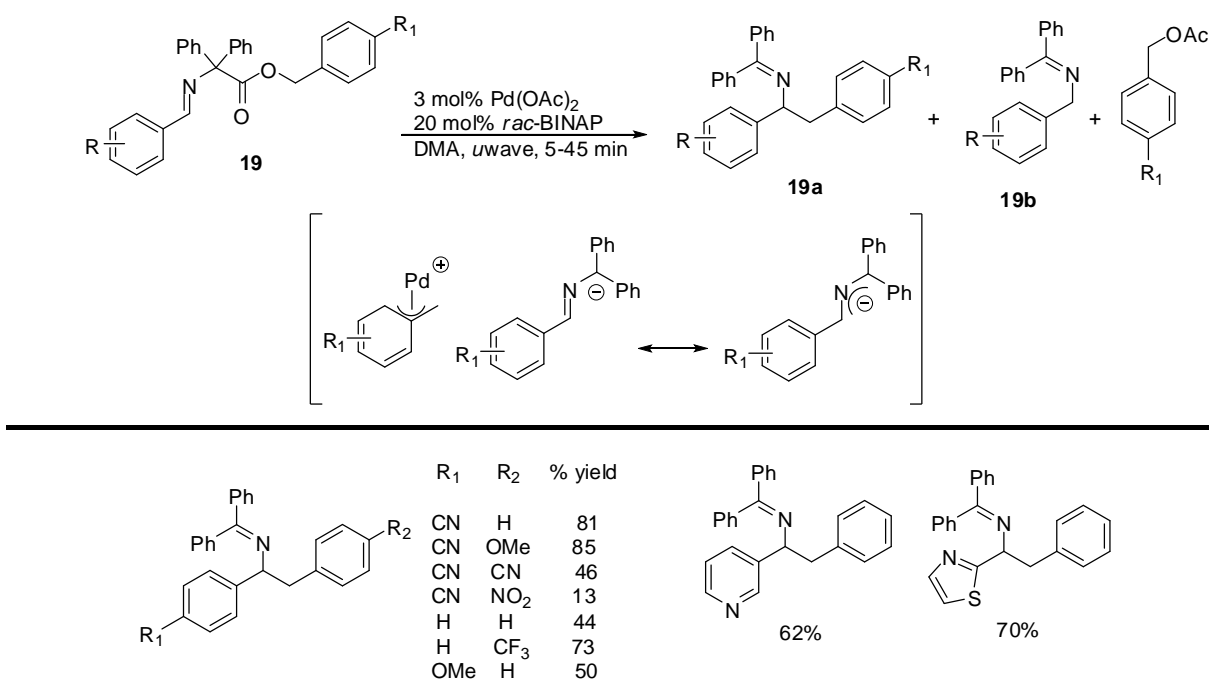
Scheme 18.



Two years after the first Pd-catalyzed DcB publication, DcB was once again highlighted by Chruma and Fields towards the synthesis of diphenylglycinate imines.⁴³ They showed that diphenylglycinate imino esters **19** undergo DcB in the presence of Pd(OAc)₂ and *rac*-BINAP

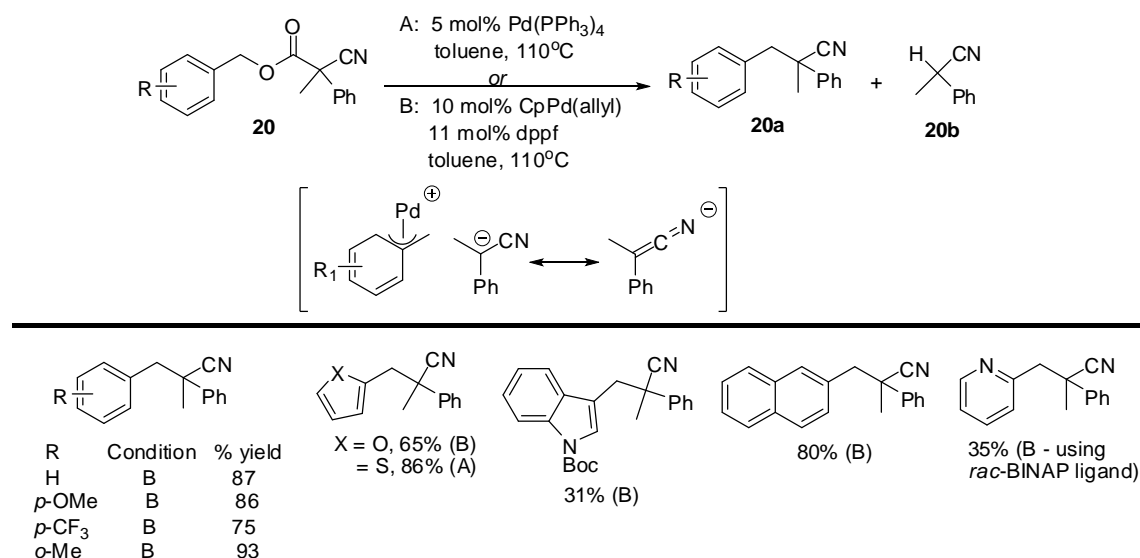
ligand under microwave conditions to generate benzyl diphenyl imines **19a** (Scheme 19). In this reaction, the nucleophile formed *in situ* from glycinate ester was a 2-azaallyl anion. In addition to **19a**, other side-products were obtained such as protonated benzyl imine **19b**.⁴³ The electronic substituents on the ring significantly affected the benzylation. In the benzyl component, incorporation of an EDG gave higher yields of benzylation than an EWG due to the greater stabilization of η^3 -Pd-benzyl complex. In the benzyl imine component, electron withdrawing groups accelerated DcB more than electron donating groups due to their greater stabilization of the azaallyl anion. Based on these results, it appears that benzyl stability depends on the substituents in which EDG stabilizes benzyl carbocation (η^3 -Pd-benzyl) while EWG stabilizes the azaallyl anion.

Scheme 19.



Pd-catalyzed DcB was also applied to the benzylation of α,α -disubstituted cyanoacetates, which was reported by a coworker from our group, Tony Recio III. He showed that benzyl cyanoacetates **20** undergo DcB in the presence of Pd(PPh₃)₄ or CpPd(allyl) and bidentate ligand to generate homobenzyl nitriles **20a** in good to high yields (Scheme 20).⁴⁴ The only side-product that was obtained in these reactions is the protonated nitrile **20b**. In this reaction, the nucleophilic partner was the ketiminate anion. While both EWG and EDG substituents are compatible with DcB, electron-donating substituents gave slightly higher benzylation yields than electron-withdrawing substituents. The reaction also tolerated several benzo-fused aromatics, albeit in low yield when nitrogen-containing heterocycles were used.

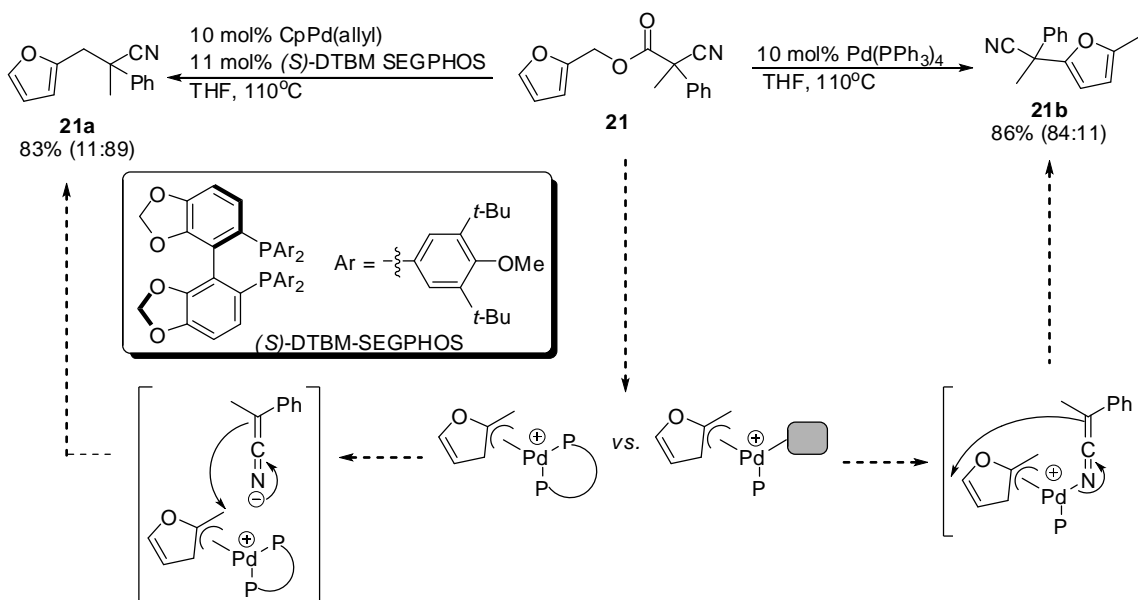
Scheme 20.



The scope of DcB was also demonstrated with heterocycles. While these substrates underwent DcB similar to benzyl nitriles, certain heteroaromatic cyanoacetates undergo DcB to generate unusual products. When furyl cyanoacetate was tried under different Pd conditions, the regioselective benzylation changed from expected C-benzylation to C-arylation depending on the

type of ligand used in conjunction with Pd catalyst (Scheme 21). When 2-furyl cyanoacetate **21** was treated with Pd(PPh₃)₄ bearing a monodentate ligand, methylfuryl nitrile **21b** was predominantly observed. On the other hand, when **21** was treated with Pd and bidentate DTBM-Segphos ligand, benzyl nitrile **21a** was the major product. The difference between the two products based on ligand selectivity was due to the availability of an open coordination site on Pd in the presence of monodentate ligand that allowed an inner-sphere attack of the ketimine, generating **21b** (arylation). In contrast, with bidentate ligand, no open coordination site was available which lead to outer-sphere attack of ketimine to the η³-Pd-furyl generating **21a**.⁴⁴ In this regard, it shows that regioselective benzylation can occur in the DcB process by simply changing the origin of benzyl electrophile and ligand coordination mode.

Scheme 21.



1.4 Conclusion

We have shown the current scope of benzylic functionalization using Pd catalysis. Based on the electrophilic nature of Pd- π -benzyl, nucleophiles such as olefins, alkylidene, arenes, and heteroatoms derived from phenols, amines, sulfinates, and phosphonates can couple with Pd complex to form newly diverse functionalized benzyl compounds. In these reactions, stoichiometric bases and/or preformed organometallics are incorporated to achieve benzylation in high yields. The scope of aromatic substrates used in coupling with these nucleophiles cover simple benzene, benzo-fused aromatics, and heterocycles making the overall Pd-catalyzed benzylation chemistry, an important class of reactions an organic chemist must include in his or her synthetic toolbox. The use of decarboxylation in Pd-catalyzed benzylation reactions avoids the need of additives since the loss of CO₂ forms the reactive intermediates *in situ* directly, which ultimately couple and form the desired benzyl compound, making the overall transformation milder and more robust compared to other benzylation methodologies.

1.5 References

1. (a) Negishi, E-i.; Liao, B. "Coupling of allyl, benzyl, or propargyl with unsaturated groups" In *Handbook of Organopalladium Chemistry for Organic Synthesis*; Negishi, E-i.; de Meijere, A., Eds.; John Wiley & Sons, Inc.; New York, **2002**; pp. 573–579. (b) Hayashi, T. "Palladium-catalyzed asymmetric cross-coupling" In *Handbook of Organopalladium Chemistry for Organic Synthesis*; Negishi, E-i.; de Meijere, A., Eds.; John Wiley & Sons, Inc.; New York, **2002**; pp. 791–806. (c) Liégault, B.; Renaud, J.-L.; Bruneau, C. "Activation and functionalization of benzylic derivatives by palladium catalysts" *Chem. Soc. Rev.* **2008**, *37*, 290–299.
2. Kuwano, R. "Catalytic transformations of benzylic carboxylates and carbonates" *Synthesis* **2009**, *7*, 1049–1061.
3. (a) Narahashi, H.; Shimizu, I.; Yamamoto, A. "Synthesis of benzylpalladium complexes through C-O bond cleavage of benzylic carboxylates: development of a novel palladium-catalyzed benzylation of olefins" *J. Organomet. Chem.* **2008**, *693*, 283–296. (b) Nagayama, K.; Shimizu, I.; Yamamoto, A. "Oxidative addition of aryl and benzyl trifluoroacetates to zerovalent palladium complexes with two modes of C-O bond cleavage processes" *Bull. Chem. Soc. Jpn.* **1999**, *72*, 799–803. (c) Rizzi, G. A.; Morandini, F.; Turco, A.; Bergamin, F. "Synthesis and characterization of $[M(X)(CH_2CH_5)(PR_3)]_2$ complexes (M = Pd, Pt; R = cyclo-C₆H₁₁; X = Cl, Br)" *Gazz. Chim. Ital.* **1993**, *123*, 359–364.
4. (a) Gatti, G.; López, J. A.; Mealli, C.; Musco, A. "Structural and NMR spectroscopic characterization of η^3 -benzyl palladium(II) complexes" *J. Organomet. Chem.* **1994**, *483*, 77–89. (b) Crascall, L. E.; Spencer, J. E. "Preparation and fluxional behavior of η^3 -methylbenzyl platinum and palladium complexes" *J. Chem. Soc. Dalton Trans.* **1992**, 3445–3452. (c) Bergamin, F.; Morandini, F.; Turco, A. "Uncharged η^3 -benzyl complexes of palladium(II)" *Gazz. Chim. Ital.* **1990**, *120*, 57–59. (d) Dewhurst, R. D.; Müller, R.; Kaupp, M.; Radacki, K.; Götz, K. "The η^3 -furfuryl ligand: plausible catalytic intermediates and heterocyclic η^3 -benzyl analogues with superior binding activity" *Organometallics*, **2010**, *29*, 4431–4433. (e) Becker, Y.; Stille, J. K. "The dynamic η^1 - and η^3 -benzylbis(triethylphosphine) palladium(II) cations. Mechanisms of interconversion" *J. Am. Chem. Soc.* **1978**, *100*, 845–850.
5. (a) Johns, A. M.; Tye, J. M.; Hartwig, J. F. "Relative rates for the amination of η^3 -allyl and η^3 -benzyl complexes of palladium" *J. Am. Chem. Soc.* **2006**, *128*, 16010–16011. (b) Johns, A. M.; Utsunomiya, M.; Incarvito, C. D.; Hartwig, J. F. "A highly active palladium catalyst for intermolecular hydroamination. Factors that control reactivity and additions of functionalized anilines to dienes and vinylarenes" *J. Am. Chem. Soc.* **2006**, *128*, 1828–1839. (c) Nettekoven, U.; Hartwig, J. F. "A new pathway for hydroamination mechanism of palladium catalyzed addition of anilines to vinylarenes" *J. Am. Chem. Soc.* **2002**, *124*, 1166–1167. (d) Onitsuka, K.; Yamamoto, M.; Suzuki, S.; Takahashi, S. "Structure and reactivity of (η^3 -indolylmethyl) palladium complexes generated by the reaction of organopalladium complexes with o-alkenylphenyl isocyanide" *Organometallics* **2002**, *21*, 5581–583.

6. (a) Crawforth, C. M.; Burling, S.; Fairlamb, I. J. S.; Kapdi, A. R.; Taylor, R. J. K.; Whitwood, A. C. "Oxidative addition of N-halosuccinimides to palladium(0): the discovery of neutral palladium(II) imidate complexes, which enhance Stille coupling of allylic and benzylic halides" *Tetrahedron* **2005**, *61*, 9736–9751. (b) Bao, M.; Nakamura, H.; Yamamoto, Y. "Facile allylative dearomatization catalyzed by palladium" *J. Am. Chem. Soc.* **2001**, *123*, 759–760.
7. Stille, J. K.; Lau, K. S. Y. "Mechanisms of oxidative addition of organic halides to group 8 transition-metal complexes" *Acc. Chem. Res.* **1977**, *10*, 434–442.
8. Zhu, Y.; Rawal, V. H. "Palladium-catalyzed C3 benzylation of indoles" *J. Am. Chem. Soc.* **2012**, *134*, 111–114.
9. Paquette, L. A.; Astles, P. C. "Total synthesis of furanocembranolides. 3. A concise convergent route to acerosolide" *J. Org. Chem.* **1993**, *58*, 165–169.
10. Chan, W. R.; Tinto, W. F.; Laydoo, R. S.; Manchand, P. S.; Reynolds, W. F.; McLean, S. "Cembrane and pseudopterane diterpenoids of the octocoral *Pseudopterogorgia acerosa*" *J. Org. Chem.* **1991**, *56*, 1773–1776.
11. Schinzer, D.; Bourguet, E.; Ducki, S. "Synthesis of furano-epothilone D" *Chem. Eur. J.* **2004**, *10*, 3217–3224.
12. Chao, T.-C.; Zhang, X.-G.; Balog, A.; Su, D.-S.; Meng, D.; Savin, K.; Bertino, J. R.; Danishefsky, S. J. "Desoxyepothilone B: an efficacious microtubule-targeted antitumor agent with a promising *in vivo* profile relative to epothilone B" *Proc. Natl. Acad. Sci. USA* **1998**, *95*, 9642–9647.
13. Heck, R. F.; Nolley, J. P., Jr. "Palladium-catalyzed vinylic hydrogen substitution reactions with aryl, benzyl, and styryl halides" *J. Org. Chem.* **1972**, *37*, 2320–2322.
14. Narahashi, H.; Yamamoto, A.; Shimizu, I. "Heck-type benzylation of olefins with benzyl trifluoroacetate" *Chem. Lett.* **2004**, *33*, 348–349.
15. Wu, G. Z.; Lamaty, F.; Negishi, E.-i. "Metal promoted cyclization. 26. Palladium-catalyzed cyclization of benzyl halides and related electrophiles containing alkenes and alkynes as a novel route to carbocycles" *J. Org. Chem.* **1989**, *54*, 2507–2508.
16. Grigg, R.; Sukirthalingam, S.; Sridharan, V. "Palladium-catalyzed tandem cyclization-anion capture processes initiated by alkyl- and π -allyl-palladium species" *Tetrahedron Lett.* **1991**, *32*, 2545–2548.
17. Hu, Y.; Zhou, J.; Lian, H.; Zhu, C.; Pan, Y. "Palladium-catalyzed cascade cyclization of benzyl halides with diethyl-diallylmalonate" *Synthesis* **2003**, *8*, 1177–1180.

18. Miura, T.; Toyoshima, T.; Takahashi, Y.; Murakami, M. "Stereoselective oxindole synthesis by palladium-catalyzed cyclization reaction of 2-(alkynyl)aryl isocyanates with amides" *Org. Lett.* **2009**, *11*, 2141–2143.
19. Messaoudi, S.; Brion, J.-D.; Alami, M. "Transition metal-catalyzed direct C-H alkenylation, alkynylation, benzylation, and alkylation of (hetero)arenes" *Eur. J. Org. Chem.* **2010**, *34*, 6495–6516.
20. Fan, S.; He, C.-Y.; Zhang, X. "Direct Pd-catalyzed benzylation of highly electron-deficient perfluoroarenes" *Chem. Commun.* **2010**, *46*, 4926–4928.
21. Verrier, C.; Hoarau, C.; Marsais, C. "Direct palladium-catalyzed alkenylation, benzylation, and alkylation of ethyl-oxazole-4-carboxylate with alkenyl-, benzyl-, and alkyl halides" *Org. Biomol. Chem.* **2009**, *7*, 647–650.
22. Lapointe, D.; Fagnou, K. "Palladium-catalyzed benzylation of heterocyclic aromatic compounds" *Org. Lett.* **2009**, *11*, 4160–4163.
23. Trost, B. M.; Czabaniuk, L. C. "Palladium-catalyzed asymmetric benzylation of 3-aryl oxindoles" *J. Am. Chem. Soc.* **2010**, *132*, 15534–15536.
24. Ackermann, L.; Barfüser, S.; Pospech, J. "Palladium-catalyzed direct arylations, alkenylations, and benzylations through C-H bond cleavages with sulfamates or phosphanates as electrophiles" *Org. Lett.* **2010**, *12*, 724–726.
25. Mukai, T.; Hirano, K.; Satoh, T.; Miura, M. "Palladium-catalyzed direct benzylation of azoles with benzyl carbonates" *Org. Lett.* **2010**, *12*, 1360–1363.
26. Kuwano, R.; Kusano, H. "Benzyl protection of phenols under neutral conditions: palladium-catalyzed benzylations of phenols" *Org. Lett.* **2008**, *10*, 1979–1982.
27. (a) Tsuji, J.; Takahashi, H.; Morikawa, M. "Organic synthesis by means of noble metal compounds. XVII. Reaction of π -allylpalladium chloride with nucleophiles" *Tetrahedron Lett.* **1965**, *6*, 4387–4388. (b) Atkins, K. E.; Walker, W. E.; Manyik, R. M. "Palladium catalyzed transfer of allylic groups" *Tetrahedron Lett.* **1970**, 3821–3824. (c) Takahashi, K.; Miyake, A.; Hata, G. "Palladium-catalyzed exchange of allylic groups of ethers and esters with active hydrogen compounds. II" *Bull. Chem. Soc. Jpn.* **1972**, *45*, 230–236. (d) Onoue, H.; Moritani, I.; Murahashi, S.-I. "Reaction of cycloalkanone enamines with allylic compounds in the presence of palladium complexes" *Tetrahedron Lett.* **1973**, 121–124. (e) Tsuji, J.; Shimizu, I.; Minami, I.; Ohashi, Y.; Sugiura, T.; Takahashi, K. "Allylic carbonates. Efficient allylating agents of carbonucleophiles in palladium-catalyzed reactions under neutral conditions" *J. Org. Chem.* **1985**, *50*, 1523–1529.
28. Kuwano, R.; Kondo, Y.; Matsuyama, Y. "Palladium-catalyzed nucleophilic benzylic substitutions of benzylic esters" *J. Am. Chem. Soc.* **2003**, *125*, 12104–12105.

29. Kuwano, R.; Kondo, Y.; Shirahama, T. "Transformation of carbonates into sulfones at the benzylic position via palladium-catalyzed benzylic substitution" *Org. Lett.* **2005**, *7*, 2973–2975.
30. Bravo-Altamirano, K.; Huang, Z.; Montchamp, J.-L. "Palladium-catalyzed phosphorus-carbon bond formation: cross-coupling reactions of alkyl phosphinates with aryl, heteroaryl, alkenyl, benzylic, and allylic halides and triflates" *Tetrahedron* **2005**, *61*, 6315–6329.
31. Lavèn, G.; Stawinski, J. "Palladium(0)-catalyzed benzylation of H-phosphonate diesters: an efficient entry to benzylic phosphonates" *Synlett* **2009**, *2*, 225–228.
32. Pèrez, I.; Sestelo, J. P.; Sarandeses, L. A. "Atom-efficient metal-catalyzed cross-coupling reaction of indium organometallics with organic electrophiles" *J. Am. Chem. Soc.* **2001**, *123*, 4155–4160.
33. Peña-Lopez, M.; Ayán-Varela, M.; Sarandeses, L. A.; Sestelo, J. P. "Palladium-catalyzed cross-coupling reactions of organogold(I) reagents with organic electrophiles" *Chem. Eur. J.* **2010**, *16*, 9905–9909.
34. Campbell, J. A.; Bordunov, V.; Broka, C. A.; Dankwardt, J.; Hendricks, R. T.; Kress, J. M.; Walker, K. A. M.; Wang, J.-H. "Preparation of 3-arylmethylindoles as selective COX-2 inhibitors" *Tetrahedron Lett.* **2004**, *45*, 3793–3796.
35. (a) Broka, C. A.; Campbell, J. A. "Indole derivatives as COX II inhibitors" PCT Int. Appl. CODEN: PIXXD2 WO-0329212 AI 20030410, **2003**, 46 pp. (b) Smith, W. L.; Garavito, R. M.; DeWitt, D. L. "Prostaglandin endoperoxide H synthases (cyclooxygenases) -1 and -2" *J. Biol. Chem.* **1996**, *271*, 33157–33160.
36. Lòpez-Pèrez, A.; Adrio, J.; Carretero, J. C. "Palladium-catalyzed cross-coupling reaction of secondary benzylic bromides with Grignard reagents" *Org. Lett.* **2009**, *11*, 5514–5517.
37. Nakao, Y.; Ebata, S.; Chen, J.; Imanaka, H.; Hiyama, T. "Cross-coupling reaction of allylic and benzylic carbonates with organo [2-(hydroxymethyl)phenyl]dimethylsilanes" *Chem. Lett.* **2007**, *36*, 606–607.
38. Milstein, D.; Stille, J. K. "Palladium-catalyzed coupling of tetraorganotin compounds with aryl and benzyl halides. Synthetic utility and mechanism" *J. Am. Chem. Soc.* **1979**, *101*, 4992–4998.
39. Lindsey, C. C.; O'Boyle, B. M.; Mercede, S. J.; Pettus, T. R. R. "Construction of previously inaccessible 2-amino-4-benzyl substituted oxazoles" *Tetrahedron Lett.* **2004**, *45*, 867–868.
40. Ohsumi, M.; Kuwano, R. "Palladium-catalyzed cross-coupling of benzylic carbonates with organostannanes" *Chem. Lett.* **2008**, *37*, 796–797.

41. (a) Kuwano, R.; Yokogi, M. "Suzuki-Miyaura cross-coupling of benzylic carbonates with arylboronic acids" *Org. Lett.* **2005**, *7*, 945–947. (b) Kuwano, R.; Yokogi, M. "Cross-coupling of benzylic acetates with arylboronic acids: one pot transformation of benzylic alcohols to diarylmethanes" *Chem. Commun.* **2005**, 5899–5901.
42. Weaver, J. D.; Recio, A., III; Grenning, A. J.; Tunge, J. A. "Transition metal-catalyzed decarboxylative allylation and benzylation reactions" *Chem. Rev.* **2011**, *111*, 1846–1913.
43. Fields, W. H.; Chruma, J. J. "Palladium-catalyzed decarboxylative benzylation of diphenylglycinate imines" *Org. Lett.* **2010**, *10*, 1979–1982.
44. Recio, A., III; Heinzman, J. D.; Tunge, J. A. "Decarboxylative benzylation and arylation of nitriles" *Chem. Commun.* **2012**, *48*, 142–144.

Chapter 2

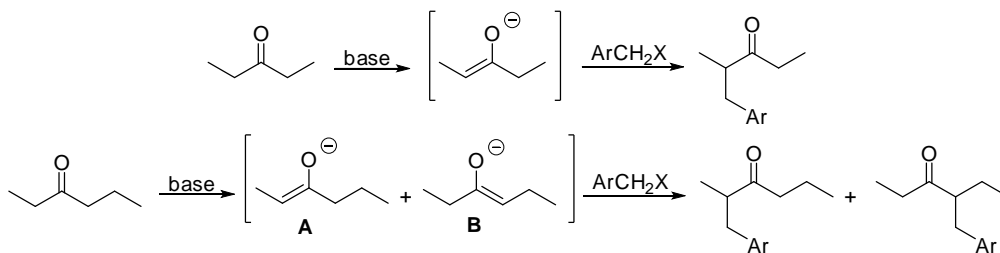
Palladium-Catalyzed Decarboxylative Benzylation of Ketones

2.1 Introduction

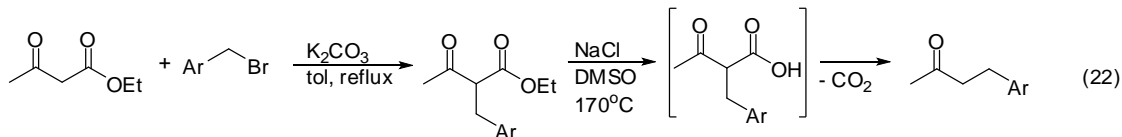
Classical strategies in α -benzyl ketone synthesis

The construction of α -benzyl ketones through alkylation of enolates with benzyl halide is a well-known synthetic method in organic chemistry.¹ Though well-known it also has limitations. First, this approach requires stoichiometric amounts of benzyl halides such as benzyl bromide and benzyl chloride. They are inexpensive and commercially available, but toxic and known to be potent lachrymators. Second, both the amount and type of base needed to deprotonate ketones to generate enolates are important. Monobenzylations require an equivalent of base and an equivalent of benzyl halide. However, typical benzylic alkylation experiments do not always yield monobenzylated ketones but rather a mixture of mono- and dibenzyl ketones. While enolate generation from symmetrical ketones is not challenging, the use of unsymmetrical ketones is also problematic (Scheme 22). Depending on the type of base used to generate enolates from such ketones, a mixture of isomeric benzyl ketones is usually obtained. The site-specific generation of enolates becomes difficult for these substrates because their α -acidic hydrogens have very close pK_a 's and the thermodynamics of enolates (A vs. B, Scheme 22) can have significant impact upon benzylation. As a result, a judicious choice of base is required to selectively generate the specific enolate needed to alkylate the benzyl halide. Other reaction conditions such as solvent and temperature are also taken into account.

Scheme 22.



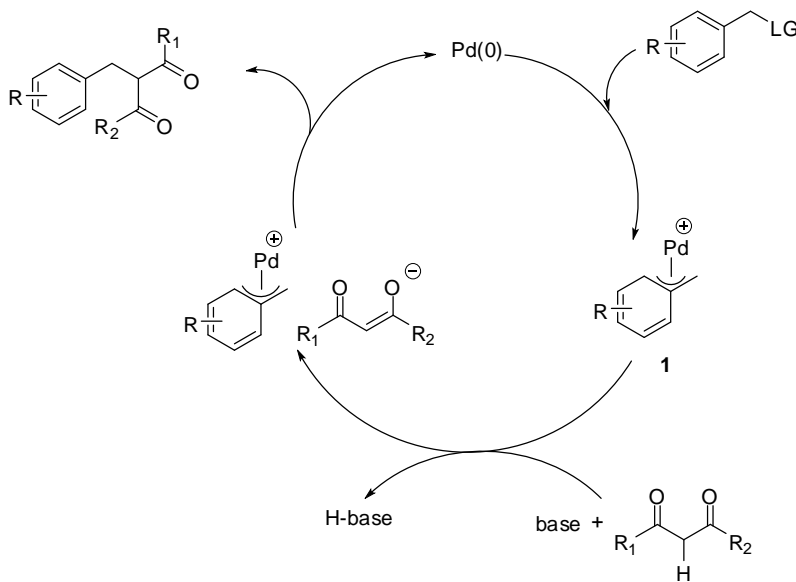
One way to address the regioselective deprotonation issue, as shown in Scheme 22, is to perform benzylation through acetoacetic ester synthesis. In this reaction, the base exclusively deprotonates at the α -carbon of the β -ketoester followed by $\text{S}_{\text{N}}2$ attack to benzyl-X, resulting in direct benzylic alkylation. Under appropriate conditions, the benzyl β -ketoester undergoes hydrolysis generating benzyl β -ketoacid, which then undergoes decarboxylation to generate the desired α -benzyl ketone (eq. 22). While site-specific enolate generation is achieved in this methodology, the formation of mono and dibenzyl ketones as a result from benzylation with β -ketoester could still occur. Walker and co-workers reported the synthesis of benzyl ketones through acetoacetate ester synthesis to generate benzyl ketones.² Unfortunately, the reaction required very high temperature to obtain the desired benzyl ketone during the decarboxylation event of the *in situ* generated benzyl β -ketoacid. Clearly, there is a need to develop new benzylation methodologies that will couple electrophilic benzylics with enolates under mild conditions while preventing the formation of isomeric benzyl ketone mixtures.



Benzyl ketone synthesis via Pd catalysis: Tsuji-Trost approach

The issues stemming from classical benzylation were significantly resolved through Pd-catalyzed reactions. Further, enolates can be coupled with benzyl electrophiles in the presence of catalytic Pd. In Pd-catalyzed benzylation of ketones, the generation of η^3 -benzyl-Pd **1** from oxidative addition of Pd with benzyl-LG is coupled to an enolate *via* nucleophilic substitution (Scheme 23). While these two benzylation reactions are similar in obtaining α -benzyl ketones (enolate generation, benzyl halide, and base), the advantage of Pd catalysis is that other benzyl-LG substrates such as benzyl acetates, carbonates, and phosphonates derived from benzyl alcohols can be used in lieu of benzyl halides.

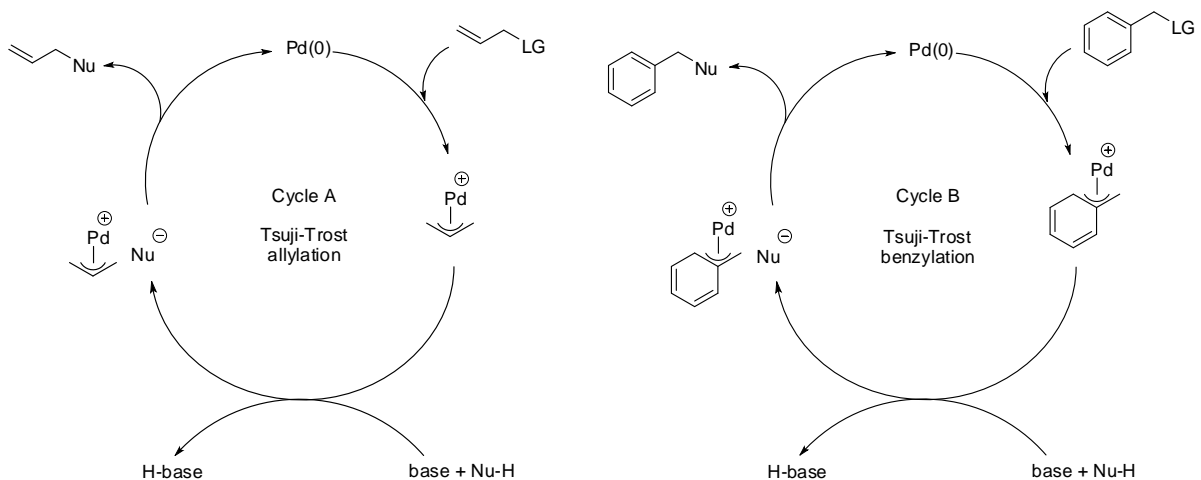
Scheme 23.



The catalytic cycle shown in Scheme 23 is reminiscent of the Tsuji-Trost reaction. The Tsuji-Trost reaction began to appear in literature as early as 1965, when the Pd-catalyzed allylic alkylation of nucleophiles with nucleophiles derived from active methylenes, amines, phenols, and other compounds with low pK_a 's (18-20), with allylic halides, acetates and carbonates in the

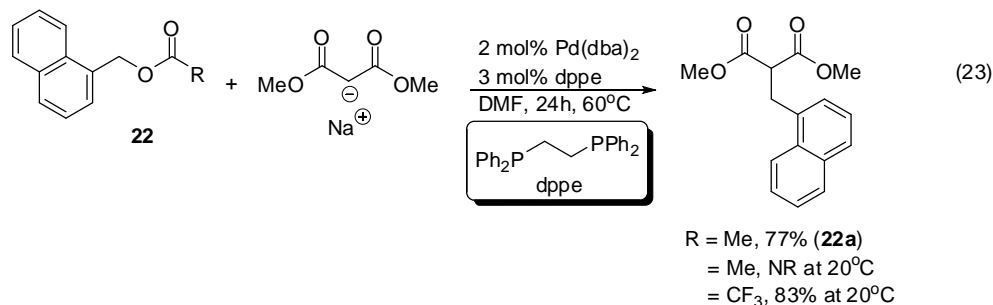
presence of base was described.² The reaction begins by coordination of Pd to an allyl substrate (Cycle A, Scheme 24). This is followed by nucleophilic displacement of the leaving group to generate electrophilic η^3 -allyl-Pd, which is subsequently attacked by a nucleophile that was deprotonated by a base to form the newly substituted allyl product. Ultimately, Pd is regenerated back into the catalytic cycle. Considering that there is similarity between η^3 -benzyl-Pd and η^3 -allyl-Pd electrophiles (Chapter 1), the scope of Tsuji-Trost reaction in allylations can be applied to benzylations (Cycle B, Scheme 24).

Scheme 24.

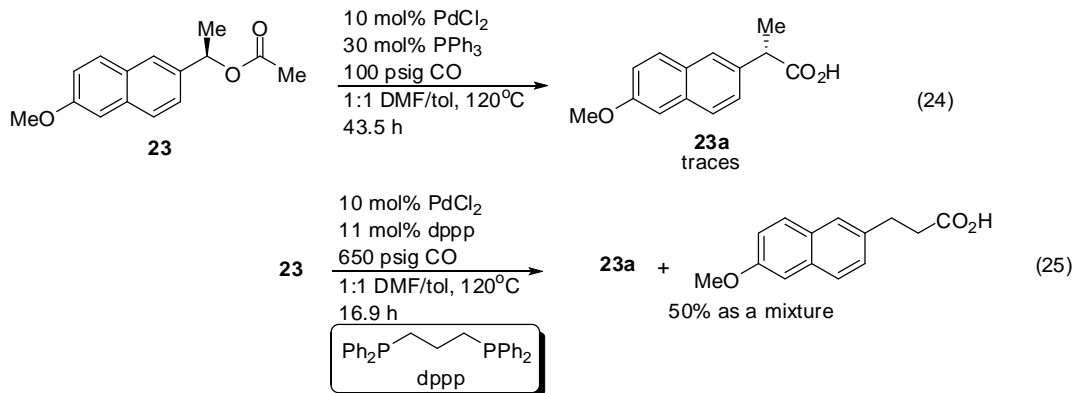


The earliest report of Tsuji-Trost benzylations utilized the cross-coupling of benzyl acetate with stabilized enolates.^{4,10} In 1992, Legros and Fiaud reported the benzylation of 1-naphthylmethyl acetate **22** with sodium dimethylmalonate in the presence of Pd(0) and bidentate dppe ligand in DMF at 60°C for 24h to generate α -1-naphthylmethyl dimethylmalonate **22a** (eq. 23).⁴ While **22** did not undergo substitution at room temperature, replacing the acetate LG with trifluoroacetate allowed benzylation to occur. This implies that the nature of the LG of benzyl moiety is important. As shown in Chapter 1, certain LG's on the benzyl moiety are reactive with

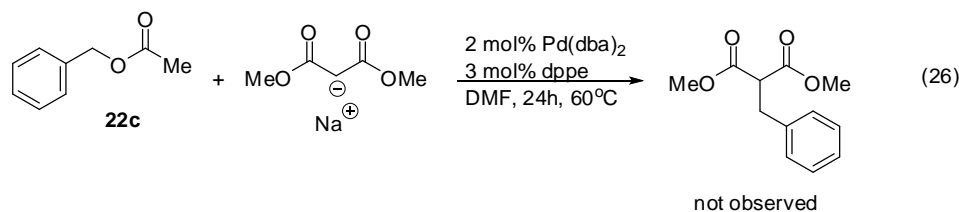
Pd. Under these conditions, benzyl trifluoroacetate is a better substrate than benzyl acetate because the former has a better LG that contains highly electronegative fluorine which presumably assists in ionization of the benzylic C-O bond of the ester, leading to generation of η^3 -benzyl-Pd complex.



The difficulty in working with benzyl acetate was also realized in Pd-catalyzed hydroxycarbonylation of 6-methoxy-2-naphthyl acetate **23** (eq. 24). As reported by Lee and coworkers in 1991, only traces of the desired 6-methoxy-2-naphthyl propanoic acid **23a** were obtained after the carbonylation reaction of **23** was run at 120°C in 43.5 hours.⁵ By switching to a bidentate ligand and increasing the CO pressure, carbonylation occurred generating the desired 2-naphthylethylpropanoic acid, yet in low yield as an inseparable mixture with demethylated propanoic acid (eq. 25). Lastly, the unreactivity of **23** to undergo substitution at room temperature suggests that benzylation reactions would require high temperatures to achieve the desired chemical transformation possibly in generating Pd- π -benzyl complex prior to nucleophilic attack of the enolate.



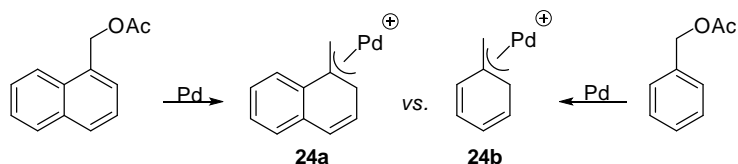
While **22** underwent substitution in high yields, the substitution of simple benzyl acetate **22c** failed to provide the desired benzyl product at room and high temperatures even though it possessed a ring similar to **22** which should also generate Pd- π -benzyl complex (eq. 26). The only difference between the two benzyl substrates, however, was the presence of an extra ring in **22** compared to **22c**. In the succeeding chapters, the word “simple” will be used throughout which will denote a substrate that does not contain extended aromatic conjugation.



The inability of **22c** to undergo substitution can be rationalized in terms of its high resonance stability. A comparison of η^3 -Pd-benzyl complexes **24a** and **24b** derived from the oxidative addition of **22** and **22c** with Pd, respectively, clearly shows that when both Pd-benzyl complexes undergo dearomatization, **24a** maintains significant aromaticity in contrast with **24b** which loses significant aromaticity (Scheme 25). Based on the calculated resonance energies of aromatic rings, it has been shown that benzo-fused rings have lower resonance energies than a simple benzene.^{6,7} These results suggest that benzo-fused substrates such as naphthalene are

highly suitable substrates in Pd-catalyzed benzylation reactions, which can be easily functionalized by any nucleophile at the benzylic position.

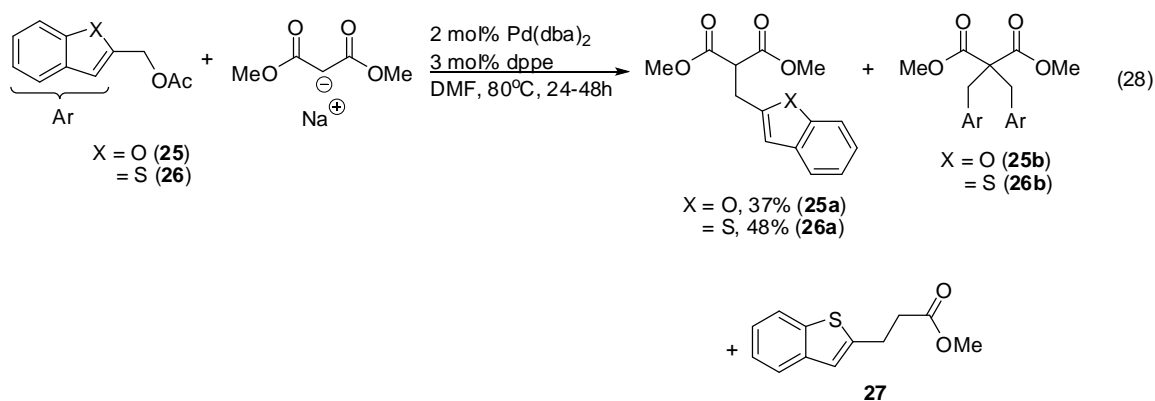
Scheme 25.



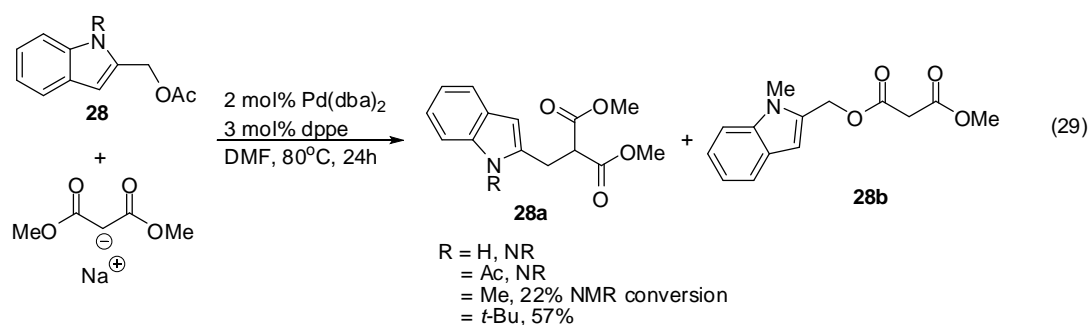
The importance of resonance energy in identifying suitable benzylic substrates towards nucleophilic substitution with malonates is the criterion in expanding the scope of benzylation towards stabilized enolates. After the seminal benzylation publication, Legros and coworkers reported the substitution of heteroaromatic benzo-fused methyl acetates such as quinoline, benzofuran, benzothiophene, and indole with metal malonates under identical conditions.⁸ In the benzylation of potassium dimethylmalonate with quinolinylmethyl acetate, the position of the benzylic moiety in quinolinylmethyl acetate significantly affected the benzylation (eq. 27). When 2-quinolinylmethyl acetate was tried, benzylation did not occur. This may be due to the generation of η^3 -Pd-quinolinyl(methyl) complex which was unstable because of interaction between the Pd- π -benzyl complex near the heteroatom. It was possible that Pd preferably coordinates with the heteroatom rather than oxidatively adding to the benzylic C-O bond. The pre-coordination of Pd to nitrogen prior to benzylation could also make the molecule unreactive towards nucleophilic enolate attack. When the location of benzylic acetate was placed farther from nitrogen, benzylation occurred producing quinolinyl acetate and protonated by-product, methylquinoline.⁸ While the formation of methylquinoline came from a formal reduction process, the authors were not able to identify the origin of the proton source.



When benzofuryl acetate **25** was treated under identical conditions to that of the naphthyl acetate shown in eq. 23, benzofuryl malonate **25a** was isolated in low yield along with dibenzofuryl malonate **25b** (eq. 28). The formation of dibenzyl ester was presumed to involve an acid-base exchange between monobenzyl ester **25a** and sodium dimethylmalonate such that a second benzylation was allowed to occur.⁹ The results in eq. 28 are interesting because the formation of dibenzyl ester was never observed with naphthyl and quinoliny acetates. In the case of benzothiophenyl acetate **26**, benzylation occurred generating a mixture of monobenzyl **26a** and dibenzyl ester **26b**, in which the yield of **26a** was higher than **25a**, the only difference between the two heterofused-benzyl acetates was the type of heteroatom. Also, benzofuryl ester **27** was isolated in this reaction. Legros and coworkers speculated that the formation of **27** came from deacylation of **26a** during the benzylation process, which somehow contributed to the low isolated yield of **26a**.

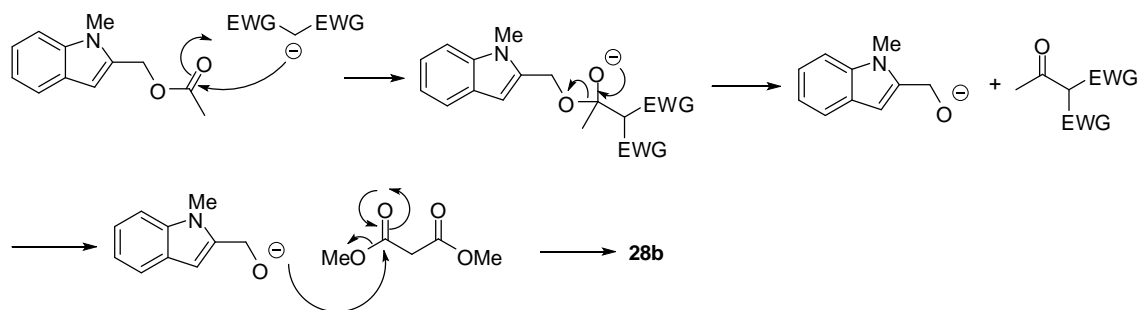


When indolymethyl acetate **28** was treated with sodium dimethylmalonate under the identical conditions as that of other heterobenzo-fused acetates, formation of the desired indole malonate ester **28a** was only achieved when nitrogen was protected with a bulky protecting group (eq. 29). No benzylation occurred when unprotected indole was used. When Ac was used as N-protecting group, benzylation did not occur but rather unprotected indole acetate was isolated which was thought to have to come from deacylation of N-acetyl indole through a hydrolytic workup.⁹ When Me was used as the N-protecting group, benzylation was observed in low conversion along with formation of N-methyl indole ester **28b**.

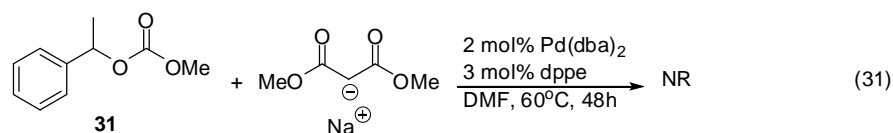
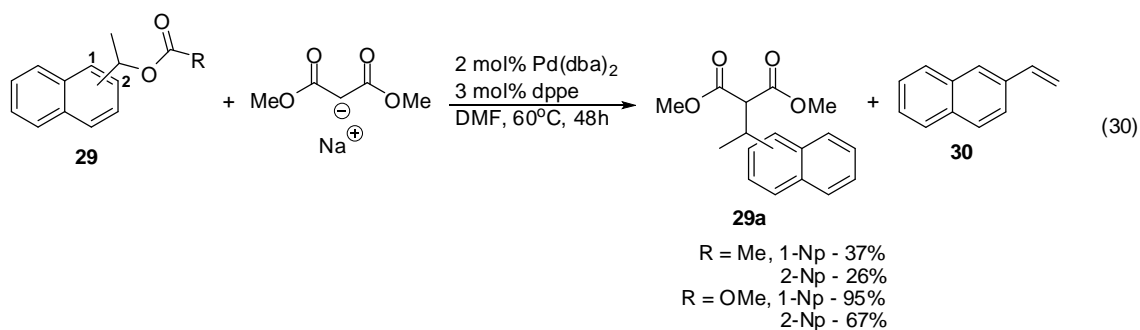


The formation of **28b** stemmed from transesterification between an indole alkoxide and a second molecule of dimethylmalonate (Scheme 26). The indole alkoxide was generated from the deacylation of malonate ketone after nucleophilic attack of the malonate ester to the carbonyl of indole ester. When a bulky *t*-Bu group was used as the N-protecting group, the formation of **28a** significantly improved and none of **28b** was observed. Based on these results, the judicious choice of protecting group is important in developing benzylation reactions with indoles. It becomes clear that an unprotected indole is not a suitable substrate because it tends to shut down the reaction via reactivity of the N-H bond with Pd, malonate anion, or other component in the reaction medium. The failed and/or poor reactivity of most heterobenzo-fused acetates under these conditions could also be due to the location of the benzyl carbon near the heteroatom.

Scheme 26.

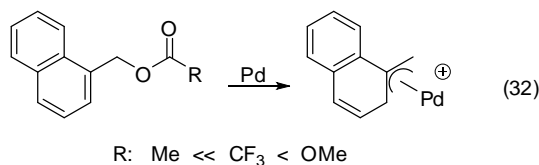


In another benzylation experiment, when 1 and 2-naphthyl carbonates **29** were allowed to react with sodium dimethylmalonate under identical conditions as shown in eq. 23, the formation of the α -substituted 1- and 2-naphthylmethyl esters **29** occurred, and more importantly, gave higher yields than the reactions performed using 1- and 2-naphthyl acetates (eq. 30).¹⁰ The difference between the two sets of benzyl substrates was the nature of the LG. Despite the difference in LG, simple benzyl carbonate **31** still failed to generate the desired benzylation product (eq. 31).



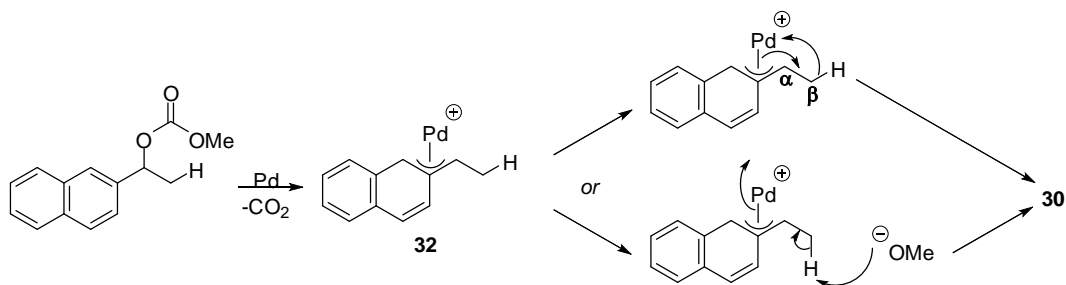
Based on these outcomes, it appears that carbonates are better leaving groups than acetates in benzylation reactions, resulting in facile generation of Pd- π -benzyl complexes. The

improved reactivity of benzyl carbonates over benzyl acetates has been demonstrated in some benzylation reactions as shown in Chapter 1 (Chapter 1.2). Previously, it has been shown that benzyl trifluoroacetate underwent benzylation faster than benzyl acetate (eq. 23). Based on these results, it is possible that a trend could be established between the three LGs used in benzylation with enolates. The trend in LG compatibility among benzyl substrates towards generation of Pd- π -benzyl complex follows the order Me \ll CF₃ < OMe (eq. 32).



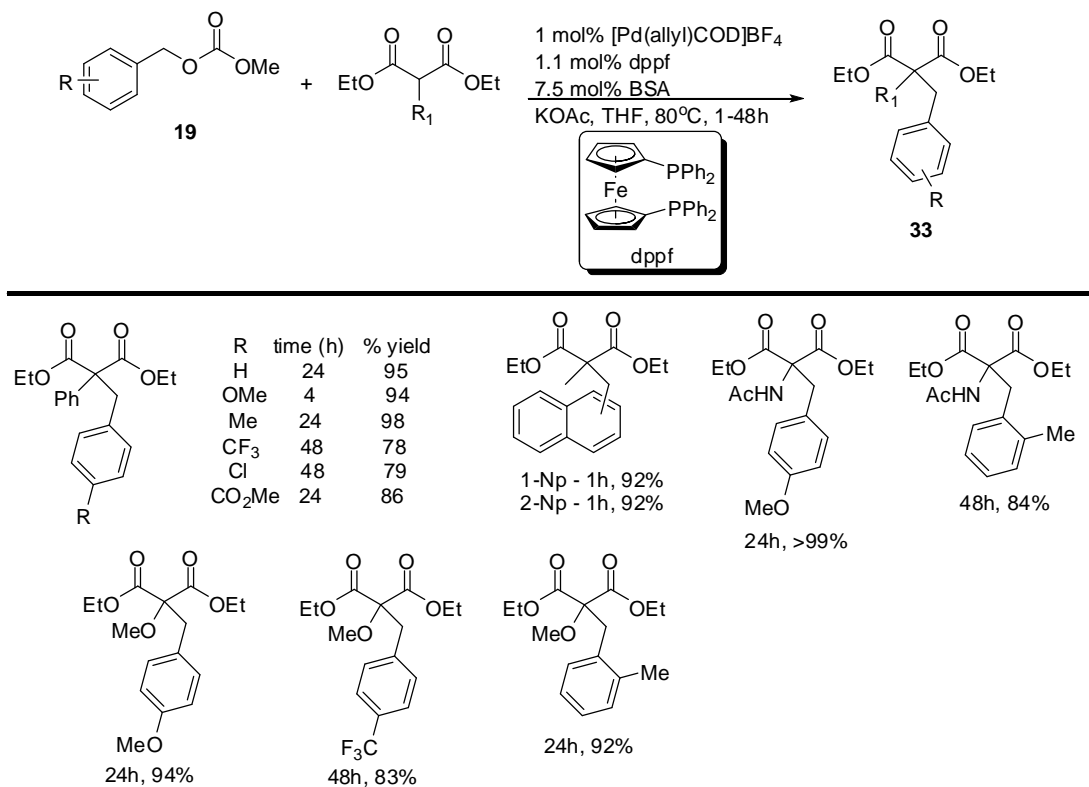
The higher benzylation yield of 1-naphthylmethyl carbonate compared to 2-naphthylmethyl carbonate could be rationalized in terms of the greater stability of the η^3 -Pd-benzyl complex at the 1-position of the naphthyl ring compared to the 2-position. Along with this result, it was interesting that the formation of vinylnaphthalene **30** was isolated from the reaction of 2-naphthylmethyl carbonate whereas none was observed from 1-naphthylmethyl carbonate, though both naphthyl carbonates have *cis* β -hydrogens near the Pd complex. The formation of **30** resulted from either direct BHE of Pd complex **32** or from displacement of Pd resulting from deprotonation of benzylic proton by an alkoxide generated from the decarboxylation of 2-naphthylcarbonate (Scheme 27).¹⁰ Overall, the position of the benzylic carbon on the aromatic ring is very important since this could potentially dictate the overall benzylation reactivity of benzyl esters towards cross-coupling with other nucleophiles while avoiding the formation of side products.

Scheme 27.



The failed reactivity of simple benzyl carbonate with sodium dimethylmalonate, as shown by Legros and coworkers, prompted other researchers to identify newer conditions that will effectively allow benzylation with this type of substrate. In 2003, Kuwano and coworkers reported that the combination of cationic $[\text{Pd}(\text{allyl})\text{COD}]\text{BF}_4$ and dppf, a more electron-rich bidentate ligand, allowed benzylation of substituted diethylmalonate with simple benzyl carbonates in the presence of BSA and base to generate α -substituted benzyl malonate **33**.¹¹ Without base, reaction did not occur. Various substituted benzyl carbonates were coupled with substituted malonates to generate a variety of benzyl malonates in good to high yields (Scheme 28).

Scheme 28.



The electronic substituents on the aromatic ring have a profound effect on benzylation. Certain benzylation reactions illustrated in Chapter 1 (Chapter 1.2) have shown that benzyl substrates which contain electron-donating substituents give higher benzylation yields than benzyl substrates containing electron-withdrawing substituents because of the greater stabilization of the cationic η^3 -Pd-benzyl complex. As shown in Scheme 28, while both *p*-methoxybenzyl carbonate and *p*-trifluoromethylbenzyl carbonate underwent nucleophilic substitution with the malonate in high yields, the former took four hours to achieve reaction completion compared to the latter which took two days. Both 1- and 2-naphthylmethyl carbonates underwent benzylation in identical yields to simple benzyl carbonates. *Ortho*-substituted benzyl carbonates gave slightly lower yields than *para*-substituted benzyl carbonates presumably due to sterics between the Pd and the substituent. It is interesting that *p*-methylester

benzyl carbonate gave higher benzylation yield than *p*-chlorobenzyl carbonate since the former is more electron-withdrawing than the latter. On the other hand, the ability of *p*-chlorobenzyl carbonate to undergo substitution with malonate suggests that inductive effects may also be important.¹¹ Ultimately, the strength and stability of η^3 -Pd-benzyl complex in cross-coupling reactions with enolates depends on the nature of substituents on the aromatic ring and their resonance, inductive, and steric effects.

Another important result was the judicious choice of ligand which had significant impact towards benzylation. As shown in eq. 23, scheme 28, and in Chapter 1.2, the use of bidentate ligands gave the desired benzylation more favorably than monodentate ligands, presumably due to chelation of two phosphorus atoms in a single backbone compared to two individual phosphine entities. While PPh_3 failed to generate the desired benzyl product, a small-sized bidentate ligand such as dppe allowed benzylation albeit with poor conversion.¹¹ Increasing the bite angle of the bidentate ligand enhanced the benzylation reactivity (Table 1).

Table 1.

entry	ligand	bite angle (deg)	% GC yield
1	2 PPh_3	-	0
2	dppe	86	2
3	dppp	91	10
4	dppb	95	41
5	dppf	99	74
6	DPEPhos	102	62
7	Xantphos	112	62

dppb

Xantphos

DPEPhos

Bite angle is defined as the preferred chelation angle determined by the phosphine ligand backbone.¹² A wider bite angle in a metal complex can exert two effects: increase in steric bulk of the whole ligand, and electronically favor or disfavor a geometry at the metal complex. In the case of the ligand screening shown in Table 1, bulky and larger bite angles containing electron-rich phosphine ligands in combination with Pd catalyst allowed oxidative addition of simple benzyl to generate Pd- π -benzyl even though it has lower resonance energy compared to benzo-fused systems. While bulky ligands with larger bite angles improved benzylation, the decent bulk and bite angle of dppf somehow fits perfectly with the formation of Pd complex and coupling with enolates compared to other bidentate ligands with comparable steric bulk and bite angles such as DPEPhos.

The benzylation mechanism was similar to the Tsuji-Trost allylation (Scheme 29). It began from the DPPF-ligated Pd complex which became a reactive Pd(0)-DPPF species, which then reacted with benzyl carbonate *via* oxidative addition to generate η^3 -benzyl-Pd(DPPF) complex **34**. At the same time decarboxylation occurred releasing the methoxide anion. The malonate anion, generated from base deprotonation of the malonate, attacked **34** to form the α -substituted benzyl product and the active Pd catalyst was regenerated.

unfavorable aggregation of the Pd(0)-DPPF complex that resulted due to formation of Pd black.^{13,14} In order to suppress the formation of undesired and inactive Pd black, an external labile ligand was thought to be necessary to be added in the reaction. A variety of ligands were, therefore, screened to evaluate their ability to suppress Pd aggregation which was a deterrent to the substitution of *p*-methoxybenzyl methyl carbonate with phenyl-dimethylmalonate (Table 2). Based on these results, DBA and TPO inhibited benzylation. While 1-octene gave slight improvement, the use of 1,5-COD showed a remarkable increase in the formation of the desired benzyl product. To this end, a variety of simple benzyl carbonates underwent substitution with different active methine compounds to generate functionalized benzyl compounds in good to high yields without the need of an external base (Scheme 31). Both EDG and EWG-containing benzyl carbonates underwent substitution in high yields, although certain substrates required longer reaction times and/or higher catalyst loading (2 mol%). Based on these results, by simply changing the Pd catalyst while maintaining the usage of more electron-rich and bulky bidentate phosphine ligands, both naphthylmethyl and simple benzyls can undergo benzylation with diverse stabilized enolates.

Scheme 30.

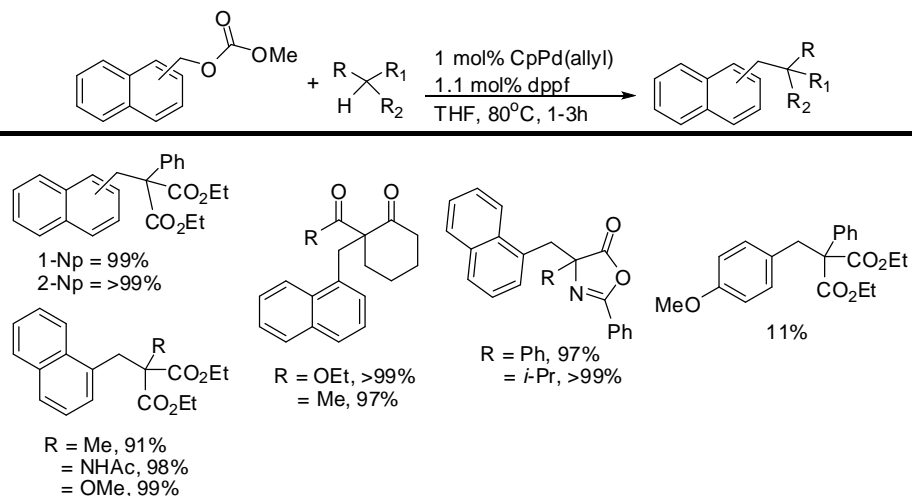
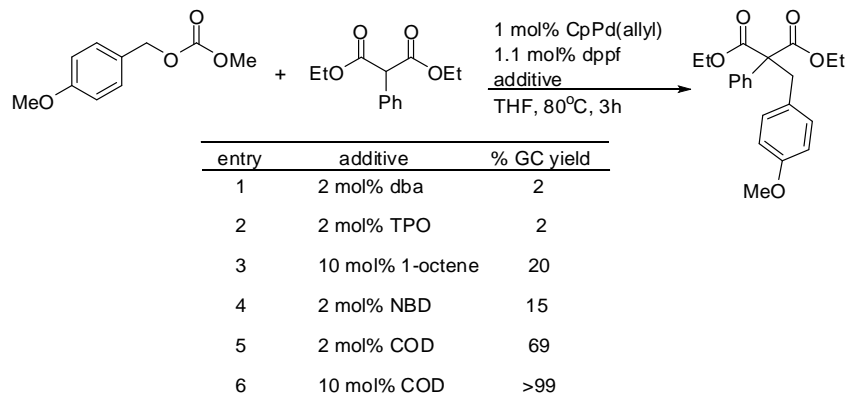
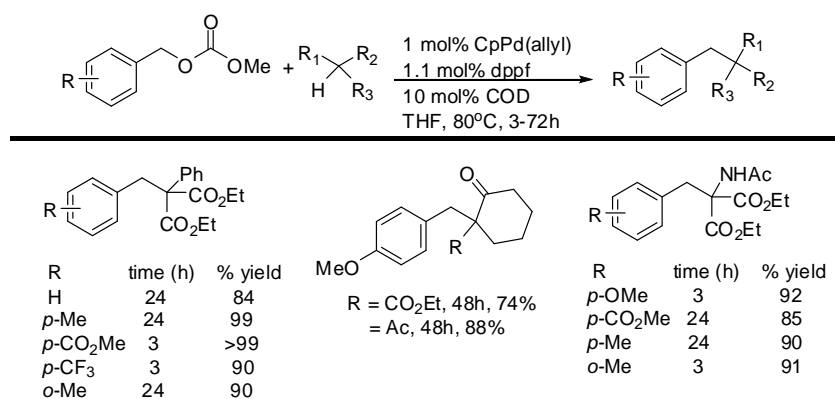


Table 2.



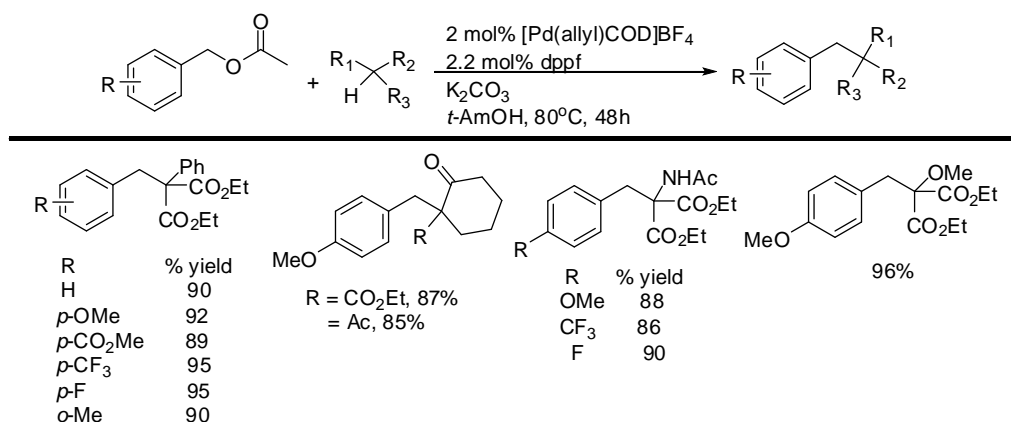
Scheme 31.



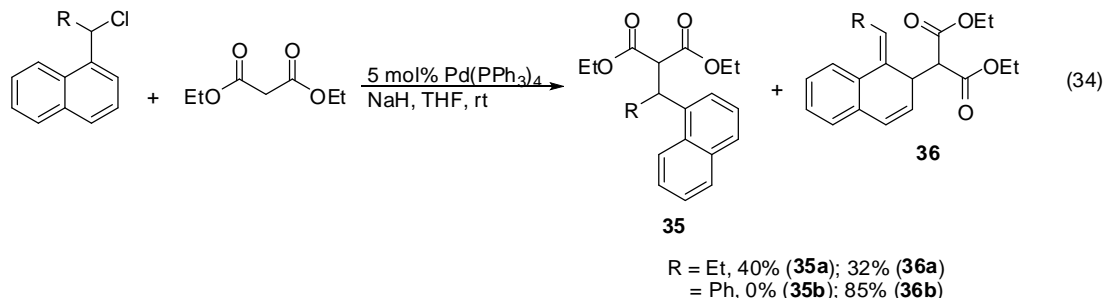
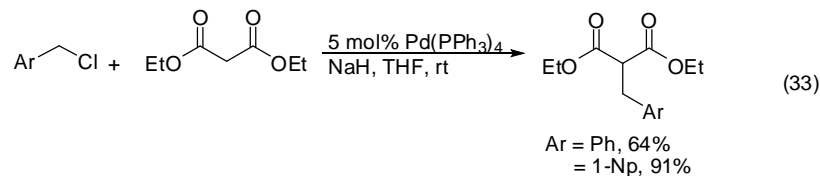
In 2007, Kuwano and Kondo reported the substitution of simple benzyl acetates using identical conditions to those used for substitution of benzyl carbonates.¹⁵ However, the use of a polar and bulky AmOH solvent was necessary to achieve the desired benzylation. A variety of benzyl acetates underwent substitution with malonates to give α -substituted benzyl malonates in high yields regardless of the electronic nature of substituents on the benzyl acetate (Scheme 32). The use of a slightly stronger base was important, presumably due to its solubility in the solvent. The authors speculated that the role of the polar solvent was to provide hydrogen bonding between the alcohol and carbonyl oxygen of the acetate which could ultimately weaken the

benzylic C-O bond, allowing oxidative addition to occur and generate the Pd- π -benzyl intermediate.¹⁵

Scheme 32.

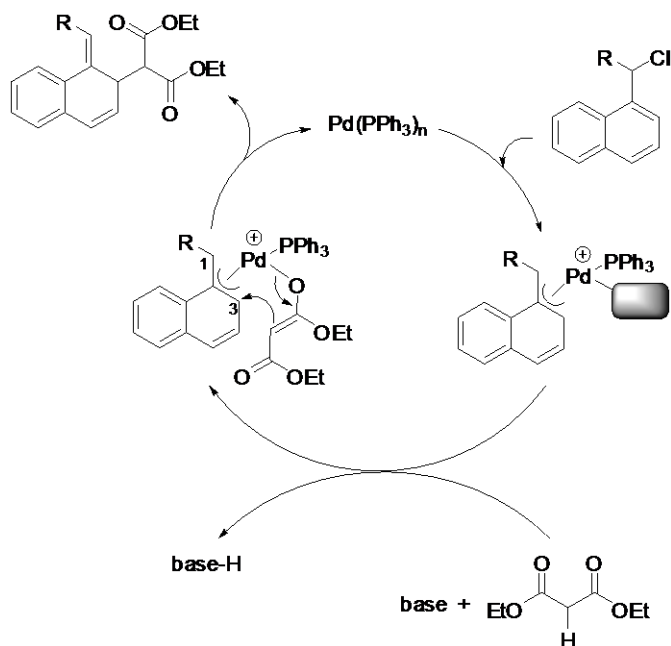


Aside from benzyl acetate and carbonate, benzyl chloride has also been utilized towards cross-coupling with enolates. Treatment of benzyl chloride and diethylmalonate with Pd(PPh₃)₄ and NaH in THF at room temperature generated the desired α -substituted benzyl malonate (eq. 33).¹⁶ The high yield of α -1-naphthyl malonate in contrast to simple benzyl malonate was the result of greater stabilization of the Pd complex with naphthyl compared to simple benzylys (*vide infra*). When naphthylethyl chloride was treated with the same conditions, an unexpected dearomatized vinyl naphthyl malonate **36** was observed along with the expected naphthylethyl malonate **35** (eq. 34). When the α -alkyl substituent was replaced with a bulky phenyl group, only aryl-vinyl naphthyl malonate **36b** was isolated in high yield.¹⁶ Unfortunately, no benzylation occurred when simple benzyl phenyl chloride was used. Based on these results, simply changing the LG allows complete regioselective attack of the nucleophile to the preformed η^3 -benzyl-Pd complex.



The use of monodentate ligand in these reactions was completely different from the previous enolate benzylations. Their utility in these type of reactions allow the generation of dearomatized products rather than the expected benzyl products. Dearomatization occurred in these reactions possibly because the use of monodentate phosphine ligand allowed the generation of an open coordination site for the enolate to access in the η^3 -Pd-benzyl complex such that the proximal distance of the enolate to C-3 of the Pd complex allowed a site-specific nucleophilic attack on this carbon rather than the C-1 benzylic carbon (Scheme 33). The steric bulk of the phenyl group in the α -position of the complex may somehow have contributed to prevent the enolate to attack at C-1 position. This explains the generation of **35a** and **36a** when the small-sized ethyl substituent was used.

Scheme 33.



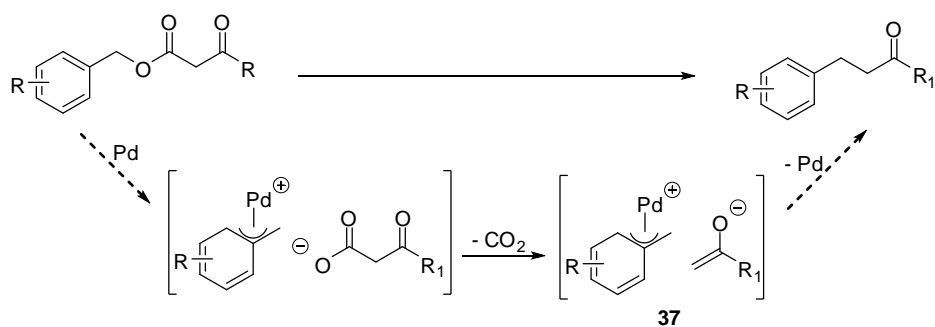
2.2 Pd-catalyzed decarboxylative allylations (DcA): Prelude to DcB

Significance of DcB from DcA

Much of the Pd-catalyzed benzylation of ketones covered until now occurs intermolecularly. The η^3 -Pd-benzyl electrophile and enolate nucleophile have to be generated separately before coupling occurs. Moreover, the nature of the enolate nucleophile in these reactions is stabilized ($\text{pK}_a < 20$). We wanted to expand the scope of benzylation from stabilized to non-stabilized enolates and avoid the need to use stoichiometric bases and/or preformed organometallics. To address these problems, we thought we could instead perform intramolecular benzylation reactions where the Pd- π -benzyl can couple with enolates through decarboxylative cross-coupling. In this reaction, the electrophilic Pd- π -benzyl complex and

enolate **37** are both generated *in situ* after decarboxylation of benzyl β -ketoester in the presence of catalytic Pd (Scheme 34). While the process would occur intramolecularly, the overall reaction would allow utilization of various non-stabilized enolates without the need of unnecessary additives. Ultimately, the ability to perform site-specific benzylations with non-stabilized enolates would enable us to synthesize diverse and functionalized benzyl ketones that cannot be traditionally accessed using standard acid-base chemistry.

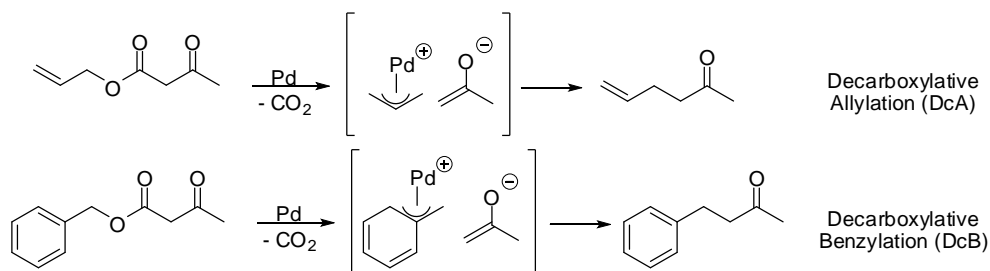
Scheme 34.



Prior to the development of α -benzyl ketone synthesis through decarboxylative benzylation (DcB) of benzyl β -ketoesters, an analogous decarboxylative allylation (DcA) of allyl β -ketoesters has been reported. Pd-catalyzed DcA reactions of allyl β -ketoesters have been known for the past 32 years since the reaction was independently discovered and reported by Tsuji and Saegusa.^{17,18} After the publication of their seminal works, several reviews have been published over the next years detailing its overall utility and chemistry in constructing allyl ketones in terms of substrate scope, application to natural product syntheses, and mechanistic studies.^{16,17,19} From the DcB perspective, we were aware that it is important to highlight important results and information from DcA since they are integral to establishing the feasibility of the benzylation project. In the simplest sense, Pd-catalyzed DcA and DcB of β -ketoesters

yield allyl and benzyl ketones through generation of enolate and alkyl electrophiles *in situ* (Scheme 35). What makes the DcA different from DcB, when all things are identical, is only the nature of electrophile.

Scheme 35.

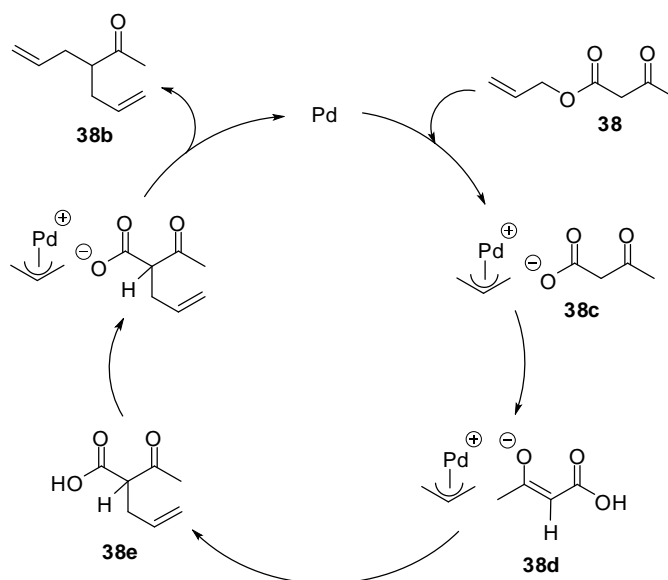


DcA of unsubstituted allyl β-ketoesters

Saegusa and Tsuji simultaneously reported that an unsubstituted allyl β-ketoester **38** underwent DcA in the presence of Pd and PPh₃ ligand to generate a mixture of allyl ketone **38a** and diallyl ketone **38b** (eq. 35).¹⁸ In this reaction, the generation of electrophilic Pd-π-allyl and nucleophilic enolate was effected by loss of CO₂. This was important because it allowed generation of reactive species *in situ* which then couple rapidly to form newly functionalized allyl ketones. More importantly, the formation of non-stabilized enolates through decarboxylation occurred under mild conditions such that the need of base and preformed organometallics were unnecessary.

from α -hydrogen of **38c** occurred to form an enolate carboxylic acid **38d** intermediate (Scheme 37). Ligand exchange from **38d** or Pd- π -allyl non-stabilized enolate intermediate formed the α -allyl β -keto-carboxylic acid **38e** via Tsuji-Trost allylation. Finally, decarboxylation of **38e** then a second allylation occurred to release **38b** and Pd is regenerated back into the catalytic cycle.

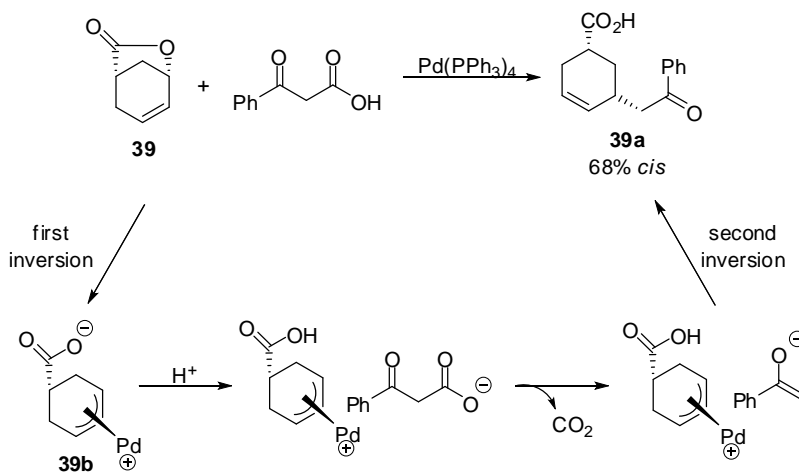
Scheme 37.



It was believed that the nature of the enolate nucleophile existed as free enolate rather than being bound to Pd.^{17,23} When *cis*-cyclohexenyl lactone **39** was treated with Pd conditions in the presence of phenylacetoacetic acid, DcA occurred giving cyclohexenyl ketone **39a** in *cis* stereochemistry (Scheme 38). The observed overall retention of the stereochemistry in the product implied that a double inversion mechanism occurred in the overall transformation. This would mean that Pd underwent backside attack to **39** generating *trans*-Pd- π -allyl intermediate **39b** as a result of first inversion. Protonation of **39b** followed by decarboxylation would lead to formation of the enolate. The enolate underwent backside attack to the Pd- π -allyl forming *cis*-allyl ketone **39a** as a result of second inversion. The double inversion mechanism has been

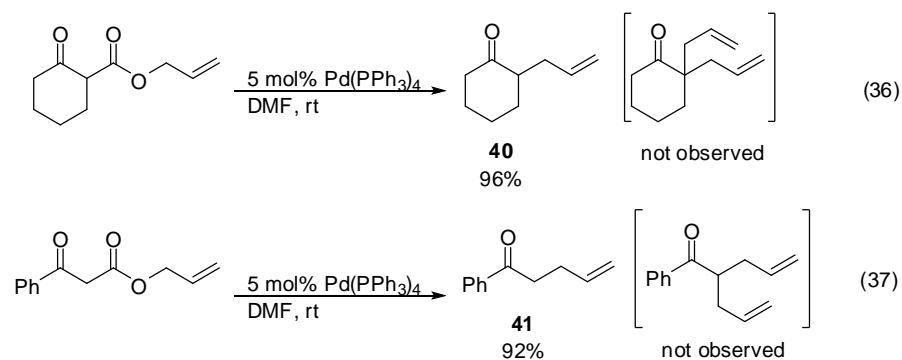
observed in allylations of ketones with stabilized nucleophiles.²⁴ The slight lower stereospecificity observed in **39a** from **39** could be attributed to competing inner-sphere reductive elimination or reactant epimerization.

Scheme 38.



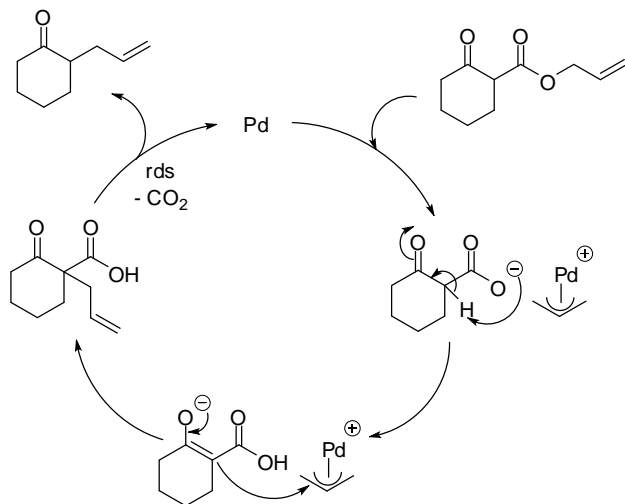
DcA of monosubstituted allyl β -ketoesters

The formation of diallyl ketones such as **38b** was prevented when the parent allyl β -ketoester contained an aryl or cyclic ketone moiety.^{18a} Tsuji and coworkers showed that an allyl cyclohexanone ester underwent DcA to generate α -allyl cyclohexanone **40** in very high yield. Formation of diallyl cyclohexanone was not observed (eq. 36). Similarly, allyl phenylacetone **41** was observed exclusively and none of undesired diallyl phenylacetone was observed in the DcA allyl phenyl β -ketoester (eq. 37).

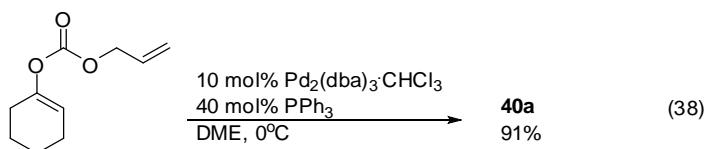


Based on several experimental and mechanistic studies, it was proposed that the catalytic cycle of DcA of allyl β -ketoesters that contain α -hydrogen undergo decarboxylation-allylation mechanism that involved an outer-sphere attack of the enolate to the η^3 -allyl-Pd complex.¹⁷ After oxidative addition to generate Pd- π -allyl complex and carboxylate, intramolecular proton transfer from the α -hydrogen occurred to generate an enolate carboxylic acid which can undergo allylation to form an α -allyl- β -ketocarboxylic acid (Scheme 39). Decarboxylation of α -allyl- β -ketocarboxylic acid furnished the allylated ketone. The overall mechanism showed similar resemblance to the diallylation mechanism. It was believed that the decarboxylation step was the rate-determining step based on several studies pertaining to the decarboxylation of similar-type allyl systems.¹⁷

Scheme 39.



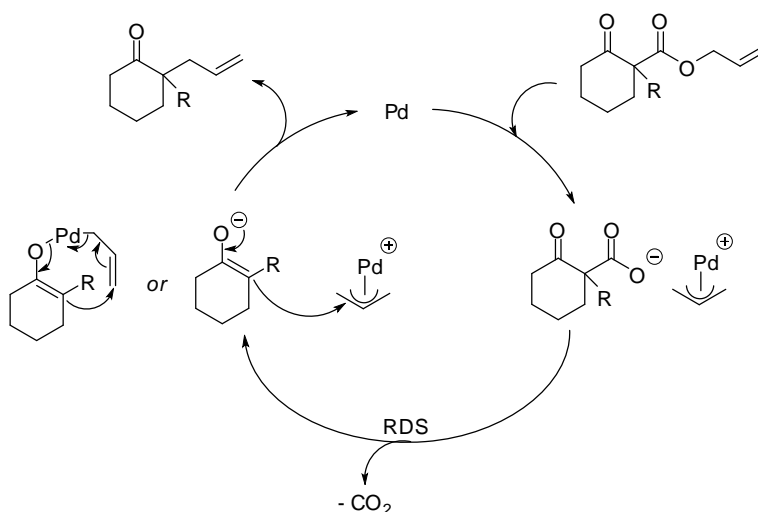
Lastly, a similar analog of allyl β -ketoester such as allyl enol carbonates can also undergo DcA giving identical allyl ketones. Tsuji and coworkers showed that an allyl cyclohexenol carbonate underwent DcA in the presence of a different Pd catalyst to generate the same allyl ketone **40a** in slightly lower yield compared with the DcA of cyclic allyl β -ketoester (eq. 38).²⁵ Since both substrates gave identical products, it was speculated that both classes of substrates underwent DcA via similar operating mechanisms though other experiments suggested otherwise.¹⁷



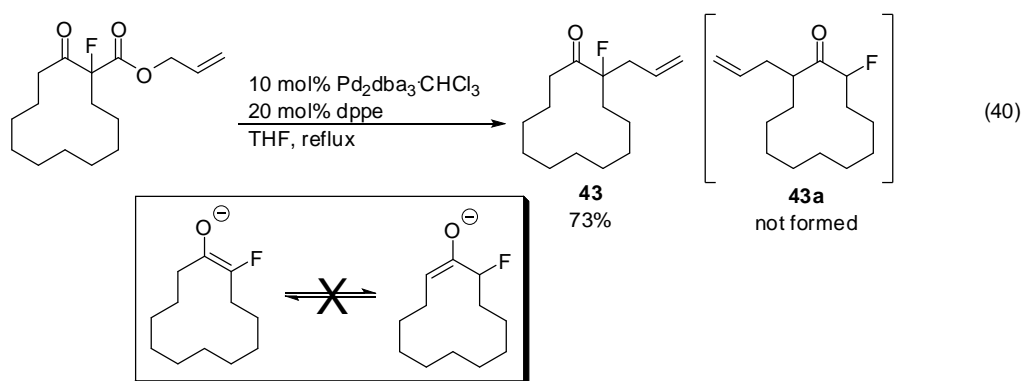
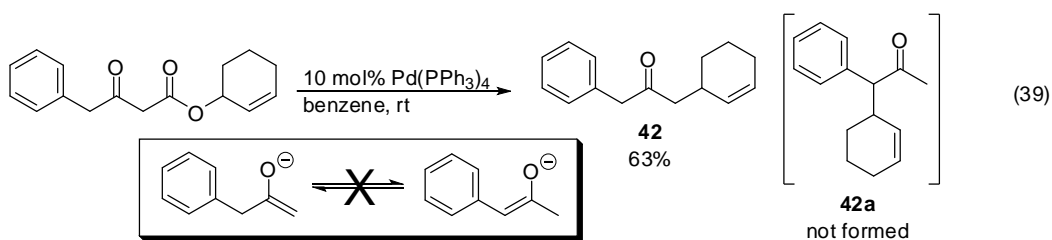
DcA of disubstituted allyl β -ketoesters

Over the 32 years since the inception of DcA of allyl β -ketoesters, the chemical literature currently contains hundreds of methodologies pertaining to the synthesis of α -disubstituted allyl functionalities. Rather than describing these reactions in detail, only the following issues will be discussed which are relevant to DcB. First, the mechanism of the DcA of α -disubstituted allyl β -ketoesters is thought to proceed *via* decarboxylation-allylation route.¹⁶ Upon generation of Pd- π -allyl complex and carboxylate intermediate after oxidative addition of Pd to the parent allyl β -ketoester, decarboxylation occurs to form the enolate. The enolate ultimately attacks the Pd electrophile to release the α -quaternary allyl ketone (Scheme 40). Mechanistic studies have shown the enolate can attack the Pd- π -allyl complex through either an outer-sphere approach or seven-membered cyclic transition state.¹⁷ Importantly, the mechanism is different from the DcA mechanism of α -monosubstituted allyl β -ketoesters (Scheme 37) when the substrates contain no α -hydrogen (Scheme 40).

Scheme 40.



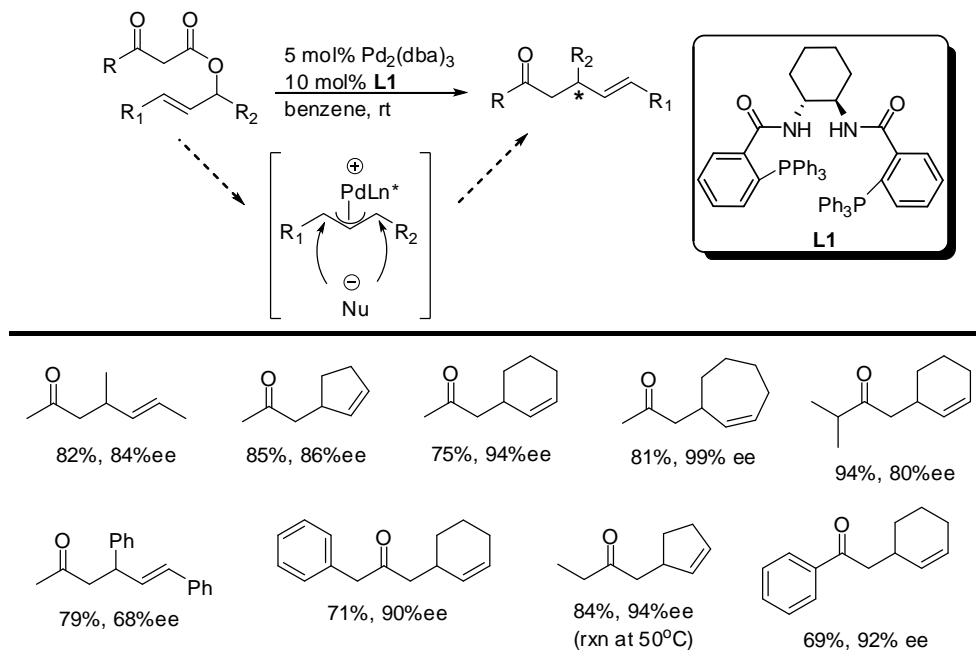
The second important feature is that the formation of α -disubstituted allyl ketones is regiospecific. Decarboxylation of the carboxylate generates the enolate at the α -position that once bore the CO_2 unit. Burger and Tunge reported the formation of **42** as the only product isolated and none of the allyl ketone isomer **42a** was observed (eq. 39). These results indicate that the kinetic enolate that was initially formed after decarboxylation does not isomerize to a more stable, thermodynamic enolate before being trapped with the electrophile.²⁰ Similarly, Shimizu and Ishii showed that an allyl α -fluoroketone- β -ketoester underwent DcA to generate fluoroketone **43** exclusively in high yield without formation of α' -allyl- α -fluoroketone **43a** (eq. 40).²⁶ The regiospecific generation of enolates through decarboxylation is advantageous because it allows access to enolates, particularly with non-stabilized enolates, which are difficult to generate using standard acid-base chemistry (Chapter 2.1).



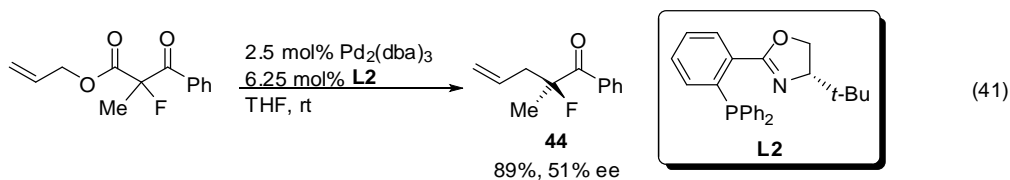
Enantioselective DcA of allyl β -ketoesters

Given the broad scope of DcA reactions with racemic substrates, its full potential was also explored towards asymmetric synthesis. In 2006, Burger and Tunge reported the first enantioselective DcA of allyl β -ketoesters in the presence of Pd and Trost ligand **L1** in benzene at room temperature.²⁰ The ability of the chiral ligand to introduce a chiral environment in the *meso*-Pd- π -allyl complex such that one face of the Pd allyl terminus is more favorable towards enolate attack allowed full control of the stereochemistry at the β -position of various allyl ketones in good to high ee's (Scheme 41). Higher enantioselectivities were obtained when the ring size of the allyl fragment was increased. The enantioselectivity was slightly influenced by the substituents at the terminal ketone position. In addition, the nature of the allyl moiety was important. If the allyl unit was cyclic, higher enantioselectivities were observed compared to acyclic allyl units. In these reactions, the origin of asymmetric control in these reactions is coming from the electrophile.

Scheme 41.

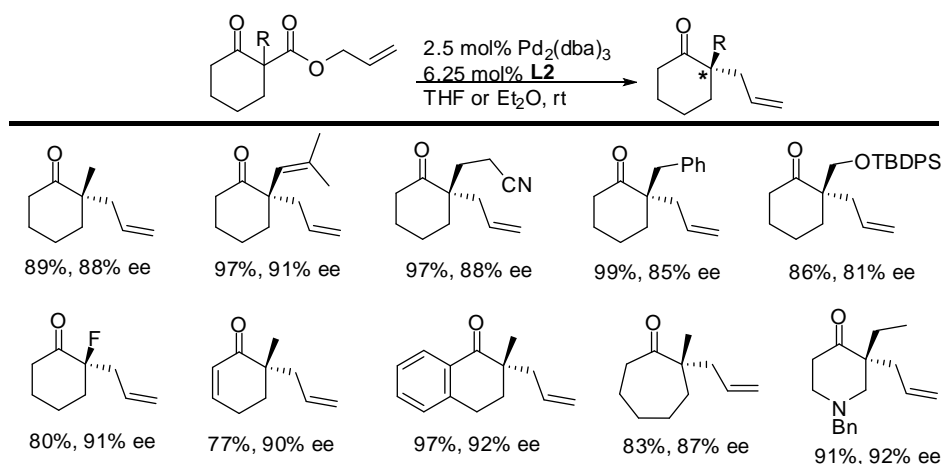


In addition to the asymmetric reaction shown in Scheme 41, in which the stereochemistry is controlled by the electrophile, other research groups performed DcA of allyl β -ketoesters in which the stereochemistry is set at the α -position of the nucleophile. Nakamura and coworkers showed that α -fluoro substituted allyl β -ketoester undergoes DcA to generate chiral α,α -disubstituted fluoroketone **44** in high yield in the presence of Pd and *t*-BuPHOX ligand **L2** (eq. 41).²⁷ While the product yield was high, the obtained ee was moderate. The low enantioselectivity observed was attributed to the formation of *E* and *Z* enolates in the reaction medium. Other acyclic α -disubstituted allyl β -ketoesters also failed to give high ee's yet high product yields resulted regardless of the kind of Pd catalyst and chiral ligand.²⁸



To minimize the inevitable low ee observed with acyclic ketones, enolates derived from cyclic ketones were used in order to generate single and fixed enolate geometry. Stoltz and coworkers showed that α -substituted 2-allyl carboxyallylcyclohexanones underwent DcA in an enantioconvergent process to generate α -substituted allyl cyclohexanones using the same chiral **L2** ligand used by Nakamura and coworkers in enantioselective DcA of α -fluoro allyl β -ketoesters.²⁹ A variety of chiral cyclic ketones were obtained in good to high yields and ee's (Scheme 71). The scope of asymmetric DcA was applied to other cyclic ketones such as tetralone, cycloheptanone, and α,β -unsaturated cyclohexanone. In addition to *t*-BuPHOX ligand, other researchers have shown that other chiral bidentate ligands were capable to perform asymmetric DcA of cyclic allyl β -ketoesters to generate enantioenriched allyl ketones.^{27,30}

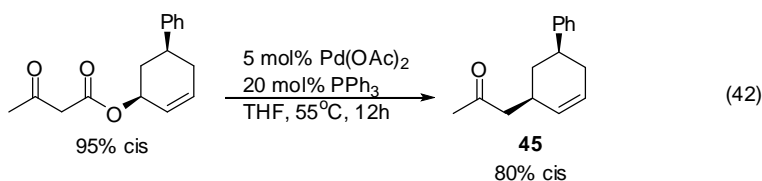
Scheme 42.



Stereospecific DcA of allyl β -ketoesters

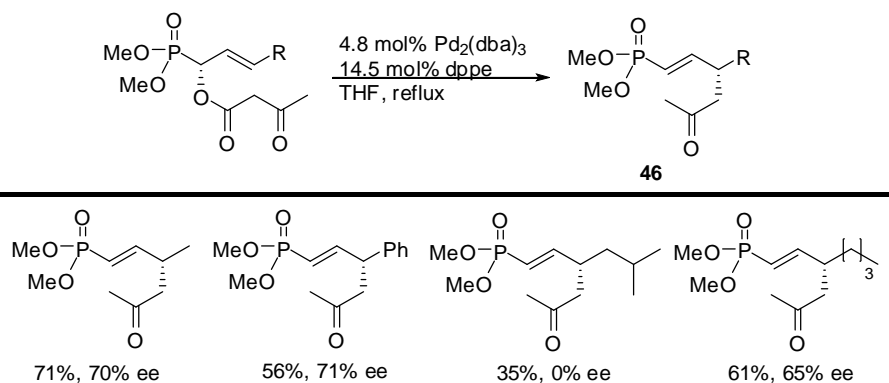
The observed retention of stereochemistry in the DcA of cyclohexenyl lactone in Scheme 38, based on double inversion mechanism, shows that the reaction is stereospecific. Further

evidence of stereospecificity of DcA was also shown by Burger and Tunge in which they reported that, when *cis*-cyclohexenyl β -ketoester was allowed to undergo DcA under appropriate conditions, cyclohexenyl ketone **45** was observed in *cis* configuration.¹⁶ (eq. 42) The slightly lower stereospecificity of **45** presumably came from competing inner-sphere reductive elimination or epimerization of the starting material.



In 2008, Yan and Spilling also reported the stereospecific DcA of phosphono allylacetate to phosphono allylketone **46** in moderate to good yields and enantioselectivity.³⁰ Unfortunately, when a *sec*-butyl group was tried, it gave racemic allyl ketone in low yield (Scheme 43).

Scheme 43.



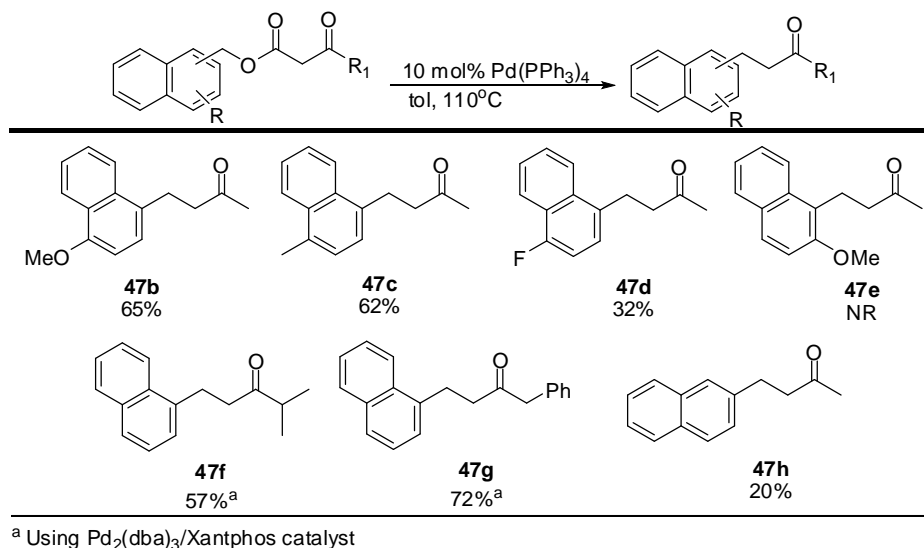
2.3 Development of DcB of benzo-fused ketones

2.3.1 DcB of unsubstituted benzo-fused β -ketoesters

Until now, benzylations have been performed by coupling Pd- π -benzyl with various substituted malonate in which the generated enolate is stabilized. Benzylic substitutions with non-stabilized enolates typically resulted to formation of mono- and dibenzyl ketone mixtures. To overcome this problem, there is a need to develop new methodology that will allow benzylic substitution with various enolates without formation of mono- and dibenzyl ketone mixtures. We think that by pursuing benzylic functionalization through decarboxylation would avoid the formation of mono- and dibenzyl ketone mixtures. Hence, to carry out research with regards to the development of Pd-catalyzed decarboxylative benzylation (DcB) of ketones is desirable because it would utilize non-stabilized enolates as the nucleophilic coupling partner with Pd- π -benzyl. Previous benzylation reactions were only restricted towards stabilized enolates ($\text{pK}_a < 15$). Moreover, these reactions used stoichiometric bases which overrides catalytic role of the reaction. To be able to perform site-specific benzylations with non-stabilized enolates ($\text{pK}_a > 15$) through decarboxylation would allow us to prepare diverse benzyl ketones that cannot be accessed using standard acid-base chemistry.

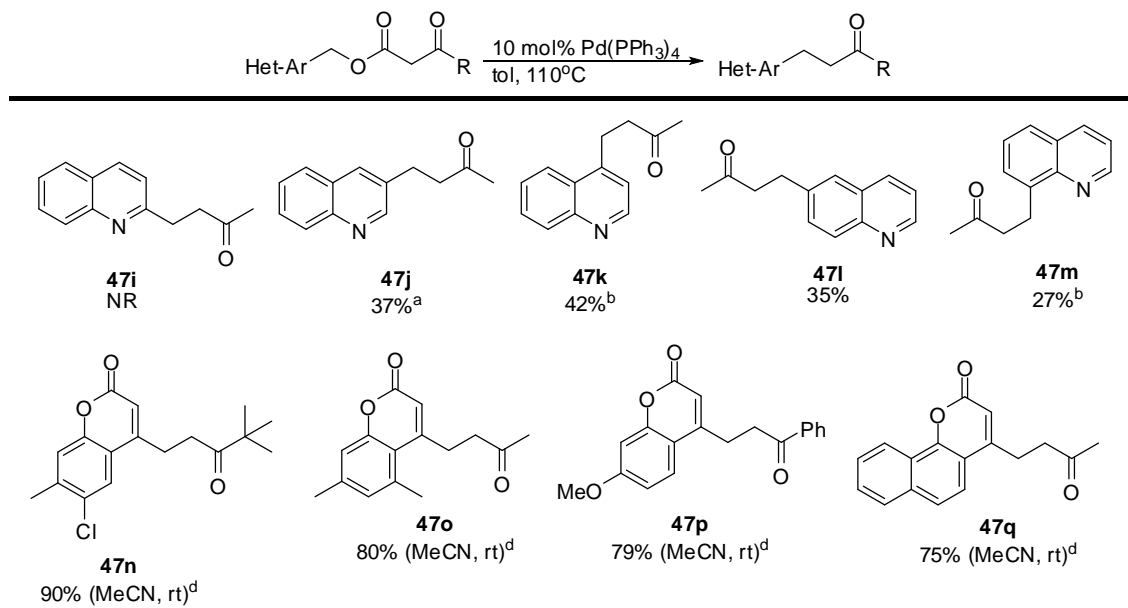
We initially began the development of decarboxylative benzylation (DcB) of ketones by using simple benzyl β -ketoesters. When an unsubstituted simple benzyl β -ketoester was treated with Pd(PPh₃)₄, the expected α -benzyl ketone was not observed and only the starting material was recovered (eq. 43). When the simple benzyl ester was replaced with 1-naphthylmethyl moiety, benzylation occurred giving a 75:12 ratio (based on crude ¹H NMR spectroscopy) of mono-naphthylmethyl ketone **47** in 40% yield and di-naphthylmethyl ketone **47a** in 8% yield.

Scheme 44.



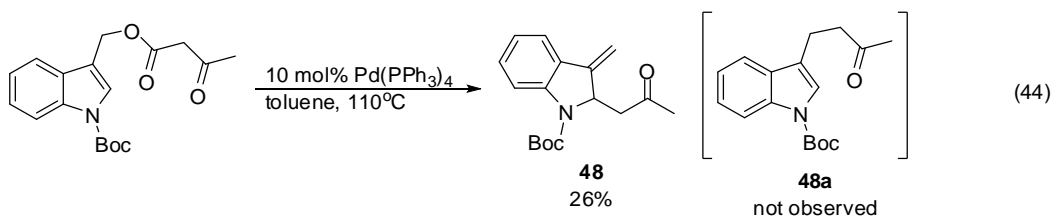
In addition to 1- and 2-naphthylmethyl electrophiles, benzo-fused heterocycles such as quinoline and coumarin β -ketoesters were also tried (Scheme 45). For these substrates, benzylation proceeded in good to high yields. Similar to the benzylation of heteroaromatics with malonates, the position of the benzyl carbon relative to the nitrogen had a profound effect on benzylation. While 2-quinoline **47i** was unreactive towards DcB, other quinoline substrates underwent substitution (**47j**, **47k**, **47l**, and **47m**) in the presence of an appropriate Pd catalyst in moderate yields. For these substrates, the benzyl carbon was located farther from nitrogen. Finally, coumarylmethyl β -ketoesters can undergo DcB at room temperature and in the presence of a polar solvent to generate coumarin ketones in good to high yields.³²

Scheme 45.



^a 2.5 mol% Pd₂(dba)₃, 10 mol% PBU₃; ^b dibenzyl-4-quinolyl ketone was isolated in 10% yield; ^c 10 mol% CpPd(allyl), 11 mol% dppf; ^d Reactions performed by Dr. Kalicharan Chattopadhyay

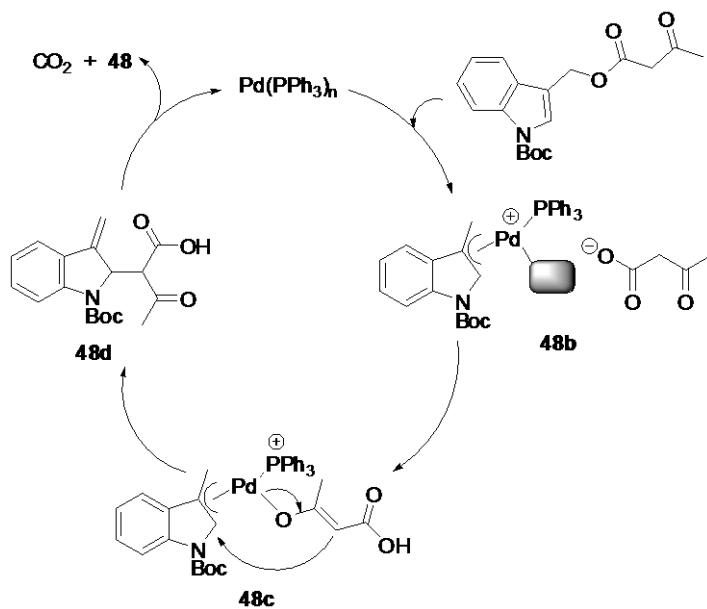
When an N-Boc protected indole β-ketoester was subjected to conditions for DcB, an unexpected indoline ketone **48** rather than desired aromatic indole ketone **48a** was isolated in low yield (eq. 44). Despite its low yield, it was interesting that a dearomatized heterocycle can be obtained coming from an aromatic starting material. While dearomatizations of naphthalene and heterocycles are known, this result highlights the first isolation of dearomatized heterocycle coming from DcB.



The formation of **48** is thought to proceed through a Carroll-type rearrangement. Carroll rearrangement is a classical reaction in which an allyl β-ketoester undergoes [3,3] sigmatropic

rearrangement to form an α -allyl- β -keto-carboxylic acid, which then undergoes decarboxylation to generate γ,δ -allylketone at high temperatures.³³ In this case, the mechanism possibly begins by oxidative addition of Pd to N-Boc protected indole β -ketoester to form Pd- π -benzyl complex and carboxylate intermediate **48b**. Proton transfer occurs to generate an enolate carboxylic acid which can occupy an open coordination site in the Pd-complex to form an O-bound Pd- π -benzyl complex **48c**. The complex undergoes reductive elimination resulting in formation of indoline β -ketoacid **48d**. Decarboxylation of **48d** ultimately furnishes the product (Scheme 46). This type of mechanism would be similar to the dearomatization of 1-naphthylaryl chlorides with diethylmalonate that generate dearomatized dihydronaphthalenes (Scheme 33).

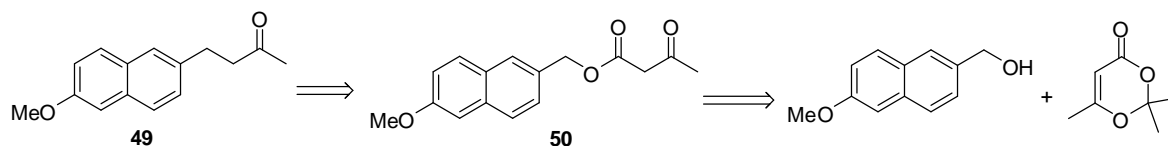
Scheme 46.



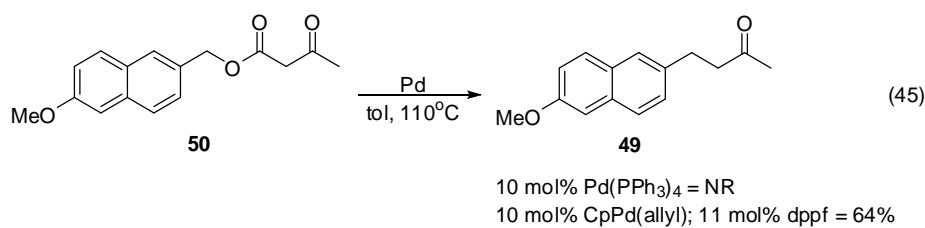
The developed DcB of benzo-fused β -ketoesters was applied towards the synthesis of a known pharmaceutical, Nabumetone. Nabumetone is a commercial NSAID developed by Beecham and is commercially sold as Relafen. It is used to relieve pain, tenderness, swelling, and stiffness caused by osteoarthritis and rheumatoid arthritis.³⁴ Looking at the parent structure

of Nabumetone **49**, it can be clearly seen that it could come from the DcB of 6-methoxy-2-naphthylmethyl β -ketoester **50**, which would then come from esterification of 6-methoxy-2-naphthylmethyl alcohol and diketene (Scheme 47).

Scheme 47.

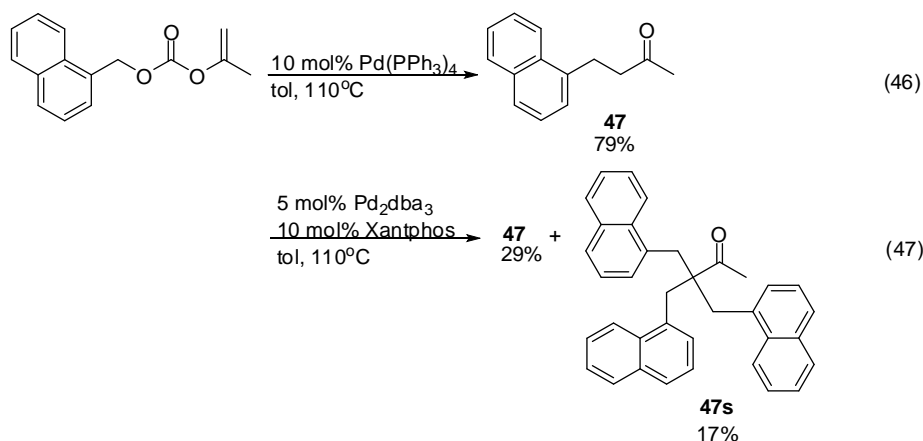


When **50** was treated with $\text{Pd}(\text{PPh}_3)_4$, we were disappointed that formation of **49** did not occur, and starting material was recovered (eq. 45). It appeared that the presence of an EDG strategically located at the 6-position of the 2-naphthyl ring inhibited benzylation, suggesting that it destabilizes the $\text{Pd}-\pi$ -benzyl complex compared to an unsubstituted 2-naphthylmethyl β -ketoester. When a more reactive Pd catalyst was used, we were pleased that benzylation occurred in good yield.



In a separate experiment, we were curious if an analog of 1-naphthylmethyl β -ketoester such as α -1-naphthyl enol carbonate can undergo DcB and give exclusively the same α -1-naphthyl ketone **47** since it has been shown that the DcA of either allyl β -ketoester or allyl enol carbonate generates the same allyl ketone (eqs. 35, 38).¹⁷ When 1-naphthyl isopropenyl enol carbonate was allowed to react with $\text{Pd}(\text{PPh}_3)_4$, it gave **47** in high yield (eq. 46). When the catalyst was replaced with $\text{Pd}_2(\text{dba})_3/\text{Xantphos}$ catalyst, it gave **47** in low yield along with tri-

benzyl ketone **47s** (eq. 47). The formation of **47s** was interesting because none of the di-benzyl ketone **35b** was observed (based on crude ^1H NMR spectrum) and for the first time, a tri-benzyl ketone was observed and isolated from the decarboxylation reaction of a benzyl enol carbonate. A similar phenomenon was also observed in the DcB of 2-naphthyl enol carbonate in the presence of $\text{CpPd}(\text{allyl})/\text{dppf}$ catalyst. Considering that triallylation was never observed in DcA reactions, these results could possibly open up newer mechanistic routes. As such, these results also suggest that there are differences in the DcB mechanism between benzyl β -ketoesters and benzyl enol carbonates.

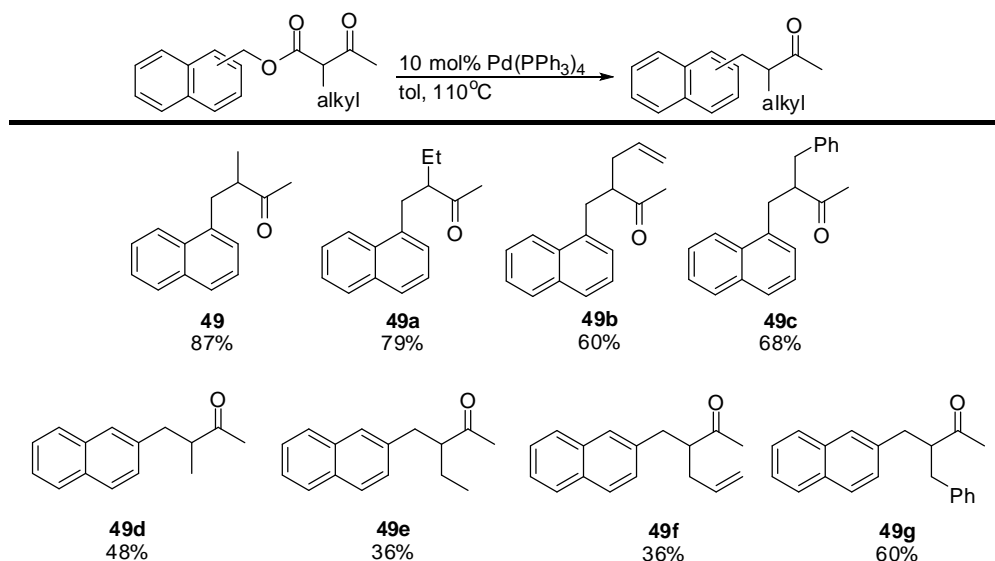


2.3.2 DcB of α -monosubstituted benzo-fused- β -ketoesters

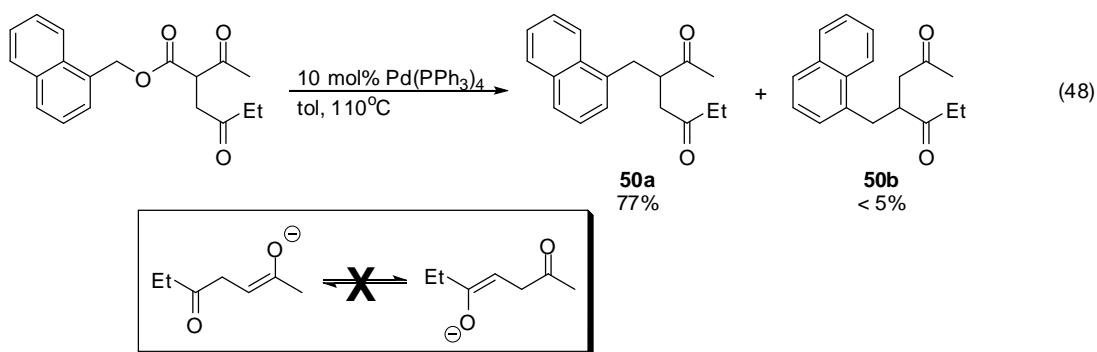
After exploring the scope of DcB towards unsubstituted benzo-fused β -ketoesters, we began to expand the scope of benzylation by exploiting the α -substitution at the β -ketoester functionality. We first explored the scope of DcB of monosubstituted naphthylmethyl β -ketoesters. We were pleased that it allowed DcB to occur generating alkyl α -naphthylmethyl ketones in good to high yields (Scheme 48). A higher yield of benzylation was observed when the α -alkyl substituent **49** was small compared to bulkier benzyl substituent **49c**. Similar to

unsubstituted naphthylmethyl β -ketoesters, α -substituted 2-naphthylmethyl β -ketoesters gave lower benzylation yields compared to 1-naphthylmethyl β -ketoesters.

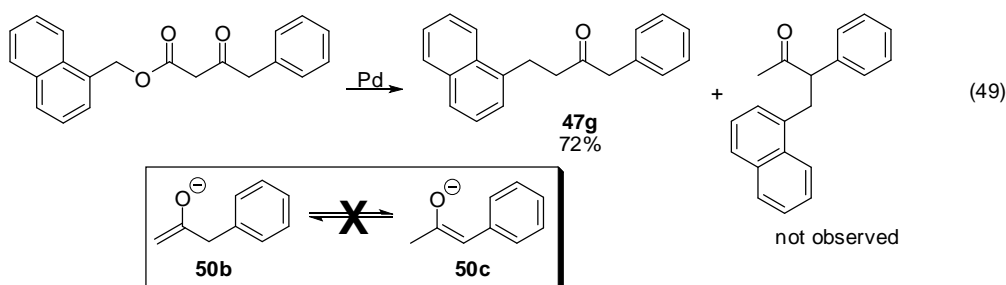
Scheme 48.



When an α -ethyl-4-oxo-1-naphthylmethyl β -ketoester was treated with $\text{Pd}(\text{PPh}_3)_4$, it also underwent DcB to give α -ethyl-4-oxo-1-naphthyl ketone **50** in high yield and none of the isomerized naphthyl ketone **50a** was observed (eq. 48). This result is consistent with the regiospecificity of DcA reactions; enolate isomerization does not occur. As a result, C-C bond formation occurs directly at the carbon where the carboxylate was initially located.

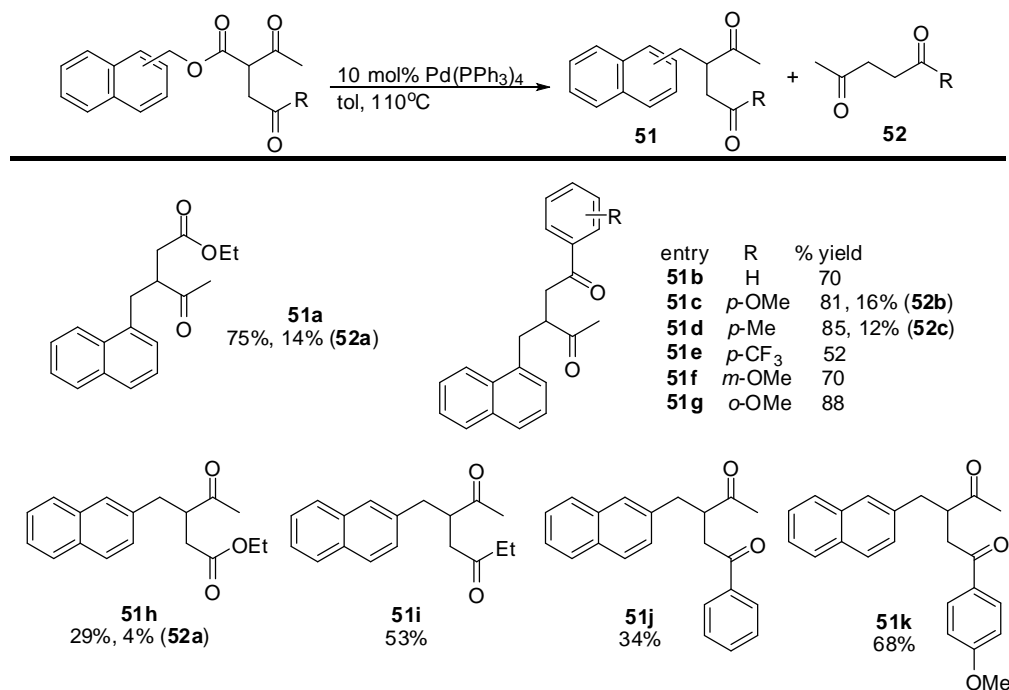


Similarly, regiospecific benzylation also occurred when unsubstituted 1-naphthylmethyl β -ketobenzyl ester underwent DcB to give 1-naphthyl-3-oxobenzylketone **47g** in high yield rather than isomeric α -1-naphthylmethyl ketone. The formation of the isomeric α -1-naphthylmethyl ketone would come from isomerization of the kinetic enolate **50b** to a more stable thermodynamic enolate **50c** (eq. 49). It has been reported that pK_a differences between **50b** and **50c** could be as high as 7.2 pK_a units.³⁵



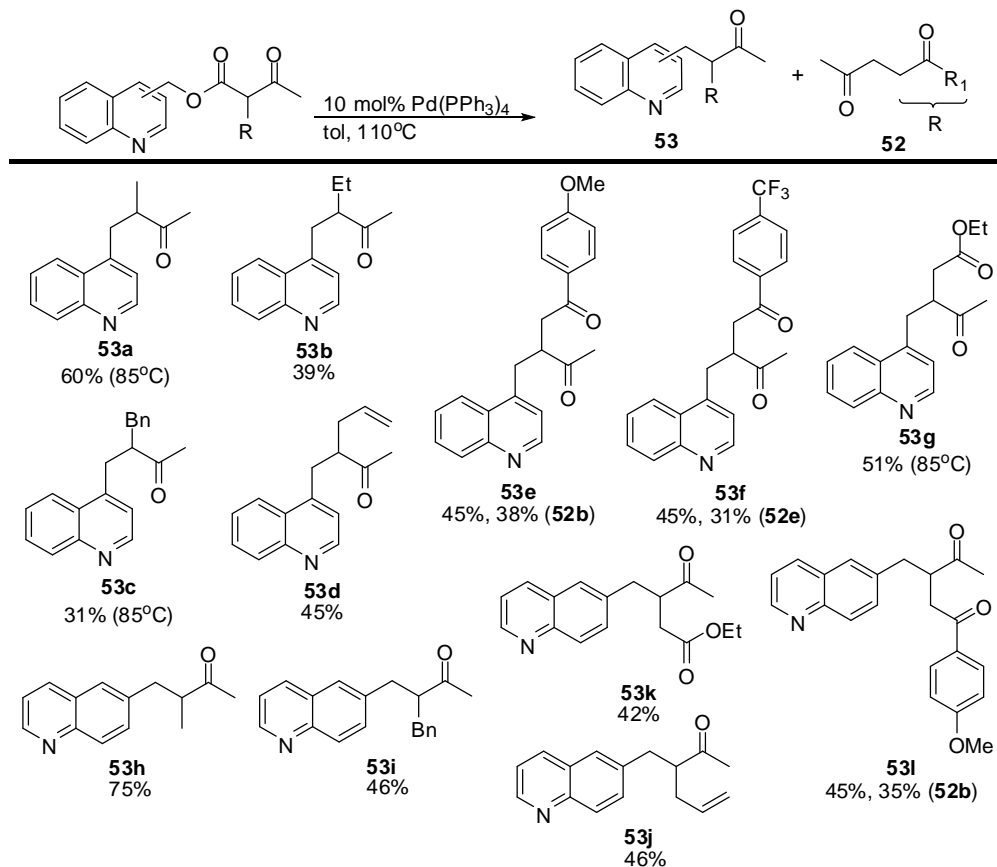
Encouraged by these results, we explored a variety of α -substituents that contain ketones and esters in DcB reactions. Indeed, all underwent regiospecific DcB to give functionalized α -substituted naphthylmethyl ketones in good to high yields using $\text{Pd}(\text{PPh}_3)_4$ (Scheme 49). In addition to α -1-naphthylmethyl ketone **51**, a protonation product **52** was also observed with some substrates. As expected, the benzylation of α -substituted ketones and esters of 2-naphthylmethyl β -ketoesters gave lower benzylation yields compared to 1-naphthylmethyl esters.

Scheme 49.

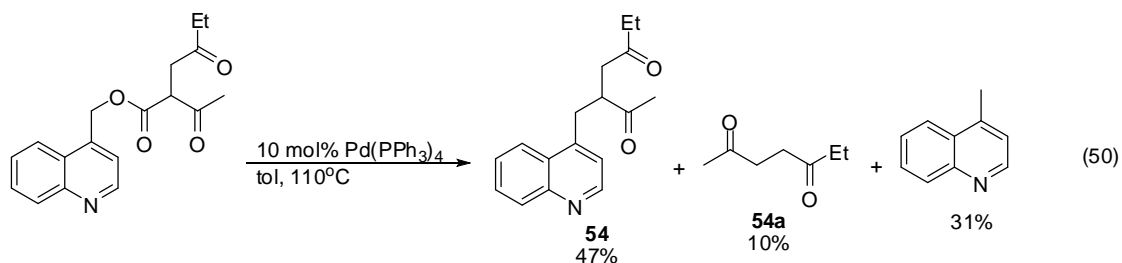


Aside from 1- and 2-naphthylmethyl β -ketoesters, quinolinylmethyl β -ketoesters were also tried. Based on the DcB of unsubstituted quinolinylmethyl β -ketoesters in Scheme 45, benzylation significantly improved when the position of benzyl carbon was located farther from the nitrogen. In this regard, we focused on using α -substituted 4- and 6-quinolinyl β -ketoesters. Gratifyingly, several monosubstituted 4- and 6-quinolinylmethyl ketones can be accessed from DcB of parent quinolinylmethyl β -ketoesters in moderate to good yields (Scheme 50). When the α -substituent was an alkyl group, α -6-quinolinylmethyl ketones gave higher yields than 4-quinolinylmethyl ketones. Once again, regioselective benzylation was also observed for ketone and ester-containing 4- and 6-quinolinylmethyl compounds, along with formation of protonation side product.

Scheme 50.



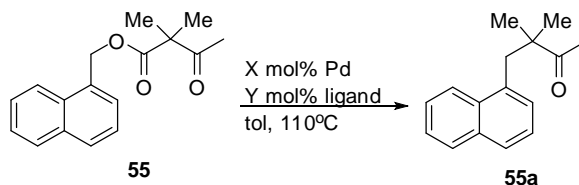
When α -ethyl-4-oxo-4-quinolinyloxy ketone was treated with $\text{Pd}(\text{PPh}_3)_4$, benzylation occurred to furnish the expected 4-quinolinyloxy ketone **54** and protonated side products such as ethyl β -ketoester **54a** and lepidine (eq. 50). Based on these results and other previous benzylations, it appears that formation of protonation products is difficult to avoid in Pd-catalyzed decarboxylation reactions. This was also observed in the DcA of allyl sulfones and allyl nitriles.³⁶ Unfortunately, the exact origin of the proton responsible for the formation of protonated side products is currently unknown despite several attempts at elucidation (Chapter 2.4.4).



2.3.3 DcB of α -disubstituted benzo-fused- β -ketoesters

When an α,α -dimethyl-1-naphthylmethyl β -ketoester **55** was treated in the presence of $\text{Pd}(\text{PPh}_3)_4$, formation of ketone **55a** occurred in 70% conversion (based on ^1H NMR spectroscopy). To improve the yield of **55a**, other Pd-based catalysts were screened (Table 3). We first considered screening a variety of monodentate ligands since the initial catalyst that was used contains monodentate PPh_3 . The results of the catalyst screening revealed that the combination of a more electron-deficient, dba-ligated Pd precatalyst with PPh_3 or PPh_2H was ineffective (entries 3 and 7). Reasoning that a more electron-rich ligand may facilitate the formation of the putative Pd- π -benzyl complex, several additional ligands were explored. While bulky, electron-rich ligands failed to promote the reaction (entries 4-6), the use of small-sized electron-rich ligands such as PMe_3 gave an improved conversion (entry 8). Ultimately, the use of PBu_3 gave the best conversion (entry 9). The Pd: PBu_3 ratio can be altered to either 1:1 or 1:2 to generate the product in very high conversion.³⁷ When the catalyst loading was reduced, the formation of **55a** was drastically reduced (entry 12). Only when the reaction was heated for more than three days, did the product conversion significantly improve.

Table 3.



entry	X	Pd	Y	ligand	% conversion ^a
1	5	Pd(PPh ₃) ₄	-	-	53
2	10	Pd(PPh ₃) ₄	-	-	70
3	5	Pd ₂ (dba) ₃	10	PPh ₃	4
4	5	Pd ₂ (dba) ₃	10	P(<i>t</i> -Bu) ₃	0
5	5	Pd ₂ (dba) ₃	10	PCy ₃	0
6	5	Pd ₂ (dba) ₃	10	P(2-TFP) ₃	3
7	5	Pd ₂ (dba) ₃	10	PPh ₂ H	0
8	5	Pd ₂ (dba) ₃	10	PMe ₃	19
9	5	Pd ₂ (dba) ₃	10	PBu ₃	>99
10	5	Pd ₂ (dba) ₃	20	PBu ₃	>99
11	2.5	Pd ₂ (dba) ₃	10	PBu ₃	>99
12	1	Pd ₂ (dba) ₃	5	PBu ₃	21 ^b

^a Based on crude ¹H NMR spectra; ^b 97% conversion after 40 h

We also surveyed several bidentate ligands to assess their reactivity towards **55** (Table 4). We were aware that bidentate ligands have been used in benzylation reactions with stabilized enolates (Chapter 2.1). When Pd₂dba₃ was used as the Pd source, all bidentate phosphine ligands that were tried gave good conversions, even the catalyst system used by Legros and coworkers in nucleophilic substitution of naphthyl acetates with malonate (entries 13, 15, 16, 18). Similar to Table 3, a 1:1 Pd:ligand ratio gave better product conversions compared to a 1:2 ratio (entry 14). The Pd catalyst used in DcB of benzyl diphenylglycinate imines also gave modest product conversion (entry 17). The dppf ligand provided the best conversion when combined with a catalyst precursor that was devoid of an electron-withdrawing dba ligand (entry 20). Interestingly, this catalyst proved to be beneficial in DcB of simple benzyl β-ketoesters (Chapter 2.4). Between the two best Pd catalyst systems, we ultimately chose the Pd₂(dba)₃/PBu₃ combination in the DcB of α-disubstituted 1-naphthyl β-ketoesters because it gave the highest product conversion.

Table 4.

$\text{55} \xrightarrow[\text{tol, 110}^\circ\text{C}]{\text{X mol\% Pd, Y mol\% ligand}} \text{55a}$

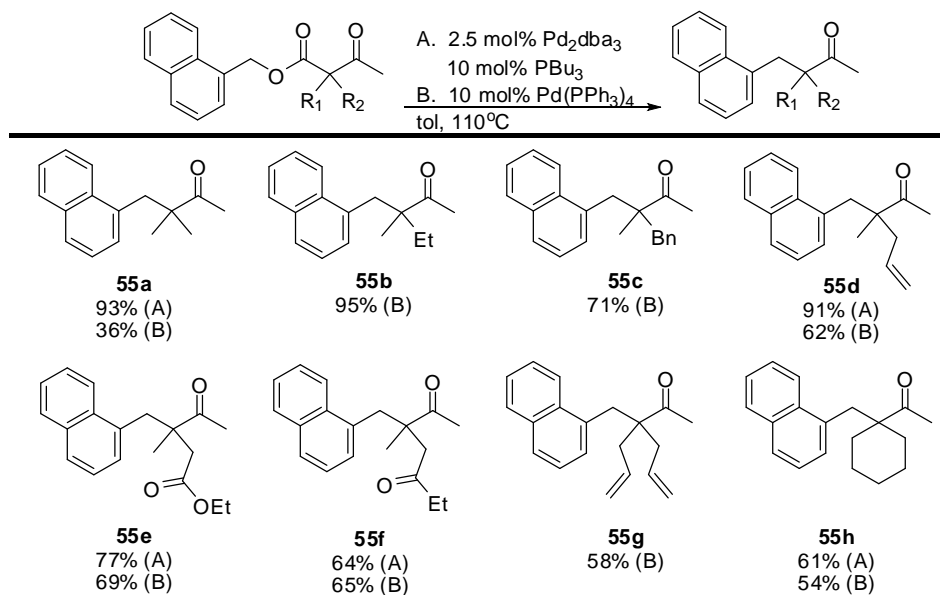
entry	X	Pd	Y	ligand	% conversion ^a
13	5	Pd ₂ (dba) ₃	10	Xantphos	88
14	5	Pd ₂ (dba) ₃	20	Xantphos	74
15	5	Pd ₂ (dba) ₃	10	<i>rac</i> -BINAP	65
16	2	Pd ₂ (dba) ₃	3	dppe	36
17	3	Pd(OAc) ₂	20	<i>rac</i> -BINAP	65
18	10	Pd ₂ (dba) ₃	11	dppf	69
19	10	[Pd(allyl)Cl] ₂	11	dppf	0
20	10	CpPd(allyl)	11	dppf	97

rac-BINAP

^a Based on crude ¹H NMR spectra

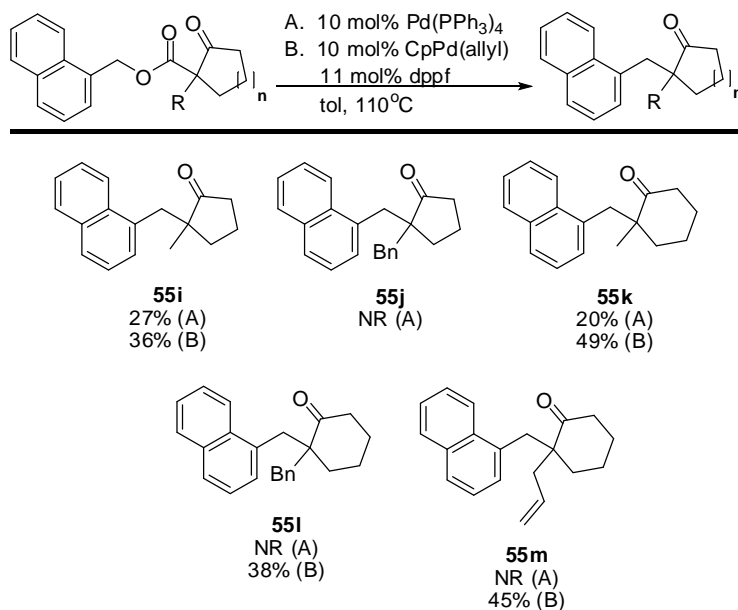
Using the chosen Pd catalyst system, a variety of α,α -disubstituted 1-naphthylmethyl β -ketoesters underwent DcB to yield α -quaternary naphthyl ketones in good to high yields (Scheme 51). Remarkably, the new catalyst system improved the generation of desired products compared to Pd(PPh₃)₄. The presence of an ester or ketone-containing α -substituent was tolerated while alkyl α -substituents gave higher benzylation yields. Nevertheless, acyclic and cyclic α -substituents were compatible under the developed DcB conditions.

Scheme 51.

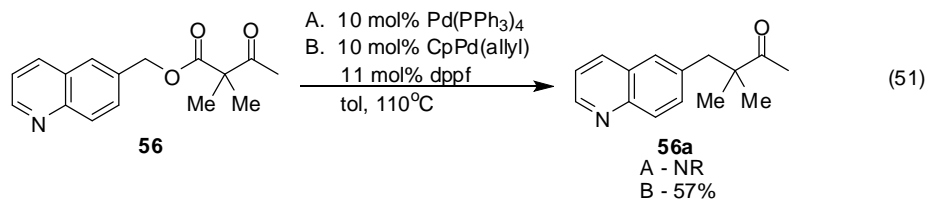


The DcB reaction was also applied towards cyclic ketones. With these substrates, Pd(PPh₃)₄ was a better catalyst than Pd₂(dba)₃/PBU₃ (Scheme 52). However, all the yields were significantly lower compared to acyclic ketones. We were pleased however that using CpPd(allyl)/dppf catalyst allowed benzylation to occur giving the desired 1-naphthylmethyl cyclic ketones in significantly improved yield. When the size of the α-substituent of the cyclic ketone **55k** was small, a higher benzylation yield was obtained compared to large size substituent **55l**. Moreover, six-membered ketones gave benzylation in high yields compared to five-membered ketones. The increase in ring size of the cyclic ketone towards decarboxylation was also observed in the DcA of allyl cyclic β-ketoesters (Scheme 36).²⁰

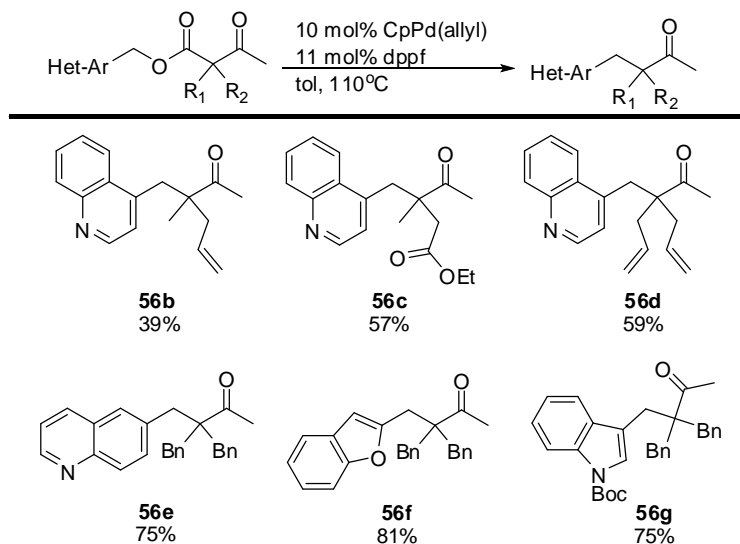
Scheme 52.



In addition to 1-naphthyl substrates, 4- and 6-quinolinyll substrates were also tried. When α,α -dimethyl-6-quinolinyll β -ketoester **56** was treated with Pd(PPh₃)₄, benzylation did not occur. This was surprising since we have shown that mono- and unsubstituted 6-quinoline β -ketoesters (Schemes 45, 50) underwent DcB in the presence of this catalyst. Gratifyingly, the use of CpPd(allyl)-dppf catalyst allowed DcB of **56** to occur, giving the desired α,α -dimethyl-6-quinolinyllmethyl ketone **56a** in good yield (eq. 51). Other heteroaromatic β -ketoesters such as indole and benzofuran underwent DcB to generate heteroaromatic ketones in good yields (Scheme 53).

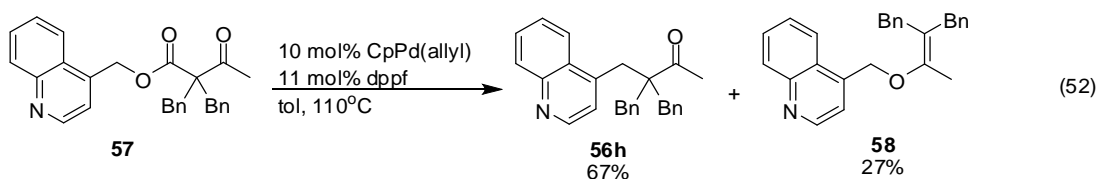


Scheme 53.

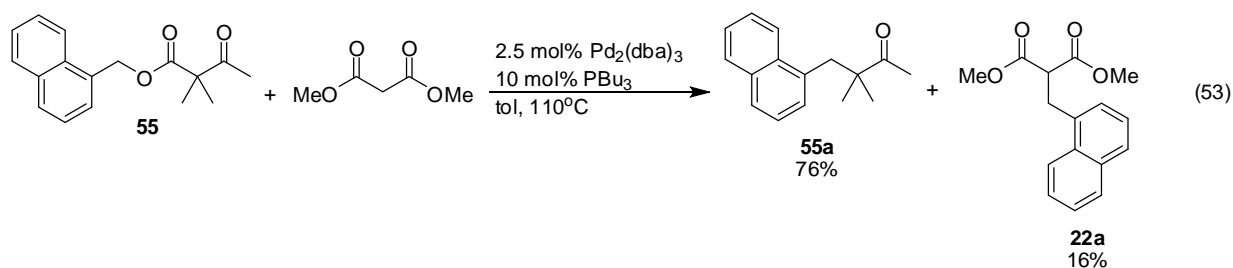


2.3.4 Regioselective benzylation

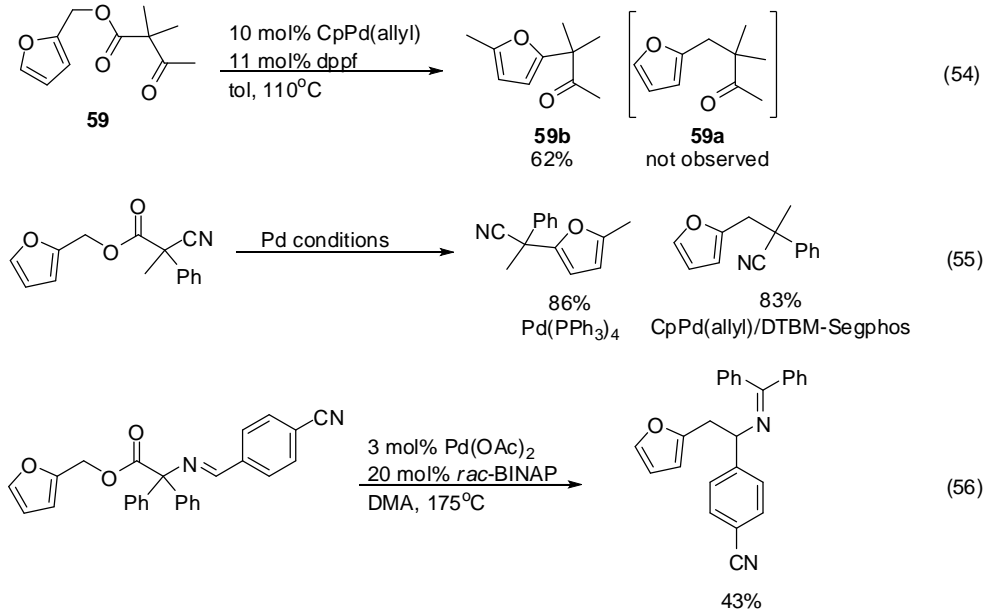
In addition to the substrates shown in Scheme 53, we also tried to perform DcB on α,α -dibenzyl-4-quinolinylmethyl β -ketoester **57**. Treatment of **57** with Pd ketone afforded **56h** in good yield. In addition to **56h**, we were also able to isolate an unknown compound which turned out to be the 4-quinolinyl enol ether **58** (eq. 52). Interestingly, other heteroaromatic β -ketoesters also showed the formation of benzyl enol ethers (based on crude ^1H NMR spectra) in addition to benzyl ketones but attempts to isolate these through flash column chromatography were not successful. Despite these drawbacks, this was the first report of achieving C and O-benylation products resulting from Pd-catalyzed DcB.



The formation of C- and O-bound 4-quinolinyll compounds (**56h** and **58**) suggests that the enolate was not bound to the metal center. The formation of freely diffusing enolates in Pd-catalyzed DcA of allyl β -ketoesters has been suggested based on crossover experiments.¹⁷ The ability of enolates to diffuse in the reaction system after decarboxylation allows the preformed enolate to be intercepted with other external pronucleophiles which could couple instead to Pd- π -allyl complex resulting in formation of newly functionalized allyl compounds instead of expected allyl ketones.³⁸ In terms of DcB, this was shown through DcB of **55** in the presence of dimethylmalonate which gave a mixture of expected 1-naphthyl ketone **55a** and α -1-naphthyl malonate **22a**. (eq. 53)

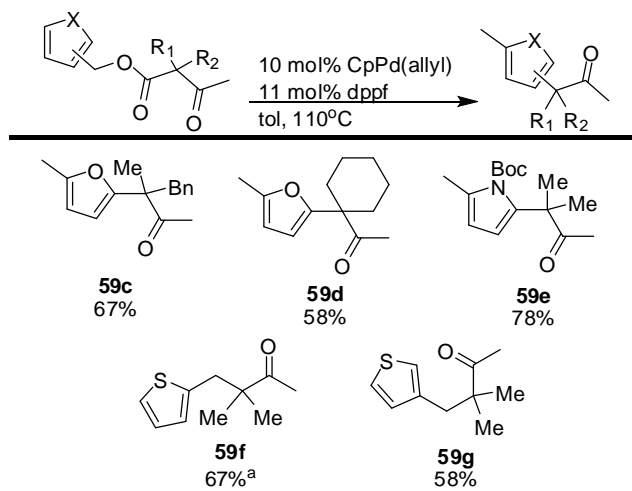


When α -dimethyl-2-furylmethyl β -ketoester **59** was treated with CpPd(allyl)-dppf catalyst, the formation of anticipated α -dimethyl-2-furyl ketone **59a** did not occur but rather an isomeric 2-dimethyl-5-methyl ketone **59b** was observed and isolated (eq. 54). The formation of aryl ketone **59b** instead of benzyl ketone **59a** was also observed in the DcB of 2-furylmethyl cyanoacetate with Pd(PPh₃)₄ (eq. 55).³⁹ When a bidentate ligand was used, benzyl nitrile was observed. Interestingly, Chruma showed that the DcB of 2-furyl-diphenylglycinate imine gave benzyl imine rather than aryl imine in the presence of bidentate ligand (eq. 56).⁴⁰



When **59** was treated with Pd(PPh₃)₄, **59b** was isolated in just 29% yield. The remaining mass balance was made up of **59a** and other unknown side products which was difficult to separate. Despite the roadblock, we could confirm that **59a** was indeed present in the reaction based on the ¹H NMR spectrum of the crude material. Attempts to isolate **59a** using other Pd-monodentate ligand catalysts regrettably gave only the starting material. Nevertheless, we briefly explored the scope of arylation with other five-membered heterocycles (Scheme 54). In addition to furan, the N-Boc pyrrole also gave the arylated ketone in high yield. When thiophene was used, benzylation was predominantly observed.

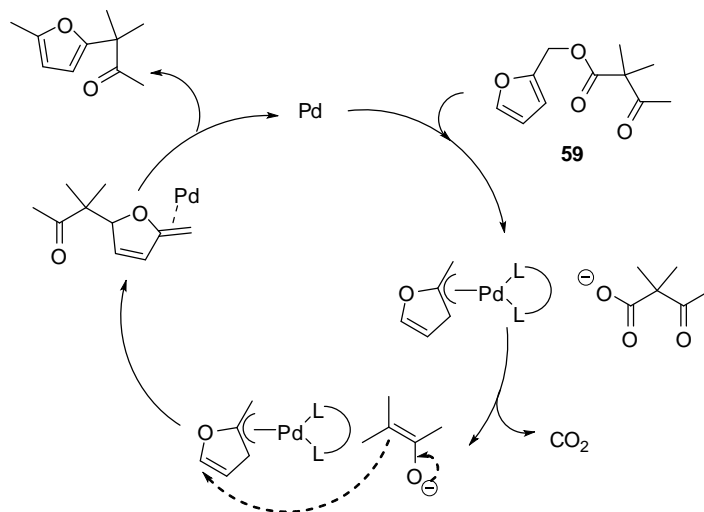
Scheme 54.



^a Two isomers of aryl-thiophenyl ketone were also isolated in 5% combined yield.

Recio and Tunge proposed in the DcB of α -disubstituted 2-furyl cyanoacetates that arylation is favored over benzylation when using monodentate ligand because of the availability of an open coordination site in the Pd- π -benzyl complex for the ketimine to access (Scheme 21).³⁹ Based on the results in Scheme 54, the formation of arylation products would possibly indicate that the enolate attacks the 5-position of the Pd-furyl complex. A plausible mechanism can be envisioned such that oxidative addition of Pd to **59** generates η^3 -Pd-furyl complex and β -ketocarboxylate. Decarboxylation occurs to generate the free enolate. Since both C-2 and C-6 positions of η^3 -furyl-Pd complex is blocked by the bidentate ligand, the free enolate attacks the C-5 position instead (Scheme 55). Rearomatization of dihydrofuryl ketone after nucleophilic attack occurs to generate the aryl ketone.

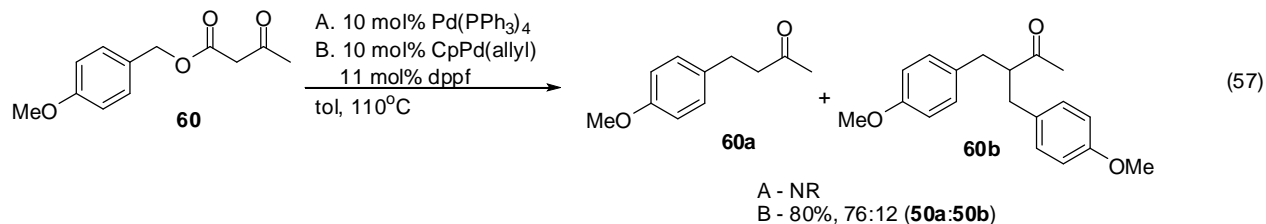
Scheme 55.



2.4 Development of DcB of simple benzyl ketones

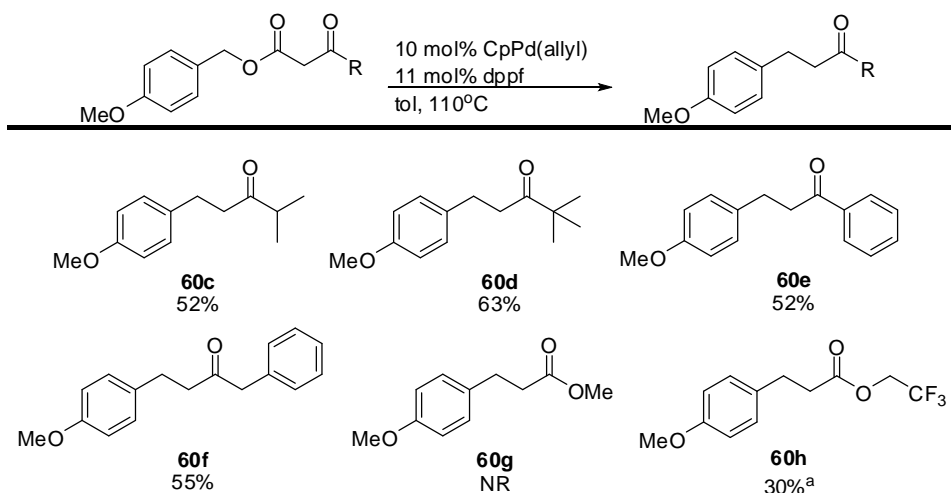
2.4.1 DcB of unsubstituted β -ketoesters

Having successfully developed a DcB methodology of benzyl-fused ketones, we turned our attention towards the initial goal of this research, which was developing DcB of simple benzyl esters. When *p*-methoxybenzyl β -ketoester **60** was treated with $\text{Pd}(\text{PPh}_3)_4$, benzylation did not occur. Other Pd/ligand combinations were also tried but they also failed to catalyze DcB. When $\text{CpPd}(\text{allyl})$ and dppf catalyst was used however, DcB occurred giving the expected mixture of **60a** and dibenzyl ketone **60b** in 80% combined yield (eq. 57). It appears that the combination of this new Pd catalyst along with a more electron-rich phosphine ligand compared to PPh_3 allowed the formation of Pd- π -benzyl species.



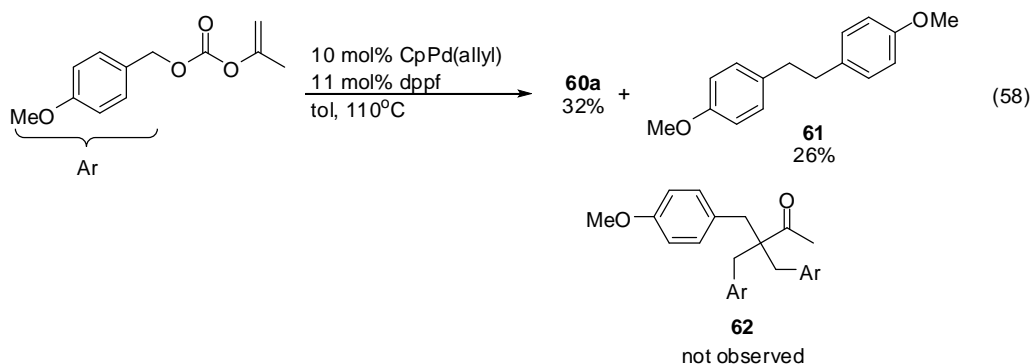
The utility of this catalyst with other unsubstituted *p*-methoxybenzyl β-ketoesters was explored (Scheme 56). A variety of *p*-methoxybenzylalkyl and aryl ketones can be accessed in good to high yields. Similar to the benzylation of benzo-fused ketones, the formation of **60f** implies that DcB of simple benzyl ketones is regiospecific, the benzyl moiety adds to the carbon at which the carboxylate was once located, indicating that isomerization of kinetic enolate to thermodynamic enolate does not occur (eq. 49). While the catalyst failed the DcB of *p*-methoxy-methylbenzyl diester to give *p*-methoxybenzyl-methyl ester **60g**, a trifluoroethyl substituent did allow DcB to occur giving the desired ester **60h** albeit in low yield.

Scheme 56.



^a Di- and tribenzyl trifluoromethyl ester were also isolated in 10% and 16% respectively.

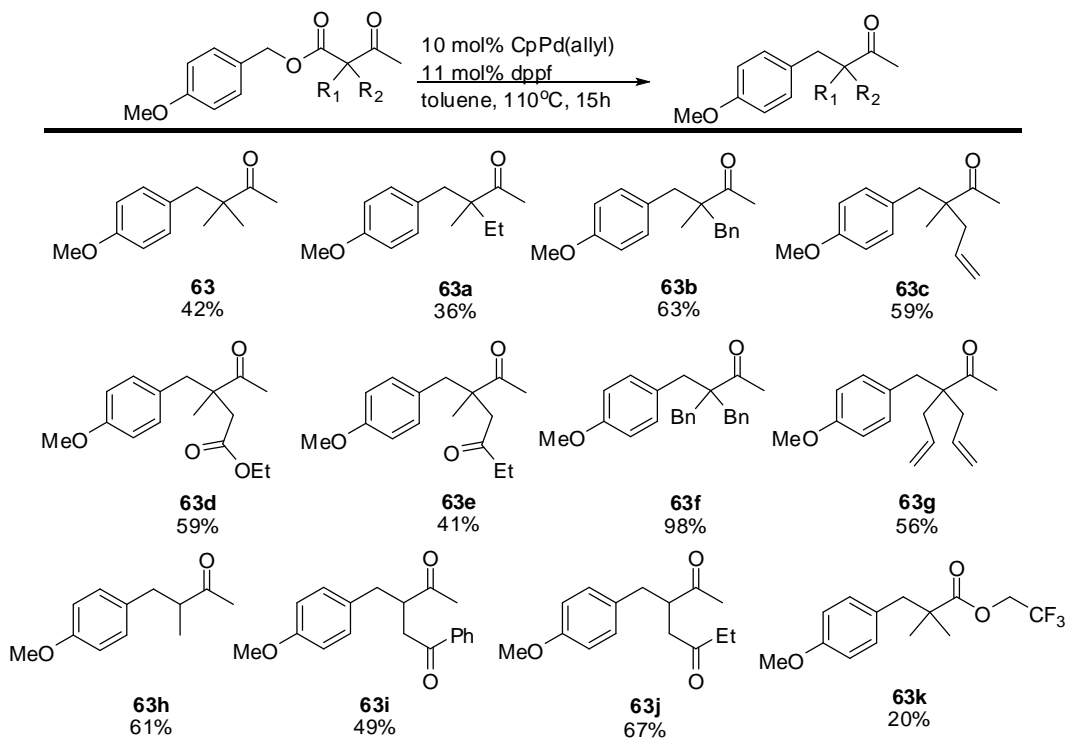
When *p*-methoxybenzyl enol carbonate was allowed to react under identical conditions, **60a** was also isolated in 32% yield along with unexpected bibenzyl **61** (eq. 58). In this case, formation of tribenzyl ketone **62** was not observed in contrast with 1-naphthyl enol carbonate (eq. 47). The formation of **61** could possibly come from ligand exchange between two Pd-benzyl-enolate species, followed by reductive elimination. Based on this intriguing result and the DcB of 1-naphthyl enol carbonate, it appears that the mechanism of DcB of simple benzyl carbonate may be different than naphthyl enol carbonate.



2.4.2 DcB of α -substituted β -ketoesters

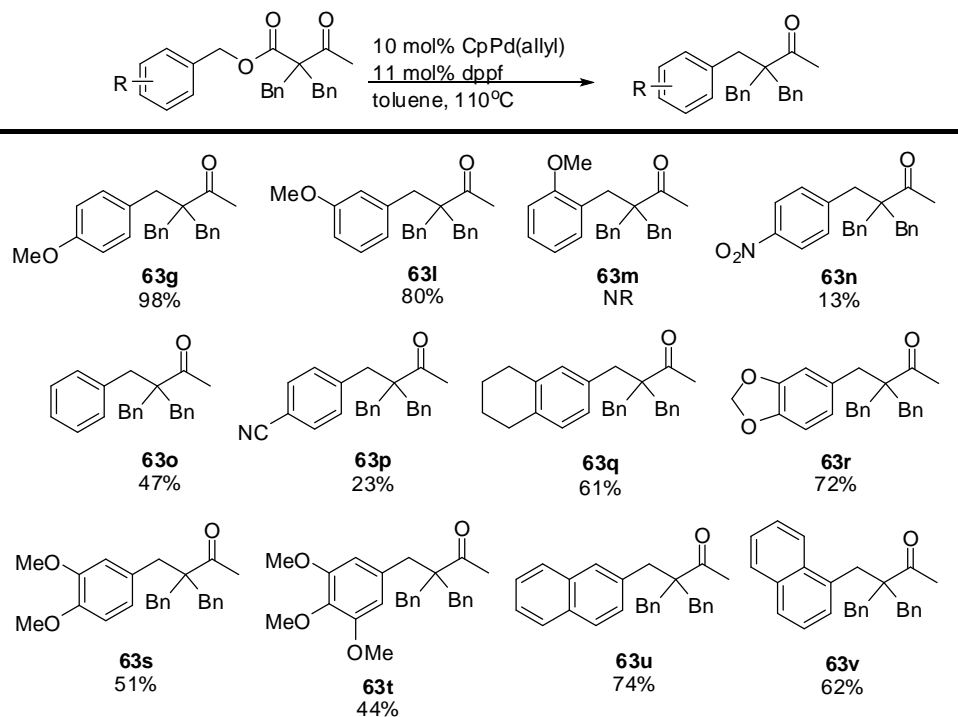
We then looked into the DcB of α -substituted simple benzyl β -ketoesters. We were pleased that a variety of α -substituted *p*-methoxybenzyl ketones can be accessed in moderate to high yields (Scheme 57). In addition, benzyl ketones containing an alkyl or ketone-containing α -substituent are compatible with benzylation. While an α -dimethyl-*p*-methoxybenzyl ketone gave benzylation in moderate yield, the α,α -dibenzyl-*p*-methoxybenzyl ketone gave the best benzylation yield. Increasing the size of the α -substituent improved the benzylation. Based on these results, it appears that the steric bulk of the enolate in relation to Pd- π -benzyl complex has significant effect on benzylation.

Scheme 57.



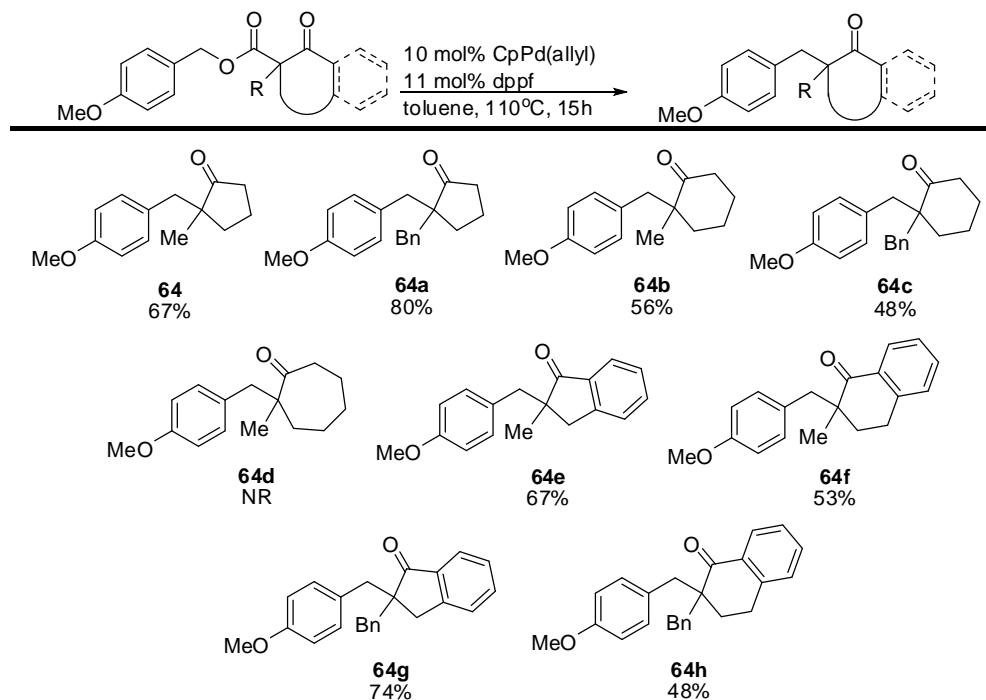
The high yield of **63f** prompted us to briefly look into the electronics of the benzyl ring towards DcB. Previous reports indicated that the presence of EDG gave high yielding benzylations than those with an EWG. Using the parent β -ketoester of **63f** as the model, a variety of EDG and EWG-substituted α -dibenzyl β -ketoesters were prepared. Consistent with earlier reports, the benzylation yield decreases dramatically for benzyl substrates containing an EWG group **63n**, **63p** (Scheme 58). The position of the benzyl substituent also affected the benzylation. While *m*-methoxy substituent **63l** gave a lower benzylation yield than **63f**, an *o*-methoxy substituent **63m** completely shut down the benzylation. The presence of two or more methoxy substituents in the ring had also significant effect in benzylation. The low yield of **63u** and **63v** compared to **63f** was due to other unknown side products present in the reaction mixture.

Scheme 58.



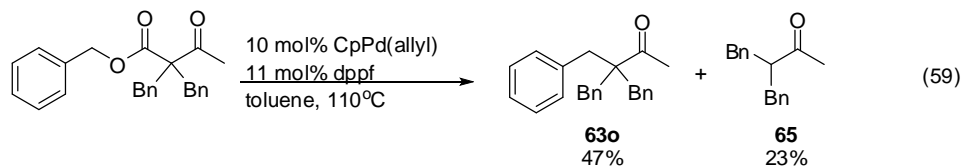
We also expanded the scope of benzylation towards cyclic ketones. In addition to 1-naphthylmethyl α -substituted cyclic ketones (Scheme 52), a variety of *p*-methoxybenzyl cyclic β -ketoesters underwent DcB giving *p*-methoxybenzyl cyclic ketones in good yields (Scheme 59). Increasing the ring size of the cyclic ketone decreased the benzylation yield. Similar to acyclic ketones (Scheme 57), the use of more bulky α -substituent gave higher benzylation yields regardless of the ring size. Other substrates that incorporate indanone and tetralone moieties were also compatible with DcB.

Scheme 59.



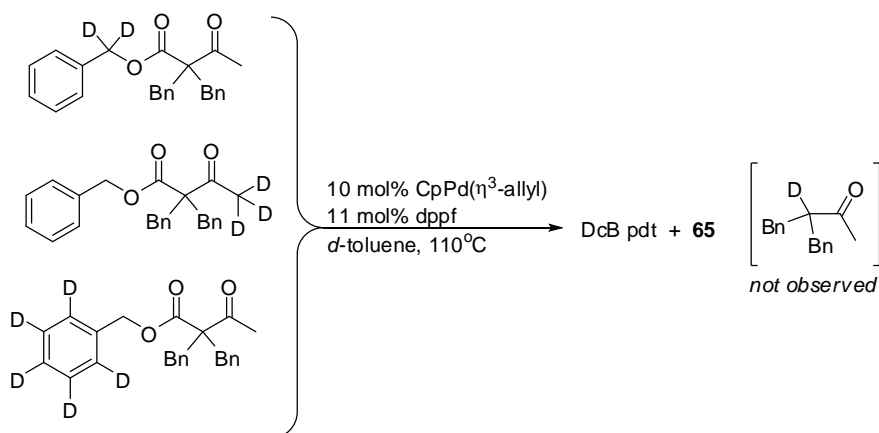
2.4.3 Efforts towards elucidating the source of protonation

During the DcB of α,α -dibenzyl-benzyl β -ketoester, we were able to isolate benzyl ketone **63o** along with dibenzyl acetone **65** (eq. 59). The generation of **65** must come from protonation of the enolate during the reaction. The same phenomenon was also observed in the DcB of α -substituted naphthyl ketones (Schemes 49 and 50). Based on these results, we were curious to identify the proton source in the reaction that could be responsible for enolate protonation.



To potentially shed light on this intriguing problem, deuterium-labeling experiments were performed hoping that a deuterium coming from different positions of the benzyl β -ketoester would be abstracted by the enolate to generate a D-labeled side product. In this regard, three separate α,α -dibenzyl benzyl β -ketoesters labeled at different positions were independently prepared and treated with Pd (Scheme 60). After the reaction proceeded, each of the crude spectra was compared to the spectrum of **65** to determine if deuterium scrambling took place. Based on their spectra, while all three D-labeled benzyl substrates indicated benzylation, the product did not show deuterium incorporation. While these results were disappointing, we speculated that the proton source could probably come from the dppf ligand.

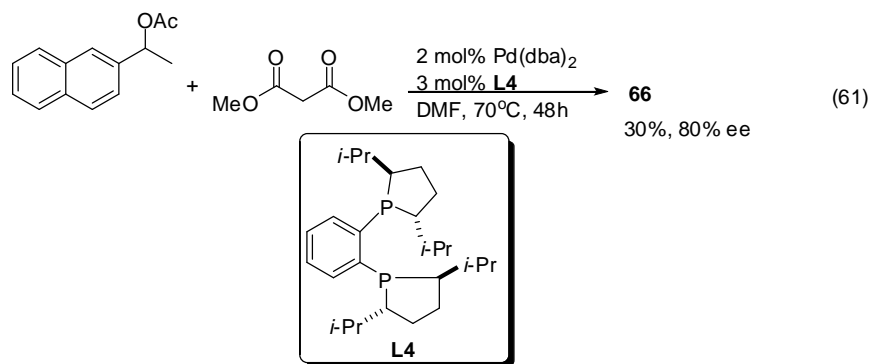
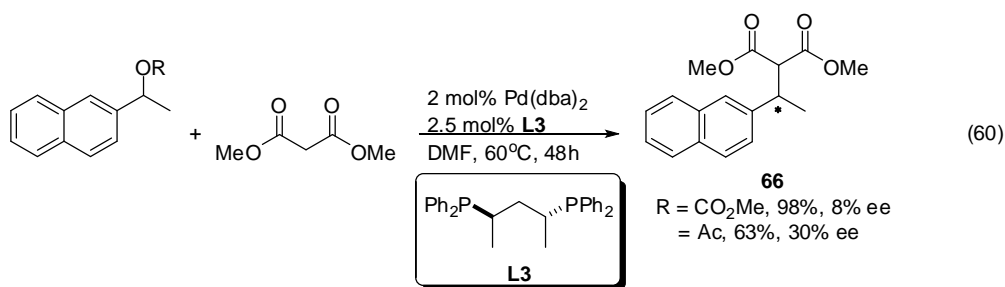
Scheme 60.



2.5 Efforts towards asymmetric benzylation

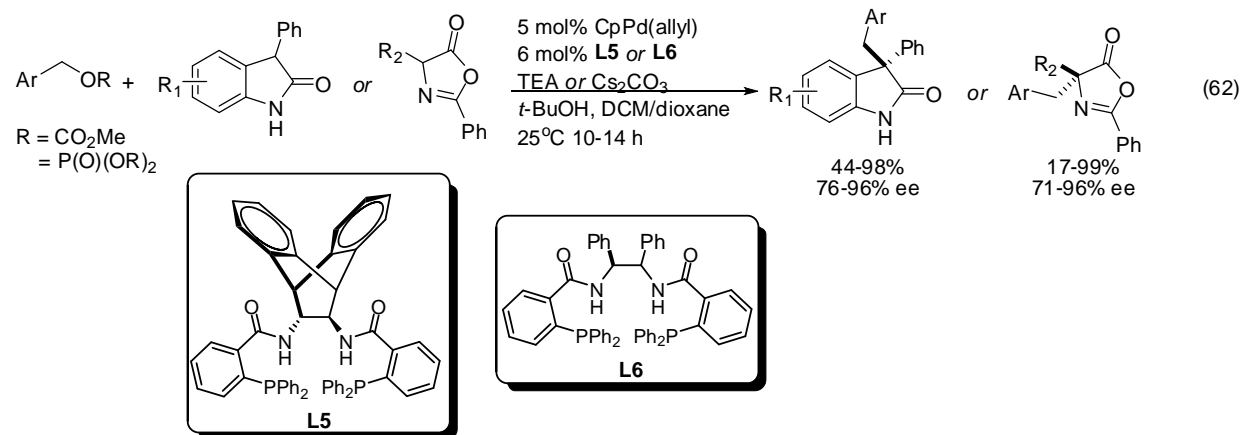
Given the success in developing a method of constructing α -substituted simple and fused-benzyl ketones, we wanted to expand the current scope of DcB of benzyl β -ketoesters towards asymmetric benzylation. While Pd-catalyzed asymmetric benzylations using secondary benzyl

halide as electrophiles have been reported,⁴¹ the use of benzyl acetate and carbonate remain limited. The first reported asymmetric benzylation was disclosed by Legros and coworkers in 1995.⁴² They have shown that 2-naphthyl methyl carbonate underwent benzylation with sodium dimethylmalonate using Pd(dba)₂ and BDPP ligand giving the desired α -substituted 2-naphthyl methyl dimethylmalonate **66** in high yield yet very low ee (eq. 60). When the carbonate LG was replaced with acetate, the yield significantly decreased but the observed enantioselectivity slightly improved. Ten years after the seminal publication, the same group reported a greatly improved enantioselectivity of **66** using DUPHOS ligand albeit in low isolated yield (eq. 61).⁴³ In these reactions, the asymmetry originates at the benzyl carbon.



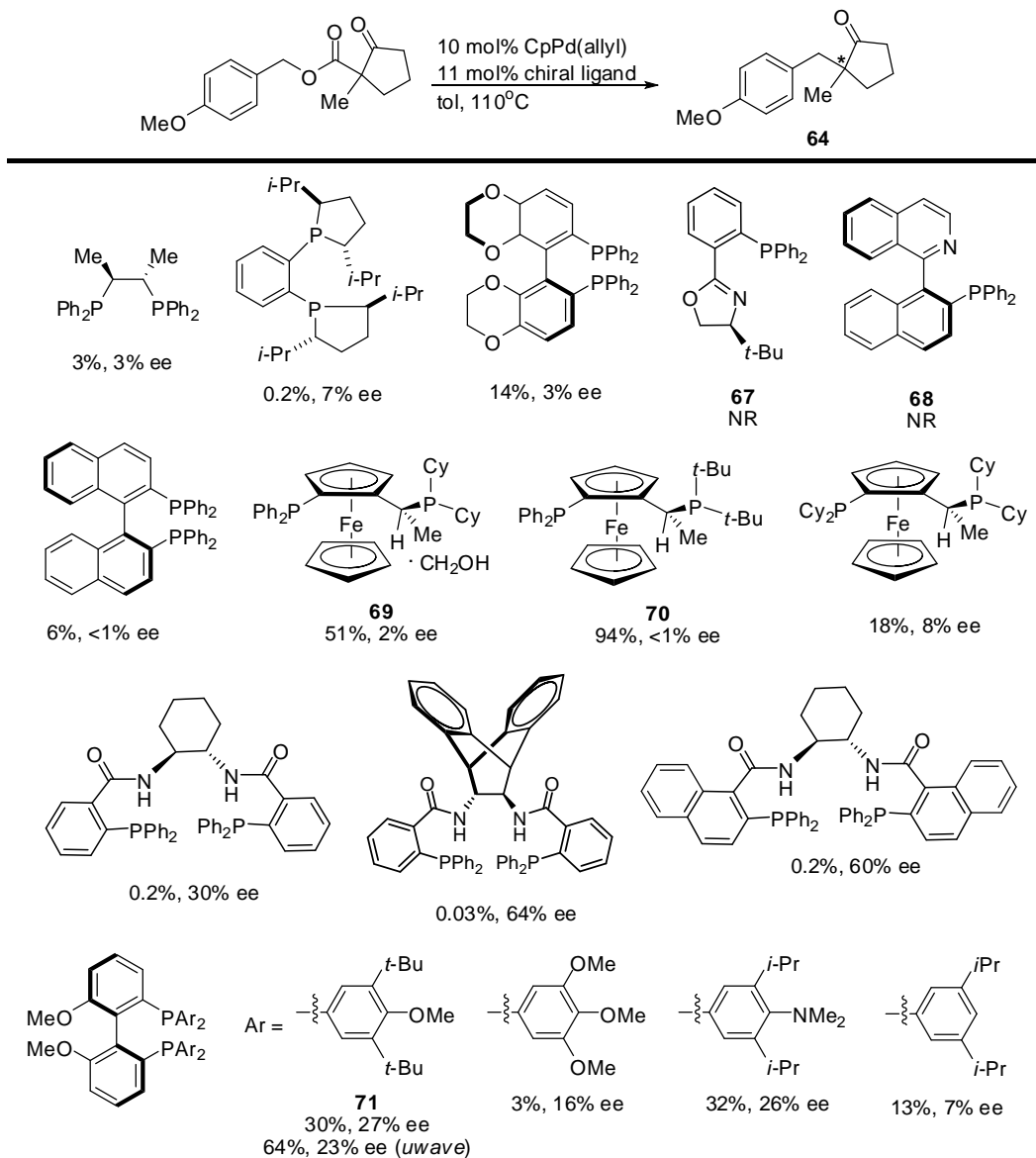
Recently, Trost and Czabaniuk reported the asymmetric benzylation using benzyl carbonate and phosphates with oxindoles and azalactones in the presence of anthracenyl or dibenzylamino Trost-type ligand in good to high yields and enantioselectivities (eq. 62).⁴⁴ In these reactions, benzylation was achieved in the presence of superstoichiometric bases and t-

BuOH additives. In contrast with the asymmetric benzylation performed by Legros and coworkers, the asymmetry is set at the α -carbon.



Based on these results, we pursued the development of an asymmetric DcB methodology of benzyl ketones. We used **64** as the model compound for asymmetric DcB analysis. Moreover, the use of **64** was also inspired by the asymmetric DcA of allyl β -ketoesters (Chapter 2.2). Using CpPd(allyl) as the Pd source, a variety of chiral ligands were screened towards the asymmetric DcB of α -methyl-*p*-methoxybenzyl cyclopentanone ester (Scheme 61). The percent conversion and ee's of each reaction were determined using chiral stationary phase GC and compared to the data of racemic compound.

Scheme 61.

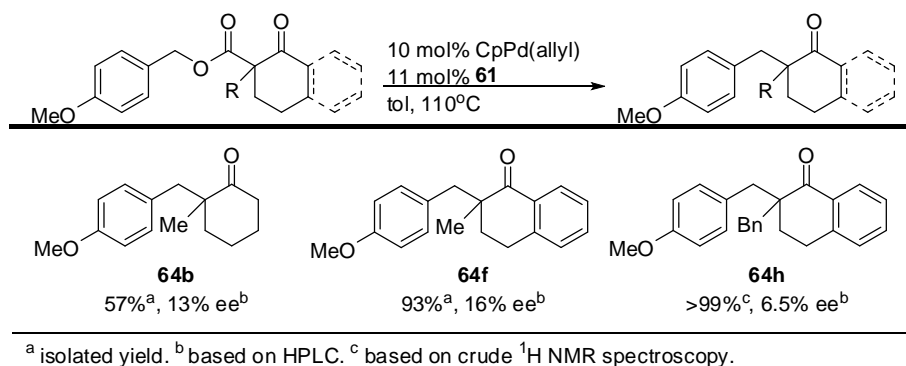


Percent values (percent conversions and ee) were obtained based from chiral GC.

The results of asymmetric DcB attempt towards **64** were disappointing but promising. It was surprising that chiral ligands such as *t*-BuPHOX **67** and QUINAP **68** which gave high enantioselectivities in DcA of allyl β -ketoesters^{29,30a} were unreactive. When Trost ligands were tried, a very low conversion despite moderate enantioselectivity was observed. The DUPHOS ligand that was reported by Legros that gave high enantioselectivity yet low benzylation yield

sadly gave even lower ee and conversion. Since dppe was the ligand used in DcB of racemic simple benzyl ketones, chiral ferrocene-derived (Josiphos) ligands were also tried. While **69** gave a moderate conversion and poor ee, the use of **70** gave a significant improvement in product formation, the difference between two ligands was the backbone of the phosphine ligand in which the latter has two more bulky *t*-Bu substituents compared to the former which has two cyclohexyl substituents. Unfortunately, both ee's were very low. When **70** was also tried with other benzyl substrates, product formation occurred in good to high yields but all gave low ee's (Scheme 62). When a methoxy-biphenyl compound containing electron rich and bulky *t*-Bu groups **71** ligand was tried, a slightly improved ee was obtained in contrast with ferrocene-derived ligands yet low product conversion. When the reaction was run in a microwave, product formation improved yet the ee was similar to the “un-microwaved” reaction. Despite these unfortunate results, one could conclude that higher enantioselectivity can be achieved using phosphine ligands containing bulky *t*-Bu and EDG substituents.

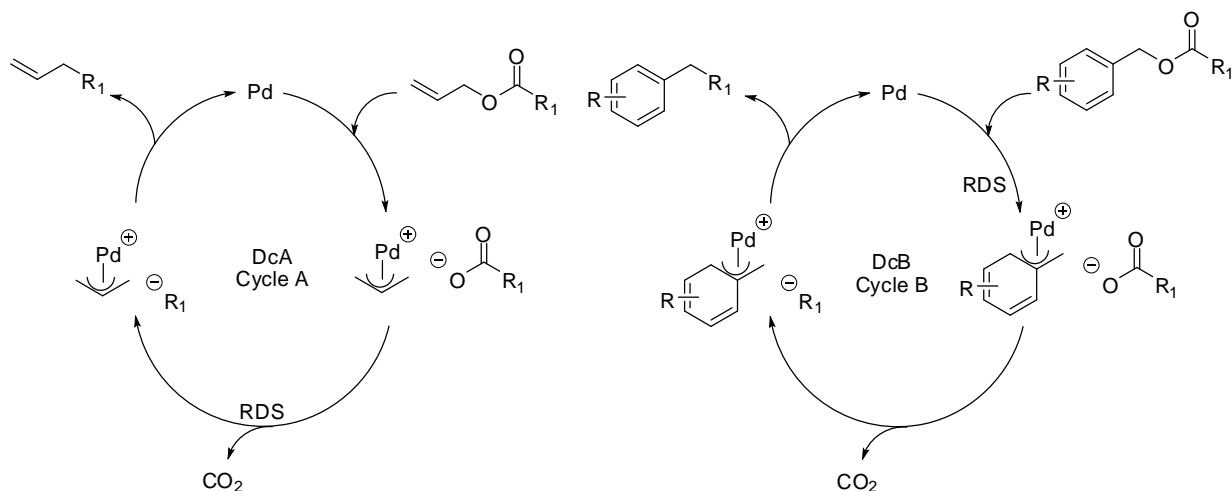
Scheme 62.



2.6 Mechanistic insights

It is likely that the mechanism of DcB of β -ketoesters should be similar to the DcA mechanism of allyl- β -ketoesters (Chapter 2.2) except the origin of Pd electrophile. Despite these similarities, it is interesting that all benzylation reactions of benzyl β -ketoesters require higher temperatures to achieve decarboxylation compared to DcA of allyl β -ketoesters that took place typically at room temperature. Their temperature differences potentially reflect a change in the rate-determining step of DcB process.¹⁷ While it has been reported that decarboxylation is the rate-determining step in the DcA of allyl β -ketoesters (Cycle A, Scheme 63), the decarboxylation might not be the slowest step in DcB of benzyl β -ketoesters but rather the ionization step leading to oxidative addition (Cycle B, Scheme 63). As a result, the ease in generation of Pd-electrophile follows a trend such that an allyl-LG generates the Pd species much faster than naphthylmethyl-LG, followed by EDG-containing simple benzyl-LG.

Scheme 63.



2.7. Conclusion

We have shown that the functionalization of simple and benzo-fused compounds with enolates via decarboxylation requires only catalytic Pd to generate the reactive η^3 -benzyl-Pd enolate species *in situ* without the need of base and other additives. In addition, a variety of non-stabilized enolates can be accessed, thus expanding the scope of enolate benzylation from previously reported stabilized nucleophiles. C-C bond formation takes place at the site where the carboxylate group was once located. This allows site-specific generation of enolates which are difficult to synthesize using classical acid-base chemistry. While certain benzyl β -ketoesters require a different kind of Pd catalyst, their reactivity allows formation of benzyl ketones (and esters) in good to high yields. These reactions significantly depend on the electronics of the aromatic ring, the position of the benzyl moiety near to an electronic substituent or heteroatom, and steric bulk of enolate. The DcB reactions of simple and benzo-fused β -ketoesters are regioselective in which enolate isomerization does not occur. In some substrates, some notable interesting compounds have been isolated. For the first time, a tribenzyl ketone and bibenzyl can be isolated using benzyl enol carbonate in contrast with benzyl β -ketoester suggesting that their mechanisms are not similar. Also, depending on appropriate reaction conditions, benzylation utilizing heteroaromatic compounds occurs giving C-benzylation, O-benzylation, or arylation depending on the nature of heterocycle. While current results did not provide high asymmetric benzylation, a lot of information can be gained from the ligands that were tried, particularly in terms of possibly designing chiral phosphine ligands that contain bulky and electron-rich substituents. Finally, the developed methodology can be applied in the synthesis of NSAID Nabumetone, thus harnessing the power of decarboxylative benzylation in constructing benzyl compounds which are relevant in medicinal chemistry.

2.8 References

1. (a) Caine, D. "Alkylation and related reactions of ketones and aldehydes via metal enolates" In *Carbon-Carbon Bond Formation*, Vol. 1, Augustine, R. L., Ed.; Marcel Dekker, New York, **1979**, Chapter 2.; (b) Carey, F. A.; Sundberg, R. J. *Advanced Organic Chemistry Part B: Reactions and Synthesis*, 4th ed.; Springer Science, **2001**, Chapter 1.
2. Walker, M. A.; Johnson, T.; Ma, Z.; Banville, J.; Remillard, R.; Kim, O.; Zhang, Y.; Staab, A.; Wong, H.; Torri, A.; Samanta, H.; Lin, Z.; Deminie, C.; Terry, B.; Krystal, M.; Meanwell, N. "Triketoacid inhibitors of HIV-integrase: A new chemotype useful for probing the integrase pharmacophore" *Bioorg. Med. Chem. Lett.* **2006**, *6*, 2920–2924.
3. (a) Tsuji, J.; Takahashi, H.; Morikawa, M. "Organic synthesis by means of noble metal compounds. XVII. Reaction of π -allylpalladium chloride with nucleophiles" *Tetrahedron Lett.* **1965**, *6*, 4387–4388. (b) Takahashi, K.; Miyake, A.; Hata, G. "Palladium-catalyzed exchange of allylic groups of ethers and esters with active hydrogen compounds. II" *Bull. Chem. Soc. Jpn.* **1972**, *45*, 230–236. (c) Tsuji, J. "Palladium-catalyzed nucleophilic substitution involving allylpalladium, propargylpalladium, and related derivatives" In *Handbook of Organopalladium Chemistry for Organic Synthesis*; Negishi, E-i.; de Meijere, A., Eds.; John Wiley & Sons, Inc.; New York, **2002**; Volume 2, pp. 1669–2027.
4. Legros, J.-Y.; Fiaud, J.-C. "Palladium-catalyzed nucleophilic substitution of naphthylmethyl and 1-naphthylethyl esters" *Tetrahedron Lett.* **1992**, *33*, 2509–2510.
5. Baird, J. M.; Kern, J. R.; Lee, G. R.; Morgans, Jr., D. J.; Sparacino, M. L. "An investigation of the palladium-catalyzed, formate mediated hydroxycarbonylation of optically active 1-arylethyl esters" *J. Org. Chem.* **1991**, *56*, 1928–1933.
6. (a) Joule, J. A.; Mills, K. *Heterocyclic Chemistry. Fifth Edition*; John Wiley & Sons, Inc.; New York, **2010**, pp. 5–18. (b) Lowry, T. H.; Richardson, K. S. *Mechanism and Theory in Organic Chemistry. Second Edition*; Harper and Row, **1981**, pp. 109–112.
7. Wheland, G. W. "The resonance energies of unsaturated and aromatic molecules" *J. Am. Chem. Soc.* **1941**, *63*, 2025–2027.
8. Legros, J.-Y.; Primault, G.; Toffano, M.; Rivière, M.-A.; Fiaud, J.-C. "Reactivity of quinoline- and isoquinoline-based heteroaromatic substrates in palladium(0)-catalyzed benzylic nucleophilic substitution" *Org. Lett.* **2000**, *2*, 433–436.
9. Primault, G.; Legros, J.-Y.; Fiaud, J.-C. "Palladium-catalyzed benzylic-like nucleophilic substitution of benzofuran-, benzothiophene- and indole-based substrates by dimethyl malonate anion" *J. Organomet. Chem.* **2003**, *687*, 353–364.

10. Legros, J.-Y.; Toffano, M.; Fiaud, J.-C. "Palladium-catalyzed substitution of esters of naphthylmethanols, 1-naphthylethanols, and analogues by sodium dimethyl malonate. Stereoselective synthesis from enantiomerically pure substrates" *Tetrahedron* **1995**, *51*, 3235–3246.
11. Kuwano, R.; Kondo, Y.; Matsuyama, Y. "Palladium-catalyzed nucleophilic benzylic substitutions of benzylic esters" *J. Am. Chem. Soc.* **2003**, *125*, 12104–12105.
12. (a) Hartwig, J. F. *Organotransition Metal Chemistry. From Bonding to Catalysis*, University Science Books, **2010**, p. 312. (b) Birkholz, M.-N.; Freixa, Z.; Leeuwen, P. W. N. M. "Bite angle effects of diphosphines in C-C and C-X bond forming cross-coupling reactions" *Chem. Soc. Rev.* **2009**, *28*, 1099–1118.
13. Kuwano, R.; Kondo, Y. "Palladium-catalyzed benzylation of active methine compounds without additional base: Remarkable effect of 1,5-cyclooctadiene" *Org. Lett.* **2004**, *6*, 3545–3547.
14. Sisak, A.; Ungávrý, F.; Kiss, G. "The formation of catalytically active species by the reduction of palladium carboxylate phosphine systems: i. Hydrogenations" *J. Mol. Catal.* **1983**, *18*, 223–225.
15. Yokogi, M.; Kuwano, R. "Use of acetate as a leaving group in palladium-catalyzed nucleophilic substitution of benzylic esters" *Tetrahedron Lett.* **2007**, *48*, 6109–6112.
16. Peng, B.; Zhang, S.; Xu, X.; Feng, X.; Bao, M. "Nucleophilic dearomatization of chloromethyl naphthalene derivatives via η^3 -benzylpalladium intermediates: a new strategy for catalytic dearomatization" *Org. Lett.* **2011**, *13*, 5402–5405.
17. Weaver, J. D.; Recio, A., III; Grenning, A. J.; Tunge, J. A. "Transition metal-catalyzed decarboxylative allylation and benzylation reactions" *Chem. Rev.* **2011**, *111*, 1846–1913.
18. (a) Shimizu, I.; Yamada, T.; Tsuji, J. "Palladium-catalyzed rearrangement of allylic esters of acetoacetic acid to give γ,δ -unsaturated methyl ketones" *Tetrahedron Lett.* **1980**, *21*, 3199–3202. (b) Tsuda, T.; Chujo, Y.; Nishi, S.; Tawara, K.; Saegusa, T. "Facile generation of a reactive palladium(II) enolate intermediate by the decarboxylation of palladium(II) β -ketocarboxylate and its utilization in allylic acylation" *J. Am. Chem. Soc.* **1980**, *102*, 6381–6384.
19. (a) Mohr, J. T.; Stoltz, B. M. "Enantioselective Tsuji allylations" *Chem. Asian. J.* **2007**, *2*, 1476–1491. (b) Mohr, J. T.; Ebner, D. C.; Stoltz, B. M. "Catalytic enantioselective stereoablative reactions: an unexploited approach to enantioselective catalysis" *Org. Biomol. Chem.* **2007**, *5*, 3571–3576. (c) You, S.-L.; Dai, L.-X. "Enantioselective palladium catalyzed decarboxylative allylic alkylations" *Angew. Chem. Int. Ed.* **2006**, *45*, 5246–5248.
20. Burger, E. C.; Tunge, J. A. "Asymmetric allylic alkylation of ketone enolates: an asymmetric Claisen surrogate" *Org. Lett.* **2004**, *6*, 4113–4115.

21. Tardibono, Jr. L. P.; Patzner, J.; Cesario, C.; Miller, M. J. "Palladium-catalyzed decarboxylative rearrangements of allyl 2,2,2-trifluoroethyl malonates: direct access to homoallylic esters" *Org. Lett.* **2009**, *11*, 4076–4079.
22. Tunge, J. A.; Burger, E. C. "Transition-metal catalyzed decarboxylative additions of enolates" *Eur. J. Org. Chem.* **2005**, *9*, 1715–1726.
23. (a) Tsuda, T.; Okada, M.; Nishi, S.; Saegusa, T. "Palladium-catalyzed decarboxylative allylic alkylation of allylic acetates with β -ketoacids" *J. Org. Chem.* **1986**, *51*, 421–426. (b) Fiaud, J.-C.; Aribé-Zouieche, L. "Stereochemistry in the palladium-catalyzed rearrangement of some cyclohex-2-enyl acetoacetates" *Tetrahedron Lett.* **1982**, *23*, 5279–5282. (c) Bäckvall, J.-E.; Nordberg, R. E.; Vågberg, J. "Stereochemistry of allylic carbon-oxygen and carbon-carbon bond formation in palladium-catalyzed decarboxylation of allylic carbonates and acetoacetates" *Tetrahedron Lett.* **1983**, *24*, 411–412.
24. Burger, E. C. "The development of catalytic, asymmetric decarboxylative coupling reactions" PhD Dissertation, The University of Kansas, **2007**, 241 pages.
25. Tsuji, J. Minami, I.; Shimizu, I. "Palladium-catalyzed allylation of ketones and aldehydes via allyl enol carbonates" *Tetrahedron Lett.* **1983**, *17*, 1793–1796.
26. Shimizu, I.; Ishii, H. "Synthesis of α -fluoroketones based on palladium-catalyzed decarboxylation reactions of allyl β -ketocarboxylates" *Tetrahedron*, **1994**, *50*, 487–495.
27. Nakamura, M.; Hajra, A.; Endo, K.; Nakamura, E. "Synthesis of chiral α -fluoroketones through catalytic enantioselective decarboxylation" *Angew. Chem. Int. Ed.* **2005**, *44*, 7248–7251.
28. Kuwano, R.; Ishida, N.; Murakami, M. "Asymmetric Carroll rearrangement of allyl α -acetamido- β -ketocarboxylates catalyzed by a chiral palladium complex" *Chem. Commun.* **2005**, 3951–3952.
29. Mohr, J. T.; Behenna, D. C.; Harned, A. M.; Stoltz, B. M. "Deracemization of quaternary stereocenters by Pd-catalyzed enantioconvergent decarboxylative allylation of racemic β -ketoesters" *Angew. Chem. Int. Ed.* **2005**, *44*, 6924–6927.
30. Burger, E. C.; Barron, B. R.; Tunge, J. A. "Catalytic asymmetric synthesis of cyclic α -allylated α -fluoroketones" *Synlett* **2006**, 2824–2826.
31. Yan, B.; Spilling, C. D. "Synthesis of cyclopentenones via intramolecular HWE and the palladium-catalyzed reactions of allylic hydroxyl phosphonate derivatives" *J. Org. Chem.* **2008**, *73*, 5385–5396.

32. Torregrosa, R. R. P.; Ariyaratna, Y.; Chattopadhyay, K.; Tunge, J. A. "Decarboxylative benzylations of alkynes and ketones" *J. Am. Chem. Soc.* **2010**, *132*, 9280–9282.
33. Carroll, M. "Addition of β,γ -unsaturated alcohols to the active methylene group. Part II. The action of ethylacetoacetate on cinnamyl alcohol and 36. Phenylvinylcarbinol." *J. Chem. Soc.* **1940**, 1266–1268.
34. (a) Goudie, A. C.; Gaster, L. M.; Lake, A. W.; Rose, C. J.; Freeman, P. C.; Hughes, B. O.; Miller, D. J. *J. Med. Chem.* **1978**, *21*, 1260–1264. (b) Hedner, T.; Samuelsson, O.; Währborg, P.; Wadenvik, H.; Ung, K.A.; Ekblom, A. *Drugs* **2004**, *64*, 2315–2343.
35. Bays, J. P. "The phenylacetone dianion: alkylation with iodomethane" *J. Org. Chem.* **1978**, *43*, 38–43.
36. (a) Weaver, J. D.; Tunge, J. A. "Decarboxylative allylation using sulfones as surrogates of alkanes" *Org. Lett.* **2008**, *10*, 4657–4660; (b) Recio III, A.; Tunge, J. A. "Regiospecific decarboxylative allylation of nitriles" *Org. Lett.* **2009**, *11*, 5630–5633.
37. Mandai, T.; Matsumoto, T.; Tsuji, J.; Saito, S. "Highly active Pd(0) catalyst from Pd(OAc)₂-Bu₃P combination in untapped 1:1 ratio: preparation, reactivity, and ³¹P-NMR" *Tetrahedron Lett.* **1993**, *34*, 2513–2516.
38. Lou, S.; Westbrook, J. A.; Schaus, S. E. "Decarboxylative aldol reactions of allyl β -ketoesters via heterobimetallic catalysis" *J. Am. Chem. Soc.* **2004**, *126*, 11440–11441.
39. Recio, A., III; Heinzman, J. D.; Tunge, J. A. "Decarboxylative benzylolation and arylation of nitriles" *Chem. Commun.* **2012**, *48*, 142–144.
40. Fields, W. H.; Chruma, J. J. "Palladium-catalyzed decarboxylative benzylolation of diphenylglycinate imines" *Org. Lett.* **2010**, *10*, 1979–1982.
41. Wong, K. P.; Lau, K. S. Y.; Stille, J. K. "Stereochemistry of oxidative addition of benzyl- α -D-chloride to tetrakis(triphenylphosphine)palladium(0). Direct evidence for configurational inversion at carbon via a nonradical mechanism" *J. Am. Chem. Soc.* **1974**, *96*, 5956–5957. (b) Lau, K. S. Y.; Wong, K. P.; Stille, J. K. "Oxidative addition of benzyl halides to zero-valent palladium complexes. Inversion of configuration at carbon" *J. Am. Chem. Soc.* **1976**, *98*, 5832–5840. (c) Becker, Y.; Stille, J. K. "Stereochemistry of oxidative addition of benzyl- α -D-chloride and bromide to tris(triethylphosphine)palladium(0). Direct observation of optical activity in a carbon-palladium σ -bonded complex" *J. Am. Chem. Soc.*, **1978**, *100*, 838–844. (d) Becker, Y.; Stille, J. K. "The dynamic η^1 - and η^3 -benzylbis(triethylphosphine)palladium(II) cations. Mechanisms of interconversion" *J. Am. Chem. Soc.*, **1978**, *100*, 845–850.
42. Legros, J.-Y.; Toffano, M.; Fiaud, J.-C. "Asymmetric palladium-catalyzed nucleophilic substitution of racemic 1-naphthylethyl esters" *Tetrahedron Asym.* **1995**, *6*, 1899–1902.

43. (a) Assié, M.; Legros, J.-Y.; Fiaud, J.-C. “Asymmetric palladium-catalyzed benzylic nucleophilic substitution: high enantioselectivity with the DUPHOS family ligands” *Tetrahedron Asym.* **2005**, *16*, 1183–1187. (b) Assié, M.; Meddour, A.; Fiaud, J.-C.; Legros, J.-Y. “Enantiodivergence in alkylation of 1-(6-methoxynaph-2-yl)ethyl acetate by potassium dimethyl malonate catalyzed by chiral palladium-DUPHOS complex” *Tetrahedron Asym.* **2010**, *21*, 1701–1708.
44. (a) Trost, B. M.; Czabaniuk, L. C. “Palladium-catalyzed asymmetric benzylation of 3-aryl oxindoles” *J. Am. Chem. Soc.* **2010**, *132*, 15534–15536. (b) Trost, B. M.; Czabaniuk, L. C. “Benzylic phosphates as electrophiles in the palladium-catalyzed asymmetric benzylation of azlactones” *J. Am. Chem. Soc.* **2012**, *134*, 5778–5781.

2.9 Methodology and compound characterizations

General Information

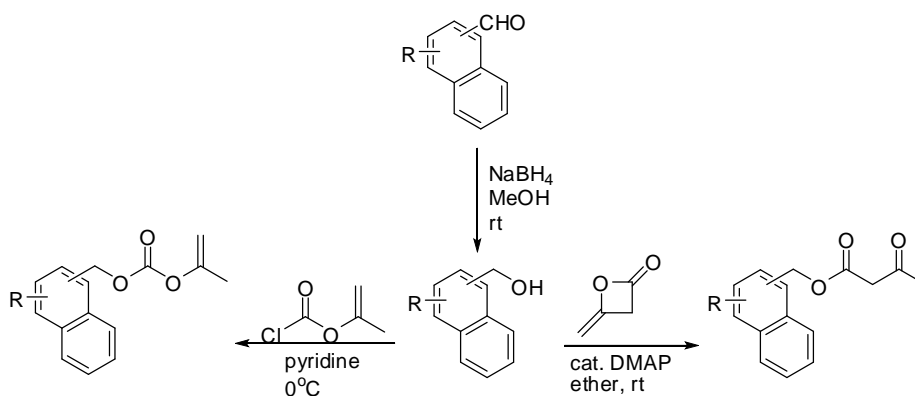
Toluene and THF were dried over sodium in the presence of benzophenone indicator. DCM and Et₂O were dried over activated alumina on a solvent system purchased from Innovative Technologies, Inc. Pd catalysts and ligands were purchased from Strem and Sigma-Aldrich. Other reagents and solvents were also obtained commercially and used without additional purification. K₂CO₃ was activated through microwave prior to use. CpPd(allyl) was prepared according to a literature procedure.¹ The isolated products were purified on silica gel from Sorbent Technologies (40-63 μm particle size, 60 Å porosity, pH 6.5-7.5). The ¹H and ¹³C NMR spectra were obtained on a Bruker Avance 400 or 500 MHz DRX spectrometer and were referenced to residual protio solvent signals. FTIR spectra were acquired on Shimadzu FTIR 8400S spectrometer. HRMS was performed on a LCT Premier TOF mass spectrometer using ESI techniques. Asymmetric analyses were performed via gas chromatography using Shimadzu GC-17A instrument with an attached AOC-20i auto injector and high performance liquid chromatography using Shimadzu SCL-10A VP instrument. Certain reactions that require very high temperatures were ran using Biotage Initiator Microwave Synthesizer equipped with Robot Eight Initiator System. Structural assignments of the isolated compounds were based on ¹H, ¹³C, DEPT 135, COSY and HSQC spectroscopies.

Preparation of Starting Materials

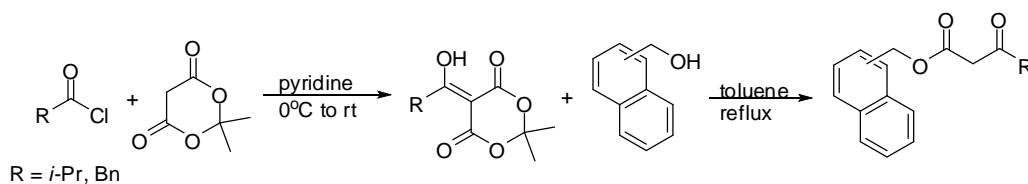
Synthesis of 1- and 2-naphthyl β-ketoesters and 1- and 2-naphthylmethyl enol carbonate

Unsubstituted 1- and 2-naphthylmethyl β-ketoesters were prepared through esterification of 1- and 2-naphthylmethanol with diketene, stabilized with Cu, and catalytic DMAP at room

temperature.² The diketene was added dropwise to prevent rapid exothermic reaction. Other substituted 1- and 2-naphthylmethanols were prepared from NaBH₄ reduction of their parent 1- and 2-naphthaldehyde. The syntheses of 1- and 2-naphthylmethyl enol carbonate were prepared by esterification of 1- and 2-naphthylmethanol and isopropenyl chloroformate.



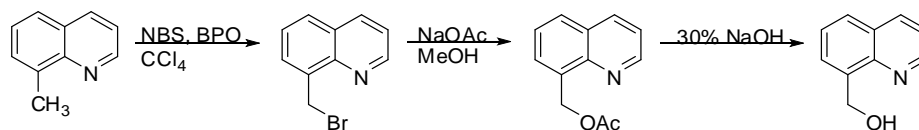
The 1-naphthylmethyl β -ketoester of **47f** and **47g** were prepared by esterification of 1-naphthylmethanol with enol-derived Meldrum acid, which was prepared by addition of isobutyryl chloride or phenylacetyl chloride to Meldrum's acid in pyridine.³ The isolated compound was used immediately without column purification.



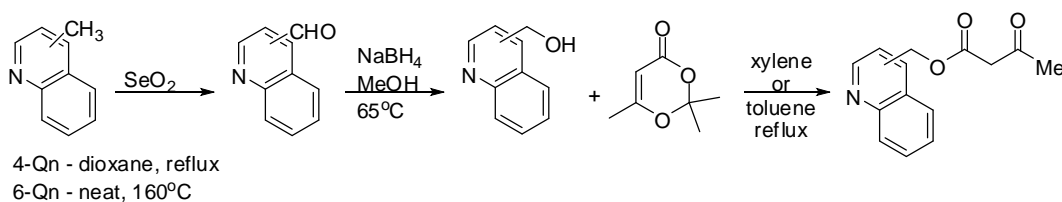
Synthesis of quinolinylmethyl, N-Boc indolylmethyl, furylmethyl, thiophenylmethyl, and N-Boc pyrrolmethyl β -ketoesters

2-, 3-, 4-, 6-, and 8-quinolinylmethyl β -ketoesters were prepared from esterification of 2-, 3-, 4-, 6-, and 8-quinolinylmethanol and 2,2,6-trimethyl-4H-1,3-dioxin-4-one in refluxing xylene.⁴ This procedure was also used in the synthesis of indolylmethyl, furylmethyl,

thiophenylmethyl, and N-Boc pyrrolylmethyl β -ketoesters using toluene as the refluxing solvent. While 2-, 3-, 4-, and 6-quinolinylmethanol were prepared from NaBH_4 reduction of their quinolinyl aldehyde, the 8-quinolinylmethanol, on the other hand, was prepared from 8-methylquinoline in three steps: NBS bromination, OAc substitution, and reduction.⁵

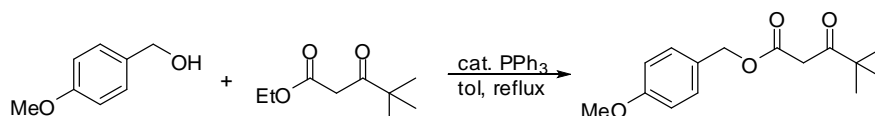


The syntheses of 3-, 4-, and 6-quinolinyl aldehydes were prepared from SeO_2 oxidation of 3-, 4- and 6-methylquinoline.⁶ Oxidations of 4- and 6-methylquinoline with SeO_2 were performed in an oil bath whereas 3-methylquinoline oxidation was performed in a microwave.



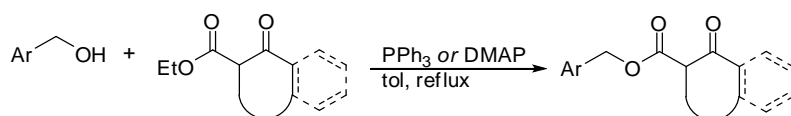
Synthesis of simple-benzyl β -ketoesters

Simple benzyl β -ketoesters were prepared similarly to the preparation of heterocyclic β -ketoesters by esterification of benzyl alcohol and 2,2,6-trimethyl-4H-1,3-dioxin-4-one using toluene in reflux. Other simple benzyl β -ketoesters that contain varied terminal ketone substituents were prepared by esterification of benzyl alcohol with an enol-derived Meldrum's acid. The synthesis of benzyl β -ketoester of **60d** was prepared from transesterification of benzyl alcohol and ethyl oxovalerate with catalytic PPh_3 .⁷



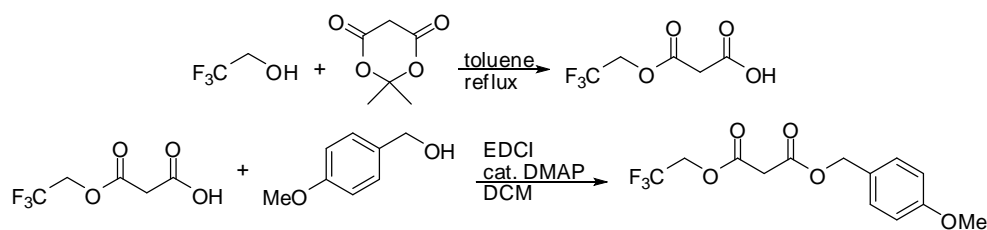
Synthesis of cyclic benzyl β -ketoesters

Cyclic benzyl β -ketoesters of **55i-55m** and **64-64h** were prepared from transesterification of *p*-methoxybenzyl alcohol or 1-naphthalene methanol with ethyl-oxocycloalkane, ethyl-oxocycloindanone, or ethyl-oxocyclohexanone in toluene at reflux with or without catalytic PPh_3 .^{7,8}



Synthesis of trifluoromethyl β -ketoester

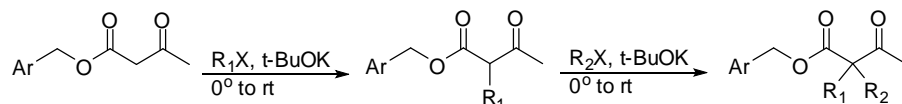
The parent β -ketoester of **60h** was prepared by esterification of *p*-methoxybenzyl alcohol and trifluoromethyl β -ketocarboxylic acid using EDCI and catalytic DMAP. The synthesis of trifluoromethyl β -ketocarboxylic acid was prepared by esterification of trifluoromethyl alcohol and Meldrum's acid in refluxing toluene.⁹



General procedure for the synthesis of α -substituted benzyl β -ketoesters¹⁰

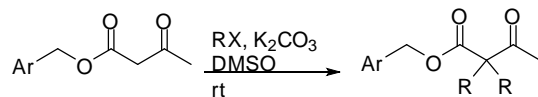
In an oven-dried 100-mL flask, a solution of benzyl β -ketoester (1.0 mmol) was dissolved in THF (10 mL). Next, *t*-BuOK (1.0 mmol) was added and the reaction was cooled in an ice bath for 30 minutes after which the alkyl halide (1.0 mmol) was added dropwise. For naphthyl esters, the solution was stirred at room temperature overnight while for quinolinyl esters, the reaction

mixture was stirred at 70°C overnight. Next, the reaction was quenched with water, extracted with ether (3 x 20 mL), washed with brine (20 mL) and dried over MgSO₄. The resulting solution was concentrated *in vacuo* before purifying via flash chromatography. To make the disubstituted ester (R₁ ≠ R₂), the above procedure was followed starting from the isolated monosubstituted aromatic β-ketoester.



General procedure for the synthesis of α,α -disubstituted benzyl β -ketoesters¹¹

In a dried 100 mL-flask under Ar, a solution of 1-naphthyl β -ketoester (1.0 mmol) in DMSO (20 mL) was prepared. Activated K₂CO₃ (4.00 mmol) was added after few minutes and the reaction was stirred at room temperature for 30 minutes. At this time, alkyl halide (2.0 mmol) or dibromoalkane (1.0 mmol) was added dropwise. The resulting solution was stirred at room temperature overnight. The yellowish solution was quenched with water extracted with DCM (3 x 20 mL), washed with brine (20 mL) and dried over MgSO₄. The resulting solution was concentrated *in vacuo* before purifying via flash chromatography.



Procedure for decarboxylative benzylation of unsubstituted ketones

In a flame-dried Schlenk tube under argon, Pd(PPh₃)₄ (0.10 mmol), or combination of either Pd₂dba₃ (0.10 *or* 0.05 mmol) and Xantphos (0.11 mmol) or CpPd(allyl) (0.10 mmol) and dppf (0.11 mmol) were dissolved in toluene (5 mL) and subsequently added to the unsubstituted benzyl β -keto ester (1.0 mmol). The resulting solution was heated at 110°C with stirring for 15 hours. After cooling the reaction mixture to room temperature, the solution was concentrated *in*

vacuo and the resulting residue was purified *via* flash chromatography using ethyl acetate and hexanes eluent.

Procedure for decarboxylative benzylation of α -monosubstituted ketones

In a flame-dried Schlenk tube under argon, Pd(PPh₃)₄ (0.10 mmol) was dissolved in toluene (5 mL) and subsequently added to the α -monosubstituted benzyl β -keto ester (1.0 mmol). The resulting solution was heated at 110°C with stirring for 15 hours. After cooling the reaction mixture to room temperature, the solution was concentrated *in vacuo* and the resulting residue was purified *via* flash chromatography using ethyl acetate and hexanes eluent.

Procedure for decarboxylative benzylation of α,α -disubstituted ketones

In a flame-dried Schlenk tube under argon, A combination of either Pd₂dba₃ (0.025 mmol) and PBU₃ (0.10 mmol) or CpPd(allyl) (0.10 mmol) and dppf (0.11 mmol) were dissolved in toluene (5 mL) and subsequently added to the α,α -disubstituted benzyl β -keto ester (1.0 mmol). The resulting solution was heated at 110°C with stirring for 15 hours. After cooling the reaction mixture to room temperature, the solution was concentrated *in vacuo* and the resulting residue was purified *via* flash chromatography using hexane and ethyl acetate eluent.

Nabumetone synthesis

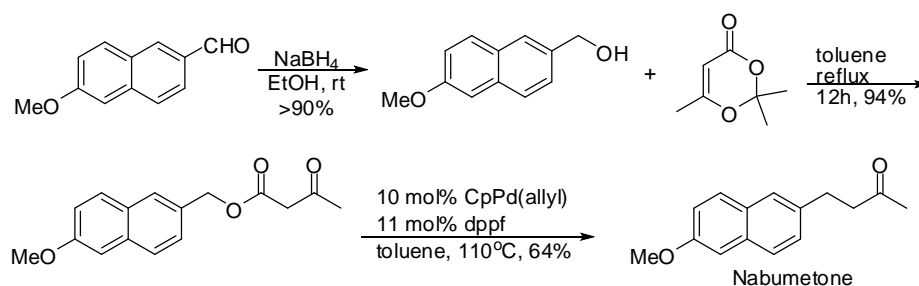
Synthesis of 6-methoxy-2-naphthyl- β -ketoester

In a dried round-bottom flask containing 6-methoxy-2-naphthylmethanol (1.0 mmol) obtained from NaBH₄ reduction of 6-methoxy-2-naphthaldehyde, 2,2,6-trimethyl-4H-1,3-dioxin-4-one (1.1 mmol) and toluene (10 mL) were added. The solution was stirred under reflux for 12 hrs. After heating, the solution was allowed to cool at room temperature. The solvent from the

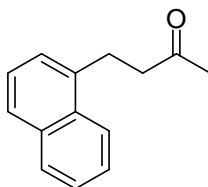
crude mixture was removed *in vacuo* prior to purification *via* column chromatography using hexanes and ethyl acetate as eluent to yield the title compound as white solid (94%).

Synthesis of Nabumetone via decarboxylative benzylation

In a dried Schlenk flask, containing **1** (1.0 mmol) and toluene (5 mL), CpPd(allyl) (0.10 mmol) and dppf (0.11 mmol) were added. The tube was stoppered with a rubber septum and was heated at 110°C for 12 hours. After heating, the tube was allowed to cool at room temperature. The solvent from the crude mixture was removed *in vacuo* prior to purification *via* column chromatography using hexanes and ethyl acetate as eluent to yield the title compound as pale-white solid.¹²



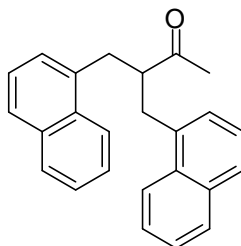
Spectroscopic Data



4-(naphthalen-1-yl)butan-2-one, **47**¹³
(RT-2-176, frac A)

¹H NMR (500 MHz, CDCl₃) δ ppm 7.97 (d, *J* = 7.9 Hz, aromatic H), 7.84 (d, *J* = 7.5 Hz, aromatic H), 7.71 (d, *J* = 8.1 Hz, aromatic H), 7.48 (dtd, *J* = 16.0, 6.8, 1.3 Hz, 2H, aromatic H), 7.37 (t, *J* = 7.6 Hz, 1H, aromatic H), 7.31 (d, *J* = 6.8 Hz, 1H, aromatic H), 3.37 – 3.32 (m, 2H, CH₂-C=O), 2.89 – 2.85 (m, 2H, O=C-CH₃), 2.14 (s, 3H, Ar-CH₂).

¹³C NMR (126 MHz, CDCl₃) δ ppm 208.45 (C=O), 140.55 (aromatic C), 137.37 (aromatic C), 134.15 (aromatic C), 131.84 (aromatic C), 131.13 (aromatic C), 129.24 (aromatic C), 127.30 (aromatic C), 126.33 (aromatic C), 125.93 (aromatic C), 123.70 (aromatic C), 44.65 (CH₂-C=O), 30.41 (C=O-CH₃), 27.06 (Ar-CH₂).



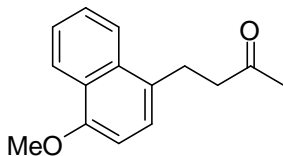
4-(naphthalen-1-yl)-3-(naphthalen-2-ylmethyl)butan-2-one, **47a**
(RT-2-176, frac B)

¹H NMR (500 MHz, CDCl₃) δ ppm 7.83 (d, *J* = 7.8 Hz, 2H, aromatic H), 7.72 (d, *J* = 8.1 Hz, 2H, aromatic H), 7.64 (d, *J* = 8.5 Hz, 2H, aromatic H), 7.43 (t, *J* = 7.5 Hz, 2H, aromatic H), 7.36 (dd, *J* = 14.5, 6.5 Hz, 3H, aromatic H), 7.31 (dd, *J* = 7.0, 2.8 Hz, 3H, aromatic H), 3.54 (dt, *J* = 14.3, 7.2 Hz, Bn-CH-Bn), 3.43 (dd, *J* = 13.7, 8.5 Hz, 2H, Ar-CH₂), 3.25 (dd, *J* = 13.8, 5.9 Hz, 2H, Ar-CH₂), 1.67 (s, 3H, CH₃).

¹³C NMR (126 MHz, CDCl₃) δ ppm 212.42 (C=O), 135.29 (aromatic C), 133.99 (aromatic C), 131.61 (aromatic C), 128.98 (aromatic C), 127.55 (aromatic C), 127.43 (aromatic C), 126.09 (aromatic C), 125.65 (aromatic C), 125.52 (aromatic C), 123.37 (aromatic C), 54.10 (Bn-CH-Bn), 35.34 (Np-CH₂), 31.98 (CH₃).

FTIR (CH₂Cl₂) $\bar{\nu}_{\max}$ cm⁻¹ 1713, 1508, 1396, 1354, 790, 777

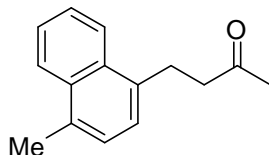
HRMS Calcd for C₂₅H₂₂O (M+H) – 339.1749, found 339.1692.



4-(4-methoxynaphthalen-1-yl)butan-2-one, **47b**¹⁴
(RT-11-200)

¹H NMR (400 MHz, CDCl₃) δ ppm 8.35 – 8.27 (m, 1H, aromatic H), 7.96 – 7.88 (d, *J* = 8.5 Hz, 1H, aromatic H), 7.64 – 7.40 (m, 2H, aromatic H), 7.25 – 7.19 (m, 1H, aromatic H), 6.77 – 6.67 (d, *J* = 8.0 Hz, 1H, aromatic H), 4.00 – 3.97 (s, 3H, O-CH₃), 3.34 – 3.22 (t, *J* = 7.7 Hz, 2H, Ar-CH₂), 2.91 – 2.80 (t, *J* = 7.7 Hz, 2H, CH₂-C=O), 2.20 – 2.08 (s, 3H, CH₃).

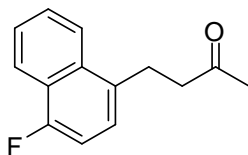
¹³C NMR (126 MHz, CDCl₃) δ ppm 208.39 (C=O), 154.48 (aromatic C), 132.47 (aromatic C), 128.92 (aromatic C), 127.47 (aromatic C), 126.67 (aromatic C), 126.10 (aromatic C), 125.91 (aromatic C), 125.13 (aromatic C), 125.06 (aromatic C), 123.38 (aromatic C), 122.90 (aromatic C), 103.51 (aromatic C), 55.62 (O-CH₃), 44.78 (CH₂-C=O), 30.24 (O=C-CH₃), 26.53 (Ar-CH₂).



4-(4-methylnaphthalen-1-yl)butan-2-one, **47c**¹⁵
(RT-10-88)

¹H NMR (400 MHz, CDCl₃) δ ppm 8.07 – 7.96 (td, *J* = 9.8, 3.3 Hz, 2H, aromatic H), 7.57 – 7.50 (dd, *J* = 6.5, 3.3 Hz, 2H, aromatic H), 7.24 – 7.21 (s, 2H, aromatic H), 3.38 – 3.29 (t, *J* = 7.8 Hz, 2H, Ar-CH₂), 2.92 – 2.83 (t, *J* = 7.8 Hz, 2H, CH₂-C=O), 2.70 – 2.63 (s, 3H, Ar-CH₃), 2.21 – 2.11 (s, 3H, CH₃).

¹³C NMR (126 MHz, CDCl₃) δ ppm 208.09 (C=O), 135.25 (aromatic C), 133.16 (aromatic C), 131.74 (aromatic C), 126.47 (aromatic C), 125.84 (aromatic C), 125.56 (aromatic C), 125.19 (aromatic C), 124.09 (aromatic C), 45.00 (Ar-CH₃), 30.08 (CH₂-C=O), 26.38 (O=C-CH₃), 19.46 (Ar-CH₂).

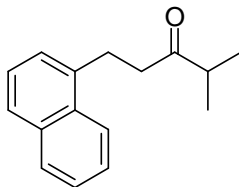


4-(4-fluoronaphthalen-1-yl)butan-2-one, **47d**
(RT-11-89)

¹H NMR (400 MHz, CDCl₃) δ ppm 8.21 – 8.09 (d, *J* = 7.7 Hz, 1H, aromatic H), 8.03 – 7.92 (d, *J* = 7.3 Hz, 1H, aromatic H), 7.62 – 7.49 (p, *J* = 6.8 Hz, 2H, aromatic H), 7.25 – 7.22 (m, 1H, aromatic H), 7.13 – 6.98 (dd, *J* = 10.3, 7.9 Hz, 1H, Ar-CH₂), 3.34 – 3.27 (t, *J* = 7.7 Hz, 2H, Ar-CH₂), 2.92 – 2.83 (t, *J* = 7.7 Hz, 2H, CH₂-C=O), 2.21 – 2.11 (s, 3H, CH₃).

¹³C NMR (126 MHz, CDCl₃) δ ppm 207.68 (C=O), 158.63 (aromatic C), 156.64 (aromatic C), 132.71 (aromatic C), 126.91 (aromatic C), 125.93 (aromatic C), 125.59 (aromatic C), 124.11 (aromatic C), 123.44 (aromatic C), 121.30 (aromatic C), 108.98 (aromatic C), 108.82 (aromatic C), 44.12 (CH₂-C=O), 29.95 (O=C-CH₃), 26.23 (Ar-CH₂).

HRMS Calcd for C₁₄H₁₄O (M+H) – 217.1029, found 217.1035.



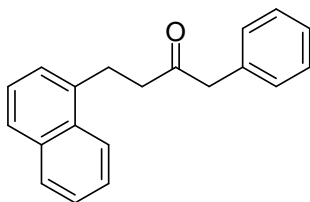
4-methyl-1-(naphthalen-1-yl)pentan-3-one, **47e**
(RT-4-37)

¹H NMR (500 MHz, CDCl₃) δ ppm 7.98 (d, *J* = 8.4 Hz, 1H, aromatic H), 7.84 (d, *J* = 8.8 Hz, 1H, aromatic H), 7.70 (d, *J* = 8.1 Hz, 1H, aromatic H), 7.49 (dtd, *J* = 16.1, 6.8, 1.4 Hz, 2H, aromatic H), 7.40 – 7.35 (m, 1H, aromatic H), 7.32 (d, *J* = 7.1 Hz, 1H, aromatic H), 3.37 – 3.31 (m, 2H, Np-CH₂), 2.91 – 2.85 (m, 2H, CH₂-C=O), 2.55 (dt, *J* = 13.9, 6.9 Hz, Me-CH-Me), 1.06 (d, *J* = 6.9 Hz, 6H, CH₃-CH-CH₃).

¹³C NMR (126 MHz, CDCl₃) δ ppm 213.90 (C=O), 137.51 (aromatic C), 134.00 (aromatic C), 131.76 (aromatic C), 128.95 (aromatic C), 127.85 (aromatic C), 127.40 (aromatic C), 126.79 (aromatic C), 126.01 (aromatic C), 125.62 (aromatic C), 123.47 (aromatic C), 41.03 (CH₃-CH-CH₃), 27.10 (CH₂-C=O), 18.11 (Np-CH₂), 16.55 (CH₃-CH-CH₃).

FTIR (CH₂Cl₂) $\bar{\nu}_{\max}$ cm⁻¹ 1711, 1597, 1466, 797, 777, 436.

HRMS Calcd for C₁₆H₁₈O (M + Na) – 249.1255, found 249.1263.



4-(naphthalen-1-yl)-1-phenylbutan-2-one, **47g**
(RT-3-297)

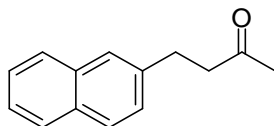
¹H NMR (500 MHz, CDCl₃) δ ppm 7.88 – 7.81 (m, 2H, aromatic C), 7.70 (d, *J* = 8.2 Hz, 1H, aromatic C), 7.49 – 7.44 (m, 2H, aromatic C), 7.37 – 7.32 (m, 1H, aromatic C), 7.32 – 7.27 (m, 2H, aromatic C), 7.25 (dd, *J* = 7.2, 2.8 Hz, 2H, aromatic C), 7.15 (d, *J* = 6.8 Hz, 2H, aromatic C), 3.66 (s, 2H, Ar-CH₂-C=O), 3.34 – 3.28 (m, 2H, Ar-CH₂), 2.91 – 2.86 (m, 2H, CH₂-C=O).

¹³C NMR (126 MHz, CDCl₃) δ 208.15 (C=O), 137.25 (aromatic C), 134.35 (aromatic C), 134.20 (aromatic C), 131.88 (aromatic C), 129.75 (aromatic C), 129.21 (aromatic C), 129.10 (aromatic C)

C), 127.41 (aromatic C), 127.31 (aromatic C), 126.42 (aromatic C), 126.36 (aromatic C), 125.91 (aromatic C), 123.74 (aromatic C), 50.88 (CH₂-Ph), 42.87 (CH₂-C=O), 27.09 (Ar-CH₂).

FTIR (CH₂Cl₂) $\bar{\nu}_{\max}$ cm⁻¹ 1713, 1597, 1495, 1454, 797, 777, 735, 698.

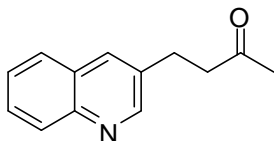
HRMS Calcd for C₂₀H₁₈O (M + Na) – 297.1255, found 297.1248.



4-(naphthalen-2-yl)butan-2-one, **47h**¹³
(RT-2-177-1)

¹H NMR (500 MHz, CDCl₃) δ ppm 7.82 – 7.75 (m, 3H, aromatic H), 7.64 – 7.60 (m, 1H, aromatic H), 7.48 – 7.40 (m, 2H, aromatic H), 7.35 – 7.30 (dd, *J* = 8.4, 1.7 Hz, 1H, aromatic H), 3.10 – 3.02 (t, *J* = 7.6 Hz, 2H, Ar-CH₂), 2.89 – 2.81 (m, 2H, O=C-CH₂), 2.20 – 2.12 (s, 3H, CH₃).

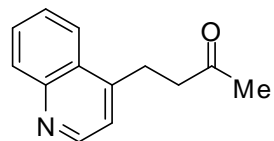
¹³C NMR (126 MHz, CDCl₃) δ ppm 208.04 (C=O), 138.59 (aromatic C), 133.68 (aromatic C), 132.12 (aromatic C), 128.24 (aromatic C), 127.74 (aromatic C), 127.58 (aromatic C), 127.17 (aromatic C), 126.53 (aromatic C), 126.17 (aromatic C), 125.47 (aromatic C), 45.24 (CH₂-C=O), 30.26 (O=C-CH₃), 29.96 (Ar-CH₂).



4-(quinolin-3-yl)butan-2-one, **47j**¹⁶
(RT-4-46)

¹H NMR (500 MHz, CDCl₃) δ ppm 8.80 – 8.75 (d, *J* = 2.2 Hz, 1H, aromatic H), 8.11 – 8.04 (m, 1H, aromatic H), 7.96 – 7.92 (m, 1H, aromatic H), 7.86 – 7.73 (m, 1H, aromatic H), 7.69 – 7.63 (m, 1H, aromatic H), 7.55 – 7.49 (m, 1H, aromatic H), 3.12 – 3.04 (t, *J* = 7.4 Hz, 2H, Ar-CH₂), 2.91 – 2.84 (t, *J* = 7.4 Hz, 2H, CH₂-C=O), 2.21 – 2.13 (s, 3H, CH₃).

¹³C NMR (126 MHz, CDCl₃) δ ppm 207.11 (C=O), 151.81 (aromatic C), 134.55 (aromatic C), 133.76 (aromatic C), 130.32 (aromatic C), 129.17 (aromatic C), 128.93 (aromatic C), 127.50 (aromatic C), 126.76 (aromatic C), 123.03 (aromatic C), 44.63 (CH₂-C=O), 30.22 (O=C-CH₃), 26.88 (Ar-CH₂).



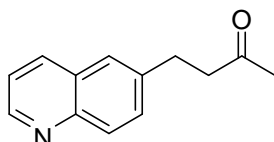
4-(quinolin-4-yl)butan-2-one, **47k**¹⁷
(RT-3-136, frac A)

¹H NMR (500 MHz, CDCl₃) δ ppm 8.77 (d, *J* = 4.4 Hz, 1H, aromatic H), 8.10 (d, *J* = 8.4 Hz, 1H, aromatic H), 7.98 (d, *J* = 8.5 Hz, 1H, aromatic H), 7.72 – 7.65 (m, 1H, aromatic H), 7.58 – 7.52 (m, 1H, aromatic H), 7.21 (d, *J* = 4.4 Hz, 1H, aromatic H), 3.37 – 3.31 (m, 2H, CH₂-C=O), 2.91 – 2.86 (m, 2H, Ar-CH₂), 2.16 (s, 3H, CH₃-C=O)

¹³C NMR (126 MHz, CDCl₃) δ ppm 207.18 (C=O), 150.52 (aromatic C), 148.59 (aromatic C), 147.25 (aromatic C), 130.65 (aromatic C), 129.52 (aromatic C), 127.56 (aromatic C), 126.93 (aromatic C), 123.52 (aromatic C), 121.09 (aromatic C), 43.60 (CH₂-C=O), 30.38 (CH₃-C=O), 25.93 (Ar-CH₂).

FTIR (CH₂Cl₂) $\bar{\nu}_{\max}$ cm⁻¹ 2341, 1717, 1593, 1364, 1163, 764

HRMS Calcd for C₁₃H₁₃NO (M+H) – 200.1075, found 200.1073.

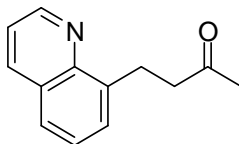


4-(quinolin-6-yl)butan-2-one, **47l**
(RT-3-258)

¹H NMR (500 MHz, CDCl₃) δ ppm 8.87 – 8.81 (d, *J* = 5.7 Hz, 1H, aromatic H), 8.10 – 8.05 (d, *J* = 9.4 Hz, 1H, aromatic H), 8.05 – 7.99 (d, *J* = 8.6 Hz, 1H, aromatic H), 7.60 – 7.57 (s, 1H, aromatic H), 7.57 – 7.52 (dd, *J* = 8.6, 2.0 Hz, 1H, aromatic H), 7.38 – 7.33 (dd, *J* = 8.3, 4.2 Hz, 1H, aromatic H), 3.10 – 3.04 (t, *J* = 7.5 Hz, 2H, Ar-CH₂), 2.88 – 2.82 (t, *J* = 7.5 Hz, 2H, CH₂-C=O), 2.18 – 2.13 (s, 3H, CH₃).

¹³C NMR (126 MHz, CDCl₃) δ ppm 207.69 (C=O), 149.95 (aromatic C), 147.19 (aromatic C), 139.48 (aromatic C), 135.70 (aromatic C), 130.73 (aromatic C), 129.51 (aromatic C), 128.28 (aromatic C), 126.40 (aromatic C), 121.32 (aromatic C), 44.89 (CH₂-C=O), 30.22 (O=C-CH₃), 29.67 (Ar-CH₂).

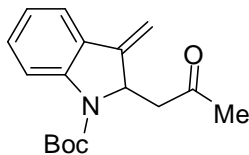
HRMS Calcd for C₁₃H₁₄NO (M+H) – 200.1075, found 200.1077.



4-(quinolin-8-yl)butan-2-one, **47m**¹⁸
(RT-4-131, frac 10-14)

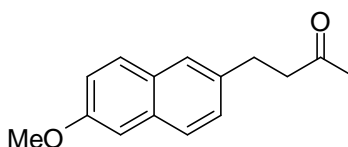
¹H NMR (500 MHz, CDCl₃) δ ppm 8.93 – 8.89 (dd, *J* = 4.2, 1.8 Hz, 1H, aromatic H), 8.15 – 8.11 (dd, *J* = 8.2, 1.8 Hz, 1H, aromatic H), 7.71 – 7.66 (dd, *J* = 8.2, 1.3 Hz, 1H, aromatic H), 7.60 – 7.56 (d, *J* = 7.0 Hz, 1H, aromatic H), 7.47 – 7.42 (m, 1H, aromatic H), 7.41 – 7.37 (dd, *J* = 8.2, 4.2 Hz, 1H, aromatic H), 3.54 – 3.48 (t, *J* = 7.6 Hz, 2H, Ar-CH₂), 3.01 – 2.95 (t, *J* = 7.6 Hz, 2H, CH₂-C=O), 2.17 – 2.12 (s, 3H, CH₃).

¹³C NMR (126 MHz, CDCl₃) δ 208.85 (C=O), 149.42 (aromatic C), 146.90 (aromatic C), 139.73 (aromatic C), 136.52 (aromatic C), 129.35 (aromatic C), 128.42 (aromatic C), 126.58 (aromatic C), 126.43 (aromatic C), 121.10 (aromatic C), 44.67 (CH₂-C=O), 30.14 (O=C-CH₃), 26.50 (Ar-CH₂).



tert-butyl 3-methylene-2-(2-oxopropyl)indoline-1-carboxylate, **48**
(RT-3-38)

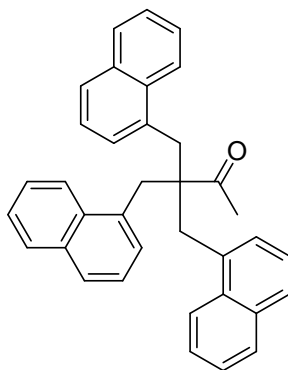
¹H NMR (400 MHz, CDCl₃) δ ppm 7.39 (d, *J* = 7.6 Hz, 1H, aromatic H), 7.29 (d, *J* = 7.8 Hz, 1H, aromatic H), 6.97 (t, *J* = 7.4 Hz, 2H, aromatic H), 5.42 (s, 1H, diastereotopic H, C=CH), 5.25 (dd, *J* = 11.9, 5.0 Hz, 1H, C-CH-CH₂), 5.01 (s, 1H, diastereotopic H, C=CH), 3.06 (d, *J* = 17.5 Hz, 1H, diastereotopic H, CH-C=O), 2.82 (dd, *J* = 16.7, 8.1 Hz, 1H, diastereotopic H, CH-C=O), 2.15 (s, 3H, CH₃-C=O), 1.57 (s, 9H, Boc)



4-(6-methoxynaphthalen-2-yl)butan-2-one, **49**¹²
(RT-11-186)

¹H NMR (400 MHz, CDCl₃) δ ppm 7.71 – 7.66 (d, *J* = 8.4 Hz, 2H, aromatic H), 7.58 – 7.53 (m, 1H, aromatic H), 7.33 – 7.29 (s, 1H, aromatic H), 7.17 – 7.11 (m, 2H, aromatic H), 3.94 – 3.93 (s, 3H, O-CH₃), 3.09 – 3.00 (t, *J* = 7.5 Hz, 2H, Ar-CH₂), 2.91 – 2.81 (m, 2H, CH₂-C=O), 2.22 – 2.15 (s, 3H, CH₃).

¹³C NMR (126 MHz, CDCl₃) δ ppm 207.98 (C=O), 157.39 (aromatic C), 136.08 (aromatic C), 134.45 (aromatic C), 133.01 (aromatic C), 128.93 (aromatic C), 127.53 (aromatic C), 126.96 (aromatic C), 126.20 (aromatic C), 118.68 (aromatic C), 105.50 (aromatic C), 55.30 (O-CH₃), 45.19 (CH₂-C=O), 30.14 (O=C-CH₃), 29.67 (Ar-CH₂).

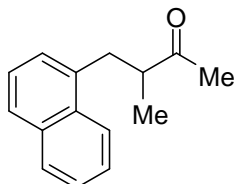


4-(naphthalen-1-yl)-3,3-bis(naphthalen-1-ylmethyl)butan-2-one, **48s**
(RT-3-291)

¹H NMR (500 MHz, CDCl₃) δ ppm 8.03 – 7.98 (d, *J* = 9.6 Hz, 3H, aromatic H), 7.87 – 7.81 (m, 3H, aromatic H), 7.75 – 7.70 (d, *J* = 8.2 Hz, 3H, aromatic H), 7.47 – 7.44 (m, 5H, aromatic H), 7.35 – 7.31 (m, 4H, aromatic H), 7.18 – 7.15 (d, *J* = 7.1 Hz, 3H, aromatic H), 3.79 – 3.67 (s, 6H, Ar-CH₂), 1.52 – 1.43 (s, 3H, CH₃).

¹³C NMR (126 MHz, CDCl₃) δ ppm 215.69 (C=O), 133.99 (aromatic C), 133.94 (aromatic C), 133.24 (aromatic C), 128.99 (aromatic C), 127.76 (aromatic C), 127.47 (aromatic C), 126.21 (aromatic C), 125.76 (aromatic C), 125.21 (aromatic C), 124.07 (aromatic C), 55.97 (CH₂-C=O), 37.18 (O=C-C), 29.94 (Ar-CH₂).

HRMS Calcd for C₃₆H₃₀ONa (M+Na) – 501.2194, found 501.2189.



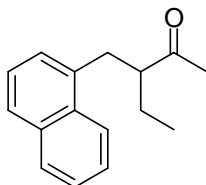
3-methyl-4-(naphthalen-1-yl)butan-2-one, **49**
(RT-2-126)

¹H NMR (500 MHz, CDCl₃) δ ppm 8.00 (d, *J* = 8.3 Hz, 1H, aromatic CH), 7.86 (d, *J* = 8.0 Hz, 1H, aromatic CH), 7.73 (d, *J* = 8.1 Hz, 1H, aromatic CH), 7.50 (dt, *J* = 14.9, 6.8 Hz, 2H, aromatic CH), 7.38 (t, *J* = 7.6 Hz, 1H, aromatic CH), 7.28 (d, *J* = 7.0 Hz, 1H, aromatic CH), 3.51 (dd, *J* = 13.4, 5.9 Hz, 1H, CH-Me), 3.00 (ddd, *J* = 28.2, 13.8, 7.4 Hz, 2H, Ar-CH₂), 2.07 (s, 3H, CH-CH₃), 1.14 (d, *J* = 6.8 Hz, 3H, CH₃-C=O)

¹³C NMR (126 MHz, CDCl₃) δ ppm 212.64 (C=O), 135.91 (aromatic C), 134.23 (aromatic C), 132.05 (aromatic C), 129.25 (aromatic C), 127.63 (aromatic C), 127.46 (aromatic C), 126.32 (aromatic C), 125.87 (aromatic C), 125.74 (aromatic C), 123.83 (aromatic C), 47.94 (Bn-CH-Me), 36.17 (Ar-CH₂), 29.39 (CH₃-C=O), 16.98 (CH-CH₃)

FTIR (CH₂Cl₂) $\bar{\nu}_{\max}$ cm⁻¹ 1711, 1458, 1396, 1356, 781, 445.

HRMS Calcd for C₁₅H₁₆O (M+Na) – 235.1099, found 235.1091.



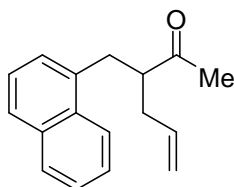
3-(naphthalen-1-ylmethyl)pentan-2-one, **49a**
(RT-2-135)

¹H NMR (500 MHz, CDCl₃) δ ppm 7.99 (d, *J* = 8.2 Hz, 1H, aromatic H), 7.85 (d, *J* = 7.9 Hz, 1H, aromatic H), 7.71 (d, *J* = 8.1 Hz, 1H, aromatic H), 7.50 (dt, *J* = 14.9, 6.8 Hz, 2H, aromatic H), 7.38 – 7.33 (m, 1H, aromatic H), 7.26 (d, *J* = 6.8 Hz, 1H, aromatic H), 3.32 (dd, *J* = 14.0, 8.1 Hz, 1H, diastereotopic H), 3.14 (dd, *J* = 14.0, 6.4 Hz, 1H, diastereotopic H), 3.02 – 2.90 (m, 1H, diastereotopic H), 1.94 (s, 3H, CH₃-C=O), 1.74 (dq, *J* = 15.2, 7.5 Hz, 1H, diastereotopic H), 1.65 – 1.53 (m, 1H, diastereotopic H), 0.92 (t, *J* = 7.4 Hz, 3H, CH₂-CH₃).

¹³C NMR (126 MHz, CDCl₃) δ ppm 213.00 (C=O), 135.91 (aromatic C), 134.25 (aromatic C), 131.99 (aromatic C), 129.28 (aromatic C), 127.55 (aromatic C), 127.47 (aromatic C), 126.36 (aromatic C), 125.89 (aromatic C), 125.79 (aromatic C), 123.83 (aromatic C), 55.16 (CH-C=O), 34.90 (Ar-CH₂), 30.88 (CH₃-C=O), 25.30 (CH-CH₂-CH₃), 11.98 (CH₂-CH₃).

FTIR (CH₂Cl₂) $\bar{\nu}_{\max}$ cm⁻¹ 2962, 2931, 1711, 1597, 1456, 1167, 777

HRMS Calcd for C₁₈H₁₆O (M+H) – 249.1279, found 249.1264.



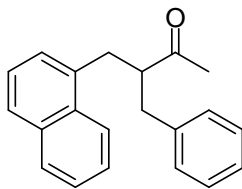
3-(naphthalen-1-ylmethyl)hex-5-en-2-one, **49b**
(RT-2-117)

¹H NMR (500 MHz, CDCl₃) δ ppm 7.98 (d, *J* = 8.4 Hz, 1H, aromatic H), 7.85 (d, *J* = 8.0 Hz, 1H, aromatic H), 7.72 (d, *J* = 8.2 Hz, 1H, aromatic H), 7.51 (dt, *J* = 14.9, 6.9 Hz, 2H, aromatic H), 7.36 (t, *J* = 7.6 Hz, 1H, aromatic H), 7.27 (d, *J* = 7.0 Hz, 1H, aromatic H), 5.77 (td, *J* = 17.1, 7.1 Hz, 1H, CH₂-CH=CH₂), 5.14 – 5.05 (m, 2H, CH=CH₂), 3.33 (dd, *J* = 14.0, 8.3 Hz, 1H, diastereotopic H), 3.18 (dd, *J* = 14.0, 6.2 Hz, 1H, diastereotopic H), 3.14 – 3.05 (m, 1H, CH₂-CH-C=O), 2.45 (dt, *J* = 14.8, 7.5 Hz, 1H, diastereotopic H), 2.33 – 2.23 (m, 1H, diastereotopic H), 1.91 (s, 3H, CH₃-C=O).

¹³C NMR (126 MHz, CDCl₃) δ ppm 212.12 (C=O), 135.66 (aromatic C), 135.37 (aromatic C), 134.27 (CH=CH₂), 131.96 (aromatic C), 129.30 (aromatic C), 127.67 (aromatic C), 127.58 (aromatic C), 126.42 (aromatic C), 125.93 (aromatic C), 125.80 (aromatic C), 123.81 (aromatic C), 117.92 (CH=CH₂), 53.02 (CH-C=O), 36.33 (Ar-CH₂), 34.45 (CH₂-CH=CH₂), 31.07 (CH₃-C=O).

FTIR (CH₂Cl₂) $\bar{\nu}_{\max}$ cm⁻¹ 3047, 3003, 2978, 1713, 1510, 1167, 918, 781

HRMS Calcd for C₁₇H₁₈O (M+Na) – 261.1255, found 261.1316.



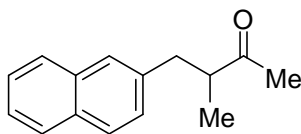
3-benzyl-4-(naphthalene-1-yl)butan-2-one, **49c**
(RT-2-151)

¹H NMR (500 MHz, CDCl₃) δ ppm 7.83 (d, *J* = 5.7 Hz, 1H, aromatic H), 7.74 (d, *J* = 8.5 Hz, 1H, aromatic H), 7.70 (d, *J* = 8.2 Hz, 1H, aromatic H), 7.47 – 7.43 (m, 2H, aromatic H), 7.34 (t, *J* = 7.5 Hz, 1H, aromatic H), 7.27 (dd, *J* = 16.1, 7.3 Hz, 3H, aromatic H), 7.21 (d, *J* = 6.9 Hz, 1H, aromatic H), 7.16 (d, *J* = 7.6 Hz, 2H, aromatic H), 3.30 (dd, *J* = 11.3, 6.9 Hz, 2H, Ar-CH₂), 3.23 (t, *J* = 9.0 Hz, 1H, diastereotopic H), 3.02 (dd, *J* = 13.2, 7.3 Hz, 1H, diastereotopic H), 2.78 (dd, *J* = 13.5, 5.4 Hz, 1H, diastereotopic H), 1.68 (s, 3H, CH₃-C=O)

¹³C NMR (126 MHz, CDCl₃) δ ppm 212.49 (C=O), 139.56 (aromatic C), 135.64 (aromatic C), 134.26 (aromatic C), 131.86 (aromatic C), 129.33 (aromatic C), 129.27 (aromatic C), 128.91 (aromatic C), 127.61 (aromatic C), 127.60 (aromatic C), 126.88 (aromatic C), 126.84 (aromatic C), 126.39 (aromatic C), 125.90 (aromatic C), 125.81 (aromatic C), 123.71 (aromatic C), 55.60 (CH₂-CH-CH₂), 38.89 (Ar-CH₂), 35.30 (Ar-CH₂), 32.17 (CH₃-C=O)

FTIR (CH₂Cl₂) $\bar{\nu}_{\max}$ cm⁻¹ 3061, 2939, 1713, 1597, 1454, 1161, 779, 700

HRMS Calcd for C₂₁H₂₀O (M+Na) – 311.1412, found 311.1424.



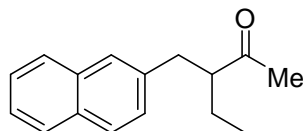
3-methyl-4-(naphthalen-2-yl)butan-2-one, **49d**
RT-2-210

¹H NMR (500 MHz, CDCl₃) δ ppm 7.75 (d, *J* = 8.1 Hz, 2H, aromatic H), 7.54 – 7.48 (m, 2H, aromatic H), 7.47 – 7.39 (m, 2H, aromatic H), 7.28 (dd, *J* = 8.4, 1.7 Hz, 1H, aromatic H), 3.15 (dd, *J* = 13.6, 6.8 Hz, 1H, diastereotopic H), 2.99 – 2.86 (m, 1H, diastereotopic H), 2.70 (dd, *J* = 13.6, 7.8 Hz, 1H, diastereotopic H), 2.09 (s, 3H, CH₃-C=O), 1.11 (d, *J* = 7.0 Hz, 3H, CH₃-CH)

¹³C NMR (126 MHz, CDCl₃) δ ppm 200.34 (C=O), 129.93 (aromatic C), 128.68 (aromatic C), 128.40 (aromatic C), 127.94 (aromatic C), 127.83 (aromatic C), 127.69 (aromatic C), 127.65 (aromatic C), 126.88 (aromatic C), 126.37 (aromatic C), 125.74 (aromatic C), 49.13, (CH-CH₃), 39.41 (Ar-CH₂), 29.27 (CH₃-C=O), 16.64 (CH-CH₃).

FTIR (CH₂Cl₂) $\bar{\nu}_{\max}$ cm⁻¹ 3045, 2922, 1710, 1663, 1358, 1240, 820, 746

HRMS Calcd for C₁₅H₁₆O (M+Na) – 253.1099, found 253.1101.



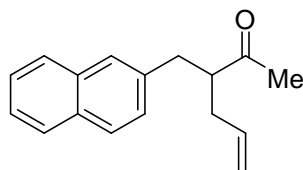
3-(naphthalen-2-ylmethyl)pentan-2-one, **49e**
(RT-4-250)

¹H NMR (500 MHz, CDCl₃) δ ppm 7.81 – 7.74 (m, 3H, aromatic H), 7.54 – 7.49 (m, 1H, aromatic H), 7.48 – 7.39 (m, 2H, aromatic H), 7.29 (dd, *J* = 8.4, 1.7 Hz, 1H, aromatic H), 3.04 (dd, *J* = 12.1, 6.8 Hz, 1H, diastereotopic H), 2.90 – 2.78 (m, 2H, CH₂-CH₃), 2.00 (s, 3H, CH₃-C=O), 1.69 (dt, *J* = 15.3, 7.6 Hz, 1H, diastereotopic H), 1.56 (s, 1H, diastereotopic H), 0.91 (t, *J* = 7.5 Hz, 3H, CH₂-CH₃).

¹³C NMR (126 MHz, CDCl₃) δ 200.46 (C=O), 137.66 (aromatic C), 133.92 (aromatic C), 132.52 (aromatic C), 128.52 (aromatic C), 128.03 (aromatic C), 127.93 (aromatic C), 127.73 (aromatic C), 127.65 (aromatic C), 126.45 (aromatic C), 125.83 (aromatic C), 56.58 (CH-C=O), 37.92 (Ar-CH₂), 30.81 (CH₃-C=O), 24.99 (CH₂-CH₃), 11.95 (CH₂-CH₃)

FTIR (CH₂Cl₂) $\bar{\nu}_{\max}$ cm⁻¹ 3051, 1666, 1634, 1504, 1277, 815

HRMS Calcd for C₁₆H₁₈O (M⁺) – 226.1358, found 226.1321.



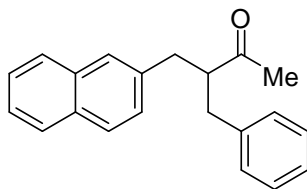
3-(naphthalen-2-ylmethyl)hex-5-en-2-one, **49f**
(YA-1-133r)

¹H NMR (500 MHz, CDCl₃) δ 7.77 (dd, *J* = 14.5, 8.7 Hz, 3H, aromatic H), 7.58 (s, 1H, aromatic H), 7.53 – 7.37 (m, 2H, aromatic H), 7.28 (d, *J* = 8.4 Hz, 1H, aromatic H), 5.74 (dt, *J* = 17.2, 7.0 Hz, 1H, CH=CH₂), 5.06 (dd, *J* = 13.6, 6.7 Hz, 2H, CH=CH₂), 3.14 – 2.93 (m, 2H, CH₂-CH=CH₂), 2.85 (dd, *J* = 12.9, 5.7 Hz, 1H, diastereotopic H), 2.48 – 2.33 (m, 1H, diastereotopic H), 2.31 – 2.19 (m, 1H, diastereotopic H), 1.99 (s, 3H, CH₃-C=O)

¹³C NMR (126 MHz, CDCl₃) δ 211.52 (C=O), 136.97 (aromatic C), 135.14 (aromatic C), 133.53 (CH=CH₂), 132.18 (aromatic C), 128.21 (aromatic C), 127.69 (aromatic C), 127.65 (aromatic C), 127.56 (aromatic C), 127.38 (aromatic C), 127.32 (aromatic C), 126.11 (aromatic C), 125.51 (aromatic C), 117.41 (CH=CH₂), 54.32 (CH₂-CH-CH₂), 37.52 (Ar-CH₂), 35.76 (CH₂-CH=CH₂), 30.82 (CH₃-C=O).

FTIR (CH₂Cl₂) $\bar{\nu}_{\max}$ cm⁻¹ 3053, 2924, 1711, 1601, 1439, 1363, 918, 820, 749

HRMS Calcd for C₁₇H₁₈O (M-H) – 237.1279, found 237.1267



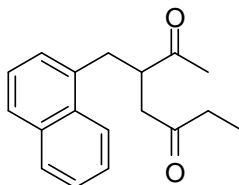
3-benzyl-4-(naphthalen-2-yl)butan-2-one, **49g**
(RT-2-194)

¹H NMR (500 MHz, CDCl₃) δ ppm 7.77 (dd, *J* = 14.7, 8.4 Hz, 3H, aromatic H), 7.57 (s, 1H, aromatic H), 7.43 (pd, *J* = 6.8, 1.5 Hz, 2H, aromatic H), 7.29 – 7.25 (m, 3H, aromatic H), 7.19 (t, *J* = 7.4 Hz, 1H, aromatic H), 7.15 (d, *J* = 8.3 Hz, 2H, aromatic H), 3.32 – 3.20 (m, 1H, diastereotopic H), 3.08 (dd, *J* = 13.6, 8.9 Hz, 1H, diastereotopic H), 2.95 (dd, *J* = 13.6, 8.8 Hz, 1H, diastereotopic H), 2.87 (dd, *J* = 13.6, 5.9 Hz, 1H, diastereotopic H), 2.76 (dd, *J* = 13.6, 6.0 Hz, 1H, diastereotopic H), 1.75 (s, 3H, CH₃-C=O)

¹³C NMR (126 MHz, CDCl₃) δ ppm 212.51 (C=O), 139.54 (aromatic C), 137.20 (aromatic C), 133.86 (aromatic C), 132.54 (aromatic C), 129.88 (aromatic C), 129.22 (aromatic C), 128.90 (aromatic C), 128.55 (aromatic C), 127.95 (aromatic C), 127.88 (aromatic C), 127.67 (aromatic C), 127.54 (aromatic C), 126.77 (aromatic C), 126.42 (aromatic C), 125.79 (aromatic C), 123.08 (aromatic C), 56.79 (CH₂-CH-CH₂), 38.53 (Ar-CH₂), 31.97 (Ar-CH₂), 32.04 (CH₃-C=O).

FTIR (CH₂Cl₂) ν_{max} cm⁻¹ 3057, 3026, 1710, 1601, 1497, 1360, 1161, 818, 700

HRMS Calcd for C₂₁H₂₀O (M+Na) – 311.1412, found 311.1368



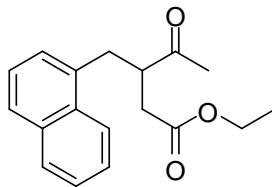
3-(naphthalen-1-ylmethyl)heptane-2,5-dione, **50**
(RT-3-43)

¹H NMR (400 MHz, CDCl₃) δ ppm 8.04 (d, *J* = 8.4 Hz, 1H, aromatic H), 7.85 (d, *J* = 8.1 Hz, 1H, aromatic H), 7.74 (d, *J* = 8.2 Hz, 1H, aromatic H), 7.52 (dt, *J* = 14.9, 6.9 Hz, 2H, aromatic H), 7.37 (dd, *J* = 8.2, 7.1 Hz, 1H, aromatic H), 7.22 (s, 1H, aromatic H), 3.56 – 3.43 (m, 1H, CH₂-CH-CH₂), 3.30 (dd, *J* = 13.7, 7.3 Hz, 1H, diastereotopic H), 3.01 (dd, *J* = 25.4, 7.5 Hz, 2H, CH₂-CH₃), 2.44 (dd, *J* = 18.1, 3.9 Hz, 1H, diastereotopic H), 2.34 (dd, *J* = 12.7, 7.3 Hz, 2H, diastereotopic H), 2.04 (s, 3H, CH₃-C=O), 0.96 (t, *J* = 7.3 Hz, 3H, CH₂-CH₃)

¹³C NMR (126 MHz, CDCl₃) δ ppm 212.20 (C=O), 210.37 (C=O), 134.77 (aromatic C), 134.29 (aromatic C), 131.94 (aromatic C), 129.34 (aromatic C), 127.96 (aromatic C), 127.75 (aromatic C), 126.70 (aromatic C), 126.16 (aromatic C), 125.75 (aromatic C), 123.73 (aromatic C), 47.74 (Np-CH₂-CH-C=O), 44.66 (CH-C(O)-CH₂), 35.98 (C(O)-CH₂-CH₃), 35.26 (Ar-CH₂), 31.18 (CH₃-C=O), 7.91 (CH₂-CH₃)

FTIR (CH₂Cl₂) $\bar{\nu}_{\max}$ cm⁻¹ 2976, 2937, 1713, 1510, 1115, 781

HRMS Calcd for C₁₈H₂₀O₂ (M+Na) – 291.1361, found 291.1361.



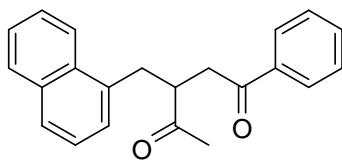
ethyl 3-(naphthalen-1-ylmethyl)-4-oxopentanoate, **51a**
(RT-2-118)

¹H NMR (500 MHz, CDCl₃) δ ppm 8.04 (d, J = 8.4 Hz, 1H, aromatic H), 7.86 (d, J = 8.1 Hz, 1H, aromatic H), 7.74 (d, J = 8.2 Hz, 1H, aromatic H), 7.52 (dt, J = 14.9, 6.9 Hz, 2H, aromatic H), 7.40 – 7.35 (m, 1H aromatic H), 7.25 (d, J = 7.2 Hz, 1H, aromatic H), 4.03 (q, J = 7.1 Hz, 2H, (O-CH₂-CH₃)), 3.51 – 3.43 (m, 1H, CH₂-CH-CH₂), 3.35 (dd, J = 13.7, 7.3 Hz, 1H, diastereotopic H), 3.06 (dd, J = 13.7, 8.2 Hz, 1H, diastereotopic H), 2.83 (dd, J = 17.1, 9.7 Hz, 1H, diastereotopic H), 2.37 (dd, J = 17.2, 4.4 Hz, 1H, diastereotopic H), 2.03 (s, 3H, CH₃-C=O), 1.18 (t, J = 7.1 Hz, 3H, CH₂-CH₃)

¹³C NMR (126 MHz, CDCl₃) δ ppm 211.20 (C=O), 172.22 (C=O), 134.20 (aromatic C), 133.99 (aromatic C), 131.59 (aromatic C), 129.05 (aromatic C), 127.70 (aromatic C), 127.60 (aromatic C), 126.39 (aromatic C), 125.82 (aromatic C), 125.47 (aromatic C), 123.34 (aromatic C), 60.74 (O-CH₂), 48.36 (CH₂-CH-CH₂), 35.88 (Np-CH₂), 35.04 (CH-CH₂-C=O), 30.77 (CH₃-C=O), 14.12 (CH₂-CH₃)

FTIR (CH₂Cl₂) $\bar{\nu}_{\max}$ cm⁻¹ 2982, 1732, 1715, 1371, 1196, 783.

HRMS Calcd for C₁₈H₂₀O₃ (M+Na) – 307.1310, found 307.1313.



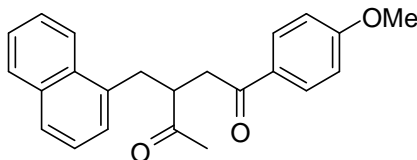
3-(naphthalen-1-ylmethyl)-1-phenylpentane-1,4-dione, **51b**
(RT-2-119)

¹H NMR (500 MHz, CDCl₃) δ ppm 8.10 (d, J = 8.4 Hz, 1H, aromatic H), 7.87 (d, J = 8.1 Hz, 3H, aromatic H), 7.75 (d, J = 8.0 Hz, 1H, aromatic H), 7.60 – 7.54 (m, 1H, aromatic H), 7.54 – 7.47 (m, 2H, aromatic H), 7.45 – 7.37 (m, 3H, aromatic H), 7.29 (d, J = 6.9 Hz, 1H, aromatic H), 3.70 (dt, J = 11.6, 5.8 Hz, 1H, CH₂-CH-CH₃), 3.59 (dd, J = 17.9, 9.7 Hz, 1H, diastereotopic H), 3.39 (dd, J = 13.7, 7.4 Hz, 1H, diastereotopic H), 3.17 (dd, J = 13.7, 8.0 Hz, 1H, diastereotopic H), 3.06 (dd, J = 18.0, 3.6 Hz, 1H, diastereotopic H), 2.09 (s, 3H, CH₃-C=O).

¹³C NMR (126 MHz, CDCl₃) δ ppm 212.13 (C=O), 198.87 (C=O), 136.61 (aromatic C), 134.85 (aromatic C), 134.30 (aromatic C), 133.64 (aromatic C), 131.96 (aromatic C), 129.36 (aromatic C), 128.91 (aromatic C), 128.35 (aromatic C), 128.01 (aromatic C), 127.70 (aromatic C), 126.80 (aromatic C), 126.18 (aromatic C), 125.79 (aromatic C), 123.79 (aromatic C), 47.51 (CH₂-CH-CH₂), 41.30 (CH₂-C=O), 35.37 (Ar-CH₂), 31.12 (CH₃-C=O).

FTIR (CH₂Cl₂) $\bar{\nu}_{\max}$ cm⁻¹ 3059, 2945, 1710, 1682, 1356, 1163, 779, 689

HRMS Calcd for C₂₂H₂₀O₂ (M+Na) – 339.1361, found 339.1346.



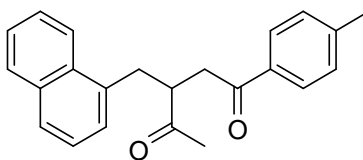
1-(4-methoxyphenyl)-3-(naphthalene-1-ylmethyl)pentane-1,4-dione, **51c**
(RT-2-162)

¹H NMR (500 MHz, CDCl₃) δ ppm 8.10 (d, *J* = 8.4 Hz, 1H, aromatic H), 7.85 (dd, *J* = 7.6, 5.4 Hz, 3H, aromatic H), 7.74 (d, *J* = 8.2 Hz, 1H, aromatic H), 7.53 (dt, *J* = 14.8, 7.1 Hz, 2H, aromatic H), 7.38 (t, *J* = 7.6 Hz, 1H, aromatic H), 7.29 (d, *J* = 6.9 Hz, 1H, aromatic H), 6.87 (d, *J* = 8.7 Hz, 2H, aromatic H), 3.83 (s, 3H, O-CH₃), 3.68 (qd, *J* = 8.0, 3.8 Hz, 1H, diastereotopic H), 3.54 (dd, *J* = 17.9, 9.6 Hz, 1H, diastereotopic H), 3.36 (dd, *J* = 13.7, 7.6 Hz, 1H, diastereotopic H), 3.17 (dd, *J* = 13.7, 7.9 Hz, 1H, diastereotopic H), 3.03 (dd, *J* = 17.9, 3.7 Hz, 1H, diastereotopic H), 2.06 (s, 3H, CH₃-C=O)

¹³C NMR (126 MHz, CDCl₃) δ ppm 212.31 (C=O), 197.18 (C=O), 163.75 (aromatic C), 134.81 (aromatic C), 134.16 (aromatic C), 131.85 (aromatic C), 130.48 (aromatic C), 129.61 (aromatic C), 129.17 (aromatic C), 127.80 (aromatic C), 127.58 (aromatic C), 126.55 (aromatic C), 126.00 (aromatic C), 125.63 (aromatic C), 123.69 (aromatic C), 113.86 (aromatic C), 55.66 (O-CH₃), 47.76 (CH₂-CH-CH₂), 41.12 (CH₂-C=O), 35.42 (Ar-CH₂), 31.27 (CH₃-C=O)

FTIR (CH₂Cl₂) $\bar{\nu}_{\max}$ cm⁻¹ 2934, 1709, 1672, 1574, 1261, 1169, 802

HRMS Calcd for C₂₃H₂₂O₃ (M+H) – 347.1647, found 347.1634.



3-(naphthalen-1-ylmethyl)-1-p-tolylpentane-1,4-dione, **51d**
(RT-2-164)

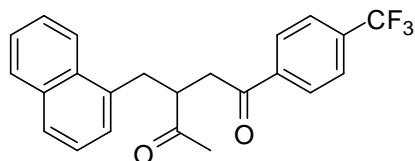
¹H NMR (500 MHz, CDCl₃) δ ppm 8.10 (d, *J* = 8.4 Hz, 1H, aromatic H), 7.86 (d, *J* = 8.1 Hz, 1H, aromatic H), 7.75 (dd, *J* = 12.9, 8.3 Hz, 3H, aromatic H), 7.56 (t, *J* = 7.6 Hz, 1H, aromatic H), 7.49 (t, *J* = 7.4 Hz, 1H, aromatic H), 7.40 – 7.34 (m, 1H, aromatic H), 7.29 (d, *J* = 6.9 Hz,

¹H, aromatic H), 7.20 (d, *J* = 8.0 Hz, 2H, aromatic H), 3.73 – 3.63 (m, 1H, diastereotopic H), 3.56 (dd, *J* = 18.0, 9.6 Hz, 1H, diastereotopic H), 3.37 (dd, *J* = 13.7, 7.6 Hz, 1H, diastereotopic H), 3.18 (dd, *J* = 13.7, 7.9 Hz, 1H, diastereotopic H), 3.05 (dd, *J* = 18.0, 3.7 Hz, 1H, diastereotopic H), 2.37 (s, 3H, Ar-CH₃), 2.06 (s, 3H, CH₃-C=O)

¹³C NMR (126 MHz, CDCl₃) δ 211.84 (aromatic C), 198.19 (aromatic C), 144.16 (aromatic C), 134.62 (aromatic C), 134.02 (aromatic C), 133.89 (aromatic C), 131.70 (aromatic C), 129.29 (aromatic C), 129.04 (aromatic C), 128.17 (aromatic C), 127.67 (aromatic C), 127.44 (aromatic C), 126.42 (aromatic C), 125.87 (aromatic C), 125.49 (aromatic C), 123.53 (aromatic C), 47.57 (CH₂-CH-CH₂), 41.20 (CH₂-C=O), 35.28 (Ar-CH₂), 31.13 (CH₃-C=O), 21.73 (Ar-CH₃)

FTIR (CH₂Cl₂) $\bar{\nu}_{\max}$ cm⁻¹ 3045, 2922, 1713, 1678, 1606, 1354, 1165, 781

HRMS Calcd for C₂₃H₂₂O₂ (M+Na) – 353.1518, found 353.1492.



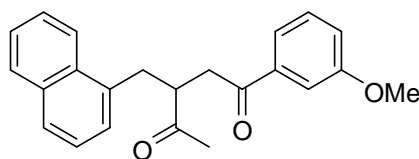
3-(naphthalen-1-ylmethyl)-1-(4-(trifluoromethyl)phenyl)pentane-1,4-dione, **51e**
(RT-2-163)

¹H NMR (500 MHz, CDCl₃) δ ppm 8.08 (d, *J* = 8.4 Hz, 1H, aromatic H), 7.94 (d, *J* = 8.0 Hz, 2H, aromatic H), 7.87 (d, *J* = 8.0 Hz, 1H, aromatic H), 7.75 (d, *J* = 8.1 Hz, 1H, aromatic H), 7.66 (d, *J* = 8.0 Hz, 2H, aromatic H), 7.60 – 7.54 (m, 1H, aromatic H), 7.50 (t, *J* = 7.4 Hz, 1H, aromatic H), 7.38 (t, *J* = 7.5 Hz, 1H, aromatic H), 7.29 (d, *J* = 6.8 Hz, 1H, aromatic H), 3.75 – 3.65 (m, 1H, diastereotopic H), 3.60 (dd, *J* = 18.0, 9.8 Hz, 1H, diastereotopic H), 3.42 (dd, *J* = 13.7, 7.1 Hz, 1H, diastereotopic H), 3.15 (dd, *J* = 13.8, 8.4 Hz, 1H, diastereotopic H), 3.00 (dd, *J* = 18.0, 3.3 Hz, 1H, diastereotopic H), 2.12 (s, 3H, CH₃-C=O)

¹³C NMR (126 MHz, CDCl₃) δ 211.80 (C=O), 197.91 (C=O), 139.24 (aromatic C), 134.93 (aromatic C), 134.72 (aromatic C), 134.52 (aromatic C), 134.30 (aromatic C), 131.97 (aromatic C), 129.43 (aromatic C), 128.67 (aromatic C), 128.15 (aromatic C), 127.77 (aromatic C), 126.76 (aromatic C), 126.25 (aromatic C), 126.00 (aromatic C), 125.97 (aromatic C), 125.80 (aromatic C), 123.65 (Ar-CF₃), 48.10 (CH₂-CH-CH₂), 41.61 (CH₂-C=O), 35.08 (Ar-CH₂), 31.11 (CH₃-C=O)

FTIR (CH₂Cl₂) $\bar{\nu}_{\max}$ cm⁻¹ 1713, 1690, 1410, 1067, 781

HRMS Calcd for C₂₃H₁₉F₃O₂ (M+Na) – 407.1235, found 407.1218



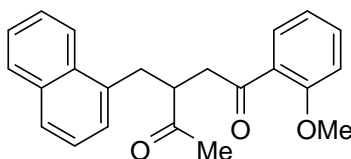
1-(3-methoxyphenyl)-3-(naphthalen-1-ylmethyl)pentane-1,4-dione, **51f**
(RT-3-296)

¹H NMR (500 MHz, CDCl₃) δ ppm 8.09 (d, *J* = 8.4 Hz, 1H, aromatic H), 7.86 (d, *J* = 7.6 Hz, 1H, aromatic H), 7.74 (d, *J* = 8.2 Hz, 1H, aromatic H), 7.67 (dd, *J* = 7.7, 1.8 Hz, 1H, aromatic H), 7.58 – 7.52 (m, 1H, aromatic H), 7.51 – 7.46 (m, 1H, aromatic H), 7.44 – 7.39 (m, 1H, aromatic H), 7.37 (dd, *J* = 8.1, 7.1 Hz, 1H, aromatic H), 7.29 (d, *J* = 6.9 Hz, 1H, aromatic H), 6.94 (t, *J* = 7.5 Hz, 1H, aromatic H), 6.89 (d, *J* = 8.4 Hz, 1H, aromatic H), 3.77 (s, 3H, O-CH₃), 3.62 (ddd, *J* = 17.1, 7.6, 3.5 Hz, 1H, diastereotopic H), 3.55 (dd, *J* = 18.3, 9.7 Hz, 1H, diastereotopic H), 3.34 (dd, *J* = 13.7, 7.4 Hz, 1H, diastereotopic H), 3.16 (dd, *J* = 5.5, 2.0 Hz, 1H), 3.13 (t, *J* = 5.5 Hz, 1H, diastereotopic H), 2.08 (s, 3H, CH₃-C=O)

¹³C NMR (126 MHz, CDCl₃) δ ppm 212.80 (C=O), 200.63 (C=O), 159.57 (aromatic C), 135.63 (aromatic C), 134.61 (aromatic C), 134.54 (aromatic C), 132.46 (aromatic C), 131.11 (aromatic C), 129.57 (aromatic C), 128.10 (aromatic C), 128.07 (aromatic C), 127.70 (aromatic C), 126.87 (aromatic C), 126.35 (aromatic C), 126.04 (aromatic C), 124.28 (aromatic C), 121.23 (aromatic C), 112.17 (aromatic C), 55.99 (O-CH₃), 48.88 (CH₂-CH-CH₂), 47.36 (CH₂-C=O), 35.69 (Ar-CH₂), 31.52 (CH₃-C=O).

FTIR (CH₂Cl₂) $\bar{\nu}_{\max}$ cm⁻¹ 1711, 1666, 1597, 1286, 1163, 779

HRMS Calcd. for C₂₃H₂₂O₃ (M+H) – 347.1647, found 347.1633.



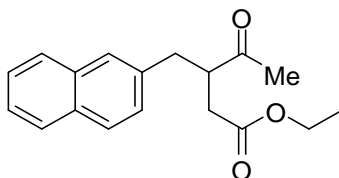
1-(2-methoxyphenyl)-3-(naphthalene-1-ylmethyl)pentane-1,4-dione, **51g**
(RT-3-295)

¹H NMR (500 MHz, CDCl₃) δ ppm 8.10 (d, *J* = 8.5 Hz, 1H, aromatic H), 7.86 (d, *J* = 8.1 Hz, 1H, aromatic H), 7.75 (d, *J* = 8.2 Hz, 1H, aromatic H), 7.57 (ddd, *J* = 8.4, 6.9, 1.3 Hz, 1H, aromatic H), 7.53 – 7.47 (m, 1H, aromatic H), 7.47 – 7.43 (m, 1H, aromatic H), 7.38 (dt, *J* = 5.6, 3.9 Hz, 2H, aromatic H), 7.31 (dt, *J* = 6.8, 3.9 Hz, 2H, aromatic h), 7.07 (ddd, *J* = 8.2, 2.6, 0.9 Hz, 1H, aromatic H), 3.80 (s, 3H, O-CH₃), 3.72 – 3.64 (m, 1H, diastereotopic H), 3.57 (dd, *J* = 18.0, 9.7 Hz, 1H, diastereotopic H), 3.38 (dd, *J* = 13.7, 7.5 Hz, 1H, diastereotopic H), 3.17 (dd, *J* = 13.8, 8.0 Hz, 1H, diastereotopic H), 3.05 (dd, *J* = 18.0, 3.6 Hz, 1H, diastereotopic H), 2.08 (s, 3H, CH₃-C=O)

¹³C NMR (126 MHz, CDCl₃) δ ppm 212.01 (C=O), 198.58 (C=O), 159.94 (aromatic C), 137.89 (aromatic C), 134.72 (aromatic C), 134.21 (aromatic C), 131.88 (aromatic C), 129.76 (aromatic C), 129.22 (aromatic C), 127.86 (aromatic C), 127.61 (aromatic C), 126.58 (aromatic C), 126.03 (aromatic C), 125.65 (aromatic C), 123.64 (aromatic C), 120.93 (aromatic C), 120.07 (aromatic C), 112.24 (aromatic C), 55.61 (O-CH₃), 47.82 (CH₂-CH-CH₂), 41.52 (CH₂-C=O), 35.37 (Ar-CH₂), 31.17 (CH₃-C=O)

FTIR (CH₂Cl₂) $\bar{\nu}_{\max}$ cm⁻¹ 1713, 1690, 1325, 1067, 781

HRMS Calcd for C₂₃H₂₂O₃ (M+H) – 347.1647, found 347.1668



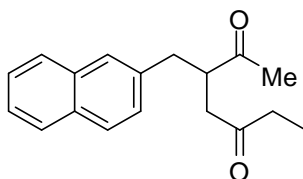
ethyl 3-(naphthalen-2-ylmethyl)-4-oxopentanoate, **51h**
(RT-3-144)

¹H NMR (500 MHz, CDCl₃) δ ppm 7.78 (dd, J = 16.5, 8.1 Hz, 3H, aromatic H), 7.58 (s, 1H, aromatic H), 7.50 – 7.40 (m, 2H, aromatic H), 7.30 (d, J = 8.4 Hz, 1H, aromatic H), 4.03 (q, J = 7.1 Hz, 2H, CH₂-CH₃), 3.46 – 3.28 (m, 1H, diastereotopic H), 3.08 (dd, J = 13.5, 6.9 Hz, 1H, diastereotopic H), 2.83 – 2.67 (m, 2H, CH₂-C=O), 2.34 (dd, J = 17.1, 4.2 Hz, 1H, diastereotopic H), 2.12 (s, 3H, CH₃-C=O), 1.18 (t, J = 7.1 Hz, 3H, CH₂-CH₃)

¹³C NMR (126 MHz, CDCl₃) δ ppm 210.93 (C=O), 172.24 (C=O), 135.75 (aromatic C), 133.49 (aromatic C), 132.26 (aromatic C), 128.49 (aromatic C), 127.72 (aromatic C), 127.64 (aromatic C), 127.58 (aromatic C), 127.06 (aromatic C), 126.27 (aromatic C), 125.76 (aromatic C), 60.46 (CH₂-CH₃), 49.67 (CH₂-CH-CH₂), 37.56 (Ar-CH₂), 35.08 (CH₂-C=O), 30.43 (CH₃-C=O), 13.75 (CH₂-CH₃)

FTIR (CH₂Cl₂) $\bar{\nu}_{\max}$ cm⁻¹ 2980, 2926, 1730, 1715, 1508, 1371, 1196, 821, 748

HRMS Calcd for C₁₈H₂₀O₃ (M+Na) – 307.1310, found 307.1325



3-(naphthalen-2-ylmethyl)heptane-2,5-dione, **51i**
(RT-3-252)

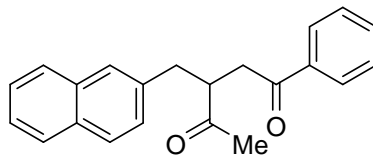
¹H NMR (500 MHz, CDCl₃) δ ppm 7.78 (dd, J = 16.5, 8.0 Hz, 3H, aromatic H), 7.57 (s, 1H, aromatic H), 7.53 – 7.37 (m, 2H, aromatic H), 7.29 (dd, J = 8.4, 1.7 Hz, 1H, aromatic H), 3.40 (td, J = 10.3, 3.6 Hz, 1H, diastereotopic H), 3.05 (dd, J = 13.5, 6.9 Hz, 1H, diastereotopic H), 2.95 (dd, J = 18.1, 10.1 Hz, 1H, diastereotopic H), 2.69 (dd, J = 13.5, 8.5 Hz, 1H, diastereotopic H), 2.44 – 2.26 (m, 3H, diastereotopic H), 2.13 (s, 3H, CH₃-C=O), 0.96 (t, J = 7.3 Hz, 3H, CH₂-CH₃)

¹³C NMR (126 MHz, CDCl₃) δ ppm 212.10 (C=O), 210.34 (C=O), 136.33 (aromatic C), 133.74 (aromatic C), 132.60 (aromatic C), 128.77 (aromatic C), 128.01 (aromatic C), 127.85 (aromatic C), 127.75 (aromatic C), 127.36 (aromatic C), 126.60 (aromatic C), 126.03 (aromatic C), 48.86

(CH₂-CH-CH₂), 44.09 (CH-CH₂-C=O), 38.04 (Ar-CH₂), 36.02 (CH₂-CH₃), 30.78 (CH₃-C=O), 7.84 (CH₂-CH₃).

FTIR (CH₂Cl₂) $\bar{\nu}_{\max}$ cm⁻¹ 2976, 2937, 1732, 1711, 1360, 1165, 822, 750

HRMS Calcd for C₁₈H₂₀O₂ (M+Na) – 291.1361, found 291.1417



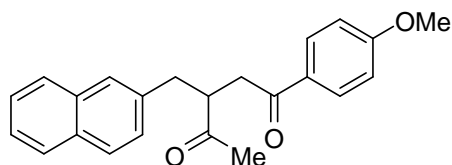
3-(naphthalen-2-ylmethyl)-1-phenylpentane-1,4-dione, **51j**
(RT-2-194)

¹H NMR (500 MHz, CDCl₃) δ ppm 7.86 (dd, *J* = 8.4, 1.2 Hz, 2H, aromatic H), 7.80 (d, *J* = 8.3 Hz, 2H, aromatic H), 7.77 (d, *J* = 7.6 Hz, 1H, aromatic H), 7.62 (s, 1H, aromatic H), 7.53 – 7.48 (m, 1H, aromatic H), 7.45 (dtd, *J* = 14.1, 6.8, 1.5 Hz, 2H, aromatic H), 7.39 (t, *J* = 7.7 Hz, 2H, aromatic H), 7.35 (dd, *J* = 8.4, 1.7 Hz, 1H, aromatic H), 3.64 – 3.58 (m, 1H, diastereotopic H), 3.55 (dd, *J* = 17.4, 9.9 Hz, 1H, diastereotopic H), 3.14 (dd, *J* = 13.5, 6.7 Hz, 1H, diastereotopic H), 3.00 (dd, *J* = 17.3, 2.7 Hz, 1H, diastereotopic H), 2.83 (dd, *J* = 13.5, 7.9 Hz, 1H, diastereotopic H), 2.19 (s, 3H, CH₃-C=O).

¹³C NMR (126 MHz, CDCl₃) δ ppm 211.52 (C=O), 198.58 (C=O), 144.99 (aromatic C), 136.39 (aromatic C), 136.07 (aromatic C), 133.52 (aromatic C), 133.30 (aromatic C), 132.30 (aromatic C), 128.58 (aromatic C), 128.52 (aromatic C), 128.05 (aromatic C), 127.71 (aromatic C), 127.58 (aromatic C), 127.49 (aromatic C), 127.08 (aromatic C), 126.29 (aromatic C), 125.73 (aromatic C), 48.41 (CH₂-CH-CH₂), 40.39 (CH₂-C=O), 37.91 (Ar-CH₂), 30.81 (CH₃-C=O).

FTIR (CH₂Cl₂) $\bar{\nu}_{\max}$ cm⁻¹ 1713, 1682, 1597, 1448, 1163, 750

HRMS Calcd for C₂₂H₂₀O₂ (M+H) – 317.1542, found 317.1526



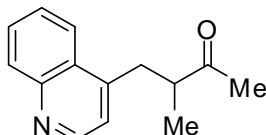
1-(4-methoxyphenyl)-3-(naphthalen-2-ylmethyl)pentane-1,4-dione, **51k**
(RT-2-196)

¹H NMR (500 MHz, CDCl₃) δ ppm 7.85 (d, *J* = 6.9 Hz, 2H, aromatic H), 7.79 (dd, *J* = 15.7, 6.8 Hz, 3H, aromatic H), 7.62 (s, 1H, aromatic H), 7.48 – 7.40 (m, 2H, aromatic H), 7.34 (dd, *J* = 8.4, 1.7 Hz, 1H, aromatic H), 6.86 (d, *J* = 9.0 Hz, 2H, aromatic H), 3.82 (s, 3H, O-CH₃), 3.63 – 3.53 (m, 1H, diastereotopic H), 3.49 (dd, *J* = 17.7, 9.9 Hz, 1H, diastereotopic H), 3.12 (dd, *J* = 13.5, 7.1 Hz, 1H, diastereotopic H), 2.97 (dd, *J* = 17.7, 3.4 Hz, 1H, diastereotopic H), 2.82 (dd, *J* = 13.5, 8.1 Hz, 1H, diastereotopic H), 2.18 (s, 3H, CH₃-C=O)

¹³C NMR (126 MHz, CDCl₃) δ 211.84 (C=O), 197.00 (C=O), 163.55 (aromatic C), 136.20 (aromatic C), 133.53 (aromatic C), 132.31 (aromatic C), 130.35 (aromatic C), 129.53 (aromatic C), 128.49 (aromatic C), 127.71 (aromatic C), 127.59 (aromatic C), 127.48 (aromatic C), 127.14 (aromatic C), 126.27 (aromatic C), 125.74 (aromatic C), 113.76 (aromatic C), 55.49 (O-CH₃), 48.75 (CH₂-CH-CH₃), 40.11 (CH₂-C=O), 37.94 (Ar-CH₂), 30.84 (CH₃-C=O).

FTIR (CH₂Cl₂) $\bar{\nu}_{\max}$ cm⁻¹ 1710, 1672, 1574, 1356, 1169, 822, 750

HRMS Calcd for C₂₃H₂₂O₃ (M+H) – 347.1647, found 347.1668



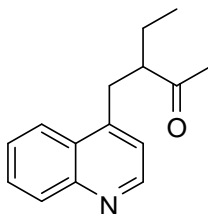
3-methyl-4-(quinolin-4-yl)butan-2-one, **53a**
(SRM-9-141)

¹H NMR (500 MHz, CDCl₃) δ ppm 8.79 (d, *J* = 4.3 Hz, 1H, aromatic H), 8.11 (d, *J* = 8.4 Hz, 1H, aromatic H), 7.98 (d, *J* = 8.4 Hz, 1H, aromatic H), 7.70 (t, *J* = 7.6 Hz, 1H, aromatic H), 7.56 (t, *J* = 7.6 Hz, 1H, aromatic H), 7.19 (d, *J* = 4.2 Hz, 1H, aromatic H), 3.51 (dd, *J* = 13.3, 5.8 Hz, 1H, CH₂-CH-CH₃), 2.98 (dt, *J* = 20.8, 7.4 Hz, 2H, CH₂-CH), 2.11 (s, 3H, CH₃-C=O), 1.16 (d, *J* = 6.8 Hz, 3H, CH-CH₃)

¹³C NMR (126 MHz, CDCl₃) δ 211.18 (C=O), 150.27 (aromatic H), 148.43 (aromatic H), 145.85 (aromatic H), 130.64 (aromatic H), 129.42 (aromatic H), 127.80 (aromatic H), 126.82 (aromatic H), 123.53 (aromatic H), 122.17 (aromatic H), 47.44 (CH-CH₃), 34.72 (Ar-CH₂), 29.11 (CH₃-C=O), 17.11 (CH-CH₃)

FTIR (CH₂Cl₂) $\bar{\nu}_{\max}$ cm⁻¹ 2970, 1713, 1508, 1360, 1169, 878, 762, 579

HRMS Calcd for C₁₄H₁₅NO (M+H) – 214.1232, found 214.1209



3-(quinolin-4-ylmethyl)pentan-2-one, **53b**
(RT-2-236)

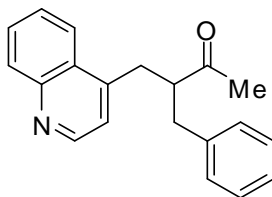
¹H NMR (500 MHz, CDCl₃) δ ppm 8.81 – 8.74 (d, *J* = 4.4 Hz, 1H, aromatic H), 8.16 – 8.09 (d, *J* = 8.4 Hz, 1H, aromatic H), 8.06 – 7.95 (d, *J* = 9.3 Hz, 1H, aromatic H), 7.76 – 7.68 (m, 1H, aromatic H), 7.63 – 7.54 (m, 1H, aromatic H), 7.23 – 7.16 (d, *J* = 4.4 Hz, 1H, aromatic H), 3.42 – 3.32 (dd, *J* = 14.0, 8.4 Hz, 1H, diastereotopic H), 3.17 – 3.09 (dd, *J* = 14.0, 6.0 Hz, 1H, diastereotopic H), 3.01 – 2.92 (m, 1H, diastereotopic H), 2.05 – 1.97 (s, 3H, O=C-CH₃), 1.82 –

1.73 (m, 1H, diastereotopic H), 1.68 – 1.58 (m, 1H, diastereotopic H), 1.00 – 0.92 (t, $J = 7.5$ Hz, 3H, $\text{CH}_2\text{-CH}_3$).

^{13}C NMR (126 MHz, CDCl_3) δ ppm 211.39 (C=O), 150.22 (aromatic C), 148.57 (aromatic C), 145.88 (aromatic C), 130.58 (aromatic C), 129.33 (aromatic C), 127.47 (aromatic C), 126.76 (aromatic C), 123.41 (aromatic C), 122.01 (aromatic C), 54.39 ($\text{CH}_2\text{-CH-C=O}$), 33.04 (Ar- CH_2), 30.44 (O=C- CH_3), 25.20 ($\text{CH}_2\text{-CH}_3$), 11.55 ($\text{CH}_2\text{-CH}_3$).

FTIR (CH_2Cl_2) $\bar{\nu}_{\text{max}}$ cm^{-1} 2962, 1711, 1591, 1508, 1352 1157, 737

HRMS Calcd for $\text{C}_{15}\text{H}_{18}\text{NO}$ (M+H) – 228.1388, found 228.1352.



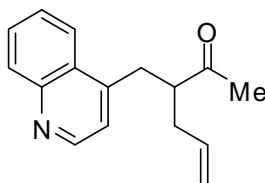
3-benzyl-4-(quinolin-4-yl)butan-2-one, **53c**
(RT-2-237)

^1H NMR (500 MHz, CDCl_3) δ ppm 8.75 (d, $J = 4.4$ Hz, 1H, aromatic H), 8.08 (d, $J = 8.7$ Hz, 1H, aromatic H), 7.70 – 7.63 (m, 2H, aromatic H), 7.48 (t, $J = 8.3$ Hz, 1H, aromatic H), 7.31 (t, $J = 7.3$ Hz, 2H, aromatic H), 7.24 (d, $J = 12.1$ Hz, 2H, aromatic H), 7.17 (dd, $J = 11.7, 5.6$ Hz, 3H, aromatic H), 3.33 (dd, $J = 13.0, 9.3$ Hz, 1H, diastereotopic H), 3.31 – 3.24 (m, 1H, diastereotopic H), 3.17 (dd, $J = 13.0, 4.1$ Hz, 1H, diastereotopic H), 3.04 (dd, $J = 13.5, 7.3$ Hz, 1H, diastereotopic H), 2.75 (dd, $J = 13.5, 7.0$ Hz, 1H, diastereotopic H), 1.77 (s, 3H, $\text{CH}_3\text{-C=O}$)

^{13}C NMR (126 MHz, CDCl_3) δ ppm 210.97 (C=O), 150.14, (aromatic H), 148.45 (aromatic H), 145.50 (aromatic H), 138.63 (aromatic H), 130.46 (aromatic H), 129.27 (aromatic H), 129.23 (aromatic H), 128.82 (aromatic H), 127.26 (aromatic H), 126.90 (aromatic H), 126.71 (aromatic H), 123.25 (aromatic H), 121.98 (aromatic H), 55.04 ($\text{CH}_2\text{-CH-CH}_2$), 38.79 (Ar- CH_2), 33.29 (Ar- CH_2), 31.51 ($\text{CH}_3\text{-C=O}$).

FTIR (CH_2Cl_2) $\bar{\nu}_{\text{max}}$ cm^{-1} 1710, 1591, 1364, 1161, 845, 764, 700

HRMS Calcd for $\text{C}_{20}\text{H}_{19}\text{NO}$ (M+H) – 290.1545, found 290.1552



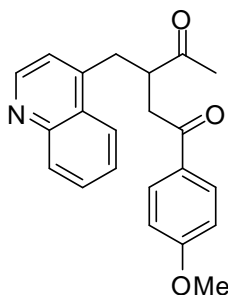
3-(quinolin-4-ylmethyl)hex-5-en-2-one, **53d**
(RT-2-235)

¹H NMR (500 MHz, CDCl₃) δ ppm 8.76 (d, *J* = 4.4 Hz, 1H, aromatic H), 8.10 (d, *J* = 8.4 Hz, 1H, aromatic H), 7.97 (d, *J* = 8.4 Hz, 1H, aromatic H), 7.70 (t, *J* = 7.6 Hz, 1H, aromatic H), 7.56 (t, *J* = 8.3 Hz, 1H, aromatic H), 7.18 (d, *J* = 4.4 Hz, 1H, aromatic H), 5.83 – 5.70 (m, 1H, CH=CH₂), 5.11 (d, *J* = 14.8 Hz, 2H, CH=CH₂), 3.34 (dd, *J* = 14.0, 8.6 Hz, 1H, diastereotopic H), 3.15 (dd, *J* = 14.0, 5.8 Hz, 1H, diastereotopic H), 3.10 – 3.02 (m, 1H, diastereotopic H), 2.44 (dt, *J* = 14.2, 8.2 Hz, 1H, diastereotopic H), 2.33 – 2.24 (m, 1H, diastereotopic H), 1.97 (s, 3H, CH₃-C=O)

¹³C NMR (126 MHz, CDCl₃) δ ppm 211.04 (C=O), 150.65 (aromatic C), 150.65 (aromatic C), 149.16 (aromatic C), 146.23 (aromatic C), 134.97 (CH=CH₂), 131.02 (aromatic C), 129.88 (aromatic C), 127.95 (aromatic C), 127.31 (aromatic C), 123.91 (aromatic C), 122.59 (aromatic C), 118.90 (CH=CH₂), 53.05 (CH₂-CH-CH₂), 36.84 (Ar-CH₂), 33.35 (CH₂-CH=CH₂), 31.15 (CH₃-C=O).

FTIR (CH₂Cl₂) $\bar{\nu}_{\max}$ cm⁻¹ 3074, 2926, 1711, 1640, 1591, 1358, 1167, 760

HRMS Calcd for C₁₆H₁₇NO (M+H) – 240.1388, found 240.1384

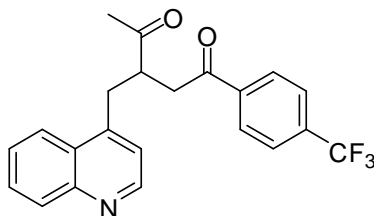


1-(4-methoxyphenyl)-3-(quinolin-4-ylmethyl)pentane-1,4-dione, **53e**
(RT-2-233)

¹H NMR (500 MHz, CDCl₃) δ ppm 8.85 – 8.79 (d, *J* = 4.4 Hz, 1H, aromatic H), 8.19 – 8.12 (m, 2H, aromatic H), 7.91 – 7.84 (d, *J* = 9.0 Hz, 2H, aromatic H), 7.79 – 7.73 (m, 1H, aromatic H), 7.68 – 7.62 (t, *J* = 7.1 Hz, 1H, aromatic H), 7.26 – 7.24 (d, *J* = 4.4 Hz, 1H, aromatic H), 6.93 – 6.88 (d, *J* = 9.0 Hz, 2H, aromatic H), 3.92 – 3.81 (s, 3H, O-CH₃), 3.73 – 3.65 (m, 1H, CH₂-CH-CH₂), 3.55 – 3.45 (dd, *J* = 17.9, 8.7 Hz, 1H, diastereotopic H), 3.43 – 3.33 (dd, *J* = 13.6, 7.8 Hz, 1H, diastereotopic H), 3.27 – 3.18 (dd, *J* = 13.7, 7.5 Hz, 1H, diastereotopic H), 3.11 – 3.01 (dd, *J* = 17.9, 4.6 Hz, 1H, diastereotopic H), 2.17 – 2.05 (s, 3H, O=C-CH₃).

¹³C NMR (126 MHz, CDCl₃) δ ppm 210.96 (C=O), 196.39 (C=O), 163.95 (aromatic C), 149.89 (aromatic C), 130.50 (aromatic C), 129.82 (aromatic C), 129.32 (aromatic C), 127.50 (aromatic C), 127.14 (aromatic C), 123.63 (aromatic C), 121.99 (aromatic C), 113.76 (aromatic C), 55.32 (CH₂-CH-CH₃), 47.03 (O-CH₃), 40.47 (CH-CH₂), 33.91 (Ar-CH₂), 30.93 (O=C-CH₃).

HRMS Calcd for C₂₂H₂₂NO₃ (M+H) – 348.1600, found 348.1565.



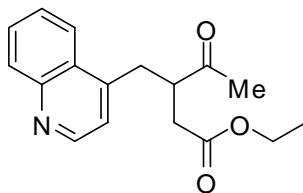
3-(quinolin-4-ylmethyl)-1-(4-(trifluoromethyl)phenyl)pentane-1,4-dione, **53f**
(RT-2-234)

¹H NMR (500 MHz, CDCl₃) δ ppm 8.85 – 8.80 (d, *J* = 4.4 Hz, 1H, aromatic H), 8.17 – 8.10 (dd, *J* = 12.5, 8.1 Hz, 2H, aromatic H), 8.00 – 7.95 (d, *J* = 8.1 Hz, 2H, aromatic H), 7.79 – 7.73 (m, 2H, aromatic H), 7.72 – 7.69 (d, *J* = 8.2 Hz, 2H, aromatic H), 7.67 – 7.63 (m, 1H, aromatic H), 3.76 – 3.66 (m, 2H, CH₂-CH-CH₂), 3.64 – 3.54 (dd, *J* = 18.1, 9.2 Hz, 1H, diastereotopic H), 3.46 – 3.38 (dd, *J* = 13.7, 7.3 Hz, 1H, diastereotopic H), 3.24 – 3.15 (dd, *J* = 13.7, 8.0 Hz, 1H, diastereotopic H), 3.10 – 3.00 (dd, *J* = 18.1, 4.0 Hz, 1H, diastereotopic H), 2.22 – 2.09 (s, 3H, O=C-CH₃).

¹³C NMR (126 MHz, CDCl₃) δ ppm 210.38 (C=O), 196.88 (aromatic C), 149.77 (aromatic C), 148.80 (aromatic C), 144.55 (aromatic C), 130.68 (aromatic C), 129.42 (aromatic C), 128.08 (aromatic C), 127.10 (aromatic C), 125.76 (aromatic C), 123.15 (CF₃), 122.11 (aromatic C), 47.42 (CH₂-CH-CH₂), 41.14 (Ar-CH₂), 34.21 (CH-CH₂C-O), 30.54 (O=C-CH₃).

FTIR (CH₂Cl₂) $\bar{\nu}_{\max}$ cm⁻¹ 3074, 2926, 1711, 1640, 1591, 1358, 1167, 760

HRMS Calcd for C₁₆H₁₇NO (M+H) – 240.1388, found 240.1384



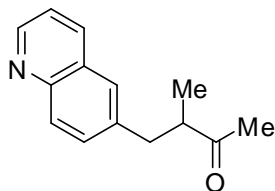
ethyl 4-oxo-3-(quinolin-4-ylmethyl)pentanoate, **53g**
(srm9146)

¹H NMR (500 MHz, CDCl₃) δ ppm 8.80 (d, *J* = 4.4 Hz, 1H, aromatic H), 8.12 (d, *J* = 8.3 Hz, 1H, aromatic H), 8.05 (d, *J* = 8.4 Hz, 1H, aromatic H), 7.73 (t, *J* = 7.0 Hz, 1H, aromatic H), 7.61 (t, *J* = 7.1 Hz, 1H, aromatic H), 7.18 (d, *J* = 4.4 Hz, 1H, aromatic H), 4.06 (q, *J* = 7.1 Hz, 2H, CH₂-CH₃), 3.45 (ddd, *J* = 12.7, 7.7, 5.4 Hz, 1H, diastereotopic H), 3.35 (dd, *J* = 13.6, 7.5 Hz, 1H, diastereotopic H), 3.08 (dd, *J* = 13.6, 7.8 Hz, 1H, diastereotopic H), 2.81 (dd, *J* = 17.1, 9.0 Hz, 1H, diastereotopic H), 2.38 (dd, *J* = 17.1, 4.9 Hz, 1H, diastereotopic H), 2.07 (s, 3H, CH₃-C=O), 1.20 (t, *J* = 7.1 Hz, 3H, CH₂-CH₃)

¹³C NMR (126 MHz, CDCl₃) δ ppm 210.19 (C=O), 172.14 (C=O), 150.29 (aromatic C), 148.71 (aromatic C), 144.35 (aromatic C), 130.74 (aromatic C), 129.70 (aromatic C), 127.21 (aromatic C), 123.38 (aromatic C), 122.34 (aromatic C), 61.17 (CH₂-CH₃), 48.25 (CH₂-CH-CH₂), 36.05 (Ar-CH₂), 33.93 (CH₂-C=O), 30.81 (CH₃-C=O), 14.31 (CH₂-CH₃)

FTIR (CH₂Cl₂) $\bar{\nu}_{\max}$ cm⁻¹ 2982, 1723, 1709, 1591, 762

HRMS Calcd for C₁₇H₁₉NO₃ (M+H) – 286.1443, found 286.1447



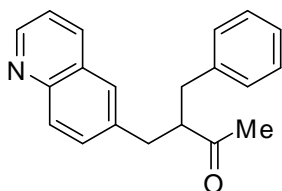
3-methyl-4-(quinolin-6-yl)butan-2-one, **53h**
(YA-1-120)

¹H NMR (500 MHz, CDCl₃) δ ppm 8.85 (d, *J* = 2.5 Hz, 1H, aromatic H), 8.07 (d, *J* = 9.3 Hz, 1H, aromatic H), 8.01 (d, *J* = 8.6 Hz, 1H, aromatic H), 7.55 (s, 1H, aromatic H), 7.52 (dd, *J* = 8.6, 2.0 Hz, 1H, aromatic H), 7.36 (dd, *J* = 8.3, 4.2 Hz, 1H, aromatic HH), 3.18 (dd, *J* = 13.7, 7.0 Hz, 1H, diastereotopic H), 2.98 – 2.87 (m, 1H, diastereotopic H), 2.73 (dd, *J* = 13.7, 7.5 Hz, 1H, diastereotopic H), 2.09 (s, 3H, CH₃-C=O), 1.12 (d, *J* = 7.0 Hz, 3H, CH-CH₃)

¹³C NMR (126 MHz, CDCl₃) δ ppm 212.13 (C=O), 150.25 (aromatic C), 147.49 (aromatic C), 138.54 (aromatic C), 135.96 (aromatic C), 131.34 (aromatic C), 129.86 (aromatic C), 128.63 (aromatic C), 127.53 (aromatic C), 121.66 (aromatic C), 49.01 (CH-CH₃), 38.83 (Ar-CH₂), 29.55 (CH₃-C=O), 16.52 (CH-CH₃)

FTIR (CH₂Cl₂) $\bar{\nu}_{\max}$ cm⁻¹ 2359, 1709, 1500, 1456, 1362, 837, 798

HRMS Calcd for C₁₄H₁₅NO (M+H) – 214.1232, found 214.1222



3-benzyl-4-(quinolin-6-yl)butan-2-one, **53i**
(RT-3-275)

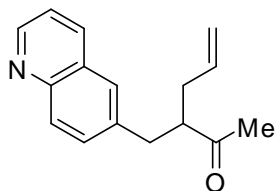
¹H NMR (500 MHz, CDCl₃) δ ppm 8.84 (dd, *J* = 4.2, 1.7 Hz, 1H, aromatic H), 8.06 (d, *J* = 6.8 Hz, 1H, aromatic H), 8.00 (d, *J* = 8.6 Hz, 1H, aromatic H), 7.53 (d, *J* = 1.7 Hz, 1H, aromatic H), 7.49 (dd, *J* = 8.6, 2.0 Hz, 1H, aromatic H), 7.36 (dd, *J* = 8.3, 4.2 Hz, 1H, aromatic H), 7.27 (t, *J* = 7.4 Hz, 2H, aromatic H), 7.19 (t, *J* = 8.0 Hz, 1H, aromatic H), 7.14 (d, *J* = 8.3 Hz, 2H, aromatic H), 3.25 (tt, *J* = 11.9, 5.9 Hz, 1H, diastereotopic H), 3.10 (dd, *J* = 13.6, 9.2 Hz, 1H, diastereotopic H), 2.96 (dd, *J* = 13.6, 8.6 Hz, 1H, diastereotopic H), 2.88 (dd, *J* = 13.6, 5.6 Hz, 1H, diastereotopic H), 2.75 (dd, *J* = 13.6, 6.2 Hz, 1H, diastereotopic H), 1.75 (s, 3H, CH₃-C=O)

¹³C NMR (126 MHz, CDCl₃) δ ppm 212.12 (C=O), 150.45 (aromatic C), 147.56 (aromatic C), 139.36 (aromatic C), 138.19 (aromatic C), 136.06 (aromatic C), 131.05 (aromatic C), 130.00 (aromatic C), 129.23 (aromatic C), 128.91 (aromatic C), 128.61 (aromatic C), 127.58 (aromatic C)

C), 126.84 (aromatic C), 121.59 (aromatic C), 56.12 (CH-CH₂), 38.85 (Ar-CH₂), 38.26 (Ar-CH₂), 32.02 (CH₃-C=O)

FTIR (CH₂Cl₂) $\bar{\nu}_{\max}$ cm⁻¹ 1711, 1499, 1369, 1161, 837, 700

HRMS Calcd for C₂₀H₁₉NO (M+H) – 290.1545, found 290.1533.



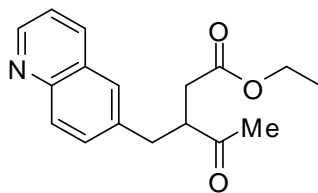
3-(quinolin-6-ylmethyl)hex-5-en-2-one, **53j**
(RT-3-274)

¹H NMR (500 MHz, CDCl₃) δ ppm 8.84 (d, *J* = 5.9 Hz, 1H, aromatic H), 8.06 (d, *J* = 7.8 Hz, 1H, aromatic H), 8.01 (d, *J* = 8.6 Hz, 1H, aromatic H), 7.57 – 7.47 (m, 2H, aromatic H), 7.35 (dd, *J* = 8.3, 4.2 Hz, 1H, aromatic H), 5.80 – 5.64 (m, 1H, CH=CH₂), 5.11 – 5.00 (m, 2H, CH=CH₂), 3.07 (dd, *J* = 13.3, 8.5 Hz, 1H, diastereotopic H), 3.04 – 2.95 (m, 1H, diastereotopic H), 2.86 (dd, *J* = 13.3, 5.8 Hz, 1H, diastereotopic H), 2.43 – 2.34 (m, 1H, diastereotopic H), 2.28 – 2.19 (m, 1H, diastereotopic H), 1.97 (s, 3H, CH₃-C=O)

¹³C NMR (126 MHz, CDCl₃) δ 211.52 (C=O), 150.35 (aromatic H), 147.48 (aromatic H), 138.24 (aromatic H), 136.04 (aromatic H), 135.12 (CH=CH₂), 131.20 (aromatic H), 129.86 (aromatic H), 128.57 (aromatic H), 127.52 (aromatic H), 121.61 (aromatic H), 117.88 (CH=CH₂), 54.02 (CH-CH₂), 37.55 (Ar-CH₂), 36.07 (CH₂-CH=CH₂), 30.73 (CH₃-C=O)

FTIR (CH₂Cl₂) $\bar{\nu}_{\max}$ cm⁻¹ 3074, 3011, 2924, 1709, 1640, 1362, 1161, 837

HRMS Calcd for C₁₆H₁₇NO (M+H) – 240.1388, found 240.1362



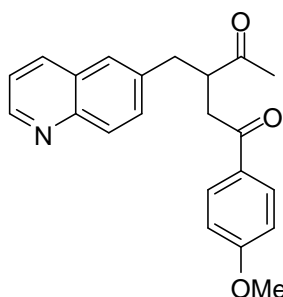
ethyl 4-oxo-3-(quinolin-6-ylmethyl)pentanoate, **53k**
(RT-3-74)

¹H NMR (500 MHz, CDCl₃) δ ppm 8.87 (d, *J* = 5.9 Hz, 1H, aromatic H), 8.06 (dd, *J* = 18.2, 8.3 Hz, 2H, aromatic H), 7.54 (d, *J* = 8.4 Hz, 2H, aromatic H), 7.38 (dd, *J* = 8.3, 4.2 Hz, 1H, aromatic H), 4.08 – 3.99 (m, 2H, CH₂-CH₃), 3.36 (dt, *J* = 14.5, 7.7 Hz, 1H, diastereotopic H), 3.10 (dd, *J* = 13.6, 7.2 Hz, 1H, diastereotopic H), 2.82 – 2.73 (m, 2H, diastereotopic H), 2.34 (dd, *J* = 17.1, 4.4 Hz, 1H, diastereotopic H), 2.11 (s, 3H, CH₃-C=O), 1.18 (t, *J* = 7.1 Hz, 3H, CH₂-CH₃)

¹³C NMR (126 MHz, CDCl₃) δ ppm 210.83 (C=O), 172.47 (C=O), 150.64, 147.43, 137.01, 136.05, 130.99, 130.29, 128.49, 127.72, 121.79, 61.13 (CH₂-CH₃), 49.77 (CH₂-CH-CH₂), 37.93 (Ar-CH₂), 35.85 (CH₂-C=O), 30.84 (CH₃-C=O), 14.44 (CH₂-CH₃)

FTIR (CH₂Cl₂) $\bar{\nu}_{\max}$ cm⁻¹ 1728, 1713, 1501, 1196, 1163, 1027, 841

HRMS Calcd for C₁₇H₁₉NO₃ (M+H) – 286.1443, found 286.1414.



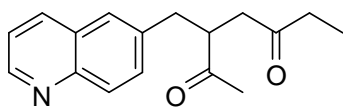
1-(4-methoxyphenyl)-3-(quinolin-6-ylmethyl)pentane-1,4-dione, **531**
(RT-3-76)

¹H NMR (500 MHz, CDCl₃) δ ppm 8.95 – 8.82 (s, 1H, aromatic H), 8.13 – 8.03 (dd, *J* = 15.6, 9.3 Hz, 2H, aromatic H), 7.90 – 7.83 (d, *J* = 9.0 Hz, 2H, aromatic H), 7.63 – 7.57 (m, 2H, aromatic H), 7.43 – 7.36 (dd, *J* = 8.3, 4.2 Hz, 1H, aromatic H), 6.92 – 6.85 (d, *J* = 9.0 Hz, 2H, aromatic H), 3.88 – 3.82 (s, 3H, O-CH₃), 3.65 – 3.57 (m, 1H, CH₂-CH-CH₂), 3.54 – 3.45 (dd, *J* = 17.7, 9.6 Hz, 1H, diastereotopic H), 3.20 – 3.12 (dd, *J* = 13.6, 7.5 Hz, 1H, diastereotopic H), 3.04 – 2.95 (dd, *J* = 17.7, 3.8 Hz, 1H, diastereotopic H), 2.92 – 2.84 (dd, *J* = 13.6, 7.7 Hz, 1H, diastereotopic H), 2.21 – 2.14 (s, 3H, O=C-CH₃).

¹³C NMR (126 MHz, CDCl₃) δ 211.73 (C=O), 196.59 (aromatic C), 163.95 (aromatic C), 150.12 (aromatic C), 147.16 (aromatic C), 136.94 (aromatic C), 135.67 (aromatic C), 131.06 (aromatic C), 130.39 (aromatic C), 129.71 (aromatic C), 129.04 (aromatic C), 127.11 (aromatic C), 121.50 (aromatic C), 113.60 (aromatic C), 55.28 (O-CH₃), 48.67 (CH₂-CH-CH₂), 40.44 (Ar-CH₂), 37.48 (CH-CH₂-C=O), 30.55 (O=C-CH₃).

FTIR (CH₂Cl₂) $\bar{\nu}_{\max}$ cm⁻¹ 1711, 1672, 1599, 1574, 1501, 1259, 1169, 833, 797

HRMS Calcd for C₂₂H₂₂NO₃ (M+H) – 348.1600, found 348.1583.



3-(quinolin-6-ylmethyl)heptane-2,5-dione, **54**
(RT-3-78)

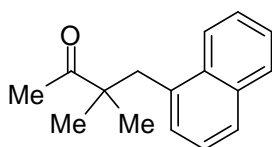
¹H NMR (500 MHz, CDCl₃) δ 8.83 – 8.79 (d, *J* = 4.4 Hz, 1H, aromatic H), 8.18 – 8.13 (d, *J* = 7.8 Hz, 1H, aromatic H), 8.11 – 8.06 (d, *J* = 8.4 Hz, 1H, aromatic H), 7.78 – 7.72 (m, 1H, aromatic H), 7.66 – 7.60 (m, 1H, aromatic H), 7.21 – 7.17 (d, *J* = 4.4 Hz, 1H, aromatic H), 3.55 – 3.46 (ddt, *J* = 12.2, 7.8, 4.4 Hz, 1H, CH₂-CH-CH₂), 3.41 – 3.26 (m, 1H, diastereotopic H), 3.11 –

2.88 (m, 2H, CH₂-CH₃), 2.52 – 2.44 (dd, *J* = 18.2, 4.4 Hz, 1H, diastereotopic H), 2.44 – 2.32 (m, 2H), 2.12 – 2.05 (s, 3H, O=C-CH₃), 1.04 – 0.95 (t, *J* = 7.3 Hz, 3H, CH₂-CH₃).

¹³C NMR (126 MHz, CDCl₃) δ 210.73 (C=O), 209.39 (C=O), 150.04 (aromatic C), 148.38 (aromatic C), 144.64 (aromatic C), 130.38 (aromatic C), 129.60 (aromatic C), 127.03 (aromatic C), 126.87 (aromatic C), 123.43 (aromatic C), 121.94 (aromatic C), 120.71 (aromatic C), 47.14 (CH₂-CH-CH₂), 44.17 (Ar-CH₂), 35.78 (CH-CH₂-C=O), 33.80 (O=C-CH₂-CH₃), 30.80 (O-C-CH₃), 7.68 (CH₂-CH₃).

FTIR (CH₂Cl₂) $\bar{\nu}_{\max}$ cm⁻¹ 1709, 1591, 1508, 1360, 1115, 764

HRMS Calcd for C₁₇H₂₀NO₂ (M+H) – 270.1494, found 270.1499.



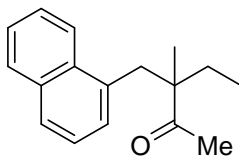
3,3-dimethyl-4-(naphthalene-1-yl)butan-2-one, **55a**
(RT-4-141)

¹H NMR (500 MHz, CDCl₃) δ ppm 8.04 (d, *J* = 8.4 Hz, 1H, aromatic H), 7.82 (d, *J* = 9.3 Hz, 1H, aromatic H), 7.72 (d, *J* = 8.2 Hz, 1H, aromatic H), 7.50 – 7.42 (m, 2H, aromatic H), 7.40 – 7.36 (m, 1H, aromatic H), 7.24 (d, *J* = 6.5 Hz, 1H, aromatic H), 3.31 (s, 2H, Ar-CH₂), 2.08 (s, 3H, CH₃-C=O), 1.15 (s, 6H, CH₃-C-CH₃)

¹³C NMR (126 MHz, CDCl₃) δ ppm 214.50 (C=O), 134.28 (aromatic C), 133.89 (aromatic C), 133.05 (aromatic C), 128.79 (aromatic C), 128.42 (aromatic C), 127.27 (aromatic C), 125.73 (aromatic C), 125.42 (aromatic C), 125.11 (aromatic C), 124.52 (aromatic C), 49.27 (CH₃-C-CH₃), 40.12 (Ar-CH₂), 26.36 (CH₃-C=O), 24.83 (CH₃-C-CH₃)

FTIR (CH₂Cl₂) $\bar{\nu}_{\max}$ cm⁻¹ 2968, 1701, 1352, 1117, 779, 453

HRMS Calcd for C₁₆H₁₈O (M+Na) – 249.1255, found 249.1263.



3-methyl-3-(naphthalene-1-ylmethyl)pentan-2-one, **55b**
(RT-4-71)

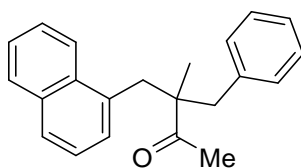
¹H NMR (500 MHz, CDCl₃) δ ppm 8.04 (d, *J* = 8.5 Hz, 1H, aromatic H), 7.82 (d, *J* = 9.5 Hz, 1H, aromatic H), 7.71 (d, *J* = 8.2 Hz, 1H, aromatic H), 7.46 (dtd, *J* = 14.5, 6.8, 1.4 Hz, 2H, aromatic H), 7.37 (dd, *J* = 8.1, 7.2 Hz, 1H, aromatic H), 3.31 (dd, *J* = 72.7, 14.3 Hz, 2H, diastereotopic H), 2.03 (s, 3H, CH₃-C=O), 1.93 (dq, *J* = 14.8, 7.4 Hz, 1H, diastereotopic H),

1.51 (dt, $J = 14.1, 7.5$ Hz, 1H, diastereotopic H), 1.06 (s, 3H, $\text{CH}_3\text{-C-C=O}$), 0.85 (t, $J = 7.5$ Hz, 3H, $\text{CH}_2\text{-CH}_3$)

^{13}C NMR (126 MHz, CDCl_3) δ ppm 214.38 (C=O), 134.29 (aromatic C), 133.90 (aromatic C), 133.12 (aromatic C), 128.82 (aromatic C), 128.15 (aromatic C), 127.25 (aromatic C), 125.75 (aromatic C), 125.43 (aromatic C), 125.17 (aromatic C), 124.47 (aromatic C), 53.24 ($\text{CH}_3\text{-C-C=O}$), 39.29 (Ar- CH_2), 31.89 ($\text{CH}_2\text{-CH}_3$), 27.04 ($\text{CH}_3\text{-C=O}$), 20.52 ($\text{CH}_3\text{-C}$), 9.19 ($\text{CH}_2\text{-CH}_3$)

FTIR (CH_2Cl_2) $\bar{\nu}_{\text{max}}$ cm^{-1} 2968, 2937, 1701, 1462, 1354, 1177, 800, 781, 434

HRMS Calcd for $\text{C}_{17}\text{H}_{20}\text{O}$ (M+H) – 241.1592, found 241.1609



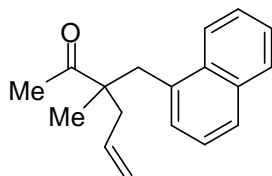
3-benzyl-3-methyl-4-(naphthalene-1-yl)butan-2-one, **55c**
(RT-4-40)

^1H NMR (500 MHz, CDCl_3) δ ppm 8.01 (dd, $J = 8.5, 7.4$ Hz, 1H, aromatic H), 7.83 (dd, $J = 7.4, 2.1$ Hz, 1H, aromatic H), 7.73 (d, $J = 8.2$ Hz, 1H, aromatic H), 7.46 (pd, $J = 6.8, 1.5$ Hz, 2H, aromatic H), 7.40 – 7.34 (m, 1H, aromatic H), 7.27 – 7.22 (m, 3H, aromatic H), 7.20 (d, $J = 7.1$ Hz, 1H, aromatic H), 7.10 – 7.07 (m, 2H, aromatic H), 3.53 (d, $J = 14.2$ Hz, 1H, diastereotopic H), 3.30 (t, $J = 13.6$ Hz, 2H, diastereotopic H), 2.72 (d, $J = 13.2$ Hz, 1H, diastereotopic H), 1.78 (s, 3H, $\text{CH}_3\text{-C=O}$), 1.10 (s, 3H, $\text{CH}_3\text{-C-C=O}$)

^{13}C NMR (126 MHz, CDCl_3) δ ppm 215.28 (C=O), 137.92 (aromatic C), 134.34 (aromatic C), 134.21 (aromatic C), 133.29 (aromatic C), 130.77 (aromatic C), 129.10 (aromatic C), 128.59 (aromatic C), 128.45 (aromatic C), 127.66 (aromatic C), 126.81 (aromatic C), 126.12 (aromatic C), 125.78 (aromatic C), 125.51 (aromatic C), 124.75 (aromatic C), 54.01 ($\text{CH}_2\text{-C-CH}_2$), 46.16 (Ph- CH_2), 40.96 (Np- CH_2), 29.24 ($\text{CH}_3\text{-C=O}$), 21.28 ($\text{CH}_3\text{-C}$)

FTIR (CH_2Cl_2) $\bar{\nu}_{\text{max}}$ cm^{-1} 2940, 1701, 1454, 1352, 1094, 779, 704

HRMS Calcd for $\text{C}_{22}\text{H}_{22}\text{O}$ (M+Na) – 325.1568, found 325.1571.



3-methyl-3-(naphthalene-1-ylmethyl)hex-5-en-2-one, **55d**
(RT-4-126)

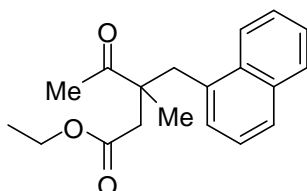
^1H NMR (500 MHz, CDCl_3) δ ppm 7.96 (d, $J = 8.2$ Hz, 1H, aromatic H), 7.85 (dd, $J = 12.6, 8.1$ Hz, 2H, aromatic H), 7.52 (td, $J = 14.2, 6.8$ Hz, 3H, aromatic H), 7.44 (d, $J = 7.2$ Hz, 1H,

aromatic H), 5.61 (d, $J = 3.1$ Hz, 2H, CH=CH₂), 5.57 (ddd, $J = 14.8, 7.9, 5.2$ Hz, 1H, CH=CH₂), 5.00 (s, 1H, diastereotopic H), 4.98 (d, $J = 8.0$ Hz, 1H, diastereotopic H), 2.61 (dd, $J = 14.0, 7.1$ Hz, 1H, diastereotopic H), 2.47 (dd, $J = 14.1, 7.5$ Hz, 1H, diastereotopic H), 1.97 (s, 3H, CH₃-C=O), 1.31 (s, 3H, CH₃-C)

¹³C NMR (126 MHz, CDCl₃) δ ppm 204.92 (C=O), 172.62 (aromatic C), 133.93 (CH=CH₂), 132.68 (aromatic C), 131.82 (aromatic C), 130.94 (aromatic C), 129.71 (aromatic C), 128.86 (aromatic C), 128.16 (aromatic C), 126.93 (aromatic C), 126.24 (aromatic C), 125.36 (aromatic C), 123.61 (aromatic C), 119.07 (CH=CH₂), 65.63 (CH₃-C-CH₂), 59.67 (CH₂-CH=CH₂), 39.37 (Ar-CH₂), 26.28 CH₃-C=O), 19.10 (CH₃-C)

FTIR (CH₂Cl₂) $\bar{\nu}_{\max}$ cm⁻¹ 3072, 2980, 2341, 1713, 1225, 1140, 777, 424

HRMS Calcd for C₁₈H₂₀O (M+H) – 253.1592, found 253.1502.



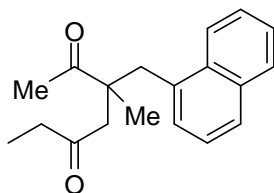
ethyl 3-methyl-3-(naphthalene-1-ylmethyl)-4-oxopentanoate, **55e**
(RT-3-123)

¹H NMR (500 MHz, CDCl₃) δ ppm 8.00 (d, $J = 8.4$ Hz, 1H, aromatic H), 7.83 (d, $J = 7.8$ Hz, 1H, aromatic H), 7.74 (d, $J = 8.2$ Hz, 1H, aromatic H), 7.47 (tdd, $J = 14.4, 6.8, 1.4$ Hz, 2H, aromatic H), 7.38 (dd, $J = 8.1, 7.1$ Hz, 1H, aromatic H), 7.25 (s, 1H, aromatic H), 4.08 (qd, $J = 7.1, 2.0$ Hz, 2H), CH₂-CH₃, 3.33 (dd, $J = 41.3, 14.0$ Hz, 2H, diastereotopic H), 2.97 (d, $J = 16.7$ Hz, 1H, diastereotopic H), 2.38 (d, $J = 16.7$ Hz, 1H, diastereotopic H), 2.06 (s, 3H, CH₃-C=O), 1.25 (s, 3H, CH₃-C), 1.20 (t, $J = 7.1$ Hz, 3H, CH₂-CH₃)

¹³C NMR (126 MHz, CDCl₃) δ ppm 213.53 (C=O), 171.99 (C=O), 134.24 (aromatic C), 133.34 (aromatic C), 133.29 (aromatic C), 129.23 (aromatic C), 129.15 (aromatic C), 128.01 (aromatic C), 126.27 (aromatic C), 125.87 (aromatic C), 125.41 (aromatic C), 124.65 (aromatic C), 60.88 (CH₂-CH₃), 50.92 (CH₃-C-C=O), 43.51 (CH₂-C=O), 40.06 (Ar-CH₂), 27.71 (CH₃-C=O), 22.31 (CH₃-C), 14.46 (CH₂-CH₃)

FTIR (CH₂Cl₂) $\bar{\nu}_{\max}$ cm⁻¹ 2975, 1709, 1703, 1460, 1111, 802, 781

HRMS Calcd for C₁₉H₂₂O₃ (M+Na) – 321.1467, found 321.1449



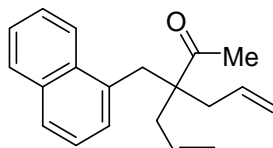
3-methyl-3-(naphthalen-1-ylmethyl)heptane-2,5-dione, **55f**
(RT-5-90)

¹H NMR (500 MHz, CDCl₃) δ ppm 7.98 (d, *J* = 8.0 Hz, 1H, aromatic H), 7.83 (d, *J* = 7.5 Hz, 1H, aromatic H), 7.74 (d, *J* = 8.0 Hz, 1H, aromatic H), 7.51 – 7.42 (m, 2H, aromatic H), 7.38 (t, *J* = 7.6 Hz, 1H, aromatic H), 7.22 (d, *J* = 7.0 Hz, 1H, aromatic H), 3.31 (s, 2H, Ar-CH₂), 3.04 (d, *J* = 18.1 Hz, 1H, diastereotopic H), 2.53 (d, *J* = 18.1 Hz, 1H, diastereotopic H), 2.32 – 2.26 (m, 2H, CH₂-CH₃), 2.06 (s, 3H, CH₃-C=O), 1.22 (s, 3H, C-CH₃), 0.98 (t, *J* = 7.3 Hz, 3H, CH₂-CH₃)

¹³C NMR (126 MHz, CDCl₃) δ ppm 213.75 (C=O), 209.37 (C=O), 133.90 (aromatic C), 133.30 (aromatic C), 132.97 (aromatic C), 128.89 (aromatic C), 128.78 (aromatic C), 127.55 (aromatic C), 125.82 (aromatic C), 125.48 (aromatic C), 124.98 (aromatic C), 124.35 (aromatic C), 51.54 (C-CH₂-C=O), 50.13 (C-CH₃), 39.79 (Ar-CH₂), 35.97 (CH₂-CH₃), 27.35 (CH₃-C=O), 22.41 (C-CH₃), 7.53 (CH₂-CH₃).

FTIR (CH₂Cl₂) $\bar{\nu}_{\max}$ cm⁻¹ 1713, 1709, 1460, 1354, 1111, 802, 781

HRMS Calcd for C₁₉H₂₂O₂ (M+Na) – 305.1518, found 305.1518.



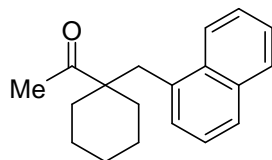
3-allyl-3-(naphthalen-1-ylmethyl)hex-5-en-2-one, **55g**
(RT-5-74)

¹H NMR (500 MHz, CDCl₃) δ ppm 8.13 (d, *J* = 8.3 Hz, 1H, aromatic H), 8.04 – 7.98 (m, 2H, aromatic H), 7.52 – 7.50 (m, 1H, aromatic H), 7.48 (dd, *J* = 3.3, 1.6 Hz, 1H, aromatic H), 7.37 (d, *J* = 3.5 Hz, 1H, aromatic H), 7.31 (d, *J* = 6.9 Hz, 1H, aromatic H), 5.79 – 5.68 (m, 2H, CH=CH₂), 5.15 – 5.04 (m, 4H, CH=CH₂), 3.36 (s, 2H, Ar-CH₂), 2.57 – 2.42 (m, 4H, CH₂-CH=CH₂), 1.88 (s, 3H, CH₃-C=O)

¹³C NMR (126 MHz, CDCl₃) δ ppm 213.71 (C=O), 138.74 (aromatic C), 134.44 (CH=CH₂), 129.47 (aromatic C), 129.15 (aromatic C), 128.02 (aromatic C), 127.47 (aromatic C), 126.58 (aromatic C), 126.17 (aromatic C), 125.70 (aromatic C), 124.71 (aromatic C), 124.56 (aromatic C), 124.30 (aromatic C), 119.61 (CH=CH₂), 53.67 (C-CH₂), 39.11 (Ar-CH₂), 37.86 (CH₂-CH=CH₂), 28.26 (CH₃-C=O).

FTIR (CH₂Cl₂) $\bar{\nu}_{\max}$ cm⁻¹ 3067, 3007, 2928, 1703, 1441, 1354, 918, 777

HRMS Calcd for C₂₀H₂₂O (M+H) – 279.1749, found 279.1750.



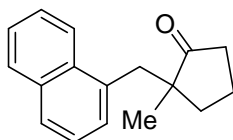
1-(1-(naphthalene-1-ylmethyl)cyclohexyl)ethanone, **55h**
(RT-5-75)

¹H NMR (500 MHz, CDCl₃) δ ppm 8.01 (d, *J* = 8.4 Hz, 1H, aromatic H), 7.82 (d, *J* = 7.9 Hz, 1H, aromatic H), 7.72 (d, *J* = 8.2 Hz, 1H, aromatic H), 7.46 (dtd, *J* = 14.5, 6.8, 1.4 Hz, 2H, aromatic H), 7.38 (dd, *J* = 8.1, 7.1 Hz, 1H, aromatic H), 7.22 (d, *J* = 7.1 Hz, 1H, aromatic H), 3.18 (s, 2H, Ar-CH₂), 2.18 (d, *J* = 13.4 Hz, 2H, Cy-CH₂), 1.94 (s, 3H, (CH₃-C=O)), 1.58 (t, *J* = 4.9 Hz, 1H, cyclohexyl H), 1.53 (d, *J* = 8.4 Hz, 1H, cyclohexyl H), 1.33 (td, *J* = 13.1, 3.4 Hz, 2H, cyclohexyl H), 1.23 – 1.13 (m, 2H, cyclohexyl H), 1.13 – 1.03 (m, 1H, cyclohexyl H)

¹³C NMR (126 MHz, CDCl₃) δ ppm 214.37 (C=O), 134.13 (aromatic H), 133.63 (aromatic H), 133.32 (aromatic H), 129.04 (aromatic H), 128.90 (aromatic H), 127.73 (aromatic H), 126.09 (aromatic H), 125.77 (aromatic H), 125.32 (aromatic H), 124.80 (aromatic H), 54.49 (C-C=O), 42.26 (Ar-CH₂), 34.21 (cyclohexyl C), 27.19 (CH₃-C=O), 25.99 (cyclohexyl C), 23.92 (cyclohexyl C)

FTIR (CH₂Cl₂) $\bar{\nu}_{\max}$ cm⁻¹ 2932, 1697, 1454, 1352, 1124, 779

HRMS Calcd. for C₁₉H₂₂O (M+Na) – 289.1568, found 289.1557.



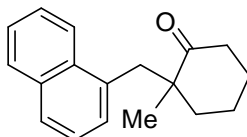
2-methyl-2-(naphthalen-1-ylmethyl)cyclopentanone, **55i**
(RT-7-135)

¹H NMR (500 MHz, CDCl₃) δ ppm 8.05 (d, *J* = 8.5 Hz, 1H, aromatic H), 7.82 (d, *J* = 8.0 Hz, 1H, aromatic H), 7.71 (d, *J* = 8.2 Hz, 1H, aromatic H), 7.47 (dtd, *J* = 16.1, 6.8, 1.3 Hz, 2H, aromatic H), 7.39 – 7.33 (m, 1H, aromatic H), 7.27 (d, *J* = 7.1 Hz, 1H, aromatic H), 3.27 (s, 2H, Ar-CH₂), 2.27 (ddd, *J* = 12.2, 8.3, 2.6 Hz, 1H, diastereotopic H), 1.98 – 1.89 (m, 1H, diastereotopic H), 1.83 (dt, *J* = 12.4, 7.5 Hz, 1H, diastereotopic H), 1.76 – 1.68 (m, 1H, diastereotopic H), 1.68 – 1.65 (m, 1H, diastereotopic H), 1.65 – 1.61 (m, 1H, diastereotopic H), 1.09 (s, 3H, C-CH₃)

¹³C NMR (126 MHz, CDCl₃) δ ppm 193.82 (C=O), 134.95, 133.99, 133.28, 128.92, 128.63, 127.36, 125.93, 125.59, 125.54, 124.68, 50.93 (C-CH₃), 38.07 (Ar-CH₂), 35.17 (CH₂-C=O), 23.67 (C-CH₃), 18.76 (CH₂-CH₂-CH₂)

FTIR (CH₂Cl₂) $\bar{\nu}_{\max}$ cm⁻¹ 2961, 2930, 1732, 1456, 1161, 1064, 800, 779

HRMS Calcd for C₁₇H₁₈O (M+H) – 239.1436, found 239.1400.

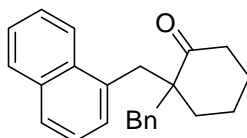


2-methyl-2-(naphthalen-1-ylmethyl)cyclohexanone, **55k**
(RT-10-67)

¹H NMR (500 MHz, CDCl₃) δ ppm 8.10 – 8.04 (d, *J* = 8.0 Hz, 1H), 7.86 – 7.80 (d, *J* = 7.6 Hz, 1H), 7.74 – 7.68 (d, *J* = 7.9 Hz, 1H), 7.50 – 7.41 (dt, *J* = 14.3, 7.3 Hz, 2H), 7.41 – 7.35 (t, *J* = 7.6 Hz, 1H), 7.31 – 7.27 (d, *J* = 7.1 Hz, 1H), 3.51 – 3.29 (dd, *J* = 66.8, 14.3 Hz, 2H), 2.55 – 2.46 (t, *J* = 6.7 Hz, 2H), 1.94 – 1.75 (m, 4H), 1.75 – 1.66 (dt, *J* = 8.8, 4.8 Hz, 1H), 1.62 – 1.55 (m, 1H), 1.08 – 1.00 (s, 3H).

¹³C NMR (126 MHz, CDCl₃) δ ppm 216.08, 134.59, 133.99, 133.54, 128.87, 128.77, 127.21, 125.70, 125.41, 125.20, 125.13, 124.83, 50.27, 39.07, 38.63, 37.88, 27.27, 23.36, 21.26.

HRMS Calcd for C₁₈H₂₀ONa (M+Na) – 275.1412, found 275.1433.

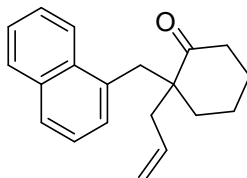


2-benzyl-2-(naphthalen-1-ylmethyl)cyclohexanone, **55l**
(RT-10-68)

¹H NMR (500 MHz, CDCl₃) δ ppm 7.87 – 7.75 (t, *J* = 7.4 Hz, 2H), 7.74 – 7.66 (d, *J* = 7.7 Hz, 1H), 7.45 – 7.30 (m, 4H), 7.29 – 7.26 (m, 1H), 7.24 – 7.17 (dd, *J* = 8.6, 4.7 Hz, 2H), 7.14 – 7.03 (d, *J* = 7.3 Hz, 2H), 3.60 – 3.49 (d, *J* = 14.6 Hz, 1H), 3.33 – 3.16 (m, 2H), 2.83 – 2.74 (d, *J* = 13.6 Hz, 1H), 2.45 – 2.34 (m, 2H), 1.77 – 1.56 (m, 6H).

¹³C NMR (126 MHz, CDCl₃) δ ppm 215.14, 137.64, 134.61, 133.91, 133.56, 130.98, 129.28, 128.90, 128.65, 128.43, 128.23, 127.17, 126.63, 125.82, 125.45, 125.39, 124.38, 54.77, 42.75, 39.96, 36.14, 33.38, 25.64, 20.88.

HRMS Calcd for C₂₄H₂₄ONa (M+Na) – 351.1725, found 351.1725.



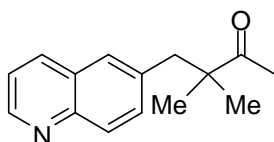
2-allyl-2-(naphthalen-1-ylmethyl)cyclohexanone, **55m**
(RT-10-101)

¹H NMR (500 MHz, CDCl₃) δ ppm 8.08 – 8.02 (d, *J* = 8.2 Hz, 1H), 7.85 – 7.79 (d, *J* = 7.7 Hz, 1H), 7.74 – 7.66 (d, *J* = 8.1 Hz, 1H), 7.51 – 7.41 (dd, *J* = 16.6, 7.7 Hz, 2H), 7.41 – 7.31 (m, 2H), 5.83 – 5.67 (m, 1H), 5.15 – 4.99 (dt, *J* = 16.9, 9.7 Hz, 2H), 3.61 – 3.21 (dd, *J* = 136.8, 14.4 Hz,

3H), 2.53 – 2.36 (m, 1H), 2.36 – 2.22 (dd, $J = 14.1, 7.7$ Hz, 1H), 1.90 – 1.74 (dt, $J = 17.6, 4.9$ Hz, 1H), 1.75 – 1.57 (m, 5H).

^{13}C NMR (126 MHz, CDCl_3) δ ppm 214.60, 134.71, 133.95, 133.83, 133.58, 128.92, 127.18, 125.75, 125.41, 125.34, 124.64, 118.59, 53.74, 40.31, 39.81, 35.61, 34.94, 26.39, 20.90.

HRMS Calcd for $\text{C}_{20}\text{H}_{22}\text{ONa}$ ($\text{M}+\text{Na}$) – 301.1568, found 301.1583.

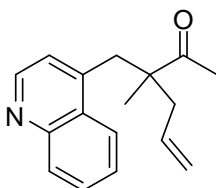


3,3-dimethyl-4-(quinolin-6-yl)butan-2-one, **56a**
(RT-11-166)

^1H NMR (400 MHz, CDCl_3) δ ppm 8.92 – 8.80 (d, $J = 4.0$ Hz, 1H), 8.14 – 8.04 (d, $J = 8.3$ Hz, 1H), 8.04 – 7.96 (d, $J = 8.6$ Hz, 1H), 3.05 – 2.94 (s, 2H), 2.17 – 2.07 (s, 1H), 1.22 – 1.11 (s, 3H).

^{13}C NMR (126 MHz, CDCl_3) δ ppm 213.63, 150.03, 147.16, 136.62, 135.64, 132.66, 128.33, 128.03, 121.11, 48.63, 44.69, 25.97, 24.61.

HRMS Calcd for $\text{C}_{15}\text{H}_{18}\text{NO}$ ($\text{M}+\text{H}$) – 228.1388; found 228.1381.

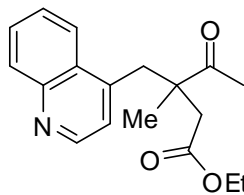


3-methyl-3-(quinolin-4-ylmethyl)hex-5-en-2-one, **56b**
(RT-11-194B)

^1H NMR (500 MHz, CDCl_3) δ ppm 8.83 – 8.75 (d, $J = 4.5$ Hz, 2H), 8.17 – 8.09 (d, $J = 8.4$ Hz, 3H), 8.09 – 8.01 (d, $J = 8.5$ Hz, 3H), 7.75 – 7.67 (m, 1H), 7.60 – 7.53 (m, 1H), 7.21 – 7.14 (d, $J = 4.5$ Hz, 2H), 5.78 – 5.65 (ddt, $J = 17.2, 10.2, 7.3$ Hz, 2H), 5.19 – 5.07 (m, 5H), 3.54 – 3.19 (dd, $J = 121.6, 14.1$ Hz, 4H), 2.61 – 2.54 (dd, $J = 14.0, 6.9$ Hz, 3H), 2.32 – 2.21 (m, 2H), 2.11 – 2.01 (s, 5H), 1.19 – 1.04 (s, 6H).

^{13}C NMR (126 MHz, CDCl_3) δ ppm 212.95, 149.43, 133.25, 130.23, 129.43, 128.63, 126.58, 124.25, 122.76, 119.12, 52.60, 43.74, 37.84, 27.25, 21.00.

HRMS Calcd for $\text{C}_{17}\text{H}_{20}\text{NO}$ ($\text{M}+\text{H}$) – 254.1545; found 254.1532.

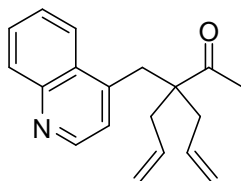


ethyl 3-methyl-4-oxo-3-(quinolin-4-ylmethyl)pentanoate, **56c**
(RT-11-165)

¹H NMR (500 MHz, CDCl₃) δ ppm 8.87 – 8.79 (d, *J* = 4.2 Hz, 1H), 8.22 – 8.15 (d, *J* = 8.4 Hz, 1H), 8.08 – 8.00 (d, *J* = 8.4 Hz, 1H), 7.79 – 7.71 (t, *J* = 7.2 Hz, 1H), 7.60 – 7.53 (t, *J* = 7.7 Hz, 1H), 7.33 – 7.28 (d, *J* = 4.2 Hz, 1H), 4.17 – 4.10 (q, *J* = 7.2 Hz, 2H), 3.69 – 3.59 (s, 2H), 2.87 – 2.76 (s, 3H), 2.10 – 2.03 (s, 3H), 1.27 – 1.22 (t, *J* = 7.1 Hz, 3H).

¹³C NMR (126 MHz, CDCl₃) δ ppm 210.99, 171.65, 130.13, 128.81, 127.16, 124.31, 123.80, 61.32, 51.87, 39.50, 35.72, 28.28, 14.44.

HRMS Calcd for C₁₈H₂₂NO₃ (M+H) – 300.1600; found 300.1618.

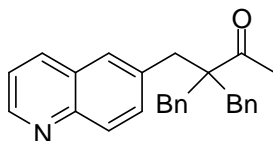


3-allyl-3-(quinolin-4-ylmethyl)hex-5-en-2-one, **56d**
(RT-10-243)

¹H NMR (500 MHz, CDCl₃) δ ppm 8.84 – 8.70 (d, *J* = 4.5 Hz, 1H), 8.14 – 7.98 (m, 2H), 7.77 – 7.65 (m, 1H), 7.62 – 7.50 (m, 1H), 7.20 – 7.09 (d, *J* = 4.5 Hz, 1H), 5.75 – 5.61 (m, 2H), 5.17 – 5.01 (m, 4H), 3.41 – 3.33 (s, 2H), 2.54 – 2.41 (m, 4H), 2.06 – 1.97 (s, 3H).

¹³C NMR (126 MHz, CDCl₃) δ 212.24, 149.81, 148.63, 144.32, 132.95, 130.43, 129.44, 128.61, 126.80, 123.84, 122.17, 119.74, 55.17, 38.68, 36.06, 27.49;

HRMS Calcd for C₁₉H₂₂NO (M+H) – 280.1701; found 280.1694.

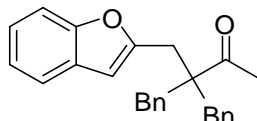


3,3-dibenzyl-4-(quinolin-6-yl)butan-2-one, **56e**
(RT-10-254)

¹H NMR (400 MHz, CDCl₃) δ ppm 8.91 – 8.83 (d, *J* = 3.3 Hz, 1H), 8.04 – 7.94 (dd, *J* = 13.4, 8.4 Hz, 2H), 7.41 – 7.33 (m, 3H), 7.28 – 7.21 (q, *J* = 8.7, 7.6 Hz, 6H), 7.07 – 7.01 (d, *J* = 7.6 Hz, 4H), 3.29 – 3.21 (s, 2H), 3.18 – 3.03 (q, *J* = 14.9 Hz, 4H), 2.03 – 1.94 (s, 3H)

^{13}C NMR (126 MHz, CDCl_3) δ ppm 213.50, 150.27, 147.38, 137.30, 136.25, 135.92, 132.45, 130.27, 129.25, 128.34, 128.02, 126.64, 121.31, 56.44, 41.35, 40.34, 29.00.

HRMS Calcd for $\text{C}_{27}\text{H}_{26}\text{NO}$ ($\text{M}+\text{H}$) – 380.2014; found 380.2005.

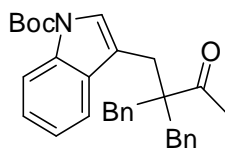


4-(benzofuran-2-yl)-3,3-dibenzylbutan-2-one, **56f**
(RT-11-105)

^1H NMR (400 MHz, CDCl_3) δ ppm 7.54 – 7.44 (dd, $J = 19.9, 7.4$ Hz, 2H), 7.32 – 7.28 (s, 3H), 7.25 – 7.19 (m, 4H), 7.18 – 7.12 (d, $J = 7.6$ Hz, 5H), 6.44 – 6.38 (s, 1H), 3.21 – 3.07 (m, 6H), 2.08 – 2.00 (s, 3H).

^{13}C NMR (126 MHz, CDCl_3) δ ppm 212.38, 212.23, 155.73, 154.59, 137.13, 130.52, 128.83, 126.85, 126.35, 123.67, 122.87, 120.71, 111.07, 105.73, 56.24, 42.10, 38.31, 31.73, 28.65.

HRMS Calcd for $\text{C}_{26}\text{H}_{24}\text{O}_2\text{Na}$ ($\text{M}+\text{Na}$) – 391.1674; found 391.1692.

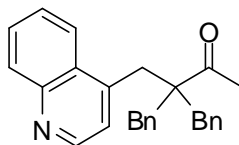


tert-butyl 3-(2,2-dibenzyl-3-oxobutyl)-1H-indole-1-carboxylate, **56g**
(RT-11-270)

^1H NMR (400 MHz, CDCl_3) δ ppm 8.22 – 8.07 (s, 1H), 7.42 – 7.33 (m, 3H), 7.27 – 7.20 (m, 7H), 7.12 – 7.02 (t, $J = 3.7$ Hz, 4H), 3.28 – 3.09 (m, 4H), 3.09 – 3.02 (s, 2H), 2.06 – 1.95 (s, 3H), 1.75 – 1.66 (s, 3H).

^{13}C NMR (126 MHz, CDCl_3) δ ppm 213.46, 137.16, 130.33, 128.48, 126.74, 124.69, 123.36, 122.57, 119.03, 116.75, 115.22, 56.13, 41.51, 28.98, 28.60, 28.38.

HRMS Calcd for $\text{C}_{31}\text{H}_{33}\text{NO}_3\text{Na}$ ($\text{M}+\text{Na}$) – 490.2358; found 490.2333.



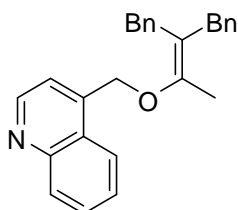
3,3-dibenzyl-4-(quinolin-4-yl)butan-2-one, **56h**
(RT-10-53fracC)

^1H NMR (400 MHz, CDCl_3) δ 8.89 – 8.77 (d, $J = 4.5$ Hz, 1H), 8.21 – 8.09 (d, $J = 8.3$ Hz, 1H), 7.99 – 7.87 (d, $J = 8.2$ Hz, 1H), 7.81 – 7.68 (t, $J = 8.2$ Hz, 1H), 7.60 – 7.50 (m, 1H), 7.25 – 7.16

(t, $J = 3.2$ Hz, 6H), 7.14 – 7.08 (d, $J = 4.6$ Hz, 1H), 7.05 – 6.96 (s, 4H), 3.56 – 3.44 (s, 2H), 3.29 – 3.13 (m, 4H), 2.02 – 1.87 (s, 3H).

^{13}C NMR (126 MHz, CDCl_3) δ ppm 213.05, 149.76, 148.12, 143.86, 136.64, 130.42, 129.39, 128.36, 126.72, 123.15, 120.83, 55.29, 41.42, 35.17, 28.88.

HRMS Calcd for $\text{C}_{27}\text{H}_{26}\text{NO}$ (M+H) – 380.2014; found 380.2001.

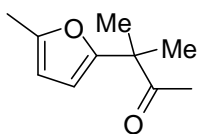


4-((3-benzyl-4-phenylbut-2-en-2-yloxy)methyl)quinoline, **58**
(RT-10-53fracA)

^1H NMR (500 MHz, CDCl_3) δ ppm 8.96 – 8.87 (d, $J = 4.2$ Hz, 1H), 8.19 – 8.09 (d, $J = 8.4$ Hz, 1H), 8.02 – 7.93 (d, $J = 8.3$ Hz, 1H), 7.78 – 7.68 (t, $J = 8.2$ Hz, 1H), 7.62 – 7.51 (m, 2H), 7.30 – 7.15 (m, 9H), 7.13 – 7.08 (t, $J = 5.8$ Hz, 5H), 5.37 – 5.24 (s, 2H), 3.45 – 3.20 (d, $J = 65.1$ Hz, 3H), 2.22 – 2.04 (s, 2H).

^{13}C NMR (126 MHz, CDCl_3) δ ppm 150.58, 148.07, 147.08, 143.49, 140.83, 140.14, 130.40, 129.41, 128.96, 128.54, 128.40, 126.88, 126.19, 125.91, 123.04, 120.09, 119.28, 67.13, 35.83, 34.25, 14.13.

HRMS Calcd for $\text{C}_{27}\text{H}_{26}\text{NO}$ (M+H) – 380.2014; found 380.1997.

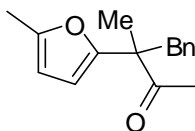


3-methyl-3-(5-methylfuran-2-yl)butan-2-one, **59b**
(RT-9-166)

^1H NMR (400 MHz, CDCl_3) δ ppm 6.08 – 6.03 (s, 1H), 5.93 – 5.89 (s, 1H), 2.28 – 2.25 (s, 3H), 2.02 – 1.99 (s, 3H), 1.44 – 1.42 (s, 6H).

^{13}C NMR (126 MHz, CDCl_3) δ ppm 209.70, 156.40, 151.47, 139.91, 109.94, 106.00, 65.81, 49.34, 25.63, 22.64, 15.43, 13.76.

HRMS Calcd for $\text{C}_{10}\text{H}_{15}\text{O}_2$ (M+ NH_4) – 167.1072; found 167.1078.

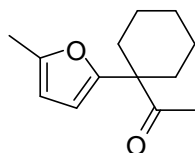


3-methyl-3-(5-methylfuran-2-yl)-4-phenylbutan-2-one, **59c**
(RT-10-82)

¹H NMR (400 MHz, CDCl₃) δ ppm 7.24 – 7.10 (s, 3H), 6.88 – 6.72 (s, 2H), 6.00 – 5.86 (s, 2H), 3.37 – 3.03 (dd, *J* = 80.8, 13.5 Hz, 2H), 2.42 – 2.28 (s, 3H), 2.13 – 2.00 (s, 3H), 1.35 – 1.20 (s, 3H).

¹³C NMR (126 MHz, CDCl₃) δ ppm 209.54, 153.87, 151.63, 137.51, 130.43, 127.88, 126.26, 108.63, 106.52, 53.76, 41.23, 26.18, 19.57, 13.82.

HRMS Calcd for C₁₆H₁₉O₂ (M+H) – 243.1385; found 243.1384.

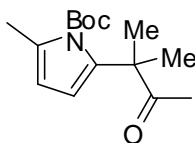


1-(1-(5-methylfuran-2-yl)cyclohexyl)ethanone, **59d**
(RT-10-84)

¹H NMR (400 MHz, CDCl₃) δ 6.13 – 5.98 (s, 1H), 5.98 – 5.82 (s, 1H), 2.32 – 2.19 (s, 3H), 2.08 – 1.86 (s, 7H), 1.60 – 1.31 (m, 6H).

¹³C NMR (126 MHz, CDCl₃) δ 209.18, 153.88, 151.37, 107.70, 106.31, 53.65, 31.25, 25.66, 25.34, 22.47, 13.54.

HRMS Calcd for C₁₃H₁₇O₂ (M-H) – 205.1229; found 205.1246.

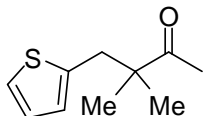


tert-butyl 2-methyl-5-(2-methyl-3-oxobutan-2-yl)-1H-pyrrole-1-carboxylate, **59e**
(RT-10-120)

¹H NMR (400 MHz, CDCl₃) δ ppm 6.09 – 6.01 (s, 1H), 5.88 – 5.80 (s, 1H), 2.37 – 2.32 (s, 3H), 2.06 – 2.02 (s, 3H), 1.55 – 1.52 (s, 9H), 1.43 – 1.39 (s, 6H).

¹³C NMR (126 MHz, CDCl₃) δ ppm 210.56, 139.28, 131.62, 110.11, 109.78, 84.32, 49.37, 27.87, 25.73, 25.69, 17.00.

HRMS Calcd for C₁₅H₂₃NO₃Na (M+Na) – 288.1576; found 288.1573.

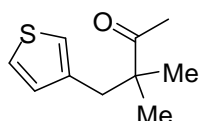


3,3-dimethyl-4-(thiophen-2-yl)butan-2-one, **59f**
(RT-9-209)

¹H NMR (500 MHz, CDCl₃) δ ppm 7.16 – 7.07 (d, *J* = 4.2 Hz, 1H), 6.94 – 6.86 (s, 1H), 6.79 – 6.70 (s, 1H), 3.08 – 2.99 (s, 2H), 2.17 – 2.09 (s, 3H), 1.20 – 1.15 (s, 6H).

¹³C NMR (126 MHz, CDCl₃) δ ppm 213.46, 139.95, 127.01, 126.72, 124.17, 48.81, 39.39, 26.01, 24.59.

HRMS Calcd for C₁₀H₁₄OSLi (M+Li) – 189.0925; found 189.0922.

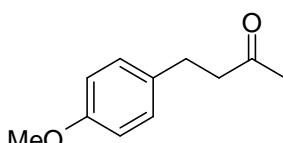


3,3-dimethyl-4-(thiophen-3-yl)butan-2-one, **59g**
(RT-9-210)

¹H NMR (400 MHz, CDCl₃) δ ppm 7.24 – 7.18 (s, 1H), 6.95 – 6.88 (s, 1H), 6.88 – 6.81 (s, 1H), 2.87 – 2.83 (s, 2H), 2.13 – 2.09 (s, 3H), 1.15 – 1.12 (s, 6H).

¹³C NMR (126 MHz, CDCl₃) δ ppm 213.83, 138.08, 129.49, 124.87, 122.26, 53.45, 39.57, 25.78, 24.07.

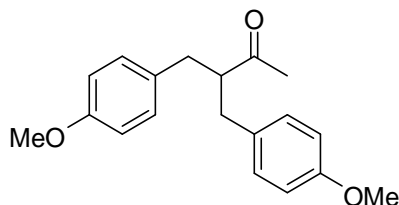
HRMS Calcd for C₁₀H₁₃OS (M-H) – 181.0687; found 181.0657.



4-(4-methoxyphenyl)butan-2-one, **60a**¹⁹
(RT-7-97)

¹H NMR (400 MHz, CDCl₃) δ ppm 7.16 – 7.02 (d, *J* = 6.5 Hz, 2H), 6.91 – 6.75 (d, *J* = 6.8 Hz, 2H), 3.83 – 3.74 (s, 3H), 2.95 – 2.80 (t, *J* = 7.6 Hz, 2H), 2.80 – 2.59 (m, 2H), 2.26 – 2.10 (d, *J* = 16.5 Hz, 3H).

¹³C NMR (126 MHz, CDCl₃) δ ppm 208.32, 158.15, 129.81, 129.35, 114.09, 56.94, 55.30, 37.20, 28.91.

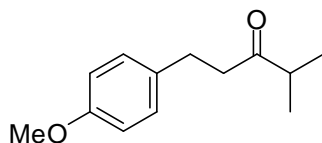


3-(4-methoxybenzyl)-4-(4-methoxyphenyl)butan-2-one, **60b**
(RT-7-97 frac)

¹H NMR (500 MHz, CDCl₃) δ ppm 7.11 – 7.08 (d, *J* = 8.7 Hz, 2H), 7.06 – 7.03 (d, *J* = 8.7 Hz, 2H), 6.83 – 6.79 (t, *J* = 8.6 Hz, 4H), 3.80 – 3.77 (s, 6H), 3.11 – 3.03 (ddd, *J* = 14.9, 9.0, 5.9 Hz, 1H), 2.87 – 2.85 (d, *J* = 3.0 Hz, 1H), 2.83 – 2.81 (d, *J* = 4.5 Hz, 1H), 2.69 – 2.64 (dd, *J* = 13.7, 5.9 Hz, 2H), 2.19 – 2.07 (s, 3H).

¹³C NMR (126 MHz, CDCl₃) δ ppm 212.76, 158.18, 132.97, 131.57, 130.02, 129.43, 113.84, 57.02, 55.37, 37.42, 31.84.

HRMS Calcd. for C₁₉H₂₂O₃Na (M+Na) – 321.1467, found 321.1435.

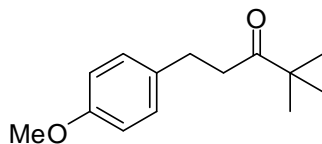


1-(4-methoxyphenyl)-4-methylpentan-3-one, **60c**
(RT-7-88)

¹H NMR (500 MHz, CDCl₃) δ ppm 7.12 – 7.07 (d, *J* = 8.7 Hz, 2H), 6.84 – 6.80 (d, *J* = 8.7 Hz, 2H), 3.83 – 3.74 (s, 3H), 2.86 – 2.79 (m, 2H), 2.76 – 2.70 (m, 2H), 2.59 – 2.52 (m, 1H), 1.10 – 1.03 (d, *J* = 6.9 Hz, 6H).

¹³C NMR (126 MHz, CDCl₃) δ ppm 214.12, 163.57, 158.03, 133.54, 129.40, 113.99, 55.40, 42.40, 41.18, 29.12, 18.28.

HRMS Calcd for C₁₃H₁₈O₂Li (M+Li) – 213.1467, found 213.1452.

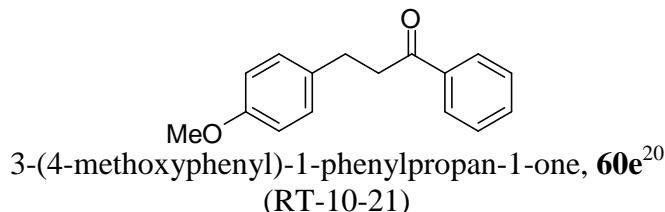


1-(4-methoxyphenyl)-4,4-dimethylpentan-3-one, **60d**
(RT-7-89)

¹H NMR (500 MHz, CDCl₃) δ ppm 7.12 – 7.08 (d, *J* = 8.6 Hz, 2H), 6.84 – 6.80 (d, *J* = 8.6 Hz, 2H), 3.80 – 3.76 (s, 3H), 2.83 – 2.78 (m, 2H), 2.78 – 2.72 (m, 2H), 1.14 – 1.05 (s, 9H).

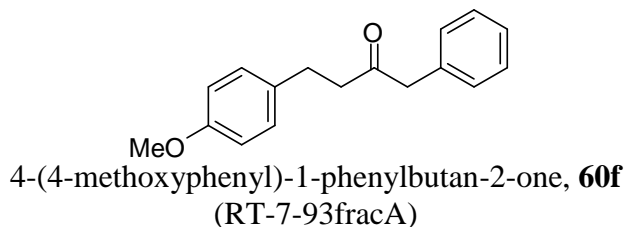
¹³C NMR (126 MHz, CDCl₃) δ ppm 215.26, 158.01, 133.77, 129.46, 113.96, 55.40, 44.23, 38.87, 29.35, 26.45.

HRMS Calcd for C₁₄H₂₁O₂ (M+H) – 221.1542, found 221.1548.



¹H NMR (400 MHz, CDCl₃) δ ppm 8.00 – 7.92 (d, *J* = 8.1 Hz, 2H), 7.60 – 7.52 (t, *J* = 7.4 Hz, 1H), 7.49 – 7.42 (m, 2H), 7.21 – 7.14 (d, *J* = 8.4 Hz, 2H), 6.89 – 6.81 (d, *J* = 8.5 Hz, 2H), 3.86 – 3.71 (s, 3H), 3.33 – 3.21 (t, *J* = 7.7 Hz, 2H), 3.07 – 2.96 (t, *J* = 7.6 Hz, 2H).

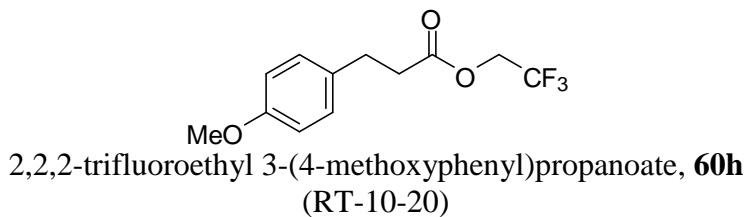
¹³C NMR (126 MHz, CDCl₃) δ ppm 199.53, 158.10, 136.96, 133.44, 133.18, 129.49, 128.67, 128.13, 114.06, 55.14, 40.97, 29.35.



¹H NMR (500 MHz, CDCl₃) δ ppm 7.98 – 7.95 (m, 2H), 7.58 – 7.54 (t, *J* = 7.4 Hz, 1H), 7.49 – 7.43 (m, 2H), 7.21 – 7.13 (d, *J* = 8.7 Hz, 2H), 6.88 – 6.80 (d, *J* = 8.7 Hz, 2H), 3.83 – 3.75 (s, 3H), 3.31 – 3.24 (m, 2H), 3.05 – 2.98 (t, *J* = 7.7 Hz, 2H), 2.66 – 2.57 (s, 2H)

¹³C NMR (126 MHz, CDCl₃) δ ppm 199.59, 157.95, 136.86, 133.40, 133.23, 133.18, 129.49, 128.74, 128.72, 128.43, 128.18, 114.00, 55.43, 40.82, 29.35, 26.82.

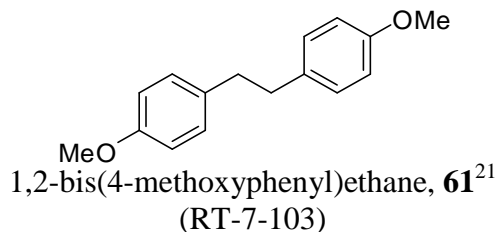
HRMS Calcd for C₁₇H₁₈O₂Li (M+Li) – 261.1467, found 261.1463.



¹H NMR (400 MHz, CDCl₃) δ ppm 7.15 – 7.08 (d, *J* = 10.3 Hz, 2H), 6.87 – 6.80 (d, *J* = 10.4 Hz, 2H), 4.50 – 4.39 (m, 2H), 3.83 – 3.75 (s, 3H), 2.98 – 2.88 (t, *J* = 7.5 Hz, 2H), 2.76 – 2.66 (t, *J* = 7.6 Hz, 2H).

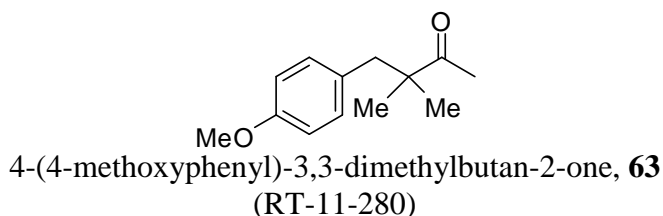
¹³C NMR (126 MHz, CDCl₃) δ ppm 210.78, 139.49, 131.89, 110.38, 109.95, 84.53, 49.49, 27.98, 25.77, 16.88.

HRMS Calcd for C₁₂H₁₂F₃O₃ (M-H) – 261.0739, found 261.0715.



¹H NMR (500 MHz, CDCl₃) δ ppm 7.15 – 7.02 (d, *J* = 8.6 Hz, 4H), 6.88 – 6.76 (s, 4H), 3.87 – 3.72 (s, 6H), 2.86 – 2.77 (s, 4H).

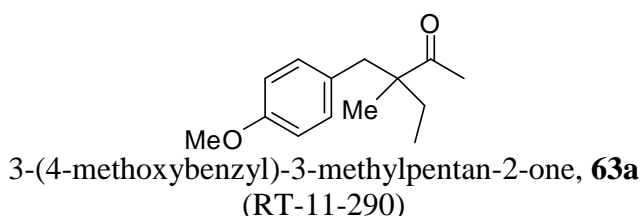
¹³C NMR (126 MHz, CDCl₃) δ ppm 157.91, 134.08, 129.50, 113.82, 55.40, 37.43.



¹H NMR (400 MHz, CDCl₃) δ ppm 7.05 – 6.95 (d, *J* = 8.6 Hz, 2H), 6.86 – 6.74 (d, *J* = 8.6 Hz, 2H), 3.80 – 3.76 (s, 3H), 2.80 – 2.68 (s, 2H), 2.14 – 2.05 (s, 3H), 1.15 – 1.05 (s, 6H).

¹³C NMR (126 MHz, CDCl₃) δ ppm 214.23, 158.40, 131.29, 129.83, 113.43, 55.20, 49.01, 44.47, 26.17, 24.12; FT-IR (CH₂Cl₂) ν_{max} cm⁻¹ 2928, 1697, 1454, 1356, 1167, 737, 700.

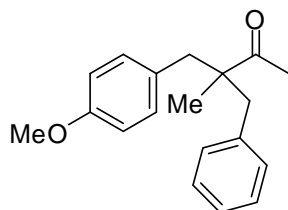
HRMS Calcd for C₁₃H₁₈O₂Li (M+Li) – 213.1467, found 213.1490.



¹H NMR (400 MHz, CDCl₃) δ ppm 7.03 – 6.95 (d, *J* = 8.4 Hz, 2H), 6.83 – 6.72 (d, *J* = 8.5 Hz, 2H), 3.79 – 3.76 (s, 3H), 2.91 – 2.57 (dd, *J* = 101.0, 13.6 Hz, 2H), 2.09 – 2.04 (s, 3H), 1.80 – 1.68 (dq, *J* = 14.4, 7.6, 7.0 Hz, 1H), 1.49 – 1.38 (dq, *J* = 15.0, 7.4 Hz, 1H), 1.08 – 1.01 (s, 3H), 0.87 – 0.78 (t, *J* = 7.5 Hz, 3H).

¹³C NMR (126 MHz, CDCl₃) δ ppm 214.15, 158.25, 131.35, 130.24, 129.64, 114.09, 113.56, 55.34, 52.87, 43.26, 31.24, 26.81, 20.40, 9.15.

HRMS Calcd for C₁₄H₂₀O₂Na (M+Na) – 243.1361, found 243.1373.

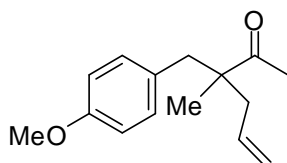


3-benzyl-4-(4-methoxyphenyl)-3-methylbutan-2-one, **63b**
(RT-7-236)

$^1\text{H NMR}$ (400 MHz, CDCl_3) δ ppm 7.10 – 7.02 (d, $J = 8.3$ Hz, 2H), 6.85 – 6.78 (d, $J = 8.7$ Hz, 2H), 3.82 – 3.75 (s, 3H), 2.97 – 2.87 (dd, $J = 13.6, 6.9$ Hz, 1H), 2.83 – 2.72 (h, $J = 6.7$ Hz, 1H), 2.56 – 2.46 (dd, $J = 13.6, 7.6$ Hz, 1H), 2.11 – 2.01 (s, 3H), 1.12 – 1.03 (d, $J = 6.9$ Hz, 3H).

$^{13}\text{C NMR}$ (126 MHz, CDCl_3) δ ppm 212.55, 158.22, 131.60, 129.88, 113.69, 55.19, 49.01, 38.25, 28.90, 16.15.

HRMS Calcd for $\text{C}_{19}\text{H}_{22}\text{O}_2\text{Na}$ ($\text{M}+\text{Na}$) – 305.1518, found 305.1524.

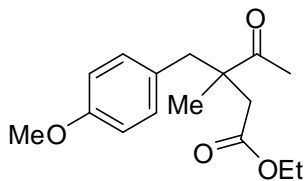


3-(4-methoxybenzyl)-3-methylhex-5-en-2-one, **63c**
(RT-10-57)

$^1\text{H NMR}$ (500 MHz, CDCl_3) δ ppm 7.04 – 6.96 (d, $J = 8.7$ Hz, 2H), 6.84 – 6.74 (d, $J = 8.7$ Hz, 2H), 5.77 – 5.62 (m, 1H), 5.09 – 5.08 (s, 1H), 5.07 – 5.03 (d, $J = 5.8$ Hz, 2H), 3.80 – 3.74 (s, 3H), 2.93 – 2.60 (dd, $J = 127.1, 13.7$ Hz, 2H), 2.49 – 2.41 (dd, $J = 14.0, 7.0$ Hz, 1H), 2.17 – 2.08 (m, 1H), 2.08 – 2.03 (s, 3H), 1.12 – 1.06 (s, 3H).

$^{13}\text{C NMR}$ (126 MHz, CDCl_3) δ ppm 213.51, 158.20, 133.97, 131.07, 129.46, 118.46, 113.54, 55.32, 52.44, 43.58, 42.89, 27.31, 20.92.

HRMS Calcd for $\text{C}_{15}\text{H}_{20}\text{O}_2\text{Na}$ ($\text{M}+\text{Na}$) – 255.1361, found 255.1364.

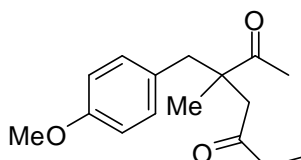


ethyl 3-(4-methoxybenzyl)-3-methyl-4-oxopentanoate, **63d**
(RT-6-203)

¹H NMR (400 MHz, CDCl₃) δ ppm 7.06 3.83 – 3.76 (s, 3H), 2.87 – 2.78 (dd, *J* = 14.9, 9.1 Hz, 2H), 2.76 – 2.69 (m, 1H), 2.38 – 2.28 (d, *J* = 16.5 Hz, 1H), 2.15 – 2.07 (s, 3H), 1.29 – 1.20 (m, 6H).

¹³C NMR (126 MHz, CDCl₃) δ ppm 213.07, 171.71, 158.63, 131.38, 128.46, 113.59, 60.63, 55.37, 50.16, 43.96, 42.53, 27.31, 21.55, 14.31.

HRMS Calcd for C₁₆H₂₂O₄Na (M+Na) – 301.1416, found 301.1422.

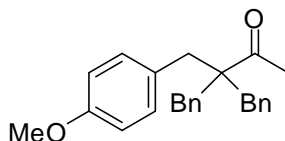


3-(4-methoxybenzyl)-3-methylheptane-2,5-dione, **63e**
(RT-6-227)

¹H NMR (400 MHz, CDCl₃) δ ppm 7.01 – 6.93 (d, *J* = 8.5 Hz, 2H), 6.85 – 6.77 (d, *J* = 8.6 Hz, 2H), 3.85 – 3.73 (s, 3H), 2.97 – 2.87 (d, *J* = 18.0 Hz, 1H), 2.82 – 2.66 (m, 2H), 2.52 – 2.42 (d, *J* = 18.0 Hz, 1H), 2.40 – 2.30 (p, *J* = 7.1 Hz, 2H), 2.15 – 2.05 (s, 3H), 1.27 – 1.17 (s, 3H), 1.06 – 0.95 (t, *J* = 7.3 Hz, 3H).

¹³C NMR (126 MHz, CDCl₃) δ ppm 213.97, 209.64, 158.46, 131.40, 128.60, 113.70, 55.36, 50.73, 49.45, 44.14, 36.10, 27.39, 21.82, 7.85.

HRMS Calcd for C₁₆H₂₂O₃Na (M+Na) – 285.1467, found 285.1469.

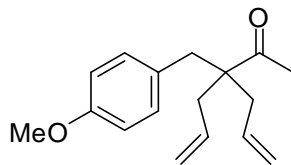


3,3-dibenzyl-4-(4-methoxyphenyl)butan-2-one, **63f**
(RT-6-202)

¹H NMR (500 MHz, CDCl₃) δ ppm 7.27 – 7.18 (m, 6H), 7.03 (d, *J* = 6.8 Hz, 4H), 6.94 (d, *J* = 8.7 Hz, 2H), 6.78 (d, *J* = 8.7 Hz, 2H), 3.77 (s, 3H), 3.04 (s, 4H), 3.00 (s, 2H), 1.95 (s, 3H).

¹³C NMR (126 MHz, CDCl₃) δ ppm 214.00, 158.45, 137.79, 131.48, 130.47, 129.54, 129.12, 128.88, 128.55, 126.74, 113.92, 56.45, 55.48, 41.01, 40.45, 29.14; FT-IR (CH₂Cl₂) ν_{max} cm⁻¹ 2932, 1699, 1497, 1454, 1250, 1032, 748.

HRMS Calcd for C₂₅H₂₆O₂ (M+H) – 359.2011, found 359.2018.

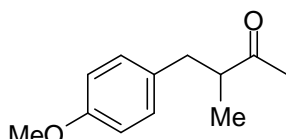


3-allyl-3-(4-methoxybenzyl)hex-5-en-2-one, **63g**
(RT-10-58)

¹H NMR (400 MHz, CDCl₃) δ ppm 7.10 – 6.95 (d, *J* = 8.6 Hz, 2H), 6.89 – 6.73 (m, 2H), 5.83 – 5.65 (m, 2H), 5.20 – 5.12 (s, 2H), 5.12 – 5.06 (d, *J* = 8.0 Hz, 2H), 3.84 – 3.73 (s, 3H), 2.91 – 2.79 (s, 2H), 2.43 – 2.23 (ddd, *J* = 37.0, 14.1, 7.7 Hz, 4H), 2.14 – 2.03 (s, 3H).

¹³C NMR (126 MHz, CDCl₃) δ ppm 212.54, 158.34, 133.61, 131.16, 129.27, 118.75, 113.72, 55.85, 55.32, 39.66, 38.17, 27.50.

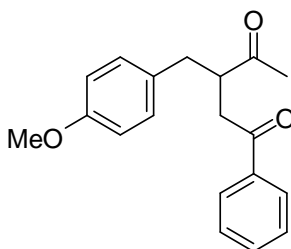
HRMS Calcd for C₁₇H₂₂O₂Na (M+Na) –281.1518, found 281.1520.



4-(4-methoxyphenyl)-3-methylbutan-2-one, **63h**²³
(RT-11-287)

¹H NMR (400 MHz, CDCl₃) δ ppm 7.13 – 6.99 (m, 2H), 6.89 – 6.77 (m, 2H), 3.82 – 3.80 (d, *J* = 1.3 Hz, 3H), 3.17 – 2.90 (m, 1H), 2.88 – 2.75 (q, *J* = 7.0 Hz, 1H), 2.60 – 2.48 (dd, *J* = 12.8, 5.0 Hz, 1H), 2.14 – 2.05 (s, 3H), 1.18 – 1.04 (m, 3H).

¹³C NMR (126 MHz, CDCl₃) δ ppm 212.60, 158.33, 131.75, 131.26, 129.81, 114.00, 113.47, 55.35, 49.15, 38.17, 29.05, 16.35.

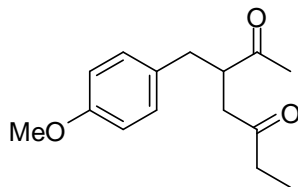


3-(4-methoxybenzyl)-1-phenylpentane-1,4-dione, **63i**
(RT-11-210)

¹H NMR (400 MHz, CDCl₃) δ ppm 7.92 – 7.87 (d, *J* = 8.3 Hz, 2H), 7.58 – 7.51 (m, 1H), 7.46 – 7.39 (t, *J* = 7.6 Hz, 2H), 7.14 – 7.08 (d, *J* = 8.6 Hz, 2H), 6.87 – 6.82 (d, *J* = 8.7 Hz, 2H), 3.82 – 3.74 (s, 3H), 3.56 – 3.43 (m, 2H), 3.02 – 2.88 (m, 2H), 2.69 – 2.60 (dd, *J* = 13.7, 7.7 Hz, 1H), 2.24 – 2.15 (s, 3H).

^{13}C NMR (126 MHz, CDCl_3) δ ppm 211.92, 198.75, 158.43, 136.62, 133.19, 130.63, 130.02, 128.77, 128.16, 114.02, 54.92, 49.04, 40.75, 37.18, 30.90

HRMS Calcd for $\text{C}_{19}\text{H}_{20}\text{O}_3\text{Na}$ ($\text{M}+\text{Na}$) – 319.1310; found 319.1311.

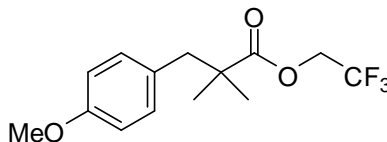


3-(4-methoxybenzyl)heptane-2,5-dione, **63j**
(RT-11-211)

^1H NMR (400 MHz, CDCl_3) δ ppm 7.09 – 7.03 (d, $J = 8.5$ Hz, 1H), 6.98 – 6.94 (m, 1H), 6.85 – 6.77 (dd, $J = 11.8, 8.6$ Hz, 2H), 3.85 – 3.70 (s, 3H), 3.34 – 3.19 (dt, $J = 13.9, 5.1$ Hz, 1H), 3.17 – 3.07 (d, $J = 13.7$ Hz, 1H), 3.01 – 2.78 (m, 2H), 2.55 – 2.45 (m, 1H), 2.42 – 2.38 (m, 1H), 2.37 – 2.33 (d, $J = 7.2$ Hz, 1H), 2.31 – 2.16 (m, 1H), 2.16 – 2.08 (s, 2H), 2.09 – 2.03 (s, 1H), 1.04 – 0.93 (t, $J = 7.3$ Hz, 2H).

^{13}C NMR (126 MHz, CDCl_3) δ ppm 211.88, 210.15, 158.31, 131.25, 130.53, 129.98, 129.11, 114.16, 113.83, 55.40, 48.96, 45.33, 43.89, 40.16, 36.97, 36.30, 35.86, 30.72, 27.85, 7.64.

HRMS Calcd for $\text{C}_{15}\text{H}_{20}\text{O}_3\text{Na}$ ($\text{M}+\text{Na}$) – 271.1310; found 271.1315.

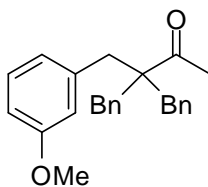


2,2,2-trifluoroethyl 3-(4-methoxyphenyl)-2,2-dimethylpropanoate, **63k**
(RT-11-197)

^1H NMR (500 MHz, CDCl_3) δ ppm 7.05 – 6.98 (d, $J = 8.7$ Hz, 2H), 6.85 – 6.77 (d, $J = 8.7$ Hz, 2H), 4.47 – 4.38 (m, 2H), 3.80 – 3.76 (s, 3H), 2.85 – 2.79 (s, 2H), 1.25 – 1.18 (s, 6H).

^{13}C NMR (126 MHz, CDCl_3) δ ppm 176.05, 158.53, 131.17, 129.26, 113.64, 60.22, 54.93, 45.08, 43.74, 24.97.

HRMS Calcd for $\text{C}_{14}\text{H}_{16}\text{F}_3\text{O}_3$ ($\text{M}-\text{H}$) – 289.1052; found 289.1054.

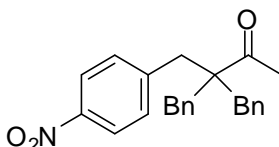


3,3-dibenzyl-4-(3-methoxyphenyl)butan-2-one, **63l**
(RT-11-289)

¹H NMR (400 MHz, CDCl₃) δ ppm 7.31 – 7.27 (d, *J* = 1.9 Hz, 2H), 7.25 – 7.13 (m, 5H), 7.09 – 7.03 (d, *J* = 8.2 Hz, 4H), 6.79 – 6.73 (d, *J* = 10.4 Hz, 1H), 6.70 – 6.63 (d, *J* = 7.6 Hz, 1H), 6.59 – 6.53 (s, 1H), 3.79 – 3.67 (s, 3H), 3.13 – 3.01 (d, *J* = 9.3 Hz, 6H), 2.03 – 1.90 (s, 3H).

¹³C NMR (126 MHz, CDCl₃) δ ppm 213.48, 159.33, 139.06, 137.42, 130.19, 129.19, 128.39, 126.60, 122.58, 115.98, 112.14, 56.12, 55.23, 41.17, 40.83, 28.99.

HRMS Calcd for C₂₅H₂₆O₂Na (M+Na) –381.1831, found 381.1844.

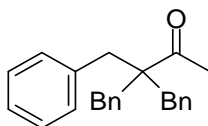


3,3-dibenzyl-4-(4-nitrophenyl)butan-2-one, **63n**
(RT-7-122)

¹H NMR (500 MHz, CDCl₃) δ ppm 8.12 – 8.04 (d, *J* = 8.8 Hz, 2H), 7.30 – 7.24 (m, 6H), 7.17 – 7.12 (d, *J* = 8.8 Hz, 2H), 7.07 – 7.00 (d, *J* = 6.6 Hz, 4H), 3.18 – 3.14 (s, 2H), 3.14 – 2.99 (m, 4H), 2.09 – 2.02 (s, 3H).

¹³C NMR (126 MHz, CDCl₃) δ ppm 212.58, 146.64, 145.90, 136.69, 131.03, 130.11, 128.61, 126.88, 123.31, 56.40, 41.57, 40.05, 28.68.

HRMS Calcd for C₂₄H₂₃NO₃ (M+) – 373.1678, found 373.1727.

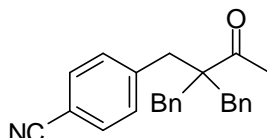


3,3-dibenzyl-4-phenylbutan-2-one, **63o**
(RT-7-138)

¹H NMR (500 MHz, CDCl₃) δ ppm 7.28 – 7.27 (d, *J* = 1.5 Hz, 1H), 7.26 – 7.19 (m, 8H), 7.15 – 7.12 (d, *J* = 8.2 Hz, 1H), 7.06 – 7.03 (d, *J* = 6.9 Hz, 5H), 3.12 – 3.04 (s, 6H), 1.99 – 1.93 (s, 3H).

¹³C NMR (126 MHz, CDCl₃) δ ppm 213.70, 139.25, 137.49, 130.29, 128.99, 128.67, 128.37, 126.60, 126.53, 56.18, 41.01, 38.30, 29.02.

HRMS Calcd for C₂₄H₂₄ONa (M+Na) –351.1725, found 351.1736.

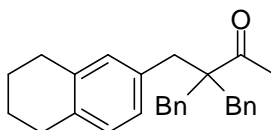


4-(2,2-dibenzyl-3-oxobutyl)benzotrile, **63p**
(RT-7-142)

¹H NMR (500 MHz, CDCl₃) δ ppm 7.55 – 7.48 (d, *J* = 8.4 Hz, 2H), 7.30 – 7.23 (m, 6H), 7.14 – 7.06 (d, *J* = 8.4 Hz, 2H), 7.06 – 6.98 (m, 4H), 3.15 – 3.06 (m, 4H), 3.05 – 2.97 (m, 2H), 2.08 – 2.00 (s, 3H).

¹³C NMR (126 MHz, CDCl₃) δ ppm 212.81, 143.65, 136.77, 131.77, 131.14, 130.12, 128.41, 126.89, 118.84, 110.48, 56.19, 41.48, 40.37, 28.69.

HRMS Calcd for C₂₅H₂₇N₂O (M+NH₄) – 371.2123, found 371.2054.

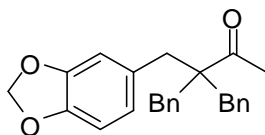


3,3-dibenzyl-4-(5,6,7,8-tetrahydronaphthalen-2-yl)butan-2-one, **63q**
(RT-7-129)

¹H NMR (500 MHz, CDCl₃) δ ppm 7.30 – 7.26 (s, 2H), 7.24 – 7.19 (m, 4H), 7.08 – 7.04 (d, *J* = 8.1 Hz, 4H), 6.97 – 6.76 (m, 2H), 6.72 – 6.67 (s, 1H), 3.10 – 3.07 (d, *J* = 4.7 Hz, 1H), 3.07 – 3.06 (s, 3H), 3.05 – 3.04 (d, *J* = 5.6 Hz, 1H), 3.04 – 2.96 (s, 2H), 2.77 – 2.63 (d, *J* = 25.9 Hz, 4H), 2.07 – 2.01 (s, 1H), 1.99 – 1.94 (s, 3H), 1.79 – 1.74 (m, 3H).

¹³C NMR (126 MHz, CDCl₃) δ ppm 213.87, 137.74, 136.80, 135.29, 134.23, 131.13, 130.31, 128.98, 128.66, 128.31, 127.34, 126.51, 56.21, 41.03, 40.62, 29.53, 29.10, 23.33.

HRMS Calcd for C₂₈H₃₁O (M+H) – 383.2375, found 383.2347.

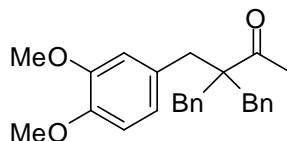


4-(benzo[d][1,3]dioxol-5-yl)-3,3-dibenzylbutan-2-one, **63r**
(RT-7-148)

¹H NMR (500 MHz, CDCl₃) δ ppm 7.28 – 7.20 (m, 6H), 7.08 – 7.01 (d, *J* = 8.3 Hz, 4H), 6.72 – 6.67 (d, *J* = 8.0 Hz, 1H), 6.55 – 6.47 (m, 2H), 5.95 – 5.90 (s, 2H), 3.11 – 3.02 (s, 4H), 3.02 – 2.94 (s, 2H), 2.02 – 1.93 (s, 3H).

¹³C NMR (126 MHz, CDCl₃) δ ppm 213.66, 147.60, 146.19, 137.42, 130.95, 130.24, 128.39, 126.60, 123.40, 110.65, 107.99, 101.03, 56.28, 40.76, 28.90.

HRMS Calcd for C₂₅H₂₈NO₃ (M+NH₄) – 390.2069, found 390.2077.

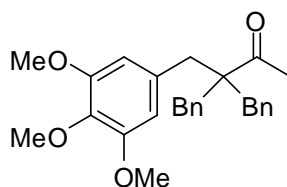


3,3-dibenzyl-4-(3,4-dimethoxyphenyl)butan-2-one, **63s**
(RT-7-144)

¹H NMR (500 MHz, CDCl₃) δ ppm 7.27 – 7.18 (m, 6H), 7.07 – 7.02 (d, *J* = 7.0 Hz, 4H), 6.77 – 6.71 (d, *J* = 8.2 Hz, 1H), 6.65 – 6.59 (dd, *J* = 8.2, 2.0 Hz, 1H), 6.45 – 6.40 (d, *J* = 2.0 Hz, 1H), 3.87 – 3.80 (s, 3H), 3.74 – 3.67 (s, 3H), 3.12 – 2.98 (m, 6H), 2.01 – 1.91 (s, 3H)

¹³C NMR (126 MHz, CDCl₃) δ ppm 213.95, 148.41, 147.66, 137.69, 130.21, 129.80, 128.39, 126.59, 122.25, 113.75, 110.90, 56.23, 55.94, 55.79, 41.18, 40.27, 29.03.

HRMS Calcd for C₂₆H₂₈O₃Na (M+Na) – 411.1936, found 411.1932.

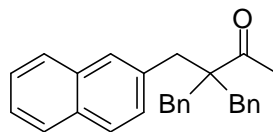


3,3-dibenzyl-4-(3,4,5-trimethoxyphenyl)butan-2-one, **63t**
(RT-11-277)

¹H NMR (400 MHz, CDCl₃) δ ppm 7.30 – 7.27 (s, 3H), 7.25 – 7.19 (m, 3H), 7.12 – 7.03 (d, *J* = 8.1 Hz, 4H), 6.22 – 6.18 (s, 2H), 3.85 – 3.77 (s, 3H), 3.76 – 3.65 (s, 6H), 3.24 – 2.99 (m, 4H), 2.06 – 1.95 (s, 4H).

¹³C NMR (126 MHz, CDCl₃) δ ppm 213.88, 152.86, 137.53, 133.16, 130.21, 128.32, 126.45, 107.25, 60.75, 56.28, 56.19, 56.09, 41.33, 40.71, 39.92, 28.99.

HRMS Calcd for C₂₇H₃₀O₄Na (M+Na) – 441.2042, found 441.2019.

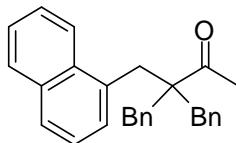


3,3-dibenzyl-4-(naphthalen-2-yl)butan-2-one, **63u**
(RT-6-267)

¹H NMR (500 MHz, CDCl₃) δ ppm 7.83 – 7.78 (m, 1H), 7.76 – 7.70 (t, *J* = 8.4 Hz, 2H), 7.48 – 7.42 (m, 3H), 7.30 – 7.22 (m, 6H), 7.20 – 7.16 (dd, *J* = 8.4, 1.7 Hz, 1H), 7.09 – 7.06 (m, 4H), 3.28 – 3.21 (s, 2H), 3.20 – 3.06 (m, 4H), 2.03 – 1.93 (s, 3H).

¹³C NMR (126 MHz, CDCl₃) δ ppm 213.77, 137.53, 135.17, 133.36, 132.25, 130.32, 128.98, 128.85, 128.78, 128.67, 128.41, 127.80, 127.65, 126.66, 126.17, 125.80, 56.36, 41.30, 40.85, 29.12.

HRMS Calcd for C₂₈H₂₇O (M+H) – 379.2062, found 379.2063.

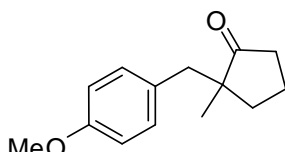


3,3-dibenzyl-4-(naphthalen-1-yl)butan-2-one, **63v**
(RT-7-76)

¹H NMR (500 MHz, CDCl₃) δ ppm 7.97 – 7.93 (dd, *J* = 6.2, 3.5 Hz, 1H), 7.89 – 7.85 (dd, *J* = 6.1, 3.4 Hz, 1H), 7.77 – 7.73 (d, *J* = 8.2 Hz, 1H), 7.53 – 7.48 (dd, *J* = 6.4, 3.3 Hz, 2H), 7.42 – 7.37 (t, *J* = 7.7 Hz, 1H), 7.25 – 7.18 (m, 7H), 7.06 – 7.00 (m, 4H), 3.52 – 3.44 (s, 2H), 3.28 – 3.16 (m, 4H), 1.85 – 1.77 (s, 3H).

¹³C NMR (126 MHz, CDCl₃) δ ppm 214.40, 137.31, 133.91, 133.40, 132.74, 130.44, 128.95, 128.56, 128.36, 127.31, 126.62, 126.28, 125.85, 125.16, 123.42, 55.66, 41.66, 36.47, 29.16.

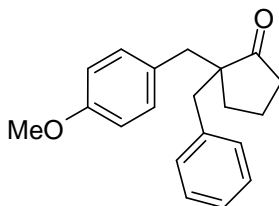
HRMS Calcd for C₂₈H₂₇O (M+H) – 379.2062, found 379.2059.



2-(4-methoxybenzyl)-2-methylcyclopentanone, **64²²**
(RT-7-149)

¹H NMR (500 MHz, CDCl₃) δ ppm 7.01 (d, *J* = 8.7 Hz, 2H), 6.78 (d, *J* = 8.7 Hz, 2H), 3.76 (s, 3H), 2.78 (d, *J* = 13.6 Hz, 1H), 2.51 (d, *J* = 13.6 Hz, 1H), 2.26 (ddd, *J* = 18.8, 8.3, 5.5 Hz, 1H), 2.08 – 1.97 (m, 1H), 1.93 (dt, *J* = 12.7, 7.6 Hz, 1H), 1.83 – 1.64 (m, 1H), 1.64 – 1.56 (m, 2H), 0.99 (s, 3H).

¹³C NMR (126 MHz, CDCl₃) δ ppm 224.02, 158.28, 131.38, 130.27, 113.72, 77.48, 77.23, 76.98, 55.37, 49.86, 41.97, 38.32, 34.77, 22.88, 18.84.



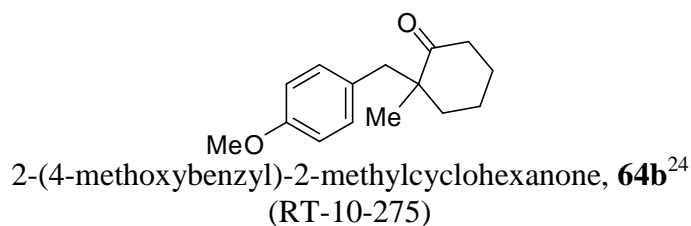
2-benzyl-2-(4-methoxybenzyl)cyclopentanone, **64a**
(RT-7-140)

¹H NMR (500 MHz, CDCl₃) δ ppm 7.26 – 7.20 (m, 3H), 7.12 – 7.07 (d, *J* = 6.9 Hz, 2H), 7.04 – 6.99 (m, 2H), 6.82 – 6.77 (d, *J* = 8.7 Hz, 2H), 3.82 – 3.73 (s, 3H), 3.04 – 2.91 (dd, *J* = 20.1, 13.3

Hz, 2H), 2.62 – 2.49 (dd, $J = 20.6, 13.3$ Hz, 2H), 1.92 – 1.80 (m, 4H), 1.36 – 1.30 (td, $J = 7.5, 3.4$ Hz, 2H).

^{13}C NMR (126 MHz, CDCl_3) δ 224.36, 158.69, 137.89, 131.60, 130.70, 129.94, 128.38, 126.76, 113.97, 55.58, 55.09, 43.28, 42.35, 39.88, 30.28, 19.07.

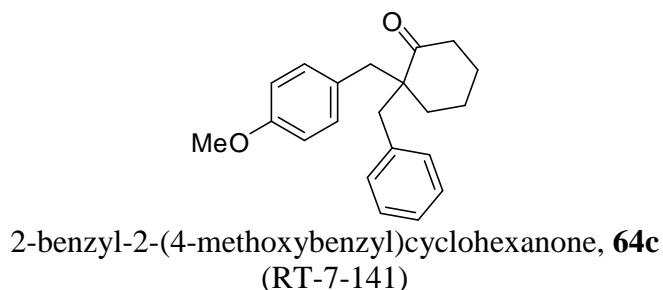
HRMS Calcd for $\text{C}_{20}\text{H}_{22}\text{O}_2\text{Na}$ ($\text{M}+\text{Na}$) – 317.1518, found 317.1545.



^1H NMR (500 MHz, CDCl_3) δ ppm 7.06 – 6.97 (d, $J = 8.6$ Hz, 2H), 6.84 – 6.75 (d, $J = 8.6$ Hz, 2H), 3.83 – 3.71 (s, 3H), 2.86 – 2.77 (s, 2H), 2.55 – 2.40 (m, 2H), 1.90 – 1.78 (m, 3H), 1.78 – 1.66 (m, 2H), 1.57 – 1.48 (m, 1H), 1.04 – 0.96 (s, 3H).

^{13}C NMR (126 MHz, CDCl_3) δ ppm 215.59, 158.00, 131.31, 129.41, 113.21, 55.08, 49.30, 42.09, 38.81, 37.91, 27.17, 22.67, 21.01.

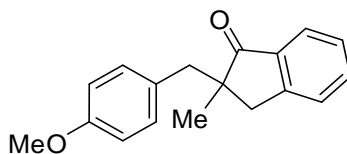
HPLC (Daicel Chiralpak OD-H HPLC column: 95% hexane/isopropanol, 0.1 mL/min) t_r = 66.990 (minor), 70.095 (major) minutes



^1H NMR (400 MHz, CDCl_3) δ ppm 7.25 – 7.15 (m, 3H), 7.13 – 7.08 (d, $J = 6.6$ Hz, 2H), 7.05 – 6.99 (d, $J = 8.7$ Hz, 2H), 6.82 – 6.76 (d, $J = 8.7$ Hz, 2H), 3.86 – 3.73 (s, 3H), 3.14 – 2.97 (dd, $J = 24.9, 13.7$ Hz, 2H), 2.71 – 2.59 (dd, $J = 13.7, 7.9$ Hz, 2H), 2.44 – 2.38 (t, $J = 6.5$ Hz, 2H), 1.78 – 1.61 (m, 6H).

^{13}C NMR (126 MHz, CDCl_3) δ 214.69, 158.01, 146.48, 137.60, 131.82, 130.93, 129.62, 128.12, 126.44, 113.21, 55.31, 53.94, 42.13, 41.45, 39.93, 33.59, 25.75, 20.92.

HRMS Calcd for $\text{C}_{21}\text{H}_{24}\text{O}_2\text{Na}$ ($\text{M}+\text{Na}$) – 331.1674, found 331.1699.

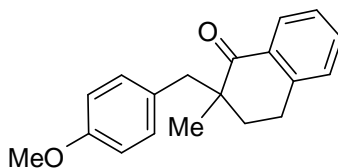


2-(4-methoxybenzyl)-2-methyl-2,3-dihydro-1H-inden-1-one, **64e**
(RT-10-226)

¹H NMR (500 MHz, CDCl₃) δ ppm 7.75 – 7.71 (d, *J* = 7.7 Hz, 1H), 7.55 – 7.50 (t, *J* = 7.4 Hz, 1H), 7.36 – 7.29 (m, 1H), 7.08 – 7.03 (d, *J* = 8.4 Hz, 2H), 6.77 – 6.72 (d, *J* = 8.6 Hz, 2H), 3.77 – 3.71 (s, 2H), 3.27 – 3.18 (d, *J* = 17.4 Hz, 1H), 3.02 – 2.94 (d, *J* = 13.8 Hz, 1H), 2.77 – 2.71 (m, 3H), 1.25 – 1.21 (s, 3H).

¹³C NMR (126 MHz, CDCl₃) δ ppm 210.75, 158.33, 152.46, 135.96, 134.64, 131.05, 129.71, 127.41, 126.43, 124.11, 113.61, 54.91, 50.66, 42.40, 38.82, 35.16, 24.65.

HRMS Calcd. for C₂₅H₂₄O₂Na (M+Na) – 289.1205, found 289.1222.



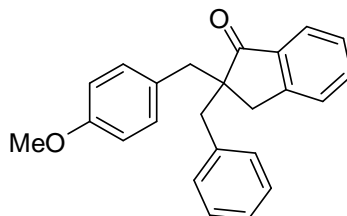
2-(4-methoxybenzyl)-2-methyl-3,4-dihydronaphthalen-1(2H)-one, **64f**
(RT-10-233)

¹H NMR (400 MHz, CDCl₃) δ ppm 8.11 – 8.01 (d, *J* = 7.9 Hz, 1H), 7.48 – 7.40 (t, *J* = 7.5 Hz, 1H), 7.33 – 7.27 (t, *J* = 7.5 Hz, 1H), 7.24 – 7.18 (d, *J* = 7.3 Hz, 1H), 7.10 – 7.03 (d, *J* = 8.5 Hz, 1H), 6.82 – 6.75 (d, *J* = 6.9 Hz, 2H), 3.82 – 3.71 (s, 3H), 3.10 – 3.01 (d, *J* = 13.6 Hz, 1H), 3.01 – 2.94 (t, *J* = 3.9 Hz, 2H), 2.81 – 2.74 (d, *J* = 13.6 Hz, 1H), 2.05 – 1.93 (m, 1H), 1.90 – 1.77 (dt, *J* = 11.8, 5.9 Hz, 1H), 1.17 – 1.13 (s, 3H).

¹³C NMR (126 MHz, CDCl₃) δ ppm 202.33, 158.26, 143.37, 133.23, 131.92, 131.74, 129.73, 128.79, 128.19, 126.80, 113.48, 55.34, 46.04, 41.92, 33.12, 25.61, 22.47.

HRMS Calcd for C₁₉H₂₀O₂Na (M+Na) – 303.1361, found 303.1364.

HPLC (Daicel Chiralpak OD-H HPLC column: 97% hexane/isopropanol, 0.1 mL/min) *t*_r = 73.113 (minor), 77.700 (major) minutes

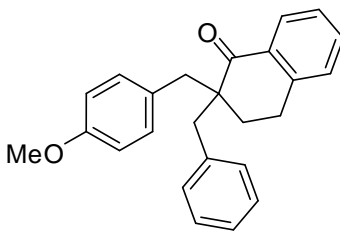


2-benzyl-2-(4-methoxybenzyl)-2,3-dihydro-1H-inden-1-one, **64g**
(RT-10-64)

¹H NMR (500 MHz, CDCl₃) δ ppm 7.65 – 7.59 (d, *J* = 7.6 Hz, 1H), 7.40 – 7.34 (t, *J* = 7.3 Hz, 1H), 7.23 – 7.17 (t, *J* = 6.6 Hz, 1H), 7.17 – 7.11 (t, *J* = 7.6 Hz, 3H), 7.11 – 7.06 (d, *J* = 6.1 Hz, 4H), 7.04 – 6.99 (d, *J* = 8.1 Hz, 2H), 6.72 – 6.65 (d, *J* = 6.3 Hz, 3H), 3.76 – 3.65 (s, 1H), 3.23 – 3.10 (t, *J* = 13.6 Hz, 2H), 3.08 – 2.98 (s, 2H), 2.87 – 2.72 (dd, *J* = 21.2, 12.7 Hz, 2H).

¹³C NMR (126 MHz, CDCl₃) δ ppm 210.68, 158.16, 153.17, 137.29, 137.04, 134.56, 131.40, 130.40, 129.26, 128.13, 127.21, 126.53, 126.07, 123.67, 113.60, 55.46, 55.27, 43.53, 42.74, 34.65.

HRMS Calcd for C₂₅H₂₄O₂Na (M+Na) – 379.1674, found 379.1657.



2-benzyl-2-(4-methoxybenzyl)-3,4-dihydronaphthalen-1(2H)-one, **64h**
(RT-7-278)

¹H NMR (400 MHz, CDCl₃) δ ppm 8.12 – 8.05 (d, *J* = 7.8 Hz, 1H), 7.46 – 7.39 (t, *J* = 8.0 Hz, 1H), 7.33 – 7.27 (m, 1H), 7.24 – 7.20 (d, *J* = 7.5 Hz, 2H), 7.19 – 7.11 (m, 4H), 7.09 – 7.02 (d, *J* = 8.6 Hz, 2H), 6.80 – 6.74 (d, *J* = 8.6 Hz, 2H), 3.81 – 3.69 (s, 3H), 3.36 – 3.19 (dd, *J* = 25.8, 13.5 Hz, 2H), 3.07 – 2.96 (t, *J* = 6.3 Hz, 2H), 2.68 – 2.56 (dd, *J* = 13.4, 10.5 Hz, 2H), 1.99 – 1.84 (t, *J* = 6.3 Hz, 2H).

¹³C NMR (126 MHz, CDCl₃) δ ppm 200.97, 158.27, 143.15, 137.60, 133.29, 132.57, 131.97, 131.06, 129.37, 128.73, 128.20, 128.10, 126.81, 126.46, 113.51, 55.30, 51.07, 41.64, 40.85, 29.22, 25.61.

HRMS Calcd for C₂₅H₂₄O₂Na (M+Na) – 379.1674, found 379.1657.

HPLC (Daicel Chiralpak OD-H HPLC column: 99% hexane/isopropanol, 0.3 mL/min) *t_r* = 46.907 (minor), 49.957 (major) minutes

References

1. Komiya, S. *Synthesis of Organometallic Compounds. A Practical Guide*; John Wiley & Sons: New York, **1997**, p. 290.
2. Wilson, S. R.; Augelli, C. E.; Vedananda, T. R.; White, J. D., "The Carroll Rearrangement: 5-dodecen-2-one." *Org. Synth.* **1993**, *8*.
3. Svenstrup, N.; Simonsen, K. B.; Thorup, N.; Brodersen, J.; Dehaen, W.; Becher, J., "A pyrazole to furan rearrangement. Thermolysis of 5-azido-4-formylpyrazoles." *J. Org. Chem.* **1999**, *64*, 2814–2820.
4. Mehdipour, A. R.; Javidnia, K.; Hemmateenejad, B.; Amirghofran, Z.; Miri, R., "Dihydropyridine derivatives to overcome atypical multidrug resistance: design, synthesis, QSAR Studies, and evaluation of their cytotoxic and pharmacological activities." *Chem. Biol. Drug Des.* **2007**, *70*, 337–346.
5. Uchida, M.; Chihiro, M.; Morita, S.; Kanbe, T.; Yamashita, H.; Yamasaki, K.; Yabuuchi, Y.; Nakagawa, K., Studies on Proton Pump Inhibitors. II. "Synthesis and antiulcer activity of 8-[(2-benzimidazolyl)sulfinylmethyl]-1,2,3,4-tetrahydroquinolines and related compounds." *Chem. Pharm. Bull.* **1989**, *37*(8), 2109–2116.
6. Achremowicz, L., "A new approach to the oxidation of methylquinolines with selenium dioxide." *Synth. Commun.* **1996**, *26*(9), 1681–1684.
7. Reddy, J. S. Y. B. V. S.; Krishna, A. D.; Reddy, C. S.; Narsaiah, A. V., "Triphenylphosphine: an efficient catalyst for transesterification of β -ketoesters." *J. Mol. Catal., A Chem.* **2007**, *261*, (1-2), 93–97.
8. Matsuo, J.-i., Okano, M., Takeuchi, K.; Tanaka, H.; Ishibashi, H. "A practical synthesis of enantiopure N-carbobenzyloxy-N'-phthaloyl-cis-1,2-cyclohexanediamine by asymmetric reductive amination and the Curtius rearrangement" *Tetrahedron Asymmetr.* **2007**, *18*, 1906–1910.
9. Tardibono, Jr. L. P.; Patzner, J.; Cesario, C.; Miller, M. J. "Palladium-catalyzed decarboxylative rearrangements of allyl 2,2,2-trifluoroethyl malonates: direct access to homoallylic esters" *Org. Lett.* **2009**, *11*, 4076–4079.
10. Lee, H.-S.; Park, J.-S.; Kim, B. M.; Gellman, S. H., "Efficient synthesis of enantiomerically pure β 2-amino acids via chiral isoxazolidinones." *J. Org. Chem.* **2003**, *68* (4), 1575–1578.
11. Gerken, J. B.; Wang, S. C.; Preciado, A. B.; Park, Y. S.; Nishiguchi, G.; Tantillo, D. J.; Little, R. D., "Remote substituent effects upon the rearrangements of housane cation radicals." *J. Org. Chem.* **2005**, *70*(12), 4598–4608.

12. Viviano, M.; Glasnov, T. N.; Reichart, B.; Tekautz, G.; Kappe, C. O. "A Scalable two-step continuous flow of Nabumetone and related 4-aryl-2-butanones" *Org. Process Res. Dev.* **2011**, *15*, 858–870.
13. Aulenta, F.; Berndt, M.; Brudgam, I.; Hartl, H.; Sorgel, S.; Reißig, H.-U., "A New, efficient and stereoselective synthesis of tricyclic and tetracyclic compounds by samarium diiodide induced cyclisations of naphthyl-substituted arylketones - an easy access to steroid-like skeletons." *Chem. Eur. J.* **2007**, *13*, 6047–6062.
14. Tateiwa, J.; Horiuchi, H.; Hashimoto, K.; Yamauchi, T.; Uemura, S.; "Cation-exchanged montmorillonite-catalyzed facile Friedel-Crafts alkylation of hydroxyl and methoxy aromatics with 4-hydroxybutan-2-one to produce raspberry ketone and pharmaceutically active compounds" *J. Org. Chem.* **1994**, *59*, 5901–5904.
15. Jefford, C.; Favarger, F.; Ferro, S.; Chambaz, D.; Bringham, A.; Bernardinelli, G.; Boukouvalas, J. "The formation of bridged bicyclic 1,2,4-trioxanes by intramolecular capture of β -hydroperoxy cations" *Helv. Chim. Acta* **1986**, *69*, 1778–1786.
16. Condon, S.; Dupré, D.; Lachaise, I.; Nédélec, J-Y. "Nickel catalyzed electrochemical heteroarylation of activated olefins" *Synthesis* **2002**, *12*, 1752–1758.
17. Cho, C. S.; Motofusa, S.-i.; Ohe, K.; Uemura, S., "Palladium(II)-catalyzed conjugate addition of aromatics to α,β -unsaturated ketones and aldehydes with arylantimony compounds." *Bull. Chem. Soc. Jpn.* **1996**, *69*(8), 2341–2348
18. Aulenta, F.; Wefelscheid, U.K.; Brüdgam, I.; Reißig, H.-U. "Nitrogen-containing tricyclic compounds by stereoselective samarium diiodide promoted cyclizations of quinoliny substituted ketones – a new access to azasteroids" *Eur. J. Org. Chem.* **2008**, *13*, 2325–2335.
19. Li, X.; Li, L.; Tang, Y.; Zhong, L.; Cun, L.; Zhu, J.; Liao, J.; Deng, J. "Chemoselective conjugate reduction of α,β -unsaturated ketones catalyzed by rhodium amido complexes in aqueous media" *J. Org. Chem.* **2010**, *75*, 2981–2988.
20. Yu, Y.; Liebeskind, L.S. "Copper-mediated, palladium-catalyzed coupling of thiol esters with aliphatic organoboron reagents" *J. Org. Chem.* **2004**, *69*, 3554–3557.
21. Oh, K.-B.; Kim, S.-H.; Lee, J.; Cho, W.-J.; Lee, T.; Kim, S. "Discovery of diarylacrylonitriles as a novel series of small molecule sortase A inhibitors" *J. Med. Chem.* **2004**, *47*, 2418–2421.
22. Gansäuer, A.; Stock, C.; Fielenbach, D.; Geich-Gimbel, D. "Catalyzed reactions of enol ethers with S_N1 active groups: a novel method for the preparation of α -alkylated ketones" *Adv. Synth. Catal.* **2003**, *345*, 1017–1030.

23. Cruz, A. C. F.; Miller, N. D.; Willis, M. C. "Intramolecular palladium-catalyzed direct arylation of alkenyl triflates" *Org. Lett.* **2007**, *9*, 4391–4393.
24. Rosa, D.; Orellana, A. "Palladium-catalyzed cross-coupling of cyclopropanols with aryl halides under mild conditions" *Org. Lett.* **2011**, *13*, 110–113.

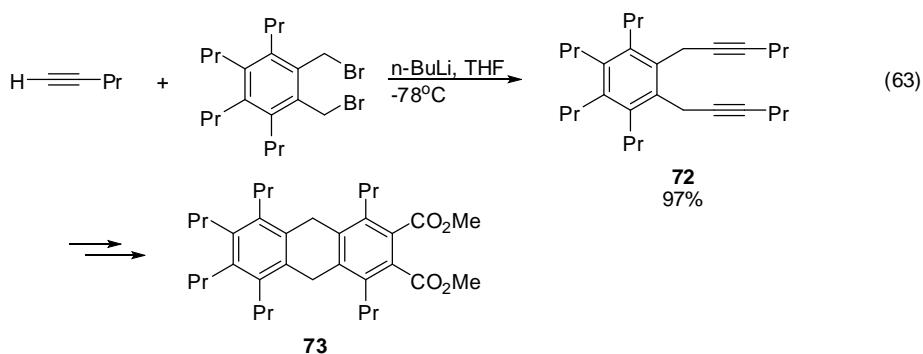
Chapter 3

Palladium-Catalyzed Decarboxylative Benzylation of Alkynes

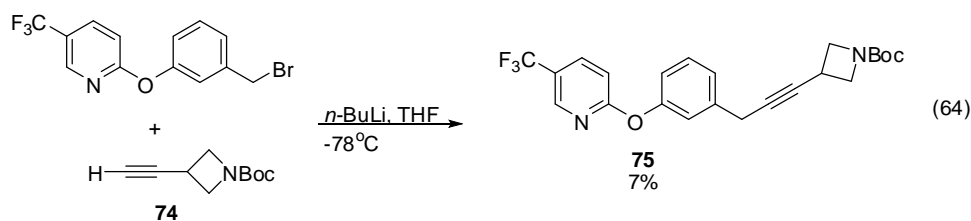
3.1 Introduction

Classical strategies in benzyl alkyne synthesis

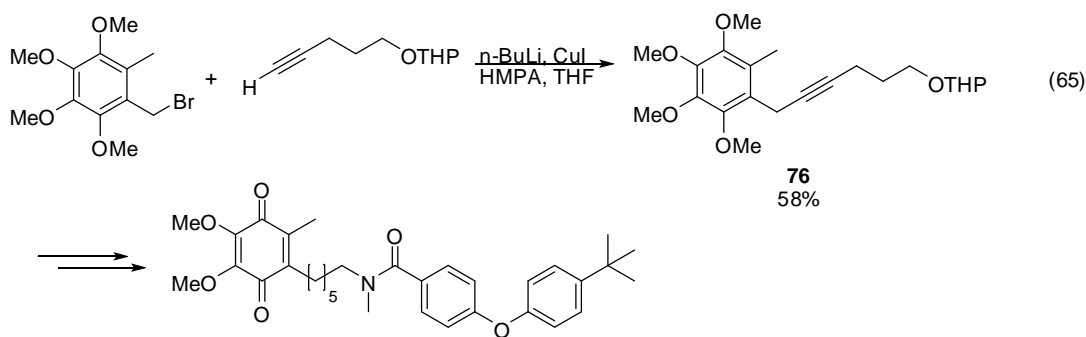
Benzyl alkyne synthesis through alkylation of alkynes with benzyl halides is a well-known synthetic method in organic chemistry.¹ In this method, the terminal hydrogen of the alkyne ($pK_a \sim 25$ in DMSO) is deprotonated with base prior to nucleophilic attack on the benzyl halide. As an example, Takahashi and coworkers used this method in constructing benzyl alkyne **72** in very high yield (eq. 63).² The formation of **72** is important in the synthesis of naphthacene **73** which could be potentially used as an organic source of conductive material.



While this synthetic method is well-known, typical benzyl alkyne preparations use *n*-BuLi as the base which is hazardous and difficult to handle. Moreover, when this is used, the reaction has to be performed at very low temperatures ($-78^\circ C$). In some cases, the use of *n*-BuLi alone at lower temperatures will not work to deprotonate the terminal hydrogen of the alkyne. Wang and coworkers attempted to prepare benzyl alkyne **75** by alkylating Boc-protected azetidine alkyne **74** with a benzyl halide derivative using *n*-BuLi at $-78^\circ C$ (eq. 64). Unfortunately, a very low yield of desired product was obtained.³ The low yield of **75** could be due to the ring opening of the azetidine in presence of the base rather than deprotonating the terminal hydrogen of the alkyne.⁴



To solve the deprotonation problem using *n*-BuLi, stoichiometric Cu(I) is added in the reaction mixture. Miyoshi and coworkers reported the addition of CuI in the alkylation of THP-protected alkyne with benzyl bromide giving benzyl alkyne **76** in high yield (eq. 65). The formation of **76** was a key step in the synthesis of a hybrid ubiquinone that potentially worked as an electron transfer substrate to bovine heart mitochondrial succinate–ubiquinone oxidoreductase and ubiquinol–cytochrome c oxidoreductase.⁵ The role of Cu when added to the reaction with *n*-BuLi is to make the alkyne more reactive by undergoing metal exchange with preformed alkyne-Li, generating a Gilman-type (acetylide)₂CuLi species. Unfortunately, this also results to formation of Li salts and other Cu by-products in the reaction mixture making product purification tedious and difficult, resulting to lower product yields.

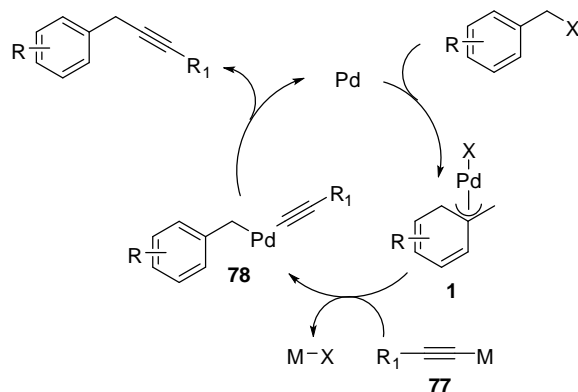


Synthesis of benzyl alkynes using palladium catalysis

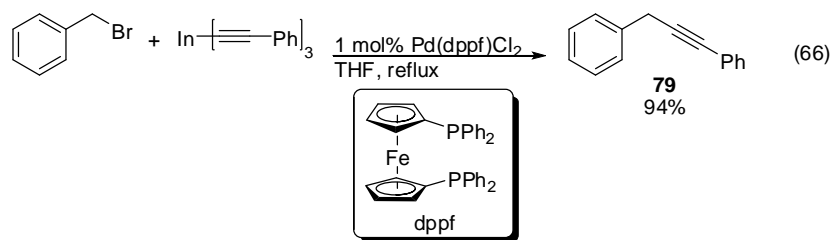
Problems arising from benzyl alkylation in the presence of *n*-BuLi at very low temperatures were significantly resolved through Pd-catalyzed reactions. In particular, the alkyne

coupling partner more commonly comes from preformed organometallics. In this method, benzyl halide undergoes oxidative addition in the presence of Pd to generate η^3 -benzyl-Pd **1**. Transmetalation of **1** with metal-acetylide **77** occurs to generate benzyl-Pd-acetylide intermediate **78**. Reductive elimination releases benzyl alkyne and Pd is regenerated back into the catalytic cycle (Scheme 64). The synthesis of **77** would come from deprotonation of the terminal hydrogen of an alkyne and its coupling with an external organometallic reagent. Ultimately, this methodology allows construction of diverse benzyl alkynes at room to high temperatures compared to classical alkylations that require *n*-BuLi and perform at very low temperatures.

Scheme 64.

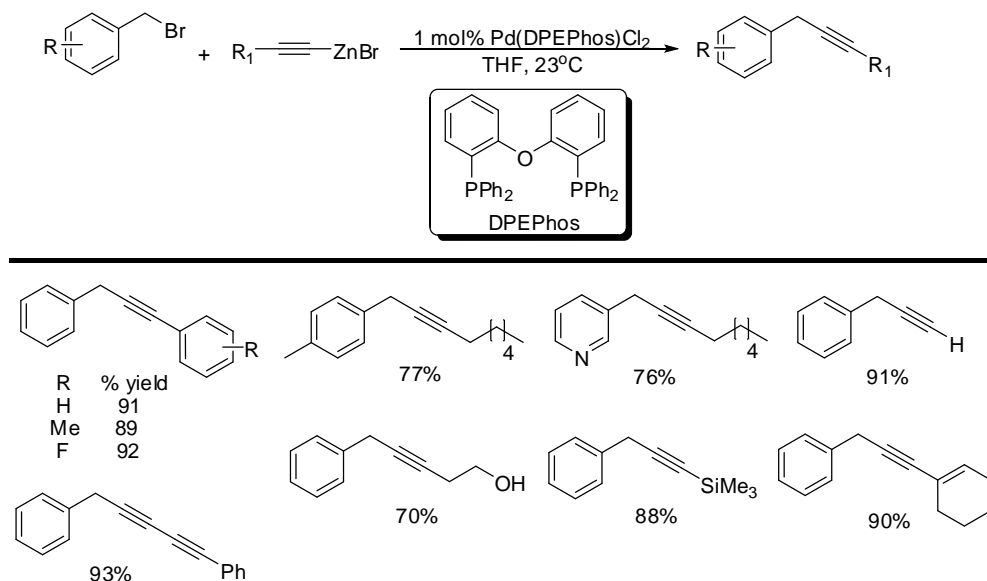


Several organometallic alkyne sources have been used to couple with Pd- π -benzyl. Sarandeses and coworkers reported the synthesis of benzyl alkyne **79** through cross-coupling between benzyl bromide and alkynylphenylindium (eq. 66).⁶ Despite the apparent low toxicity associated with In metal, alkynylphenylindium is extremely reactive such that it must be stored in THF when not in used to prevent immediate decomposition.

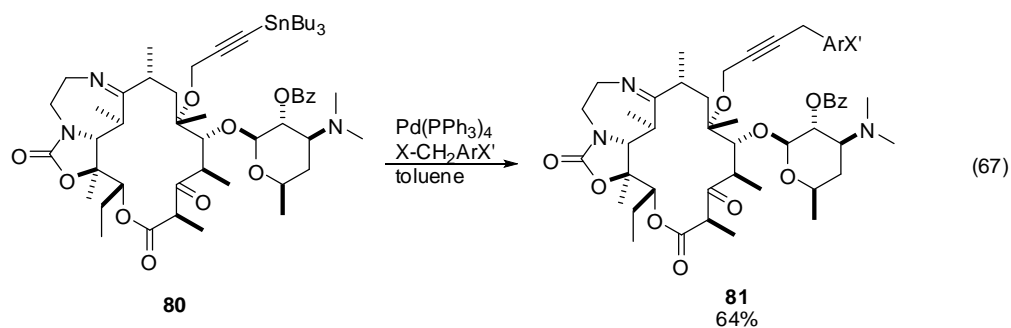


Qian and Negishi reported the use of zinc as the source of metal that can form an organometallic reagent, alkynylzinc which was used to couple with benzyl bromide to generate benzyl alkynes at room temperature. (Scheme 65) Both EWG and EDG substituents in the benzyl bromide underwent cross-coupling with alkynylzinc in good to high yields. When an aliphatic alkynylzinc was used, benzylation with benzyl bromide occurred in slightly lower yields compared with aromatic alkynylzinc.⁷

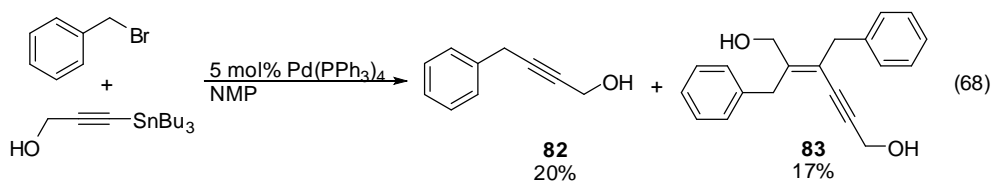
Scheme 65.



Another source of metal used in Pd catalysis was Sn. Yong and coworkers reported the synthesis of diazolid **81** via Stille cross-coupling of diazolid-stannane **80** with benzyl dihalide to generate benzyl alkyne in good yield (eq. 67).⁸ The formation of **81** was essential in evaluation of its antibacterial activity against erythromycin-resistant respiratory tract pathogens.



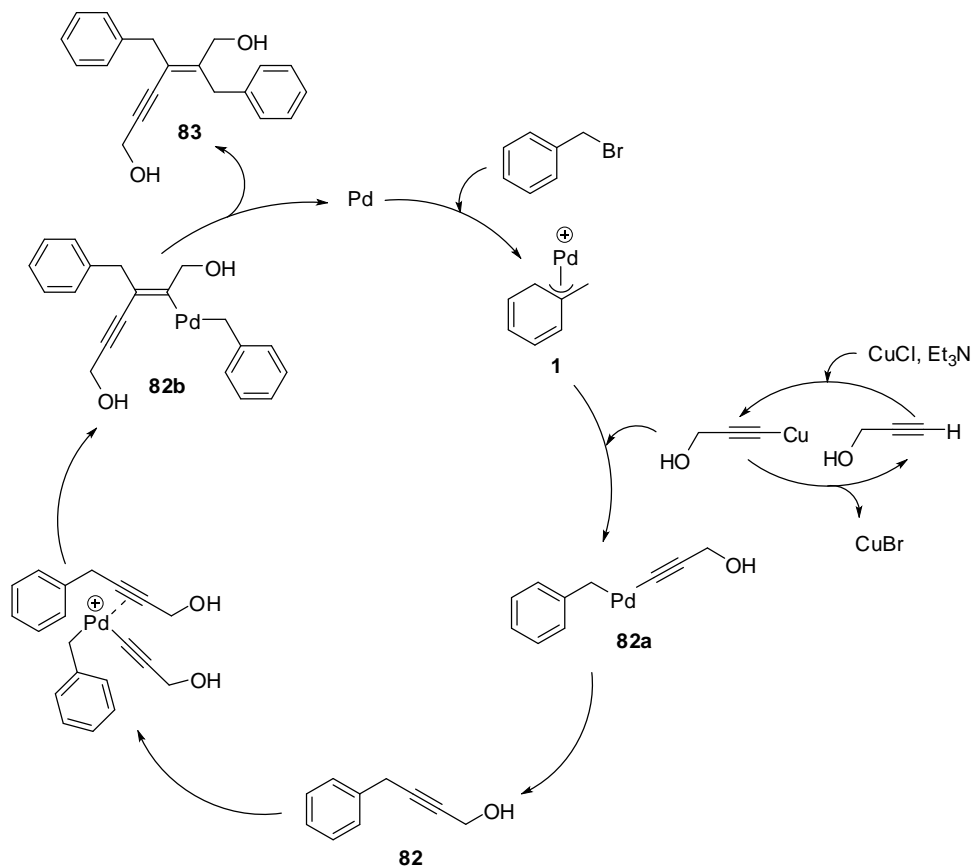
The use of Sn in Stille cross-coupling of benzyl halides with alkynylstannanes was also used by Alami and coworkers. They showed that tributyltin propargyl alcohol couples with benzyl bromide in the presence of NMP to generate benzyl alkyne **82**. This also results to formation of benzyl enyne **83** in the reaction hence giving an overall low yield of **82**. (eq. 68) The authors postulated that the formation of **83** came from tandem Stille-carbopalladation-Stille sequence.⁹



Lastly, the use of Cu metal in benzyl alkynylations *via* Sonogahsira cross-coupling has also been utilized.¹⁰ This was highlighted by Alami and coworkers, in which they reported the cross-coupling of benzyl bromide and propargyl alcohol in the presence of CuI, and BnNET₃Cl salt to generate benzyl alkyne **82** in low yield (condition A, eq. 69). When other Pd catalysts, Cu salts, and ammonium salt additives were tried, an unprecedented enyne **83** in moderate yield was also observed rather than desired benzyl alkyne **82** (condition B, eq. 69). The formation of **83** was similar to the Stille cross-coupling of tributylstannane propargyl alcohol with benzyl bromide (eq. 68). The double bond stereochemistry of the enyne was unambiguously assigned as *E* based on NOESY, HMBC and HSQC experiments. Despite the inability to synthesize **82**, they took advantage in expanding the scope of benzyl enyne formation. A variety of benzyl enynes

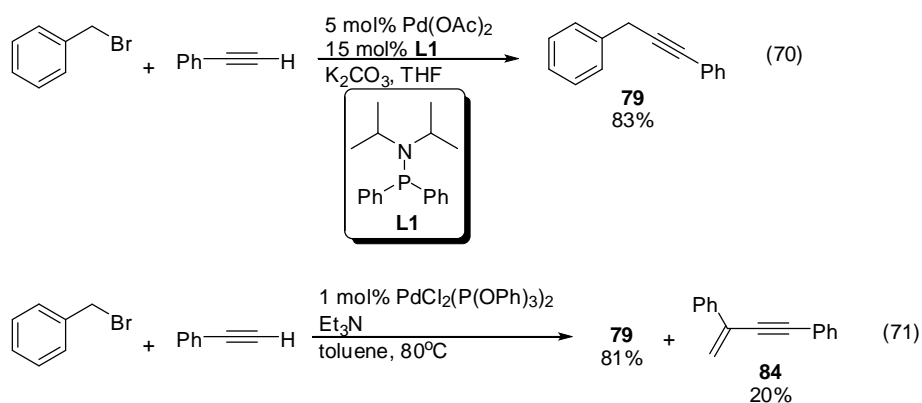
benzyl-Pd-alkyne intermediate **82a**. Reductive elimination of **82a** leads to formation of benzyl alkyne **82**. It is believed that at this stage, the Pd of a second **82a** intermediate coordinates to **82**. This results to carbopalladation to generate a σ -vinyl-Pd complex **82b**. Reductive elimination of **82b** ultimately releases benzyl enyne **83** and Pd is regenerated back in the catalytic cycle.

Scheme 67.



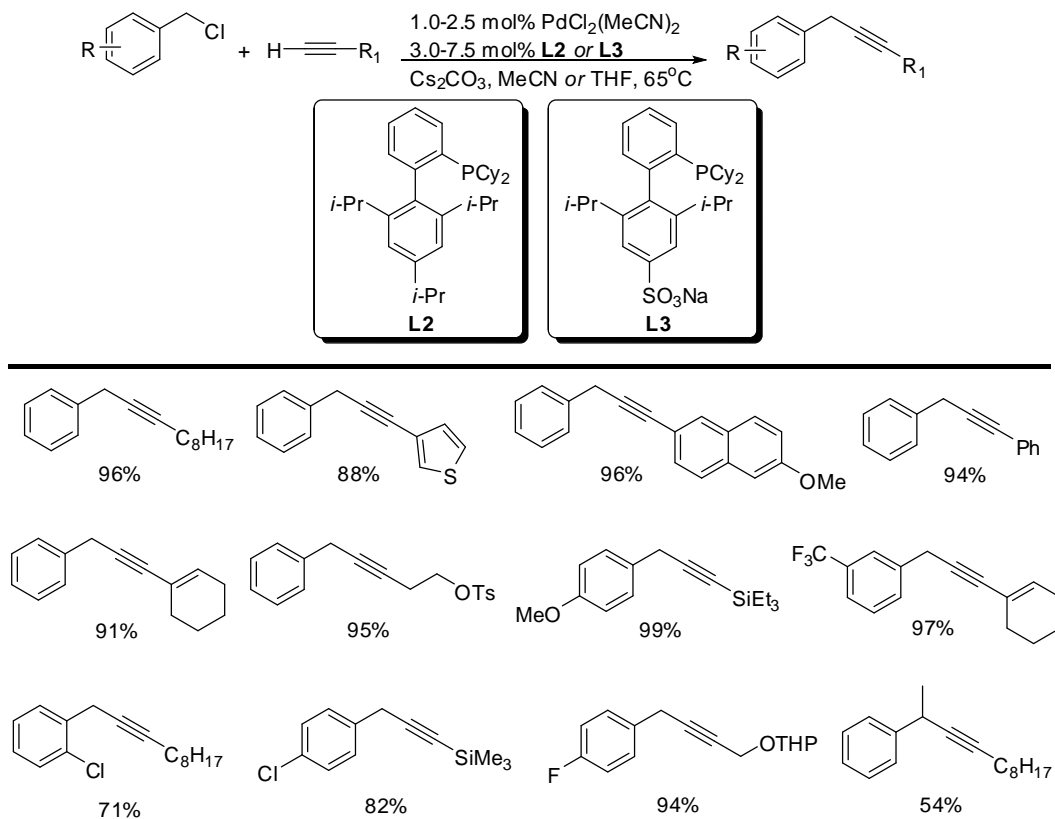
The use of other catalysts and additives also gave benzyl alkynes while preventing the formation of benzyl enynes. Zhang and coworkers showed that an electron-poor monodentate aminophosphine ligand can be used to generate benzyl alkyne **79** in high yield without the need of Cu additive (eq. 70).¹¹ Trzeciak and coworkers on the other hand, showed that Cu-free Sonogashira reactions can be performed to generate the same benzyl alkyne using a monodentate phosphite ligand (eq. 71). However, they also observed significant formation of the isomeric

phenyl vinyl enyne **84** along with the benzyl alkyne which presumably resulted from “head-to-tail” dimerization of phenylacetylene.¹²

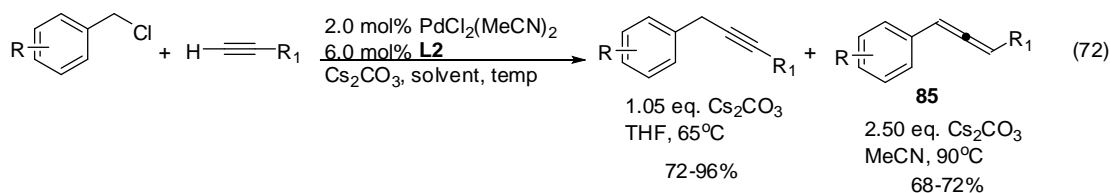


An improved synthesis of **79** and other benzyl alkynes was reported by Buchwald through the coupling of benzyl chlorides with acetylene derivatives in the presence of monodentate ligand that contain the biphenyl backbone (Scheme 68).¹³ A variety of benzyl alkynes can be accessed under these conditions in good to high yields. Both aromatic and aliphatic acetylenes were compatible substrates with benzyl chloride. In addition, both EDG and EWG-containing benzyl chlorides were tolerable. More importantly, formation of undesired isomers such as aryl allenes and benzyl enynes were not observed. The authors reasoned that difference of this method compared to Trzeciak and Alami’s protocols was that the use of a more bulky electron-rich monodentate phosphine ligand suppresses the occurrence of Pd being bound to the arene and alkyne that will lead to a second carbometallation step that would result in the formation of **82b**.

Scheme 68.



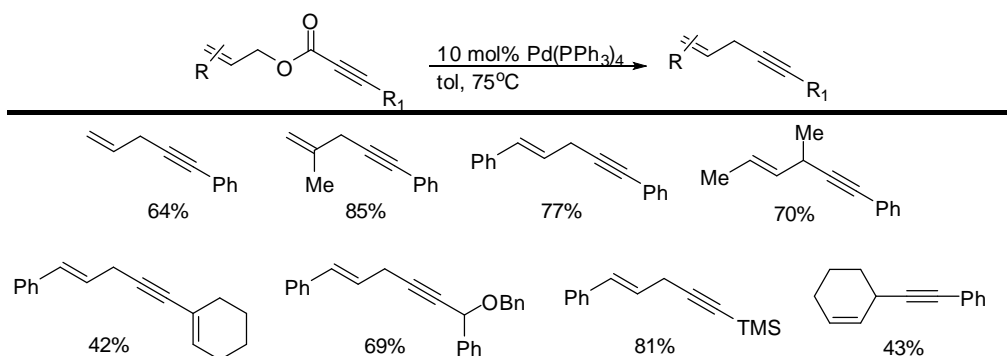
While the reaction worked with various substituted benzyl chlorides and alkynes, a major limitation of the methodology was that the formation of benzyl alkyne significantly depended on the amount of base, nature of solvent and temperature. When reactions were ran using stoichiometric base, less polar solvent such as THF, and heated at lower temperatures, benzyl alkynes were formed. When the reactions were ran in excess base, more polar solvent such as MeCN, and heated above 80°C , aryl allenes **85** were formed (eq. 72). These results suggest that the formation of alkyne at lower temperatures is kinetically driven whereas the formation of phenyl allene, resulted from isomerization of benzyl alkyne at higher temperatures is thermodynamically driven.



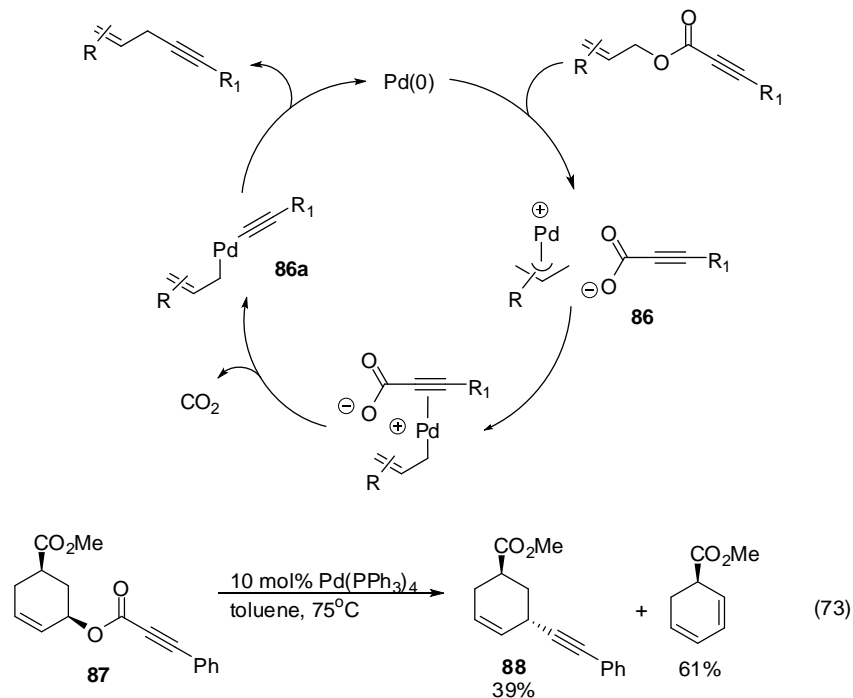
3.2 Decarboxylative allylation of alkynes: prelude to DcB of alkynes

Prior to the development of DcB of alkynes, it was disclosed in 2005 by Rayabarapu and Tunge that allyl propiolates undergo decarboxylation in the presence of $\text{Pd}(\text{PPh}_3)_4$ giving 1,4-enynes in good to high yields (Scheme 69). They proposed that the DcA mechanism begins through oxidative addition of allyl propiolate with Pd to generate an η^3 -allyl-Pd carboxylate complex **86**. Alkynyl metalation occurs in which η^1 -allyl-Pd coordinates to the alkyne. This undergoes decarboxylation to give an allyl-Pd-alkyne intermediate **86a**. Finally, reductive elimination forms the enyne (Scheme 70). The formation of allyl-Pd-alkyne **86a**, in which Pd is bound to acetylide was rationalized based on the observed inversion of stereochemistry of *trans*-1,4 cyclohexenyl phenyl alkyne **87** resulting from the DcA of *cis*-cyclohexenyl phenyl propiolate **87** (eq. 73).¹⁴

Scheme 69.

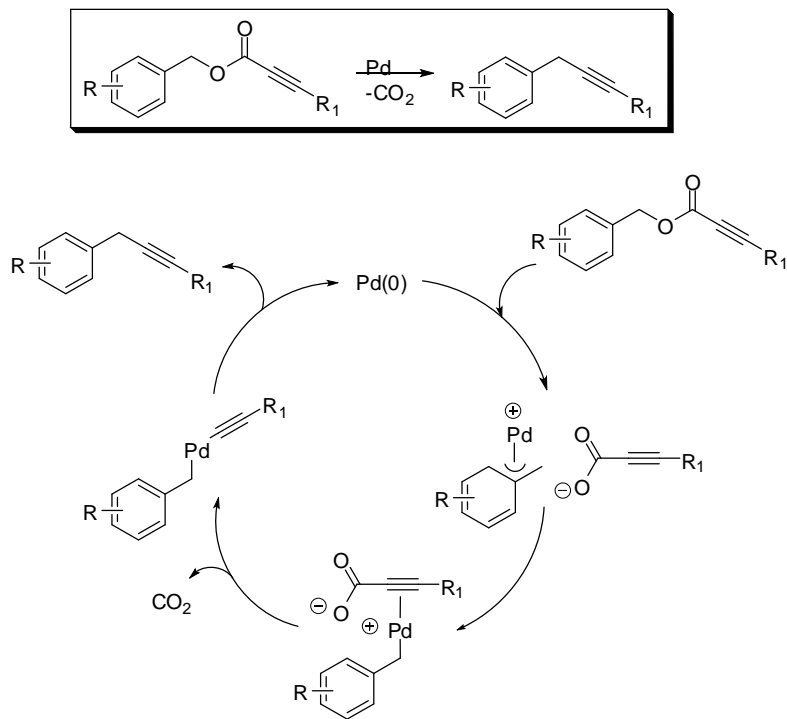


Scheme 70.



Inspired by these results, we wanted to develop a decarboxylative strategy towards the synthesis of benzyl alkynes. To be able to perform DcB of alkynes will allow us to construct benzyl alkynes under milder conditions without the need of base or any preformed organometallics, which were utilized in previous benzyl alkylation chemistries. In terms of the mechanism of DcB, it will be similar to the DcA of alkynes mechanism since both will generate the same reactive nucleophile (Scheme 71).

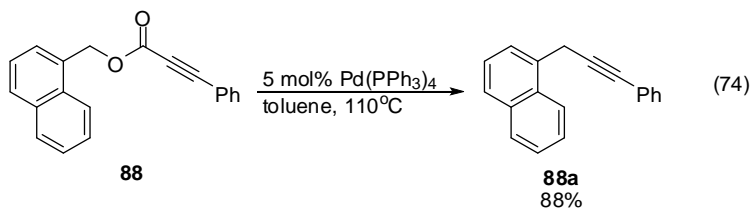
Scheme 71.



3.3 Development of DcB of benzo-fused alkynes

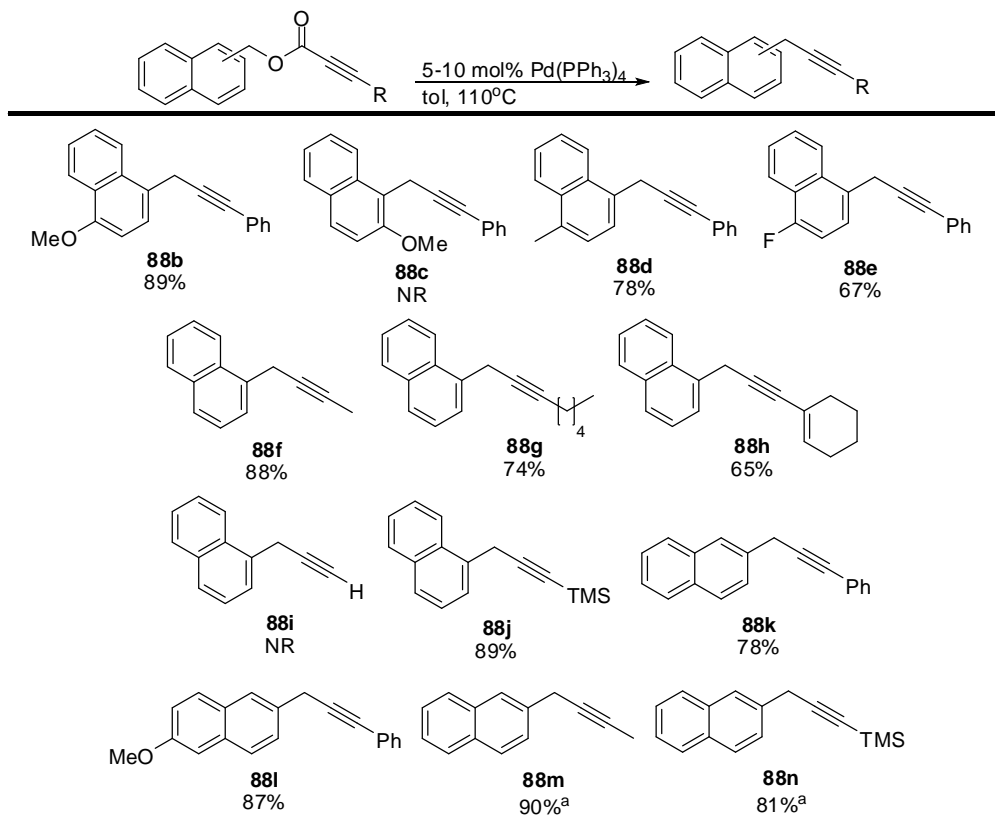
3.3.1 Substrate Scope

We began the development of DcB of alkynes using benzo-fused propiolates. When 1-naphthylmethyl phenyl propiolate **88** was tried using the standard reaction conditions used in DcA of alkynes, we were pleased that the reaction proceeded smoothly to give 1-naphthylmethyl phenyl alkyne **88a** in high yield (eq. 74).¹⁵



Based on this promising result, we also explored other substrates to examine the scope of DcB (Scheme 72). Various naphthylmethyl propiolates undergo decarboxylation to generate naphthylmethyl alkynes in good to high yields. The position and nature of the substituents near to the benzyl alkyne significantly affected the benzylation. While (4-methoxy) 1-naphthylmethyl phenyl propiolate **88b** undergoes DcB in very high yield, (2-methoxy) 1-naphthylmethyl phenyl propiolate **84c** regrettably did not undergo DcB. The use of EDG substituents (**88b** and **88d**) gave higher yields than a substrate with an EWG substituent **88e**. Both 1- and 2-naphthylmethyl propiolates underwent DcB although a higher catalyst loading (10 mol%) was necessary for 2-naphthylmethyl propiolates. In addition to phenyl alkynes, other aliphatics such as methyl, pentyl, and cyclohexenyl alkynes can be used with little to no effect on yield of benzylation. This is in contrast with the DcA of alkynes in which aromatic propiolates are superior substrates.¹⁵ While a terminal alkyne **88i** failed to undergo DcB, a TMS group **88j** can be used in lieu of the hydrogen.¹⁵

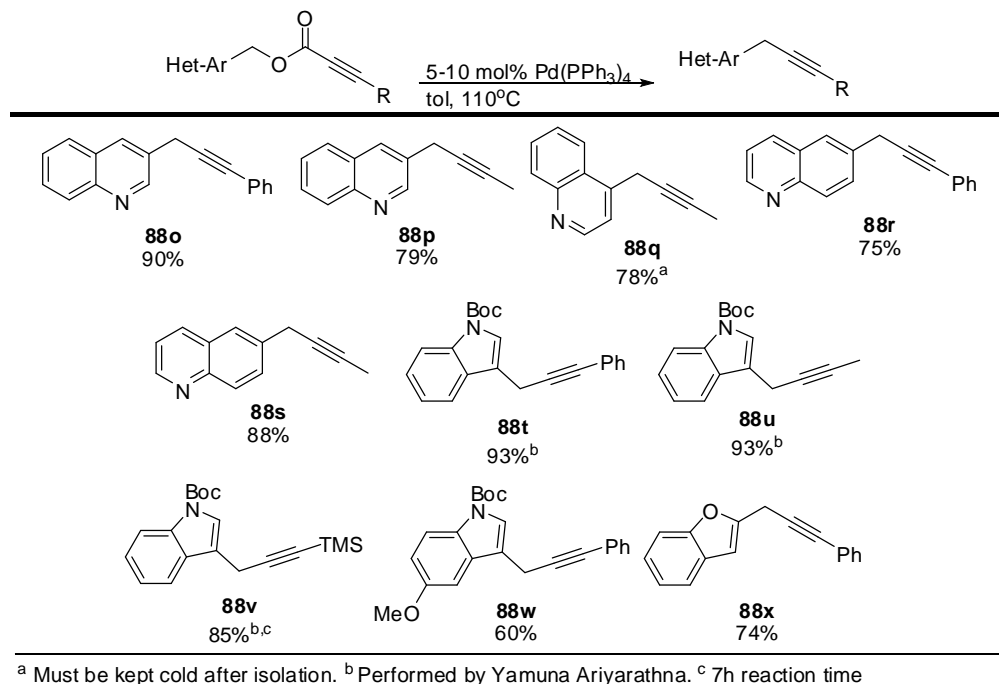
Scheme 72.



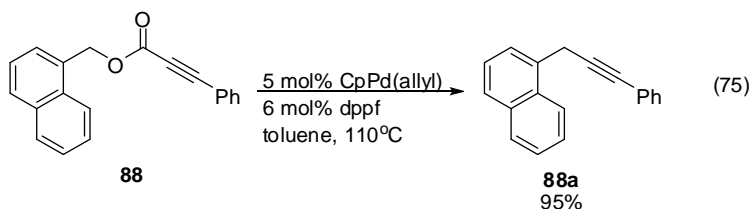
^a Performed by Yamuna Ariyaratna

We also expanded the scope of DcB using heterocycles. We were pleased that quinolinylmethyl, indolylmethyl, and benzofurylmethyl propiolates undergo DcB in good to excellent yields (Scheme 73). The position of the nitrogen near to the benzyl carbon in quinolines did not seem to affect benzylation. While we were able to obtain 4-quinolinylmethyl methyl alkyne **88q** in good yield, it has to be kept cold after isolation to prevent isomerization to 4-quinolinyl butadiene.¹⁵

Scheme 73.

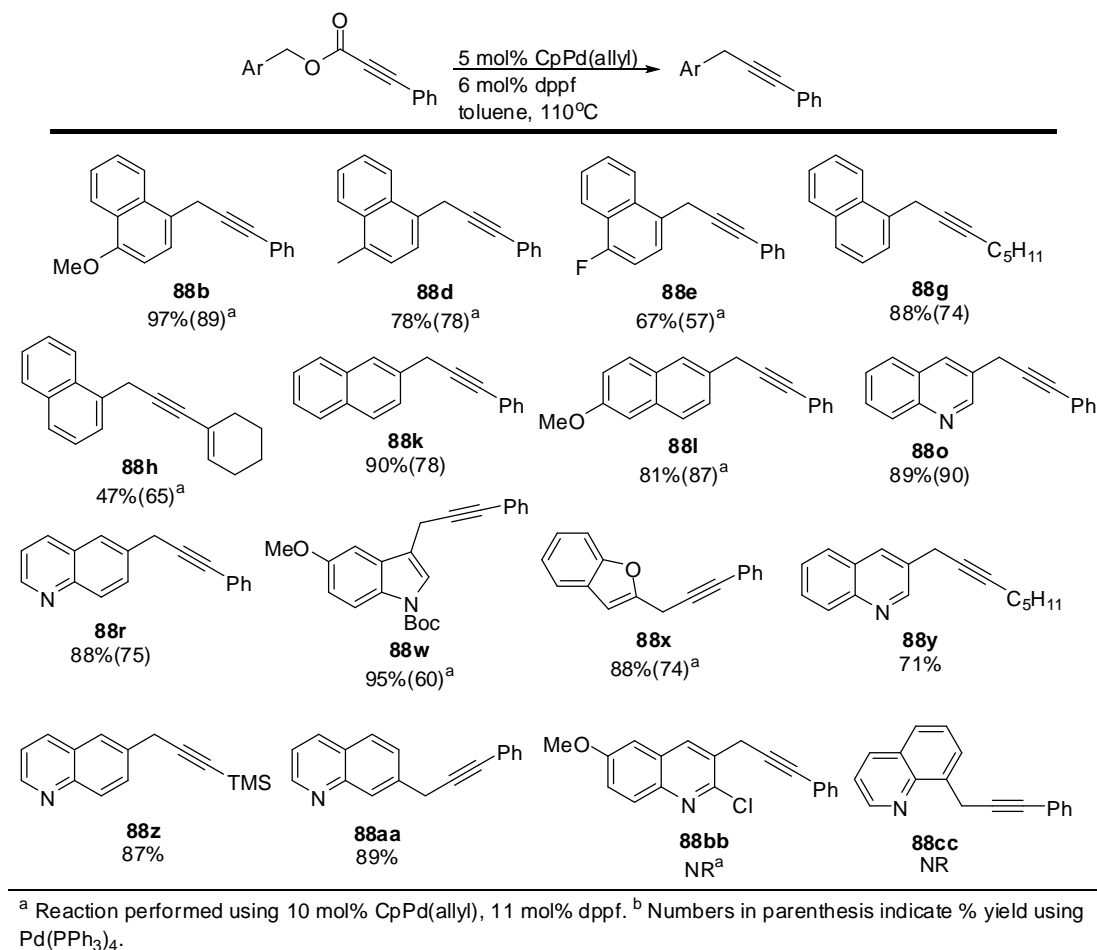


While we were working towards expanding the scope of DcB using Pd(PPh₃)₄, we were curious if other Pd catalysts could also be used instead of Pd(PPh₃)₄. More specifically, we were curious if we could use the catalyst inspired from our first project in which CpPd(allyl)/dppf catalyst was a very useful catalyst in the DcB of simple benzyl β-ketoesters (Chapter 2.3). To test our hypothesis, 1-naphthylmethyl phenyl alkyne **88** was treated with CpPd(allyl)/dppf catalyst. We were delighted that it gave **88a** cleanly at a lower catalyst loading and in higher yield compared to Pd(PPh₃)₄ catalyst (eq. 75).



Gratified by this result, we briefly looked into some of the substrates that were coupled previously using Pd(PPh₃)₄ and compared these results using CpPd(allyl)/dppf (Scheme 74). We were pleased that CpPd(allyl)/dppf catalyst also effectively allowed DcB of aromatic and heteroaromatic benzo-fused propiolates into their corresponding alkynes in higher and comparable yields to the Pd(PPh₃)₄ catalyst. Other quinolinylmethyl alkynes (**88y** and **88z**) can also be accessed using this catalyst system. While a 2-chloro-6-methoxy-3-quinolinylmethyl phenyl propiolate **88bb** failed to undergo DcB, 7-quinolinylmethyl phenyl alkyne **88aa** was an excellent substrate. The inability of 8-quinolinylmethyl phenyl propiolate **84cc** to undergo DcB supports the idea that the position of the heteroatom near to the benzylic carbon is important.

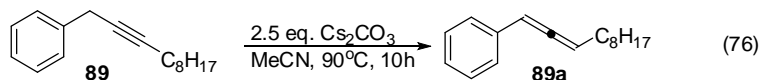
Scheme 74.



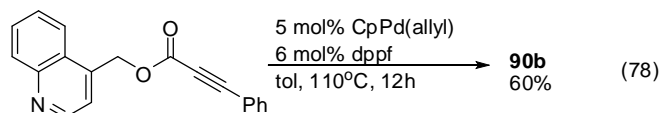
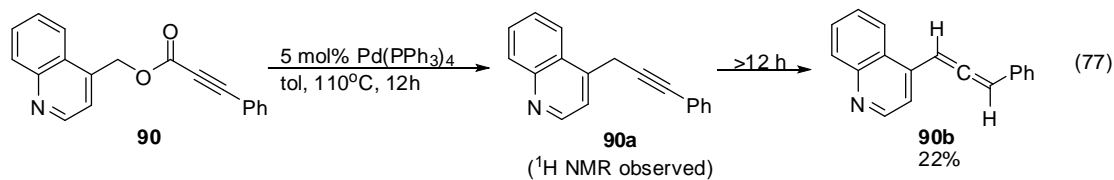
3.3.2 Inevitable isomerizations

One of the key experiments reported by Buchwald and coworkers showed that benzyl octyne **89** underwent isomerization giving benzyl allene **89a** in presence of base (eq. 76).¹³ This implies that the role of base has significant impact in alkyne-allene isomerizations. Alkyne-allene isomerization of this kind is known as prototropic rearrangement in which there is migration of a non-cumulated π -bond into cumulation with a second π -bond.¹⁶ Based on the

results shown in Schemes 72-74, we did not see any formation of aryl allene from benzyl alkyne, but rather decomposition when benzyl alkynes were kept at room temperature.

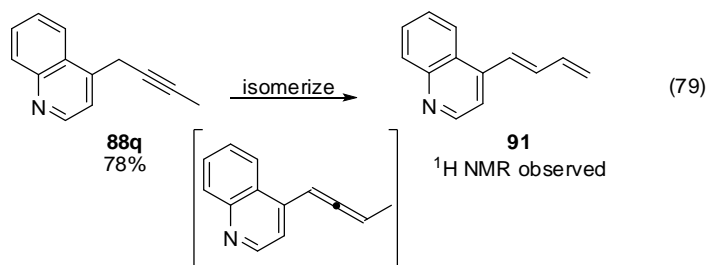


When 4-quinolinylmethyl phenyl propiolate **90** was treated with Pd(PPh₃)₄ for 12 hours, the expected 4-quinolinylmethyl phenyl alkyne **90a** was observed (eq. 77). However, when we let the reaction run longer; we no longer observed **90a** (based on ¹H NMR spectroscopy) but rather 4-quinolinyl phenyl allene **90b**. The formation of **90a** can also be bypassed by simply heating **90** longer than 12 hours albeit in low yield. When CpPd(allyl)-dppf catalyst was used, **90b** was isolated in good yield and none of **90a** was observed (eq. 78). This implies that formation of **90a** is kinetically driven while **90b** is thermodynamic. Since we could only see benzyl alkyne **90a** on NMR scale, attempts to isolate it proved difficult. While isolation of **90a** was not possible, it was interesting that other benzo-fused alkynes did not isomerize to aryl allenes, even when reactions were heated for more than 12 hours.



Another substrate that also underwent isomerization was the product of DcB of 4-quinolinylmethyl methyl propiolate. For this substrate, formation of 4-quinolinyl butadiene **91** occurred from isomerization of 4-quinolinylmethyl methyl alkyne **88q**. This concomitant

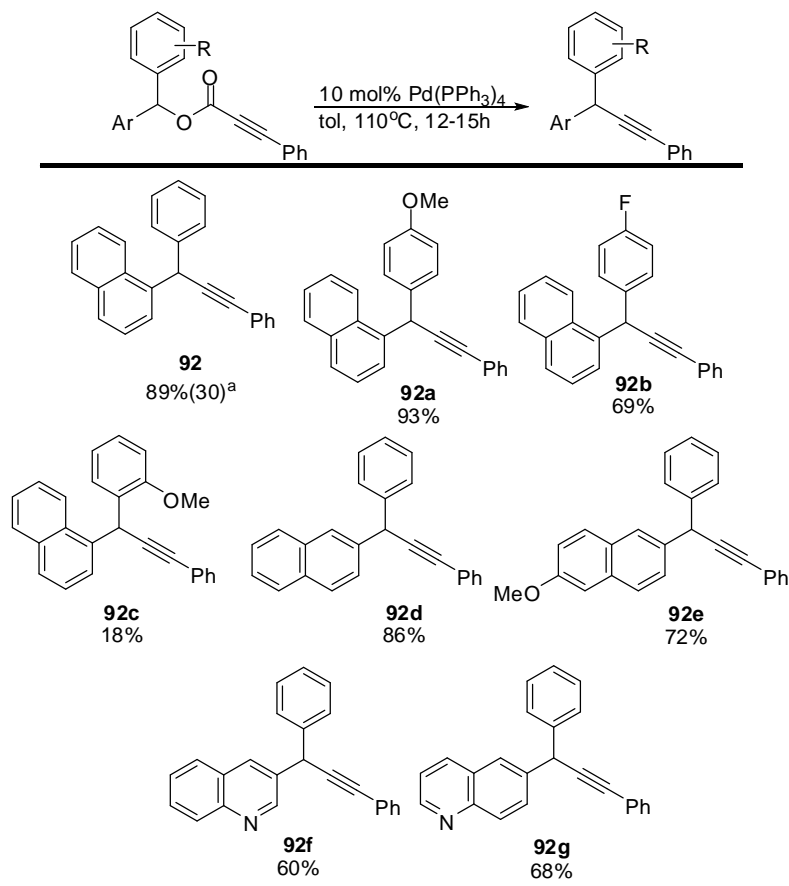
isomerization event was observed during the course of reaction (eq. 79). While we could get a clean ^1H NMR spectrum of **88q**, a clean ^{13}C NMR spectrum of it was difficult because we could notice the formation and appearance of olefin signals pertaining to **91** during acquisition. Considering that the thermodynamic stability of isomeric acetylenes and dienes, in which 1,3-dienes are the most stable compounds, we were pleased that diene formation was not observed in other substrates.¹⁷



3.3.3 Diaryl alkyne synthesis

We also looked into the DcB of diaryl alkynes (Scheme 75). For these reactions, $\text{Pd}(\text{PPh}_3)_4$ proved to be a better catalyst. While a higher catalyst loading was necessary to achieve a high yield of benzylation, both aromatic and heteroaromatic substrates underwent benzylation in good to high yields. Similar to previous DcB results, the electronics and position of the substituent on the ring affected the overall reaction.

Scheme 75.



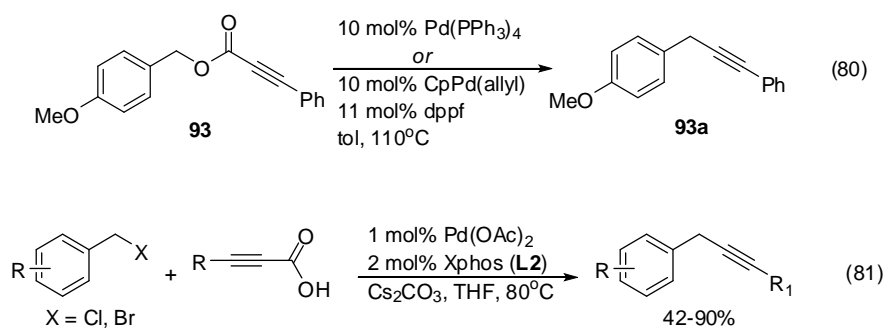
^a Number in parenthesis is the % yield using 5 mol% Pd.

3.4 Development of DcB of simple benzyl alkynes

3.4.1 Background

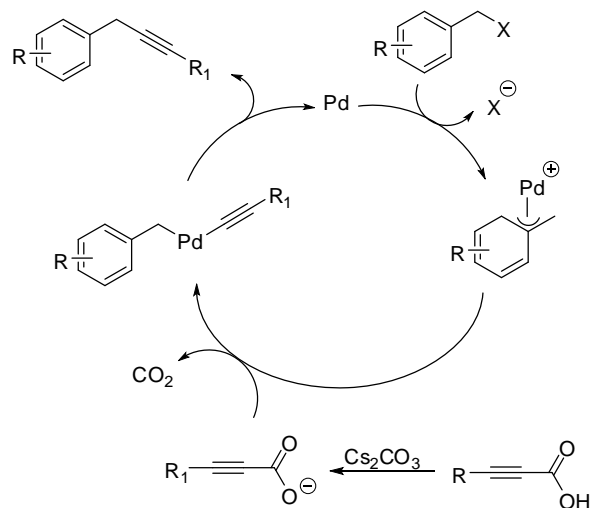
The ability of benzo-fused propiolates to undergo DcB inspired us to investigate the scope of alkyne DcB using simple benzyl esters. To begin, when *p*-methoxybenzylmethyl phenyl propiolate **93** was subjected to Pd conditions used in the DcB of benzo-fused propiolates, formation of benzyl alkyne **93a** did not occur (eq. 80). Saddened by these results, we looked into the literature with the hope to find publications that describe in some way regarding

decarboxylative benzylations of simple benzyls. We were able to find an interesting publication reported by Li and coworkers in 2010, in which they reported the benzylation of propiolic acids with benzyl halide in the presence of base and XPhos ligand giving simple benzyl alkynes (eq. 81). A variety of benzyl halides can be used as coupling partner with aromatic and aliphatic propiolic acids in good to high yields.¹⁸

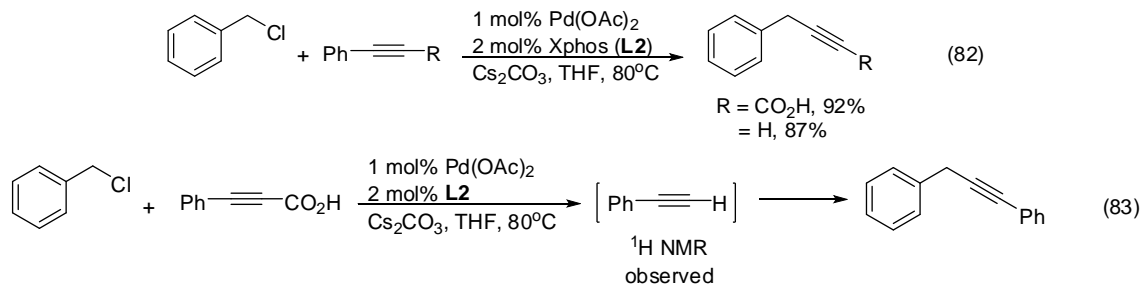


The proposed mechanism occurs starting from oxidative addition of benzyl halide with Pd to generate Pd- π -benzyl complex. Cs₂CO₃ deprotonates phenyl propiolic acid giving phenyl alkynyl carboxylate which then undergoes decarboxylation to generate phenyl alkynyl anion. This leads to formation of alkyne-Pd-benzyl intermediate (Scheme 76). Reductive elimination ultimately releases benzyl alkyne and Pd is regenerated back into the catalytic cycle.¹⁹

Scheme 76.



One interesting feature of this reaction was phenylacetylene can undergo substitution with benzyl chloride to give benzyl alkyne in comparable yield with that of phenylpropionic acid (eq. 82). This suggests that formation of phenylacetylene occurs in the reaction *in situ*. If phenylacetylene is present in the reaction, then decarboxylation would become unnecessary since deprotonation of the terminal alkyne from phenylacetylene will also generate the alkynyl anion needed to form the alkyne-Pd-benzyl intermediate. Based on a series of ¹H NMR experiments, we were able to observe the formation of phenylacetylene in the reaction of phenyl propionic acid and benzyl bromide (eq. 83). It appears that while the overall chemistry leads to generation of benzyl alkynes, synthetic preparations required more expensive propiolic acids rather than acetylenes to generate the alkynyl anion. Despite the disadvantage, the overall benzylation could be beneficial to our chemistry.



3.4.2 Substrate methodology and reaction scope

The inability of *p*-methoxybenzylmethyl phenyl propiolate **93** to undergo DcB prompted us to try other catalysts. Initial screening results showed that while bidentate and monodentate ligands that contain (PPh_x) in their ligand backbone failed (entries 1-4), the use of alkylphosphine monodentate ligands incredibly gave the desired *p*-methoxybenzyl phenyl alkyne **93a** in moderate to good conversions. Switching from CpPd(allyl) to Pd₂(dba)₃ as Pd source, we were able to notice improved product conversion. When we switched from alkyl phosphines to electron-rich biphenyl-derived phosphines, identical to the catalyst used by Li¹⁸ and Buchwald.¹³ We were pleased that higher product conversions were observed. Finally, the use of XPhos ligand gave the best conversion. When the catalyst loading was lowered, the conversion to product dropped drastically. Ultimately, we chose the combination of Pd₂dba₃/XPhos catalyst for DcB of simple benzyl propiolates.

Table 5.

Entry	X	Pd	Y	Ligand	%Conversion ^a
1	10	CpPd(allyl)	11	dppf	0
2	10	CpPd(allyl)	11	dppe	0
3	10	CpPd(allyl)	11	Xantphos	0
4	10	CpPd(allyl)	20	PPh ₃	0
5	10	CpPd(allyl)	20	PMe ₃	67
6	10	CpPd(allyl)	20	PBu ₃	47
7	10	CpPd(allyl)	20	P(<i>t</i> -Bu) ₃	0
8	10	CpPd(allyl)	20	PCy ₂ bp	72 ^b
9	5	Pd ₂ dba ₃	20	PCy ₂ bp	63
10	5	Pd ₂ dba ₃	20	SPhos	77
11	5	Pd ₂ dba ₃	20	XPhos	94
12	2.5	Pd ₂ dba ₃	10	XPhos	11
13	1	Pd ₂ dba ₃	5	XPhos	0

SPhos

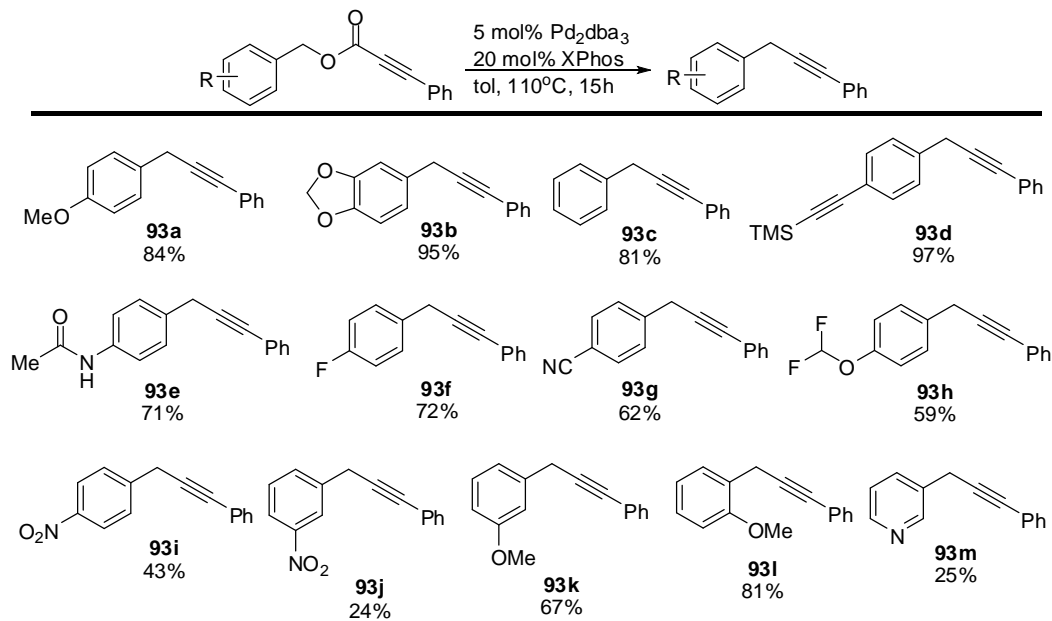
dppe

Xantphos

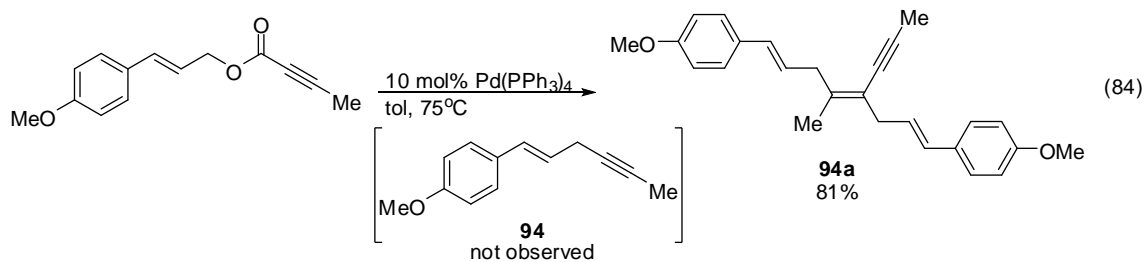
^a Determined by ¹H NMR spectroscopy. ^b The ¹H NMR spectrum gave messy mixtures.

Having the optimized reaction conditions at hand, we tried it to utilize various simple benzyl propiolates in DcB reactions. We first looked into the effect of substituents around the aromatic ring towards DcB. (Scheme 77) As expected, EDG-containing substituents gave products in higher yields compared to substrates containing EWG substituents, We were also pleased that 2-methoxy-1-naphthylmethyl phenyl propiolate underwent DcB giving 2-methoxy-1-naphthyl phenyl alkyne in high yield when a more reactive Pd catalyst was used.

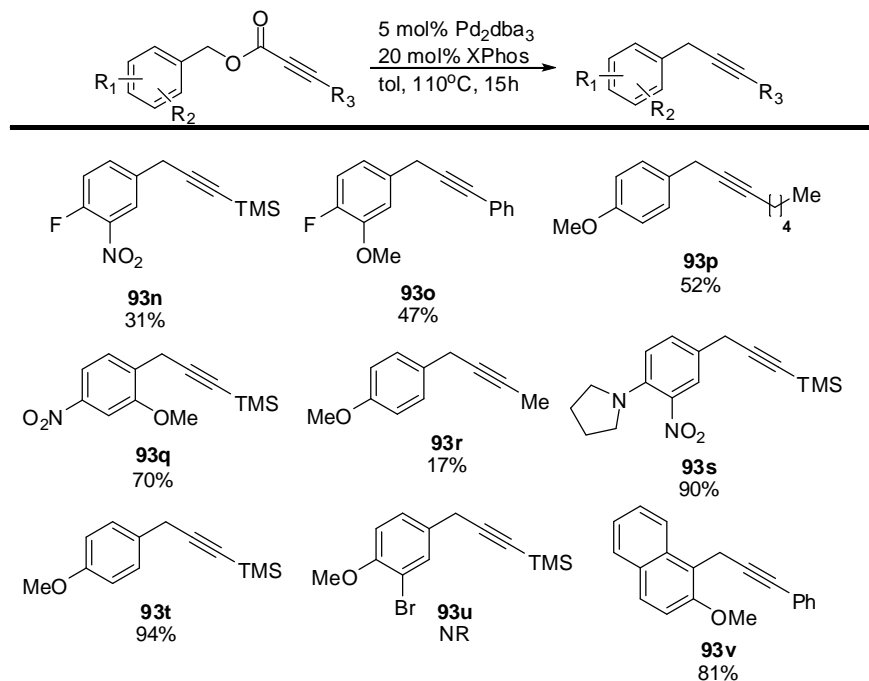
Scheme 77.



We also looked into exploring the scope of DcB with other substituted benzyl alkynes (Scheme 78). While the formation of **93u** did not occur, presumably because of the presence of bromine substituent, a fluoro substituent (**93n** and **93o**) underwent benzylation in low to moderate yields. When a terminal alkyne was replaced with a bulky group such as pentyl or TMS, DcB proceeded in high yield compared to smaller group Me. This lies in contrast with DcA of alkynes in which a dimeric-type enyne **94a** was obtained rather than the desired enyne **94** when Me-substituent was used (eq. 84).¹⁴

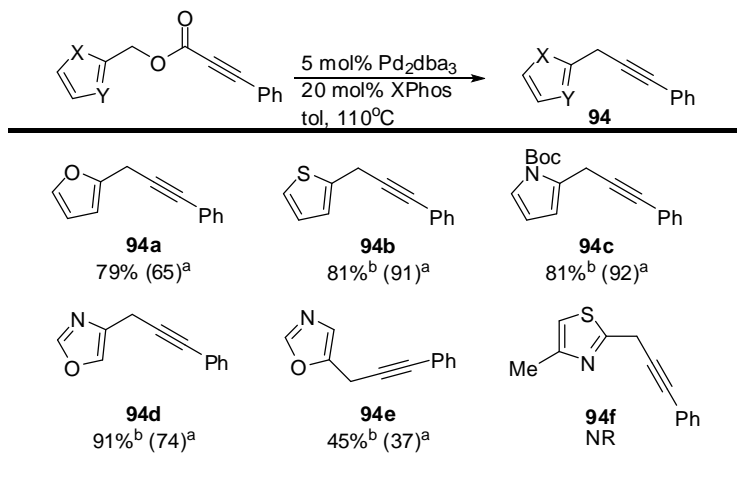


Scheme 78.



Finally, we looked into the DcB of benzyl alkynes using five-membered heterocycles as the benzyl coupling partner (Scheme 79). We were pleased that furanylmethyl, thiophenylmethyl, and Boc-protected pyrrolylmethyl phenyl propiolates undergo DcB giving the corresponding five-membered heterocyclic alkynes in high yields. Pd(PPh₃)₄ can also be used in these reactions and still generate benzylation compounds in high yields. When an oxazole was tried, it appeared that the position of the benzyl next to an electronegative atom has significant effect on DcB. While 4-oxazolylmethyl phenyl alkyne **94e** was obtained in high yield, 5-oxazolylmethyl phenyl alkyne **94f** gave a lower benzylation yield. When the benzyl moiety is in between two heteroatoms (**94g**), DcB did not occur.

Scheme 79.

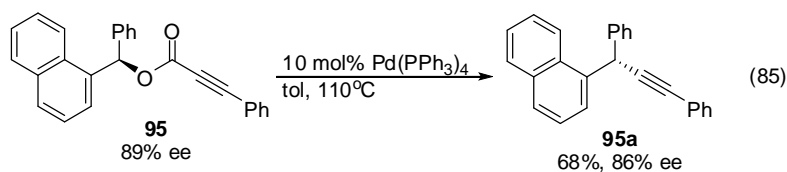


^a Numbers in parenthesis indicate % yield using 10 mol% Pd(PPh₃)₄.

^b Performed by Shehani Mendis.

3.5 Mechanistic insights

We think that the DcB mechanism of benzyl alkynes should be similar to the DcA mechanism of allyl alkynes; the only difference is the type of Pd electrophile. Also in this mechanism, the nucleophile is bound to the metal compared to enolate which is not bound (Chapter 2.3). To test whether the alkyne is bound to Pd after decarboxylation, an enantiopure 1-naphthylphenyl phenyl propiolate **95** was treated under identical reaction conditions as that of benzo-fused phenyl propiolates. It gave the expected 1-naphthylphenyl phenyl alkyne **95a** in good yield with high conservation of enantiomeric excess (eq. 85). While we were not able to determine the absolute configuration of **95a**, we think that the reaction would proceed with inversion. This assumption is based on the stereochemical probe in the DcA of allyl phenyl propiolate (eq. 73).¹⁴



3.6 Conclusion

We have shown that simple benzyl and benzo-fused propiolates undergo DcB in the presence of appropriate Pd catalyst to generate benzyl alkynes. While benzo-fused propiolates can undergo DcB with either Pd(PPh₃)₄ or CpPd(allyl)/dppf catalyst, simple benzyl propiolates undergo DcB in the presence of electron-rich monodentate biphenyl-containing phosphine ligands. With the exception of a few 4-quinolinyl propiolates, the developed methodology allows construction of various substituted benzyl alkynes in good to high yields without formation of side products such as allenes and benzyl enynes. Similar to the DcB of benzyl β-ketoesters, the DcB of alkynes depends on the electronics of substituent and its position next to the benzylic carbon. Both simple aromatic and heteroaromatics can be utilized using the developed methodology. Also, the developed DcB of alkynes allows generation of diaryl methane containing alkynes in good yields, which can be applied towards the development of asymmetric DcB. Finally, the utility of DcB for functionalization of heterocycles makes this method an attractive tool useful in pharmaceutical synthesis and medicinal chemistry.

3.7 References

1. (a) Buck, M.; Chong, J. M. "Alkylation of 1-alkynes in THF" *Tetrahedron Lett.* **2001**, *42*, 5825-5827.; (b) Brandsma, L. *Preparative Acetylenic Chemistry*, 2nd ed.; Elsevier: Amsterdam, **1988**, 322 pp.; (c) Raphael, R. A. *Acetylene Compounds in Organic Synthesis*; Butterworths: London, **1955**, 219 pp.
2. Takahashi, T.; Kitamura, M.; Shen, B.; Nakajima, K. "Straightforward method for synthesis of highly alkyl-substituted naphthacene and pentacene derivatives by homologation" *J. Am. Chem. Soc.* **2000**, *122*, 12876-12877.
3. Wang, J. L.; Bowen, S. J.; Schweitzer, B. A.; Madsen, H. M.; McDonald, J.; Pelc, M. J.; Tenbrink, R. E.; Beidler, D.; Thorarensen, A. "Structure based design of novel irreversible FAAH inhibitors" *Bioorg. Med. Chem. Lett.* **2009**, *19*, 5970-5974.
4. Gaertner, V. R. "Ring-opening nucleophilic alkylations by tertiary azetidines" *J. Heterocycl. Chem.* **1969**, *6*, 273-277.
5. Yabunaka, H.; Kenmochi, A.; Nakatogawa, Y.; Sakamoto, K.; Miyoshi, H. "Hybrid ubiquinone: novel inhibitor of mitochondrial complex I" *Biochim. Biophys. Acta* **2002**, *1556*, 106-112.
6. Pérez, I.; Sestelo, J. P.; Sarandeses, L. A. "Atom-efficient metal-catalyzed cross-coupling reaction of indium organometallics with organic electrophiles" *J. Am. Chem. Soc.* **2001**, *123*, 4155-4160
7. Qian, M.; Negishi, E.-i. "Palladium-catalyzed cross-coupling reaction of alkynylzincs with benzylic electrophiles" *Tetrahedron Lett.* **2005**, *46*, 2927-2930.
8. Yong, H.; Gu, Y. G.; Clark, R. F.; Marron, T.; Ma, Z.; Soni, N.; Stone, G. G.; Nilius, A. M.; Marsh, K.; Djuric, S. W. "Design, synthesis and structure-activity relationships of 6-*O*-arylpropargyl diazalides with potent activity against multidrug-resistant *Streptococcus pneumoniae*" *Bioorg. Med. Chem. Lett.* **2005**, *15*, 2653-2658.
9. Pottier, L. R.; Peyrat, J.-F.; Alami, M.; Brion, J.-D. "Highly substituted enynes via a palladium-catalyzed tandem three carbon-carbon bonds forming reaction procedure from benzyl halides and alkynyl tributyltin reagents" *Tetrahedron Lett.* **2004**, *45*, 4035-4038.
10. (a) Pottier, L. R.; Peyrat, J.-F.; Alami, M.; Brion, J.-D. "Unexpected tandem Sonogashira-carbopalladation-Sonogashira coupling reaction of benzyl halides with terminal alkynes: a novel four-component domino sequence to highly substituted enynes" *Synlett* **2004**, *9*, 1503-1508.; (b) Arcadi, A.; Cacchi, S.; Ianelli, S.; Marinelli, F.; Pietroni, B. "The palladium-tributylammonium formate reagent in the stereoselective hydrogenation, and stereo- and regioselective hydroarylation of alkyl 4-hydroxy-2-alkynoates: a route to substituted butenolides" *Tetrahedron* **1988**, *44*, 481-490.

11. Cheng, J.; Sun, Y.; Wang, F.; Guo, M.; Xu, J.-H.; Pan, Y.; Zhang, Z. "A copper- and amine-free Sonogashira reaction employing aminophosphines as ligands" *J. Org. Chem.* **2004**, *69*, 5428–5432.
12. Sans, V.; Trzeciak, A. M.; Luis, S.; Ziolkowski, J. J. "PdCl₂(P(OPh)₃)₂ catalyzed coupling and carbonylative coupling of phenylacetylenes with aryl iodides in organic solvents and in ionic liquids" *Catal. Lett.* **2006**, *109*, 37–41.
13. Larsen, C. H.; Anderson, K. W.; Tundel, R. E.; Buchwald, S. L. "Palladium-catalyzed Heck alkylation of benzyl chlorides" *Synlett* **2006**, *18*, 2941–2946.
14. Rayabarapu, D. K.; Tunge, J. A. "Catalytic decarboxylative sp–sp³ coupling" *J. Am. Chem. Soc.* **2005**, *127*, 13510–13511.
15. Torregrosa, R. R. P.; Ariyaratna, Y.; Chattopadhyay, K.; Tung, J. A. "Decarboxylative benzylations of alkynes and ketones" *J. Am. Chem. Soc.* **2010**, *132*, 9280–9282.
16. Hashmi, A. S. K. "Synthesis of allenes by isomerization reactions" In *Modern Allene Chemistry*; Krause, N.; Hashmi, A. S. K., Eds.; John Wiley & Sons, Germany, **2004**, pp. 3–50.
17. Olah, G. A.; Mólnar, A. "Hydrocarbon Chemistry, 2nd Edition" John Wiley and Sons, p. 180.
18. Zhang, W.-W.; Zhang, X.-G.; Li, J.-H. "Palladium-catalyzed decarboxylative coupling of alkynyl carboxylic acids with benzyl halides or aryl halides" *J. Org. Chem.* **2010**, *75*, 5259–5264.
19. Weaver, J. D.; Recio, A., III; Grenning, A. J.; Tunge, J. A. "Transition metal-catalyzed decarboxylative allylation and benzylation reactions" *Chem. Rev.* **2011**, *111*, 1846–1913.

3.8 Methodology and Compound Characterizations

General Information

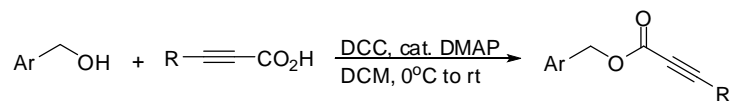
Toluene and THF were dried over sodium in the presence of benzophenone indicator. DCM and Et₂O were dried over activated alumina on a solvent system purchased from Innovative Technologies, Inc. Pd catalysts and ligands were purchased from Strem and Sigma-Aldrich. Other reagents and solvents were also obtained commercially and used without additional purification unless specified. Chiral 1-naphthylphenyl methanol was prepared according to a literature procedure.¹ CpPd(allyl) was prepared according to another literature procedure.² The isolated products were purified on silica gel from Sorbent Technologies (40-63 μm particle size, 60 Å porosity, pH 6.5-7.5). The ¹H and ¹³C NMR spectra were obtained on a Bruker Avance 400 or 500 MHz DRX spectrometer and were referenced to residual protio solvent signals. FTIR spectra were acquired on Shimadzu FTIR-8400S spectrometer. HRMS was performed on a LCT Premier TOF mass spectrometer using ESI techniques. Asymmetric analyses were performed via HPLC using Shimadzu SCL-10A VP instrument equipped with a chiral OD-H column. Structural assignments of the isolated compounds were based on ¹H, ¹³C, DEPT 135, COSY and HSQC spectroscopies.

Synthesis of Starting Materials

Synthesis of fused and simple benzyl propiolates

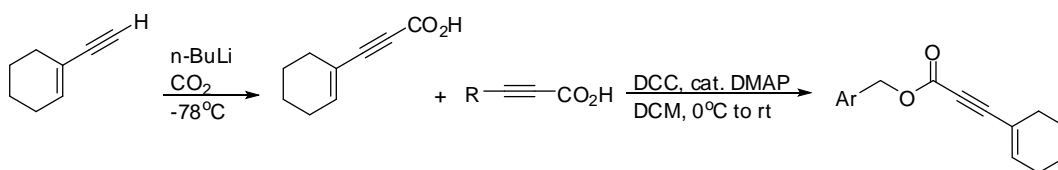
In an oven-dried 100 mL-flask were added the benzyl alcohol (1.0 mmol), propiolic acid (1.0 mmol) and DCM (10 mL). The mixture was stirred in an ice bath for 30 minutes, after which, a DCM (3 mL) solution containing DCC (1.0 mmol) and DMAP (0.10 mmol) was added dropwise to the cooled flask. The reaction was stirred at room temperature overnight. The

resulting solution was filtered through a pad of celite in a funnel fitted with a filter paper. The celite mixture was washed with small amounts of DCM. The collected filtrate was concentrated *in vacuo* before purifying *via* flash chromatography over silica gel.



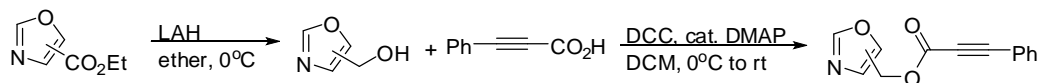
Synthesis of 1-naphthyl cyclohexenyl ester

The benzyl propiolate ester of **88h** was made by DCC-DMAP coupling of 1-naphthalenemethanol and 3-cyclohexenyl propiolic acid. 3-cyclohexenyl propiolic acid was prepared from the addition of CO₂, in the form of dry ice, to the mixture containing n-BuLi and 1-ethynylcyclohex-1-ene at -78°C followed by acidic workup at room temperature.



Synthesis of 4- and 5-oxazole phenyl propiolates

The parent benzyl propiolate of **94d** and **94e** were prepared by DCC-DMAP coupling of phenyl propiolic acid and oxazole alcohol. The alcohols were prepared by LAH reduction of 4 and 5-oxazole ethyl esters at 0°C.



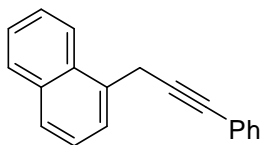
Procedure for decarboxylative benzylation of alkynes

In a flame-dried Schlenk tube under argon, Pd(PPh₃)₄ (0.05 mmol) or the combination of Pd₂(dba)₃ (0.05 mmol) and XPhos (0.20 mmol) was dissolved in toluene (5 mL) and was added to the benzyl propiolic ester (1.0 mmol). The reaction was stirred at 110°C for 7 – 15 hours depending on the compound. After cooling the reaction mixture at room temperature, the reaction was concentrated *in vacuo* and was purified *via* flash chromatography using hexane and ethyl acetate as eluent. The isolated compound was kept in the freezer.

Note on storage of benzylic alkynes

We observed that some of the isolated benzylic alkynes - especially quinolinyl alkynes - decomposed over time when stored at room temperature. To avoid the risk of decomposition and degradation of other substrates in the future, all benzylic alkynes were stored in a freezer after isolation.

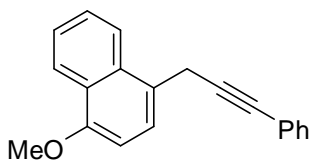
Spectroscopic Data



1-(3-phenylprop-2-ynyl)naphthalene, **88a**³
(YA-1-24)

¹H NMR (500 MHz, CDCl₃) δ ppm 8.10 (d, *J* = 8.3 Hz, 1H, aromatic H), 7.89 (d, *J* = 8.0 Hz, 1H, aromatic H), 7.79 (d, *J* = 8.2 Hz, 1H, aromatic H), 7.71 (d, *J* = 7.0 Hz, 1H, aromatic H), 7.59 – 7.54 (m, 1H, aromatic H), 7.54 – 7.49 (m, 1H, aromatic H), 7.49 – 7.43 (m, 3H, aromatic H), 7.29 (dd, *J* = 5.1, 1.9 Hz, 3H, aromatic H), 4.24 (s, 2H, Ar-CH₂)

¹³C NMR (126 MHz, CDCl₃) δ ppm 134.16 (aromatic C), 132.94 (aromatic C), 132.10 (aromatic C), 131.92 (aromatic C), 129.20 (aromatic C), 128.69 (aromatic C), 128.30 (aromatic C), 128.06 (aromatic C), 126.64 (aromatic C), 126.21 (aromatic C), 126.19 (aromatic C), 126.07 (aromatic C), 124.11 (aromatic C), 123.85 (aromatic C), 87.69 (CH₂-C-C-Ar) 84.01 (CH₂-C-C-Ar), 24.14 (Ar-CH₂)



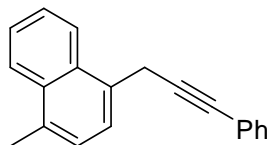
1-methoxy-4-(3-phenylprop-2-ynyl)naphthalene, **88b**
(RT-4-283)

¹H NMR (500 MHz, CDCl₃) δ ppm 8.35 (d, *J* = 8.3 Hz, 1H, aromatic H), 8.04 (d, *J* = 8.3 Hz, 1H, aromatic H), 7.64 – 7.56 (m, 2H, aromatic H), 7.56 – 7.50 (m, 1H, aromatic H), 7.46 (dd, *J* = 7.0, 2.6 Hz, 2H, aromatic H), 7.33 – 7.27 (m, 3H, aromatic H), 6.79 (d, *J* = 7.8 Hz, 1H, aromatic H), 4.15 (s, 2H, Ar-CH₂), 3.99 (s, 3H, O-CH₃).

¹³C NMR (126 MHz, CDCl₃) δ ppm 154.87 (aromatic C), 132.23 (aromatic C), 131.61 (aromatic C) (aromatic C), 128.18 (aromatic C), 127.73 (aromatic C), 126.64 (aromatic C), 125.89 (aromatic C), 125.61 (aromatic C), 125.06 (aromatic C), 124.35 (aromatic C), 123.77 (aromatic C), 123.24 (aromatic C), 122.63 (aromatic C), 103.29 (aromatic C), 87.63 (CH₂-C-C-Ar), 83.24 (CH₂-C-C-Ar), 55.40 (O-CH₃), 23.20 (Ar-CH₂).

FTIR (CH₂Cl₂) $\bar{\nu}_{\max}$ cm⁻¹ 2938, 2359, 2332, 1489, 1437, 1119, 756.

HRMS Calcd for C₂₀H₁₆O (M+H) – 273.1279, found 273.1273.



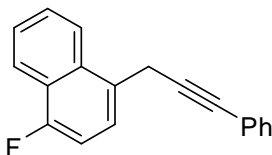
1-methyl-4-(3-phenylprop-2-ynyl)naphthalene, **88d**
(RT-9-282)

¹H NMR (400 MHz, CDCl₃) δ ppm 8.14 – 8.11 (dd, *J* = 6.6, 3.2 Hz, 1H, aromatic H), 8.07 – 8.03 (dd, *J* = 7.6, 2.1 Hz, 1H, aromatic H), 7.60 – 7.53 (td, *J* = 6.3, 5.8, 2.4 Hz, 3H, aromatic H), 7.47 – 7.41 (dd, *J* = 6.0, 2.3 Hz, 2H, aromatic H), 7.32 – 7.27 (m, 4H, aromatic H), 4.24 – 4.16 (s, 2H, Ar-CH₂), 2.72 – 2.68 (s, 3H, Ar-CH₃).

¹³C NMR (126 MHz, CDCl₃) δ ppm 133.66 (aromatic C), 132.77 (aromatic C), 131.57 (aromatic C), 131.47 (aromatic C), 130.51 (aromatic C), 128.11 (aromatic C), 127.63 (aromatic C), 126.29 (aromatic C), 125.70 (aromatic C), 125.46 (aromatic C), 125.37 (aromatic C), 124.85 (aromatic C), 123.83 (aromatic C), 123.62 (aromatic C), 87.57 (Ar-C-C-CH₂), 83.18 (Ar-C-C-CH₂), 23.55 (Ar-CH₂), 19.49 (CH₃).

FTIR (CH₂Cl₂) $\bar{\nu}_{\max}$ cm⁻¹ 2995, 2246, 1686, 1390, 1094, 758, 432.

HRMS Calcd for C₂₀H₁₇ (M+H) – 257.1330, found 257.1328.



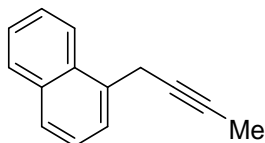
1-fluoro-4-(3-phenylprop-2-ynyl)naphthalene, **88e**
(RT-9-52)

¹H NMR (400 MHz, CDCl₃) δ ppm 8.22 – 8.13 (d, *J* = 8.2 Hz, 1H, aromatic H), 8.13 – 8.05 (d, *J* = 7.9 Hz, 1H, aromatic H), 7.66 – 7.55 (t, *J* = 8.9 Hz, 3H, aromatic H), 7.50 – 7.41 (s, 2H, aromatic H), 7.33 – 7.27 (m, 3H, aromatic H), 7.18 – 7.06 (t, *J* = 8.6 Hz, 1H, aromatic H), 4.23 – 4.13 (s, 2H, Ar-CH₂).

¹³C NMR (126 MHz, CDCl₃) δ ppm 159.44 (aromatic C), 157.39 (aromatic C), 132.55 (aromatic C), 131.77 (aromatic C), 128.39 (aromatic C), 127.98 (aromatic C), 127.21 (aromatic C), 126.24 (aromatic C), 125.44 (aromatic C), 123.56 (aromatic C), 121.27 (aromatic C), 109.11 (aromatic C), 108.92 (aromatic C), 87.16 (Ar-C-C-CH₂), 83.83 (Ar-C-C-CH₂), 23.48 (Ar-CH₂).

FTIR (CH₂Cl₂) $\bar{\nu}_{\max}$ cm⁻¹ 2926, 2359, 2189, 1603, 1238, 1055, 690.

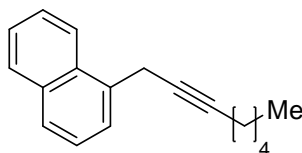
HRMS Calcd for C₁₉H₁₃FLi (M+Li) – 267.1161, found 267.1203.



1-(but-2-ynyl)naphthalene, **88f**⁴
(RT-4-294)

¹H NMR (500 MHz, CDCl₃) δ ppm 8.04 (d, *J* = 8.3 Hz, 1H, aromatic H), 7.87 (d, *J* = 7.9 Hz, 1H, aromatic H), 7.76 (d, *J* = 8.0 Hz, 1H, aromatic H), 7.63 (d, *J* = 7.0 Hz, 1H, aromatic H), 7.52 (dt, *J* = 22.5, 7.3 Hz, 3H, aromatic H), 7.47 – 7.42 (m, 1H, aromatic H), 3.96 (s, 2H, Ar-CH₂), 1.87 (s, 3H, C-CH₃).

¹³C NMR (126 MHz, CDCl₃) δ ppm 133.62 (aromatic C), 133.24 (aromatic C), 131.38 (aromatic C), 128.61 (aromatic C), 127.31 (aromatic C), 125.93 (aromatic C), 125.58 (aromatic C), 125.51 (aromatic C), 125.50 (aromatic C), 123.39 (aromatic C), 78.69 (Ar-C-C-CH₂), 76.39 (Ar-C-C-CH₂), 22.78 (Ar-CH₂), 3.75 (C-CH₃).



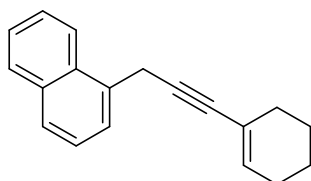
1-(oct-2-ynyl)naphthalene, **88g**
(RT-6-7)

¹H NMR (500 MHz, CDCl₃) δ ppm 8.04 (d, *J* = 8.4 Hz, 1H, aromatic H), 7.86 (d, *J* = 7.7 Hz, 1H, aromatic H), 7.75 (d, *J* = 8.2 Hz, 1H, aromatic H), 7.64 (d, *J* = 6.6 Hz, 1H, aromatic H), 7.51 (dt, *J* = 20.8, 7.5 Hz, 2H, aromatic H), 7.46 – 7.42 (m, 1H, aromatic H), 3.98 (s, 2H, Ar-CH₂), 2.23 (t, *J* = 7.1 Hz, 2H, C-CH₂-CH₂), 1.57 – 1.50 (m, 2H, CH₂-CH₂), 1.42 – 1.36 (m, 2H, CH₂-CH₂), 1.33 (dd, *J* = 14.1, 7.2 Hz, 2H, CH₂-CH₃), 0.89 (t, *J* = 7.2 Hz, 3H, CH₂-CH₃)

¹³C NMR (126 MHz, CDCl₃) δ ppm 133.65 (aromatic C), 133.39 (aromatic C), 131.51 (aromatic C), 128.62 (aromatic C), 127.28 (aromatic C), 125.39 (aromatic C), 123.44 (aromatic C), 83.69 (C-CH₂-CH₂), 77.19 (Ar-CH₂-C-C), 30.71 (C-C-CH₂-CH₂), 28.82 (CH₂-CH₂), 23.23 (Ar-CH₂), 22.27 (CH₂-CH₃), 18.55 (C-CH₂-CH₂), 13.87 (CH₂-CH₃).

FTIR (CH₂Cl₂) $\bar{\nu}_{\max}$ cm⁻¹ 2930, 2230, 1597, 1510, 1396, 987, 769

HRMS Calcd for C₁₈H₂₀ (M+H) – 237.1643, found 237.1634.



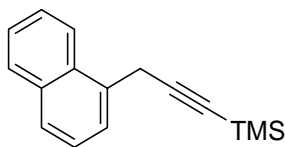
1-(3-cyclohexenylprop-2-ynyl)naphthalene, **88h**
(RT-9-287)

¹H NMR (400 MHz, CDCl₃) δ ppm 8.08 – 8.00 (d, *J* = 8.2 Hz, 1H, aromatic H), 7.89 – 7.83 (d, *J* = 7.1 Hz, 1H, aromatic H), 7.78 – 7.73 (d, *J* = 8.3 Hz, 1H, aromatic H), 7.67 – 7.62 (d, *J* = 7.0 Hz, 1H, aromatic H), 7.55 – 7.43 (ddd, *J* = 21.8, 13.6, 8.1 Hz, 3H, aromatic H), 6.11 – 6.05 (s, 1H, vinyl H), 4.15 – 4.05 (s, 2H, Ar-CH₂), 2.20 – 2.11 (s, 2H, C-CH₂), 2.11 – 2.00 (s, 2H, C-CH₂), 1.67 – 1.55 (m, 4H, (CH₂-CH₂)).

¹³C NMR (126 MHz, CDCl₃) δ ppm 134.03 (vinyl C), 133.79 (aromatic C), 133.00 (aromatic C), 131.56 (aromatic C), 128.79 (aromatic C), 127.55 (aromatic C), 126.19 (aromatic C), 125.80 (aromatic C), 125.70 (aromatic C), 123.53 (aromatic C), 120.98 (vinyl C), 85.53 (Ar-C-C-CH₂), 84.32 (Ar-C-C-CH₂), 29.61 (CH₂), 25.72 (CH₂), 23.69 (CH₂), 22.51 (CH₂), 21.71 (CH₂).

FTIR (CH₂Cl₂) $\bar{\nu}_{\max}$ cm⁻¹ 3047, 2932, 2361, 2214, 1690, 1508, 790

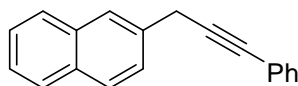
HRMS Calcd for C₁₉H₁₇ (M-H) – 245.1330, found 245.1367.



trimethyl(3-(naphthalene-1-yl)prop-1-ynyl)silane, **88j**⁵
(RT-4-284)

¹H NMR (500 MHz, CDCl₃) δ ppm 7.91 (d, *J* = 8.3 Hz, 1H, aromatic H), 7.78 (d, *J* = 8.3 Hz, 1H, aromatic H), 7.68 (d, *J* = 8.2 Hz, 1H, aromatic H), 7.57 (d, *J* = 7.0 Hz, 1H, aromatic H), 7.46 – 7.34 (m, 4H, aromatic H), 3.97 (s, 2H, Ar-CH₂), 0.11 (s, 9H, (CH₃-Si))

¹³C NMR (126 MHz, CDCl₃) δ ppm 133.79 (aromatic C), 133.63 (aromatic C), 132.08 (aromatic C), 131.39 (aromatic C), 128.65 (aromatic C), 128.42 (aromatic C), 127.48 (aromatic C), 126.02 (aromatic C), 125.66 (aromatic C), 125.55 (aromatic C), 123.25 (aromatic C), 103.75 (CH₂-C-C-TMS), 87.89 (CH₂-C-C-TMS), 23.84 (Ar-CH₂), 0.06 (CH₃-Si)



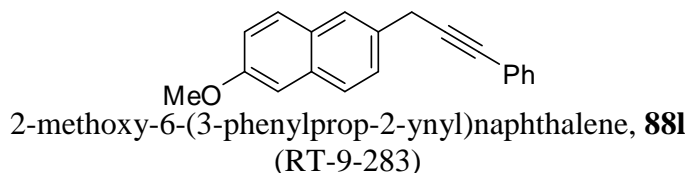
2-(3-phenylprop-2-ynyl)naphthalene, **88k**
(YA-1-47)

¹H NMR (500 MHz, CDCl₃) δ ppm 7.87 (s, 1H, aromatic H), 7.82 (dd, *J* = 7.3, 2.1 Hz, 2H, aromatic H), 7.50 (dd, *J* = 8.4, 1.8 Hz, 1H, aromatic H), 7.48 (dd, *J* = 3.3, 1.2 Hz, 1H, aromatic H), 7.47 (d, *J* = 1.9 Hz, 1H, aromatic H), 7.45 (dd, *J* = 2.0, 0.8 Hz, 1H, aromatic H), 7.43 (dd, *J* = 6.7, 1.4 Hz, 1H, aromatic H), 7.30 (dt, *J* = 4.7, 2.4 Hz, 3H, aromatic H), 3.99 (s, 2H, Ar-CH₂)

¹³C NMR (126 MHz, CDCl₃) δ ppm 134.54 (aromatic C), 133.86 (aromatic C), 132.68 (aromatic C), 132.01 (aromatic C), 128.59 (aromatic C), 128.53 (aromatic C), 128.21 (aromatic C), 127.98 (aromatic C), 126.84 (aromatic C), 126.56 (aromatic C), 126.46 (aromatic C), 125.92 (aromatic C), 123.97 (aromatic C), 87.70 (CH₂-C-C-Ar), 83.05 (CH₂-C-C-Ar), 26.46 (Ar-CH₂)

FTIR (CH₂Cl₂) $\bar{\nu}_{\max}$ cm⁻¹ 3053, 2251, 1694, 1489, 1269, 812, 690.

HRMS Calcd for C₁₉H₁₄ (M+H) – 243.1174, found 243.1174.

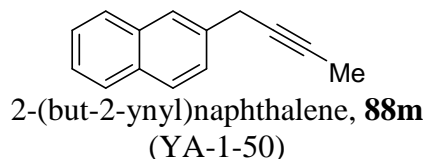


¹H NMR (400 MHz, CDCl₃) δ ppm 7.84 – 7.77 (s, 1H, aromatic H), 7.77 – 7.70 (d, *J* = 9.2 Hz, 2H, aromatic H), 7.53 – 7.45 (s, 3H, aromatic H), 7.36 – 7.29 (t, *J* = 3.4 Hz, 3H, aromatic H), 7.19 – 7.11 (m, 2H, aromatic H), 4.02 – 3.95 (d, *J* = 2.8 Hz, 2H, Ar-CH₂), 3.95 – 3.87 (d, *J* = 3.9 Hz, 3H, O-CH₃).

¹³C NMR (126 MHz, CDCl₃) δ ppm 157.55 (aromatic C), 133.51 (aromatic C), 131.96 (aromatic C), 131.72 (aromatic C), 129.26 (aromatic C), 129.10 (aromatic C), 128.39 (aromatic C), 127.88 (aromatic C), 127.14 (aromatic C), 126.17 (aromatic C), 123.80 (aromatic C), 118.99 (aromatic C), 105.79 (aromatic C), 87.75 (Ar-C-C-CH₂), 82.83 (Ar-C-C-CH₂), 55.44 (Ar-CH₂), 25.91 (O-CH₃).

FTIR (CH₂Cl₂) $\bar{\nu}_{\max}$ cm⁻¹ 2935, 2359, 2332, 1606, 1265, 1229, 756.

HRMS Calcd for C₂₀H₁₇O (M+H) – 273.1279, found 273.1266.

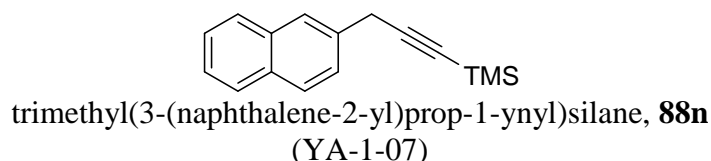


¹H NMR (400 MHz, CDCl₃) δ ppm 7.80 (s, 4H, aromatic H), 7.43 (s, 3H, aromatic H), 3.71 (s, 2H, Ar-CH₂), 1.88 (s, 3H, C-CH₃)

¹³C NMR (126 MHz, CDCl₃) δ ppm 135.17 (aromatic C), 133.74 (aromatic C), 132.48 (aromatic C), 128.27 (aromatic C), 127.78 (aromatic C), 126.74 (aromatic C), 126.24 (aromatic C), 125.66 (aromatic C), 78.37 (CH₂-C-C-CH₃), 76.89 (CH₂-C-C-CH₃), 25.68 (Ar-CH₂), 3.73 (C-CH₃).

FTIR (CH₂Cl₂) $\bar{\nu}_{\max}$ cm⁻¹ 3053, 2243, 1693, 1265, 748

HRMS Calcd for C₁₄H₁₂ (M+Li) – 187.1099, found 187.0987.

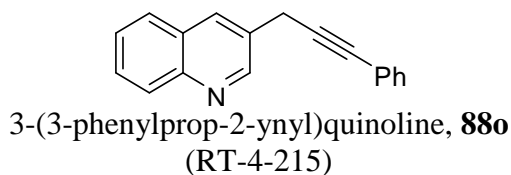


¹H NMR (500 MHz, CDCl₃) δ ppm 7.81 (t, *J* = 8.3 Hz, 4H, aromatic H), 7.50 – 7.42 (m, 3H, aromatic H), 3.81 (s, 2H, aromatic H), 0.22 (s, 9H, CH₃-Si).

¹³C NMR (126 MHz, CDCl₃) δ ppm 134.17 (aromatic C), 133.82 (aromatic C), 132.65 (aromatic C), 128.45 (aromatic C), 127.97 (aromatic C), 126.76 (aromatic C), 126.55 (aromatic C), 126.43 (aromatic C), 125.90 (aromatic C), 104.57 (CH₂-C-C-Si), 87.55 (CH₂-C-C-Si), 26.73 (Ar-CH₂), 0.45 (Si-CH₃).

FTIR (CH₂Cl₂) $\bar{\nu}_{\max}$ cm⁻¹ 2959, 2176, 1601, 1508, 1250, 842.

HRMS Calcd for C₁₆H₁₈Si (M+H) – 239.1256, found 239.1270.

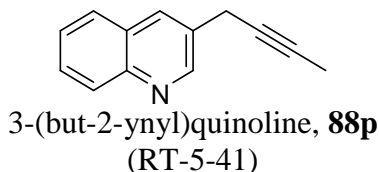


¹H NMR (500 MHz, CDCl₃) δ 8.92 ppm (d, *J* = 2.2 Hz, 1H, aromatic H), 8.19 (s, 1H, aromatic H), 8.09 (d, *J* = 8.4 Hz, 1H, aromatic H), 7.81 (d, *J* = 8.1 Hz, 1H, aromatic H), 7.70 – 7.66 (m, 1H, aromatic H), 7.54 (t, *J* = 7.5 Hz, 1H, aromatic H), 7.46 (dd, *J* = 5.8, 3.8 Hz, 2H, aromatic H), 7.31 (dd, *J* = 4.4, 2.2 Hz, 3H, aromatic H), 4.01 (s, 2H, Ar-CH₂).

¹³C NMR (126 MHz, CDCl₃) δ ppm 150.97 (aromatic C), 147.07 (aromatic C), 134.21 (aromatic C), 131.64 (aromatic C), 129.61 (aromatic C), 129.15 (aromatic C), 129.08 (aromatic C), 128.29 (aromatic C), 128.11 (aromatic C), 127.98 (aromatic C), 127.51 (aromatic C), 126.82 (aromatic C), 122.95 (aromatic C), 85.81 (CH₂-C-C-Ar), 83.65 (CH₂-C-C-Ar), 23.25 (Ar-CH₂).

FTIR (CH₂Cl₂) ν_{\max} cm⁻¹ 3057, 2924, 2177, 1691, 1267, 432

HRMS Calcd for C₁₈H₁₃N (M+H) – 244.1126, found 244.1122.

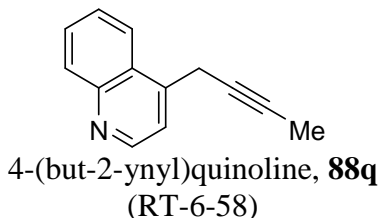


¹H NMR (500 MHz, CDCl₃) δ 8.82 ppm (d, *J* = 2.1 Hz, 1H, aromatic H), 8.09 (s, 1H), 8.06 (d, *J* = 8.4 Hz, 1H), 7.77 (d, *J* = 8.1 Hz, 1H), 7.64 (t, *J* = 7.6 Hz, 1H), 7.50 (t, *J* = 7.5 Hz, 1H), 3.70 (s, 2H), 1.86 (s, 3H).

¹³C NMR (126 MHz, CDCl₃) δ ppm 151.39, 147.23, 134.41, 130.72, 129.40, 129.30, 128.38, 127.83, 127.08, 79.40, 75.65, 23.03, 3.87.

FTIR (CH₂Cl₂) $\bar{\nu}_{\max}$ cm⁻¹ 3057, 2918, 2278, 1641, 1377, 1196, 752.

HRMS Calcd for C₁₃H₁₁N (M+H) – 182.0970, found 182.0958.

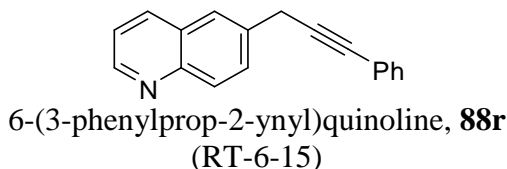


¹H NMR (400 MHz, CDCl₃) δ ppm 8.85 (s, 1H), 8.10 (t, *J* = 7.7 Hz, 1H), 7.98 (d, *J* = 5.9 Hz, 1H), 7.69 (d, *J* = 6.9 Hz, 1H), 7.57 (s, 2H), 3.95 (s, 2H), 1.86 (s, 3H).

¹³C NMR (101 MHz, CDCl₃) δ ppm 150.64, 148.16, 143.31, 130.36, 129.37, 126.77, 123.19, 120.56, 80.29, 74.71, 22.59, 3.62.

FTIR (CH₂Cl₂) $\bar{\nu}_{\max}$ cm⁻¹ 2923, 2176, 1655, 1379, 1020, 762.

HRMS Calcd for C₁₃H₁₁N (M+H) – 182.0970, found 182.0957.

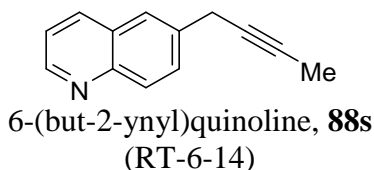


¹H NMR (500 MHz, CDCl₃) δ ppm 8.88 (d, *J* = 4.2 Hz, 1H, aromatic H), 8.13 (d, *J* = 8.2 Hz, 2H, aromatic H), 8.08 (d, *J* = 8.6 Hz, 1H, aromatic H), 7.85 (s, 1H, aromatic H), 7.73 (dd, *J* = 8.6, 1.8 Hz, 1H, aromatic H), 7.47 (dd, *J* = 6.7, 2.9 Hz, 3H, aromatic H), 7.38 (dd, *J* = 8.3, 4.2 Hz, 1H, aromatic H), 7.30 (dd, *J* = 5.0, 2.0 Hz, 1H, aromatic H), 4.00 (s, 2H, Ar-CH₂)

¹³C NMR (126 MHz, CDCl₃) δ 150.36, 147.72, 135.94, 135.34, 131.85, 130.30, 129.88, 128.42, 128.18, 126.25, 123.44, 121.22, 86.87 (CH₂-C-C-Ar), 83.38 (Ar-C-C-CH₂), 25.97 (Ar-CH₂)

FTIR (CH₂Cl₂) $\bar{\nu}_{\max}$ cm⁻¹ 2926, 2199, 1595, 1277, 827, 692.

HRMS Calcd for C₁₈H₁₃N (M+H) – 244.1126, found 244.1125.

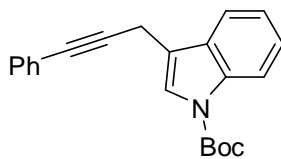


¹H NMR (500 MHz, CDCl₃) δ ppm 8.86 (d, *J* = 4.1 Hz, 1H, aromatic H), 8.12 (d, *J* = 8.1 Hz, 1H, aromatic H), 8.03 (d, *J* = 8.6 Hz, 1H, aromatic H), 7.77 (s, 1H, aromatic H), 7.65 (d, *J* = 8.6 Hz, 1H, aromatic H), 7.37 (dd, *J* = 8.2, 4.2 Hz, 1H, aromatic H), 3.72 (s, 2H, Ar-CH₂), 1.87 (s, 3H, C-CH₃).

¹³C NMR (126 MHz, CDCl₃) δ ppm 150.50, 147.71, 136.47, 130.87, 129.87, 128.68, 126.48, 121.80, 78.97 (CH₂-C-C-CH₃), 76.66 (CH₂-C-C-CH₃), 25.55 (Ar-CH₂), 4.03 (C-CH₃)

FTIR (CH₂Cl₂) $\bar{\nu}_{\max}$ cm⁻¹ 2959, 2228, 1500, 1117, 827, 615.

HRMS Calcd for C₁₃H₁₁N (M+H) – 182.0970, found 182.0939.



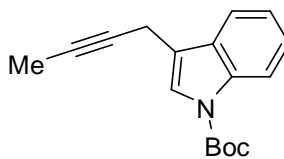
tert-butyl-3-(3-phenylprop-2-ynyl)-1*H*-indole-1-carboxylate, **88t**
(YA-1-30)

¹H NMR (400 MHz, CDCl₃) δ ppm 8.11 (s, 1H, aromatic H), 7.62 (dd, *J* = 10.9, 3.1 Hz, 2H, aromatic H), 7.43 – 7.40 (m, 2H, aromatic H), 7.35 – 7.30 (m, 1H, aromatic H), 7.27 (dd, *J* = 4.0, 2.5 Hz, 4H, aromatic H), 3.83 (s, 2H, Ar-CH₂), 1.65 (s, 9H, CH₃-C=O).

¹³C NMR (126 MHz, CDCl₃) δ ppm 150.22, (C=O peak) 131.60 (aromatic C), 128.19 (aromatic C), 127.82 (aromatic C), 124.48 (aromatic C), 123.53 (aromatic C), 123.37 (aromatic C), 122.48 (aromatic C), 118.89 (aromatic C), 116.22 (aromatic C), 115.30 (aromatic C), 86.30 (Ar-CH₂-C), 83.51 (O=C-C-CH₃), 81.62 (CH₂-C-C-Ar), 27.90 (CH₃-C-C=O), 15.96, (Ar-CH₂).

FTIR (CH₂Cl₂) $\bar{\nu}_{\max}$ cm⁻¹ 2250, 1707, 1491, 1232, 754

HRMS Calcd for C₂₂H₂₁NO₂ (M+H) – 332.1651, found 332.1649.



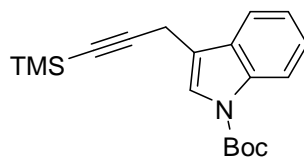
tert-butyl 3-(but-2-ynyl)-1*H*-indole-1-carboxylate, **88u**
(YA-1-40)

¹H NMR (400 MHz, CDCl₃) δ ppm 8.04 (s, 1H, aromatic H), 7.47 (d, *J* = 7.5 Hz, 2H, aromatic H), 7.21 (s, 1H, aromatic H), 7.16 (d, *J* = 6.2 Hz, 1H, aromatic H), 3.47 (s, 2H, Ar-CH₂), 1.76 (s, 3H, C-C-CH₃), 1.58 (s, 9H, O=C-C-CH₃).

¹³C NMR (126 MHz, CDCl₃) δ ppm 149.83 (C=O), 133.85 (aromatic C), 133.64 (aromatic C), 128.56 (aromatic C), 124.49 (aromatic C), 123.24 (aromatic C), 122.46 (aromatic C), 118.89 (aromatic C), 117.14 (aromatic C), 115.33 (aromatic C), 83.38 (O=C-C-CH₃), 75.65 (Ar-C-C-CH₃), 27.98 (Ar-C-C-CH₃), 15.32 (Ar-CH₂), 3.57 (Ar-C-C-CH₃).

FT-IR (CH₂Cl₂) $\bar{\nu}_{\max}$ cm⁻¹ 2978, 2931, 1732, 1256, 1155, 748, 542

HRMS Calcd for C₁₇H₁₉NO₂ (M+H) – 270.1494, found 270.1529.



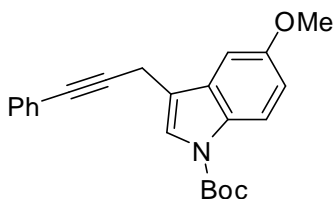
tert-butyl 3-(3-(trimethylsilyl)prop-2-ynyl)-1*H*-indole-1-carboxylate, **88v**
(YA-1-41)

¹H NMR (500 MHz, CDCl₃) δ ppm 8.12 (s, 1H, aromatic H), 7.53 (d, *J* = 7.6 Hz, 2H, aromatic H), 7.31 (t, *J* = 7.7 Hz, 1H, aromatic H), 7.22 (d, *J* = 7.2 Hz, 1H, aromatic H), 3.63 (s, 2H, Ar-CH₂), 1.65 (s, 9H, C-CH₃), 0.17 (s, 9H, Si-CH₃)

¹³C NMR (126 MHz, CDCl₃) δ ppm 149.93 (C=O), 129.83 (aromatic C), 124.71 (aromatic C), 123.67 (aromatic C), 122.64 (aromatic C), 119.04 (aromatic C), 116.22 (aromatic C), 115.51 (aromatic C), 103.53 (C-Si-CH₃), 86.71 (O=C-C-CH₃), 83.66 (CH₂-C-C), 28.47 (O=C-C-CH₃), 16.89 (Ar-CH₂), 0.00 (Si-CH₃)

FTIR (CH₂Cl₂) $\bar{\nu}_{\max}$ cm⁻¹ 2976, 2961, 2179, 1736, 1369, 1157, 844.

HRMS Calcd for C₁₉H₂₅NO₂Si (M+H) – 328.1733, found 328.1736.



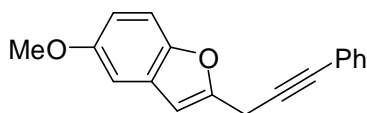
tert-butyl 5-methoxy-3-(3-phenylprop-2-ynyl)-1*H*-indole-1-carboxylate, **88w**
(RT-9-117)

¹H NMR (400 MHz, CDCl₃) δ ppm 8.10 – 7.93 (s, 1H, aromatic H), 7.62 – 7.56 (s, 1H, aromatic H), 7.47 – 7.41 (dd, *J* = 6.5, 3.1 Hz, 2H, aromatic H), 7.30 – 7.28 (d, *J* = 3.5 Hz, 2H, aromatic H), 7.20 – 7.15 (m, 1H, aromatic H), 7.10 – 7.09 (d, *J* = 2.5 Hz, 1H, aromatic H), 6.97 – 6.91 (dd, *J* = 9.0, 2.5 Hz, 1H, aromatic H), 3.92 – 3.84 (s, 3H, O-CH₃), 3.84 – 3.76 (s, 2H, Ar-CH₂), 1.67 – 1.66 (s, 9H, Boc).

¹³C NMR (126 MHz, CDCl₃) δ ppm 185.92 (C=O), 155.91 (aromatic C), 133.93 (aromatic C), 131.56 (aromatic C), 130.02 (aromatic C), 128.38 (aromatic C), 127.79 (aromatic C), 116.30 (aromatic C), 115.70 (aromatic C), 113.08 (aromatic C), 103.98 (C-Si-CH₃), 101.60 (O=C-C-CH₃), 86.32 (alkyne C), 82.15 (alkyne C), 56.14 (Ar-CH₂), 27.92 (O-Me), 16.39 (Boc).

FTIR (CH₂Cl₂) $\bar{\nu}_{\max}$ cm⁻¹ 2978, 2359, 2195, 1730, 1383, 1076, 758.

HRMS Calcd for C₂₃H₂₇N₂O₃ (M+NH₄) – 379.2022, found 379.2036.



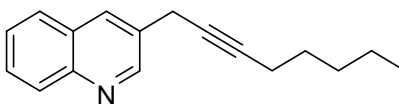
5-methoxy-2-(3-phenylprop-2-ynyl)benzofuran, **88x**
(RT-9-285)

¹H NMR (400 MHz, CDCl₃) δ ppm 7.57 – 7.51 (d, *J* = 7.5 Hz, 1H, aromatic H), 7.51 – 7.43 (m, 3H, aromatic H), 7.37 – 7.29 (s, 3H, aromatic H), 7.29 – 7.26 (s, 1H, aromatic H), 7.25 – 7.20 (m, 1H, aromatic H), 6.74 – 6.68 (s, 1H, aromatic H), 4.02 – 3.94 (s, 2H, Ar-CH₂).

¹³C NMR (126 MHz, CDCl₃) δ ppm 155.10 (aromatic C), 153.56 (aromatic C), 131.82 (aromatic C), 128.38 (aromatic C), 128.12 (aromatic C), 123.71 (aromatic C), 123.13 (aromatic C), 122.85 (aromatic C), 120.58 (aromatic C), 111.06 (aromatic C), 103.38 (aromatic C), 83.92 (Ar-C-C-CH₂), 82.67 (Ar-C-C-CH₂), 20.04 (Ar-CH₂).

FTIR (CH₂Cl₂) $\bar{\nu}_{\max}$ cm⁻¹ 3057, 2932, 2359, 2220, 1599, 1165, 752.

HRMS Calcd for C₁₇H₁₂ONa (M+Na) – 255.0786, found 255.0869.



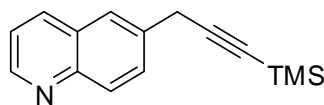
3-(oct-2-ynyl)quinoline, **88y**
(RT-9-293)

¹H NMR (400 MHz, CDCl₃) δ ppm 8.90 – 8.84 (s, 1H, aromatic H), 8.16 – 8.12 (s, 1H, aromatic H), 8.12 – 8.06 (d, *J* = 8.4 Hz, 1H, aromatic H), 7.84 – 7.77 (d, *J* = 8.2 Hz, 1H, aromatic H), 7.73 – 7.65 (t, *J* = 7.7 Hz, 1H, aromatic H), 7.58 – 7.50 (t, *J* = 7.0 Hz, 1H, aromatic H), 3.83 – 3.71 (s, 2H, Ar-CH₂), 2.32 – 2.20 (t, *J* = 7.1 Hz, 2H, C-CH₂), 1.61 – 1.57 (m, 1H, diastereotopic H), 1.56 – 1.52 (m, 1H, diastereotopic H), 1.44 – 1.31 (m, 4H, CH₂-CH₂), 0.95 – 0.88 (t, *J* = 7.1 Hz, 3H, CH₃).

¹³C NMR (126 MHz, CDCl₃) δ ppm 150.97 (aromatic C), 134.53 (aromatic C), 130.72 (aromatic C), 129.25 (aromatic C), 128.90 (aromatic C), 128.20 (aromatic C), 127.67 (aromatic C), 127.00 (aromatic C), 84.25 (Ar-C-C-CH₂), 76.11 (Ar-C-C-CH₂), 31.27 (Ar-CH₂), 28.71 (CH₂), 23.09 (CH₂), 22.33 (CH₂), 18.89 (CH₂), 14.17 (CH₃).

FT-IR (CH₂Cl₂) $\bar{\nu}_{\max}$ cm⁻¹ 2955, 2359, 2216, 1496, 1285, 787.

HRMS Calcd for C₁₇H₂₀N (M+H) – 238.1596, found 238.1586.



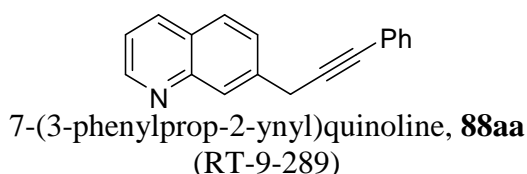
6-(3-(trimethylsilyl)prop-2-ynyl)quinoline, **88z**
(RT-10-11)

¹H NMR (400 MHz, CDCl₃) δ ppm 8.91 – 8.81 (d, *J* = 4.1 Hz, 1H, aromatic H), 8.17 – 8.09 (d, *J* = 8.3 Hz, 1H, aromatic H), 8.09 – 7.96 (d, *J* = 8.8 Hz, 1H, aromatic H), 7.82 – 7.71 (s, 1H), 7.71 – 7.61 (d, *J* = 8.7 Hz, 1H, aromatic H), 7.44 – 7.31 (dd, *J* = 8.2, 4.2 Hz, 1H, aromatic H), 3.91 – 3.72 (s, 2H, Ar-CH₂), 0.26 – 0.18 (s, 9H, TMS).

¹³C NMR (126 MHz, CDCl₃) δ ppm 150.29 (aromatic C), 147.58 (aromatic C), 135.80 (aromatic C), 134.90 (aromatic C), 130.19 (aromatic C), 129.69 (aromatic C), 128.22 (aromatic C), 126.16 (aromatic C), 121.43 (aromatic C), 103.76 (Ar-C-C-CH₂), 87.90 (Ar-C-C-CH₂), 26.29 (Ar-CH₂), -0.02 (TMS).

FTIR (CH₂Cl₂) $\bar{\nu}_{\max}$ cm⁻¹ 2959, 2359, 2176, 1645, 1250, 1022, 847.

HRMS Calcd for C₁₅H₁₈NSi (M+H) – 240.1209, found 240.1198.

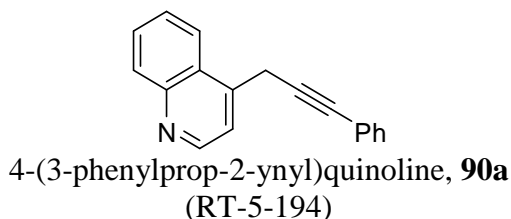


¹H NMR (400 MHz, CDCl₃) δ ppm 8.98 – 8.88 (d, *J* = 3.9 Hz, 1H, aromatic H), 8.23 – 8.12 (m, 2H, aromatic H), 7.85 – 7.78 (d, *J* = 8.3 Hz, 1H, aromatic H), 7.65 – 7.58 (d, *J* = 8.5 Hz, 1H, aromatic H), 7.51 – 7.46 (t, *J* = 3.5 Hz, 2H, aromatic H), 7.43 – 7.37 (dd, *J* = 8.0, 4.2 Hz, 1H, aromatic H), 7.34 – 7.29 (t, *J* = 2.9 Hz, 3H, aromatic H), 4.09 – 4.05 (s, 2H, Ar-CH₂).

¹³C NMR (126 MHz, CDCl₃) δ 150.69 (aromatic C), 136.10 (aromatic C), 131.86 (aromatic C), 128.39 (aromatic C), 128.11 (aromatic C), 127.90 (aromatic C), 127.42 (aromatic C), 127.21 (aromatic C), 123.58 (aromatic C), 121.00 (aromatic C), 86.91 (Ar-C-C-CH₂), 83.63 (Ar-C-C-CH₂), 26.26 (Ar-CH₂).

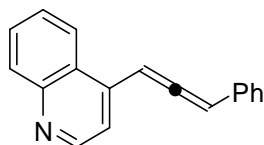
FTIR (CH₂Cl₂) $\bar{\nu}_{\max}$ cm⁻¹ 2926, 2359, 2201, 1630, 1448, 1281, 773, 690.

HRMS Calcd for C₁₈H₁₄N (M+H) – 244.1126, found 244.1115.



¹H NMR (500 MHz, CDCl₃) δ 8.89 (d, *J* = 4.3 Hz, 1H, aromatic H), 8.14 (d, *J* = 8.6 Hz, 1H, aromatic H), 8.05 (d, *J* = 8.5 Hz, 1H, aromatic H), 7.75 – 7.71 (m, 1H, aromatic H), 7.66 (d, *J* = 3.8 Hz, 1H, aromatic H), 7.46 – 7.44 (m, 2H, aromatic H), 7.38 (d, *J* = 7.9 Hz, 1H, aromatic H), 7.34 (d, *J* = 9.4 Hz, 1H, aromatic H), 7.31 (d, *J* = 3.1 Hz, 2H, aromatic H), 4.25 (s, 2H, Ar-CH₂).

HRMS Calcd for C₁₈H₁₄N (M+H) – 244.1126, found 244.1108.

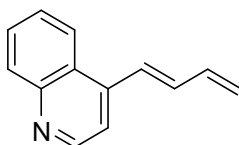


4-(3-phenylpropa-1,2-dienyl)quinoline, **90b**
(RT-11-142)

¹H NMR (400 MHz, CDCl₃) δ ppm 8.81 (d, *J* = 4.5 Hz, 1H, aromatic H), 8.24 (d, *J* = 8.5 Hz, 1H, aromatic H), 8.12 (d, *J* = 8.5 Hz, 1H, aromatic H), 7.72 (t, *J* = 7.6 Hz, 1H, aromatic H), 7.56 (t, *J* = 7.1 Hz, 1H, aromatic H), 7.45 (d, *J* = 4.5 Hz, 1H, aromatic H), 7.40 – 7.29 (m, 5H, aromatic H), 7.26 (d, *J* = 7.0 Hz, 1H, diastereotopic H), 7.23 (s, 1H, aromatic H), 6.72 (d, *J* = 6.6 Hz, 1H, diastereotopic H).

¹³C NMR (126 MHz, CDCl₃) δ ppm 210.65 (Ar-C-C-C-Ar), 150.11 (aromatic C), 148.86 (aromatic C), 139.12 (aromatic C), 132.54 (aromatic C), 130.29 (aromatic C), 129.43 (aromatic C), 128.94 (aromatic C), 127.92 (aromatic C), 127.31 (aromatic C), 126.65 (aromatic C), 126.09 (aromatic C), 123.33 (aromatic C), 119.26 (aromatic C), 98.50 (Ar-C-C-C-Ar), 93.57 (Ar-C-C-C-Ar).

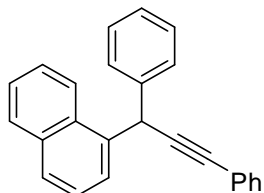
HRMS Calcd for C₁₈H₁₃N (M+H) – 244.1126, found 244.1146.



(E)-4-(buta-1,3-dienyl)quinoline, **91**
(RT-5-195)

¹H NMR (400 MHz, CDCl₃) δ ppm 8.84 (d, *J* = 4.5 Hz, 1H, aromatic H), 8.10 (t, *J* = 8.6 Hz, 2H, aromatic H), 7.70 (t, *J* = 5.6 Hz, 1H, aromatic H), 7.55 (t, *J* = 7.0 Hz, 1H, aromatic H), 7.50 (d, *J* = 4.5 Hz, 1H, aromatic H), 7.27 (d, *J* = 15.4 Hz, 1H, aromatic H), 7.00 (dd, *J* = 15.0, 10.7 Hz, 1H, Ar-CH=CH), 6.72 – 6.53 (m, 1H, Ar-CH=CH=CH₂), 5.50 (d, *J* = 16.8 Hz, 1H, diastereotopic H), 5.36 (d, *J* = 9.9 Hz, 1H, diastereotopic H).

¹³C NMR (126 MHz, d-Tol) δ ppm 150.64 (aromatic C), 142.22 (aromatic C), 137.64 (CH=CH=CH=CH₂), 135.66 (CH=CH=CH=CH₂), 131.45 (Ar-CH), 129.56 (aromatic C), 128.63 (aromatic C), 127.76 (aromatic C), 126.73 (aromatic C), 123.81 (aromatic C), 120.87 (aromatic C), 120.25 (aromatic C), 117.40 (CH=CH=CH=CH₂).



1-(1,3-diphenylprop-2-ynyl)naphthalene, **92** and **95a**
(RT-7-248, RT-9-150)

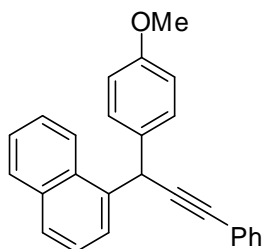
¹H NMR (500 MHz, CDCl₃) δ ppm 8.13 (dd, *J* = 6.2, 2.8 Hz, 1H), 7.88 – 7.82 (m, 1H), 7.79 (d, *J* = 8.2 Hz, 1H), 7.67 (dd, *J* = 6.9, 2.4 Hz, 1H), 7.48 – 7.39 (m, 7H), 7.33 – 7.24 (m, 6H), 7.22 – 7.18 (m, 1H), 5.91 (s, 1H).

¹³C NMR (126 MHz, CDCl₃) δ ppm 141.00, 136.83, 134.17, 131.68, 128.82, 128.58, 128.20, 128.10, 128.02, 127.96, 126.87, 126.70, 126.13, 125.61, 125.51, 124.19, 123.50, 90.15, 85.22, 40.68.

FTIR (CH₂Cl₂) $\bar{\nu}_{\max}$ cm⁻¹ 3057, 2116, 1948, 1597, 1491, 797, 756.

HRMS Calcd for C₂₅H₁₈ (M+H) – 319.1487, found 319.1495.

HPLC (Daicel Chiralpak OD-H HPLC column: 95% hexane/isopropanol, 0.5 mL/min) *t*_r = 10.330 (major), 12.242 (minor) minutes



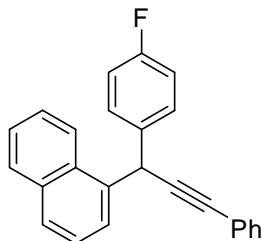
1-(1-(4-methoxyphenyl)-3-phenylprop-2-ynyl)naphthalene, **92a**
(RT-10-124)

¹H NMR (500 MHz, CDCl₃) δ ppm 8.20 – 8.10 (t, *J* = 4.6 Hz, 1H), 7.92 – 7.84 (m, 1H), 7.83 – 7.77 (d, *J* = 8.4 Hz, 1H), 7.73 – 7.65 (d, *J* = 6.7 Hz, 1H), 7.51 – 7.42 (m, 4H), 7.40 – 7.34 (d, *J* = 8.7 Hz, 2H), 7.31 – 7.27 (t, *J* = 3.0 Hz, 3H), 7.27 – 7.26 (s, 1H), 6.93 – 6.79 (d, *J* = 8.6 Hz, 2H), 5.98 – 5.83 (s, 1H), 3.87 – 3.73 (s, 3H).

¹³C NMR (126 MHz, CDCl₃) δ ppm 158.56, 137.25, 134.28, 133.29, 131.80, 131.13, 129.15, 128.94, 128.32, 128.16, 128.05, 126.67, 126.22, 125.72, 125.64, 124.33, 123.71, 114.07, 90.72, 85.17, 55.40, 40.12.

FTIR (CH₂Cl₂) $\bar{\nu}_{\max}$ cm⁻¹ 2930, 2359, 2199, 1597, 1173, 781.

HRMS Calcd for C₂₆H₂₀ONa (M+H) – 371.1412, found 371.1426.



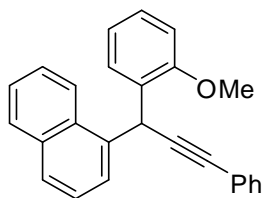
1-(1-(4-fluorophenyl)-3-phenylprop-2-ynyl)naphthalene, **92b**
(RT-9-187)

¹H NMR (400 MHz, CDCl₃) δ ppm 8.14 – 8.06 (t, *J* = 4.6 Hz, 1H), 7.93 – 7.86 (t, *J* = 4.6 Hz, 1H), 7.86 – 7.79 (d, *J* = 8.0 Hz, 1H), 7.71 – 7.65 (d, *J* = 7.1 Hz, 1H), 7.52 – 7.38 (m, 8H), 7.31 – 7.29 (d, *J* = 3.0 Hz, 2H), 7.04 – 6.95 (t, *J* = 8.7 Hz, 2H), 5.95 – 5.80 (s, 1H).

¹³C NMR (126 MHz, CDCl₃) δ ppm 162.89, 160.85, 136.81, 136.63, 134.25, 132.60, 131.76, 131.05, 129.66, 128.95, 128.40, 128.21, 126.85, 126.37, 125.83, 125.61, 124.08, 123.35, 115.54, 115.34, 90.19, 85.27, 40.15.

FTIR (CH₂Cl₂) $\bar{\nu}_{\max}$ cm⁻¹ 3057, 2359, 2216, 1598, 1157, 756, 690.

HRMS Calcd for C₂₅H₁₈F (M-H) – 335.1236, found 335.1242.



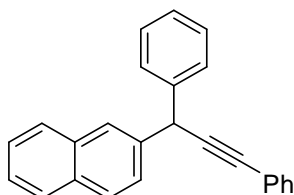
1-(1-(2-methoxyphenyl)-3-phenylprop-2-ynyl)naphthalene, **92c**
(RT-10-250)

¹H NMR (500 MHz, CDCl₃) δ ppm 8.22 – 8.12 (d, *J* = 8.2 Hz, 1H), 7.90 – 7.82 (d, *J* = 7.6 Hz, 1H), 7.81 – 7.75 (d, *J* = 8.2 Hz, 1H), 7.74 – 7.69 (d, *J* = 7.0 Hz, 1H), 7.53 – 7.39 (m, 6H), 7.31 – 7.20 (m, 4H), 6.97 – 6.87 (m, 4H), 6.41 – 6.33 (s, 1H), 3.97 – 3.78 (s, 3H).

¹³C NMR (126 MHz, CDCl₃) δ ppm 156.23, 156.03, 137.36, 134.01, 131.84, 131.36, 129.76, 129.60, 128.78, 128.35, 128.25, 127.88, 126.15, 125.86, 125.55, 124.07, 123.91, 120.97, 110.94, 90.85, 83.92, 55.96, 33.22.

FTIR (CH₂Cl₂) $\bar{\nu}_{\max}$ cm⁻¹ 3057, 2933, 2334, 2216, 1597, 1103, 757.

HRMS Calcd for C₂₆H₂₀O (M+Na) – 371.1412, found 371.1396



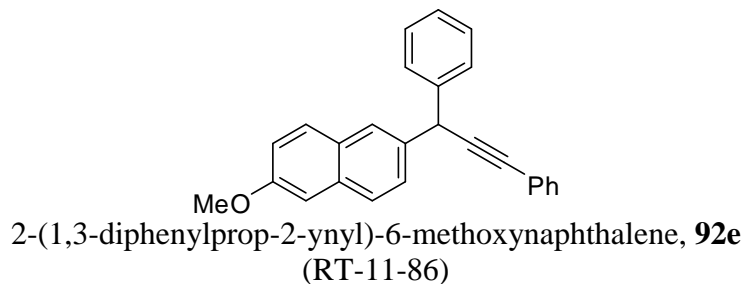
2-(1,3-diphenylprop-2-ynyl)naphthalene, **92d**
(RT-7-241)

¹H NMR (500 MHz, CDCl₃) δ ppm 7.92 (d, *J* = 4.4 Hz, 1H), 7.85 – 7.76 (m, 3H), 7.53 – 7.46 (m, 5H), 7.46 – 7.42 (m, 2H), 7.36 – 7.28 (m, 9H), 7.25 (s, 1H), 5.37 (d, *J* = 5.9 Hz, 1H).

¹³C NMR (126 MHz, CDCl₃) δ ppm 141.52, 139.13, 133.83, 133.68, 133.50, 132.47, 131.77, 128.76, 128.56, 128.50, 128.30, 128.09, 127.92, 127.71, 127.05, 126.34, 126.18, 125.87, 123.53, 90.18, 85.26, 43.77.

FTIR (CH₂Cl₂) $\bar{\nu}_{\max}$ cm⁻¹ 3026, 2334, 1950, 1599, 1491, 1271, 1028, 756, 694.

HRMS Calcd HRMS for C₂₅H₁₈ (M+H) – 319.1487, found 319.1481.

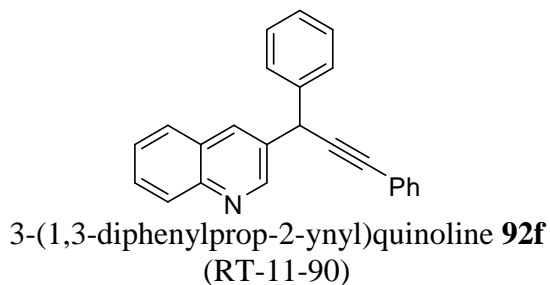


¹H NMR (400 MHz, CDCl₃) δ ppm 7.87 – 7.82 (s, 1H), 7.75 – 7.66 (dd, *J* = 16.0, 8.7 Hz, 2H), 7.52 – 7.44 (qd, *J* = 8.8, 8.4, 3.1 Hz, 5H), 7.36 – 7.29 (m, 5H), 7.26 – 7.23 (d, *J* = 4.0 Hz, 1H), 7.16 – 7.09 (m, 2H), 5.40 – 5.27 (s, 1H), 3.94 – 3.85 (s, 3H).

¹³C NMR (126 MHz, CDCl₃) δ ppm 157.78, 141.84, 136.98, 133.61, 131.85, 129.52, 128.94, 128.81, 128.75, 128.38, 128.14, 127.43, 127.04, 126.96, 126.25, 123.65, 119.06, 105.79, 90.29, 85.30, 55.33, 43.68.

FTIR (CH₂Cl₂) $\bar{\nu}_{\max}$ cm⁻¹ 3057, 2220, 1607, 1235, 1030, 756.

HRMS Calcd for C₂₆H₁₉O (M-H) – 347.1436, found 347.1470.

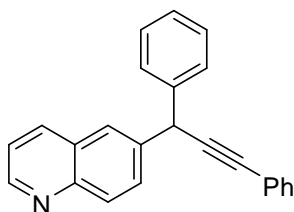


¹H NMR (500 MHz, CDCl₃) δ ppm 9.02 – 8.94 (s, 1H), 8.22 – 8.16 (s, 1H), 8.12 – 8.06 (d, *J* = 8.3 Hz, 1H), 7.84 – 7.78 (d, *J* = 8.0 Hz, 1H), 7.72 – 7.66 (t, *J* = 7.7 Hz, 1H), 7.59 – 7.53 (d, *J* = 7.0 Hz, 1H), 7.54 – 7.47 (t, *J* = 6.4 Hz, 4H), 7.39 – 7.31 (m, 4H), 7.31 – 7.26 (m, 3H), 5.47 – 5.41 (s, 2H).

¹³C NMR (126 MHz, CDCl₃) δ ppm 151.15, 147.22, 140.54, 134.74, 134.12, 131.81, 129.48, 129.32, 129.07, 128.47, 128.13, 127.95, 127.54, 127.05, 123.15, 88.79, 86.00, 41.71.

FTIR (CH₂Cl₂) $\bar{\nu}_{\max}$ cm⁻¹ 2341, 1656, 1598, 1377, 756, 692.

HRMS Calcd for C₂₄H₁₈N (M+H) – 320.1439, found 320.1431.



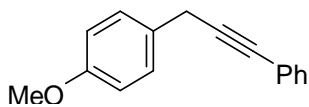
6-(1,3-diphenylprop-2-ynyl)quinoline, **92g**
(RT-11-91)

$^1\text{H NMR}$ (500 MHz, CDCl_3) δ ppm 8.92 – 8.85 (dd, $J = 4.2, 1.6$ Hz, 1H), 8.18 – 8.11 (d, $J = 8.1$ Hz, 1H), 8.09 – 8.02 (d, $J = 8.8$ Hz, 1H), 7.93 – 7.87 (d, $J = 1.7$ Hz, 1H), 7.78 – 7.72 (dd, $J = 8.8, 2.0$ Hz, 1H), 7.55 – 7.45 (m, 4H), 7.42 – 7.38 (dd, $J = 8.3, 4.2$ Hz, 1H), 7.37 – 7.31 (m, 5H), 7.29 – 7.26 (m, 1H), 5.48 – 5.34 (s, 1H).

$^{13}\text{C NMR}$ (126 MHz, CDCl_3) δ ppm 150.46, 147.63, 141.22, 140.14, 136.22, 131.86, 130.13, 130.04, 128.92, 128.43, 128.33, 128.16, 127.33, 126.17, 123.37, 121.48, 89.67, 85.71, 43.85.

FT-IR (CH_2Cl_2) $\bar{\nu}_{\text{max}}$ cm^{-1} 3028, 1596, 1491, 1265, 1028, 842, 756.

HRMS Calcd for $\text{C}_{24}\text{H}_{18}\text{N}$ (M+H) – 320.1439, found 320.1449.



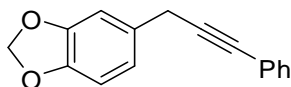
1-methoxy-4-(3-phenylprop-2-ynyl)benzene, **93a**
(RT-11-160)

$^1\text{H NMR}$ (400 MHz, CDCl_3) δ ppm 7.47 – 7.40 (dd, $J = 6.6, 3.0$ Hz, 2H), 7.35 – 7.31 (m, 2H), 7.31 – 7.28 (dd, $J = 4.8, 2.1$ Hz, 3H), 6.92 – 6.84 (d, $J = 8.6$ Hz, 2H), 3.83 – 3.80 (s, 3H), 3.79 – 3.76 (s, 2H).

$^{13}\text{C NMR}$ (126 MHz, CDCl_3) δ ppm 158.50, 131.76, 129.07, 128.92, 128.36, 123.71, 114.03, 88.16, 82.45, 55.58, 24.66.

FTIR (CH_2Cl_2) $\bar{\nu}_{\text{max}}$ cm^{-1} 2928, 2835, 2359, 2191, 1670, 1510, 1037, 756.

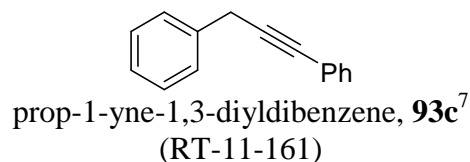
HRMS Calcd for $\text{C}_{16}\text{H}_{15}\text{O}$ (M+H) – 223.1123; found 223.1097.



5-(3-phenylprop-2-ynyl)benzo[d][1,3]dioxole, **93b**⁶
(RT-11-65)

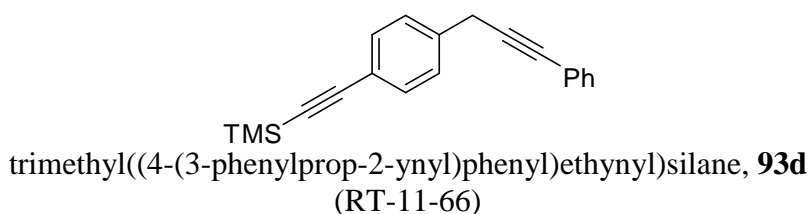
$^1\text{H NMR}$ (500 MHz, CDCl_3) δ 7.48 – 7.42 (dd, $J = 6.5, 3.2$ Hz, 2H), 7.33 – 7.27 (m, 3H), 6.97 – 6.90 (d, $J = 1.5$ Hz, 1H), 6.89 – 6.83 (dd, $J = 8.0, 1.6$ Hz, 1H), 6.80 – 6.75 (m, 1H), 5.99 – 5.92 (s, 2H), 3.80 – 3.69 (s, 2H).

^{13}C NMR (126 MHz, CDCl_3) δ 147.92, 146.42, 131.69, 130.58, 128.81, 128.30, 127.98, 127.05, 123.65, 120.90, 108.70, 108.35, 101.12, 87.69, 82.69, 25.30.



^1H NMR (400 MHz, CDCl_3) δ ppm 7.52 – 7.40 (m, 4H), 7.38 – 7.32 (t, $J = 7.6$ Hz, 2H), 7.32 – 7.28 (m, 3H), 7.28 – 7.27 (s, 1H), 3.93 – 3.75 (s, 2H).

^{13}C NMR (126 MHz, CDCl_3) δ ppm 136.89, 131.78, 128.69, 128.37, 128.10, 127.96, 126.77, 123.79, 87.65, 82.78, 25.89.

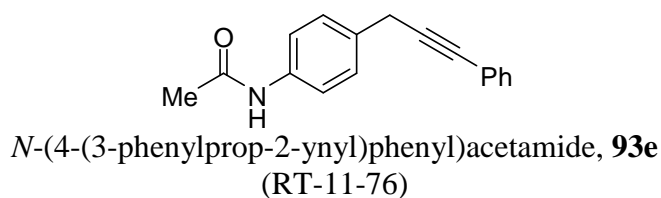


^1H NMR (500 MHz, CDCl_3) δ ppm 7.49 – 7.40 (dt, $J = 5.0, 3.2$ Hz, 4H), 7.37 – 7.33 (d, $J = 7.9$ Hz, 2H), 7.33 – 7.28 (dd, $J = 4.9, 1.9$ Hz, 3H), 3.89 – 3.75 (s, 2H), 0.32 – 0.18 (s, 9H).

^{13}C NMR (126 MHz, CDCl_3) δ ppm 137.38, 132.26, 131.78, 128.41, 128.08, 127.97, 123.51, 121.58, 105.11, 94.08, 86.88, 83.14, 25.85, 0.15.

FTIR (CH_2Cl_2) $\bar{\nu}_{\text{max}}$ cm^{-1} 2959, 2349, 2156, 1599, 1489, 1250, 864, 690.

HRMS Calcd for $\text{C}_{20}\text{H}_{24}\text{NSi}$ ($\text{M}+\text{NH}_4$) – 306.1678, found 306.1640.

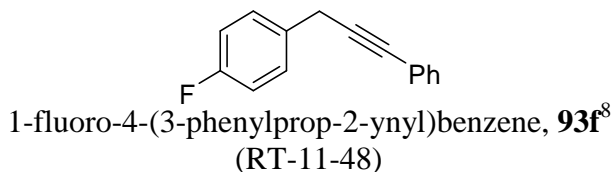


^1H NMR (500 MHz, CDCl_3) δ ppm 7.49 – 7.41 (td, $J = 10.1, 9.2, 3.7$ Hz, 4H), 7.38 – 7.33 (d, $J = 8.0$ Hz, 2H), 7.32 – 7.27 (m, 3H), 7.23 – 7.17 (m, 1H), 3.83 – 3.73 (s, 2H), 2.19 – 2.14 (m, 3H).

^{13}C NMR (126 MHz, CDCl_3) δ ppm 168.36, 136.53, 132.86, 131.69, 130.24, 129.54, 128.64, 128.38, 127.99, 123.72, 120.23, 87.58, 82.81, 25.34, 24.75.

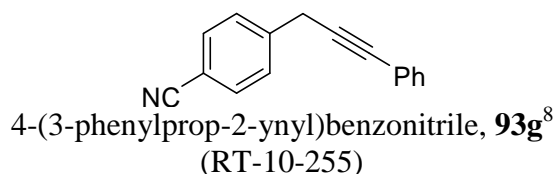
FTIR (CH_2Cl_2) $\bar{\nu}_{\text{max}}$ cm^{-1} 3303, 3059, 2349, 2197, 1666, 1537, 1319, 1020, 756, 692.

HRMS Calcd for C₁₇H₁₆NO (M+H) – 250.1232; found 250.1237.



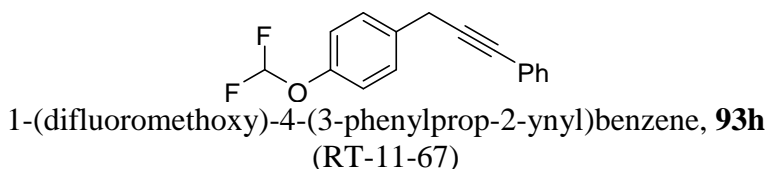
¹H NMR (400 MHz, CDCl₃) δ ppm 7.47 – 7.42 (dd, *J* = 6.6, 3.0 Hz, 2H), 7.41 – 7.35 (dd, *J* = 8.3, 5.4 Hz, 2H), 7.33 – 7.28 (t, *J* = 3.3 Hz, 3H), 7.06 – 7.00 (t, *J* = 8.7 Hz, 3H), 3.90 – 3.72 (s, 2H).

¹³C NMR (101 MHz, CDCl₃) δ ppm 162.95, 160.59, 133.12, 132.42, 131.72, 130.86, 129.49, 128.41, 127.97, 123.49, 115.43, 87.37, 82.66, 25.15.



¹H NMR (500 MHz, CDCl₃) δ ppm 7.67 – 7.57 (d, *J* = 8.1 Hz, 2H), 7.57 – 7.48 (d, *J* = 7.9 Hz, 2H), 7.48 – 7.38 (dd, *J* = 6.5, 3.1 Hz, 3H), 7.36 – 7.28 (dd, *J* = 4.4, 2.1 Hz, 2H), 3.93 – 3.81 (s, 2H).

¹³C NMR (126 MHz, CDCl₃) δ ppm 142.45, 132.52, 131.78, 128.91, 128.48, 128.37, 123.18, 119.01, 110.81, 85.27, 83.91, 25.98.

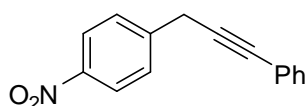


¹H NMR (500 MHz, CDCl₃) δ ppm 7.47 – 7.37 (m, 4H), 7.34 – 7.27 (m, 3H), 7.13 – 7.05 (d, *J* = 8.5 Hz, 2H), 6.68 – 6.31 (t, *J* = 74.1 Hz, 1H), 3.87 – 3.73 (s, 2H).

¹³C NMR (126 MHz, CDCl₃) δ ppm 149.96, 133.94, 131.71, 129.45, 128.42, 128.11, 119.94, 117.93, 116.12, 114.06, 86.92, 83.05, 25.11.

FTIR (CH₂Cl₂) $\bar{\nu}_{\max}$ cm⁻¹ 2959, 2199, 1703, 1603, 1508, 1223, 1018, 758, 692.

HRMS Calcd. for C₁₆H₁₆F₂NO (M+NH₄) – 276.1200; found 276.1171.



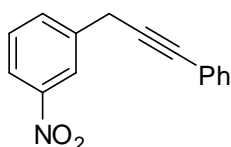
1-nitro-4-(3-phenylprop-2-ynyl)benzene, **93i**
(RT-11-47)

¹H NMR (400 MHz, CDCl₃) δ ppm 8.30 – 8.15 (d, *J* = 8.7 Hz, 2H), 7.64 – 7.56 (dd, *J* = 8.9, 2.1 Hz, 2H), 7.50 – 7.43 (dd, *J* = 6.6, 3.0 Hz, 2H), 7.38 – 7.30 (dd, *J* = 8.7, 4.2 Hz, 3H), 4.02 – 3.90 (s, 2H).

¹³C NMR (126 MHz, CDCl₃) δ ppm 147.12, 144.17, 131.79, 129.08, 128.96, 128.50, 128.42, 123.96, 123.12, 85.56, 83.92, 25.99.

FTIR (CH₂Cl₂) $\bar{\nu}_{\max}$ cm⁻¹ 2853, 2349, 1597, 1518, 1344, 1109, 858, 756.

HRMS Calcd for C₁₅H₁₀NO₂ (M-H) – 236.0712; found 236.0708.



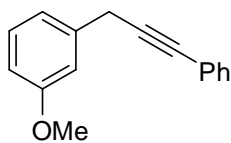
1-nitro-3-(3-phenylprop-2-ynyl)benzene, **93j**
(RT-11-35)

¹H NMR (400 MHz, CDCl₃) δ ppm 8.34 – 8.27 (s, 1H), 8.16 – 8.10 (dd, *J* = 7.9, 1.9 Hz, 1H), 7.81 – 7.73 (m, 1H), 7.56 – 7.49 (t, *J* = 7.9 Hz, 1H), 7.49 – 7.44 (td, *J* = 4.2, 2.2 Hz, 2H), 7.35 – 7.29 (t, *J* = 3.2 Hz, 3H), 3.96 – 3.92 (s, 2H).

¹³C NMR (126 MHz, CDCl₃) δ ppm 139.03, 134.30, 131.83, 129.60, 128.49, 128.40, 123.16, 122.07, 85.66, 84.02, 25.70.

FTIR (CH₂Cl₂) $\bar{\nu}_{\max}$ cm⁻¹ 3080, 2920, 2210, 1594, 1354, 1101, 757.

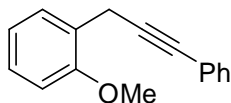
HRMS Calcd for C₁₅H₁₅N₂O₂ (M+NH₄) – 255.1134; found 255.1178.



1-methoxy-3-(3-phenylprop-2-ynyl)benzene, **93k⁵**
(RT-11-33)

¹H NMR (500 MHz, CDCl₃) δ ppm 7.50 – 7.40 (m, 2H), 7.32 – 7.28 (m, 3H), 7.28 – 7.24 (m, 2H), 7.03 – 6.94 (m, 2H), 6.83 – 6.77 (m, 1H), 3.83 – 3.82 (s, 3H), 3.82 – 3.81 (s, 2H).

¹³C NMR (126 MHz, CDCl₃) δ ppm 159.93, 138.46, 131.77, 129.65, 128.40, 128.37, 127.97, 123.77, 120.47, 113.84, 112.19, 87.49, 82.84, 55.37, 25.90.



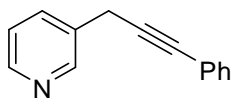
1-methoxy-2-(3-phenylprop-2-ynyl)benzene, **93l**
(RT-11-34)

$^1\text{H NMR}$ (500 MHz, CDCl_3) δ ppm 7.62 – 7.57 (dd, $J = 7.5, 1.5$ Hz, 1H), 7.50 – 7.44 (m, 2H), 7.33 – 7.28 (m, 3H), 7.27 – 7.23 (m, 1H), 7.03 – 6.94 (td, $J = 7.5, 1.0$ Hz, 1H), 6.91 – 6.81 (d, $J = 8.1$ Hz, 1H), 3.91 – 3.83 (s, 3H), 3.83 – 3.74 (s, 2H).

$^{13}\text{C NMR}$ (126 MHz, CDCl_3) δ ppm 156.89, 131.80, 129.04, 128.34, 127.94, 127.83, 125.24, 124.02, 120.66, 110.07, 87.70, 82.84, 55.50, 20.22.

FTIR (CH_2Cl_2) $\bar{\nu}_{\text{max}}$ cm^{-1} 3060, 2940, 2370, 2230, 1604, 1484, 1243, 1103, 755.

HRMS Calcd for $\text{C}_{16}\text{H}_{13}\text{O}$ (M-H) – 221.0966; found 221.0962.

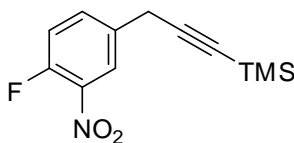


3-(3-phenylprop-2-ynyl)pyridine, **93m**
(RT-11-226)

$^1\text{H NMR}$ (400 MHz, CDCl_3) δ ppm 8.70 – 8.62 (m, 2H), 8.56 – 8.47 (d, $J = 4.2$ Hz, 1H), 7.81 – 7.73 (d, $J = 7.9$ Hz, 1H), 7.51 – 7.39 (m, 1H), 7.36 – 7.29 (dt, $J = 4.9, 2.5$ Hz, 5H), 3.94 – 3.74 (s, 2H).

$^{13}\text{C NMR}$ (126 MHz, CDCl_3) δ ppm 149.46, 148.33, 135.65, 132.55, 131.78, 128.45, 128.25, 123.60, 123.33, 86.23, 83.25, 23.00.

HRMS Calcd for $\text{C}_{14}\text{H}_{12}\text{N}$ (M+H) – 194.0970; found 194.0971.



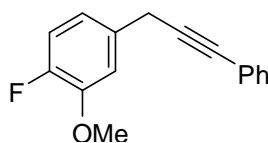
(3-(4-fluoro-3-nitrophenyl)prop-1-ynyl)trimethylsilane, **93n**
(RT-11-80)

$^1\text{H NMR}$ (400 MHz, CDCl_3) δ ppm 8.10 – 8.05 (d, $J = 7.6$ Hz, 1H), 7.65 – 7.57 (m, 1H), 7.28 – 7.27 (s, 1H), 3.77 – 3.62 (s, 2H), 0.22 – 0.19 (s, 9H).

$^{13}\text{C NMR}$ (126 MHz, CDCl_3) δ ppm 155.58, 153.48, 135.00, 125.49, 118.66, 102.01, 89.18, 29.85, 25.43, 0.09.

FTIR (CH_2Cl_2) $\bar{\nu}_{\text{max}}$ cm^{-1} 2959, 2392, 2179, 1622, 1539, 1350, 844, 760.

HRMS Calcd for $\text{C}_{12}\text{H}_{18}\text{FN}_2\text{O}_2\text{Si}$ (M+ NH_4) – 269.1122, found 269.1132.



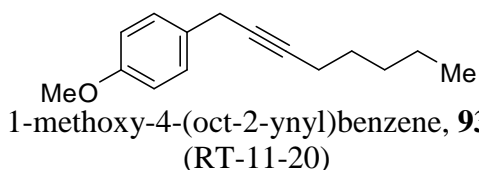
1-fluoro-2-methoxy-4-(3-phenylprop-2-ynyl)benzene, **93o**
(RT-11-79)

$^1\text{H NMR}$ (400 MHz, CDCl_3) δ ppm 7.50 – 7.41 (t, $J = 3.5$ Hz, 2H), 7.34 – 7.28 (d, $J = 3.8$ Hz, 3H), 7.21 – 7.06 (dd, $J = 25.1, 11.3$ Hz, 2H), 6.98 – 6.87 (t, $J = 8.6$ Hz, 1H), 3.94 – 3.85 (s, 3H), 3.80 – 3.74 (s, 2H).

$^{13}\text{C NMR}$ (126 MHz, CDCl_3) δ ppm 131.79, 128.40, 128.08, 123.58, 115.92, 113.78, 87.09, 83.08, 56.69, 25.01.

FTIR (CH_2Cl_2) $\bar{\nu}_{\text{max}}$ cm^{-1} 2932, 2349, 2039, 1518, 1277, 1122, 1027.

HRMS Calcd for $\text{C}_{16}\text{H}_{14}\text{FO}$ (M+H) – 241.1029; found 241.1023.



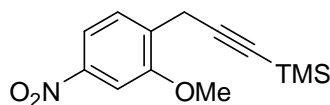
1-methoxy-4-(oct-2-ynyl)benzene, **93p**
(RT-11-20)

$^1\text{H NMR}$ (400 MHz, CDCl_3) δ ppm 7.28 – 7.24 (m, 2H), 6.90 – 6.82 (d, $J = 8.5$ Hz, 1H), 3.85 – 3.76 (s, 2H), 3.57 – 3.47 (s, 1H), 2.27 – 2.15 (t, $J = 7.1$ Hz, 1H), 1.39 – 1.29 (m, 2H), 1.23 – 1.16 (d, $J = 6.8$ Hz, 1H), 0.93 – 0.87 (t, $J = 6.7$ Hz, 2H).

$^{13}\text{C NMR}$ (126 MHz, CDCl_3) δ ppm 158.31, 129.79, 128.91, 113.94, 82.43, 78.06, 55.44, 31.18, 28.80, 24.41, 22.31, 18.86, 14.08.

FTIR (CH_2Cl_2) $\bar{\nu}_{\text{max}}$ cm^{-1} 2965, 2935, 2865, 2195, 1602, 1514, 1461, 1248, 1176, 1026, 825.

HRMS Calcd for $\text{C}_{15}\text{H}_{19}\text{O}$ (M-H) – 215.1436; found 215.1445.



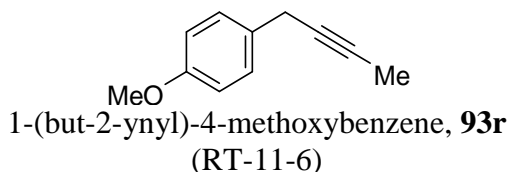
(3-(2-methoxy-4-nitrophenyl)prop-1-ynyl)trimethylsilane, **93q**
(RT-11-130)

$^1\text{H NMR}$ (500 MHz, CDCl_3) δ ppm 7.89 – 7.85 (dd, $J = 8.3, 2.1$ Hz, 1H), 7.71 – 7.68 (d, $J = 8.4$ Hz, 1H), 7.68 – 7.67 (d, $J = 2.1$ Hz, 1H), 3.99 – 3.85 (s, 3H), 3.72 – 3.58 (s, 2H), 0.26 – 0.15 (s, 9H).

¹³C NMR (126 MHz, CDCl₃) δ ppm 156.74, 147.79, 132.63, 128.92, 115.74, 104.57, 102.10, 88.55, 55.76, 20.51, 0.07.

FTIR (CH₂Cl₂) $\bar{\nu}_{\max}$ cm⁻¹ 2959, 2179, 1526, 1493, 1416, 1288, 1094, 1034, 845, 760.

HRMS Calcd for C₁₃H₂₁N₂O₃Si (M+NH₄) – 281.1321; found 281.1329.

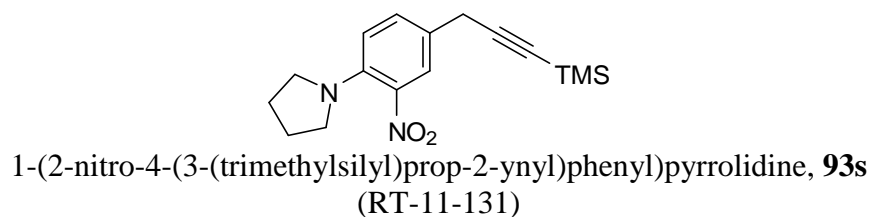


¹H NMR (400 MHz, CDCl₃) δ ppm 7.26 – 7.21 (d, *J* = 4.8 Hz, 2H), 6.89 – 6.81 (d, *J* = 8.7 Hz, 2H), 3.85 – 3.73 (s, 3H), 3.53 – 3.41 (d, *J* = 2.5 Hz, 2H), 1.92 – 1.77 (s, 3H).

¹³C NMR (126 MHz, CDCl₃) δ ppm 158.35, 129.75, 128.96, 114.03, 113.99, 77.67, 77.35, 55.45, 24.39, 3.76.

FTIR (CH₂Cl₂) $\bar{\nu}_{\max}$ cm⁻¹ 2922, 2215, 1599, 1514, 1253, 1026, 833.

HRMS Calcd for C₁₁H₁₁O (M-H) – 159.0810; found 159.0823.

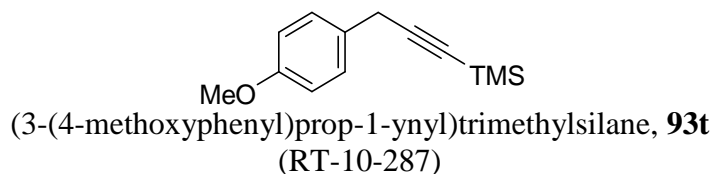


¹H NMR (400 MHz, CDCl₃) δ ppm 7.77 – 7.68 (d, *J* = 2.1 Hz, 1H), 7.38 – 7.29 (dd, *J* = 8.7, 2.0 Hz, 1H), 6.92 – 6.83 (d, *J* = 8.8 Hz, 1H), 3.62 – 3.51 (s, 2H), 3.24 – 3.16 (t, *J* = 6.4 Hz, 4H), 2.04 – 1.91 (p, *J* = 3.6 Hz, 4H), 0.26 – 0.12 (s, 9H).

¹³C NMR (126 MHz, CDCl₃) δ ppm 141.88, 136.85, 132.83, 125.86, 123.80, 116.29, 103.82, 87.59, 50.58, 25.89, 24.88, 0.21.

FTIR (CH₂Cl₂) $\bar{\nu}_{\max}$ cm⁻¹ 2959, 2176, 2118, 1630, 1463, 1306, 845, 760.

HRMS Calcd for C₁₆H₂₃N₂O₂Si (M+H) – 303.1529; found 303.1531.

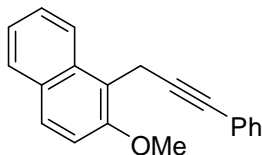


¹H NMR (400 MHz, CDCl₃) δ ppm 7.26 – 7.21 (s, 2H), 6.91 – 6.82 (d, *J* = 8.5 Hz, 2H), 3.88 – 3.74 (s, 3H), 3.65 – 3.51 (s, 2H), 0.23 – 0.15 (s, 9H).

¹³C NMR (126 MHz, CDCl₃) δ ppm 158.51, 128.97, 128.43, 114.02, 104.91, 86.62, 55.29, 25.33, 0.26.

FTIR (CH₂Cl₂) $\bar{\nu}_{\max}$ cm⁻¹ 2960, 2170, 2125, 1614, 1509, 1243, 1036, 840.

HRMS Calcd for C₁₃H₁₇OSi (M-H) – 217.1049; found 217.1066.



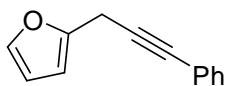
2-methoxy-1-(3-phenylprop-2-ynyl)naphthalene, **93v**
(RT-11-53)

¹H NMR (400 MHz, CDCl₃) δ ppm 8.20 – 8.15 (d, *J* = 8.8 Hz, 1H), 7.84 – 7.78 (d, *J* = 10.3 Hz, 1H), 7.59 – 7.51 (t, *J* = 7.7 Hz, 1H), 7.41 – 7.35 (t, *J* = 7.5 Hz, 1H), 7.35 – 7.29 (m, 2H), 7.24 – 7.19 (dd, *J* = 4.4, 2.1 Hz, 3H), 4.25 – 4.17 (s, 1H), 4.06 – 3.96 (s, 1H):

¹³C NMR (126 MHz, CDCl₃) δ ppm 154.13, 133.01, 131.79, 129.44, 128.93, 128.54, 128.16, 127.61, 126.78, 124.07, 123.82, 123.67, 118.31, 113.87, 88.67, 80.24, 57.09, 15.54.

FTIR (CH₂Cl₂) $\bar{\nu}_{\max}$ cm⁻¹ 2934, 2210, 1949, 1626, 1512, 1089, 756, 692.

HRMS Calcd for C₂₀H₁₇O (M+H) – 273.1279; found 273.1282.



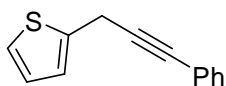
2-(3-phenylprop-2-ynyl)furan, **94a**
(RT-10-246)

¹H NMR (500 MHz, CDCl₃) δ ppm 7.47 – 7.39 (m, 2H), 7.38 – 7.33 (m, 1H), 7.32 – 7.27 (t, *J* = 3.2 Hz, 3H), 6.37 – 6.24 (d, *J* = 33.9 Hz, 2H), 4.01 – 3.50 (s, 2H).

¹³C NMR (126 MHz, CDCl₃) δ ppm 150.45, 141.90, 131.83, 131.75, 128.49, 128.37, 128.33, 128.14, 123.44, 110.60, 110.43, 106.38, 84.64, 81.98, 19.59.

FTIR (CH₂Cl₂) $\bar{\nu}_{\max}$ cm⁻¹ 3057, 2924, 2189, 1657, 1597, 1315, 1070, 756.

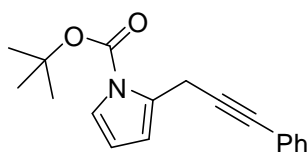
HRMS Calcd for C₁₃H₉O (M-H) – 181.0653, found 181.0638.



2-(3-phenylprop-2-ynyl)thiophene, **94b**⁸
(RT-11-57)

¹H NMR (500 MHz, CDCl₃) δ ppm 7.51 – 7.41 (dd, *J* = 6.5, 3.0 Hz, 2H), 7.36 – 7.28 (dd, *J* = 6.4, 2.7 Hz, 3H), 7.23 – 7.17 (dd, *J* = 5.1, 1.1 Hz, 1H), 7.06 – 7.00 (d, *J* = 4.5 Hz, 1H), 7.00 – 6.93 (m, 1H), 4.06 – 3.95 (s, 2H).

¹³C NMR (126 MHz, CDCl₃) δ ppm 139.72, 131.78, 128.38, 128.35, 128.13, 127.00, 125.20, 124.25, 123.47, 86.82, 82.46, 20.81.



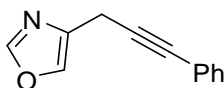
tert-butyl 2-(3-phenylprop-2-ynyl)-1H-pyrrole-1-carboxylate, **94c**
(RT-11-58)

¹H NMR (400 MHz, CDCl₃) δ ppm 7.50 – 7.39 (m, 2H), 7.32 – 7.27 (t, *J* = 2.8 Hz, 3H), 7.27 – 7.24 (s, 1H), 6.37 – 6.31 (t, *J* = 2.2 Hz, 1H), 6.15 – 6.11 (t, *J* = 3.3 Hz, 1H), 4.07 – 3.94 (s, 2H), 1.68 – 1.56 (s, 9H).

¹³C NMR (126 MHz, CDCl₃) δ ppm 149.40, 131.82, 130.12, 128.32, 127.93, 123.81, 121.70, 112.70, 110.15, 86.81, 84.12, 81.84, 27.93, 20.33

FTIR (CH₂Cl₂) $\bar{\nu}_{\max}$ cm⁻¹ 2978, 2931, 2359, 1740, 1491, 1340, 1119, 756.

HRMS Calcd for C₁₈H₁₉NO₂ (M+Na) – 304.1313, found 304.1313.



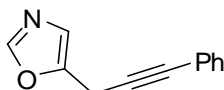
4-(3-phenylprop-2-ynyl)oxazole, **94d**
(RT-11-60)

¹H NMR (400 MHz, CDCl₃) δ ppm 7.88 – 7.84 (s, 1H), 7.69 – 7.65 (dd, *J* = 2.4, 1.4 Hz, 1H), 7.47 – 7.41 (m, 2H), 7.33 – 7.28 (m, 3H), 3.78 – 3.70 (s, 2H).

¹³C NMR (126 MHz, CDCl₃) δ ppm 151.36, 136.92, 135.67, 131.81, 128.40, 128.22, 123.31, 84.99, 82.17, 18.02.

FTIR (CH₂Cl₂) $\bar{\nu}_{\max}$ cm⁻¹ 3134, 3057, 2361, 2203, 1699, 1488, 1061, 914, 756.

HRMS Calcd for C₁₂H₈NO (M+H) – 184.0762, found 184.0774.



5-(3-phenylprop-2-ynyl)oxazole, **94e**
(RT-11-59)

¹H NMR (400 MHz, CDCl₃) δ ppm 7.87 – 7.79 (s, 1H), 7.51 – 7.38 (d, *J* = 5.8 Hz, 2H), 7.36 – 7.28 (t, *J* = 2.8 Hz, 3H), 7.28 – 7.26 (s, 1H), 7.06 – 6.99 (s, 1H), 4.14 – 3.62 (s, 2H).

¹³C NMR (126 MHz, CDCl₃) δ ppm 150.76, 147.91, 131.84, 128.45, 123.40, 122.94, 82.81, 82.55, 17.34.

FTIR (CH₂Cl₂) $\bar{\nu}_{\text{max}}$ cm⁻¹ 3134, 3057, 2361, 2203, 1699, 1488, 1061, 914, 756.

HRMS Calcd for C₁₂H₈NO (M+H) – 184.0762, found 184.0756.

References:

1. Qin, Y.-C., Pu, L. "Highly enantioselective addition of diphenylzinc to aliphatic and aromatic aldehydes catalyzed by a readily available H₈-BINOL derivative" *Angew. Chem. Int. Ed.* **2005**, *45*, 273–277.
2. Komiya, S. *Synthesis of Organometallic Compounds. A Practical Guide*; John Wiley & Sons: New York, **1997**, p. 290.
3. Nishibayashi, Y.; Shinoda, A.; Miyake, Y.; Matsuzawa, H.; Sato, M., "Ruthenium-Catalyzed Propargylic Reduction of Propargylic Alcohols with Silanes." *Angew. Chem. Int. Ed.* **2006**, *45*, 4835–4839.
4. Erenler, R., "Synthesis of Allenic Naphthalene Derivatives." *Bull. Chem. Soc. Ethiop.* **2007**, *21*, (2), 241–247.
5. Zhang, W.-W.; Zhang, X.-G.; Li, J.-H. "Palladium-catalyzed decarboxylative coupling of alkynyl carboxylic acids with benzyl halides or aryl halides" *J. Org. Chem.* **2010**, *75*, 5259–5264.
6. Ma, S.; He, Q.; Zhang, X. "Pd(0)-catalyzed highly selective synthesis of 1,1-diarylpropadienes and 1,3-diarylpropynes from 1-aryl-1-propynes and aryl halides" *J. Org. Chem.* **2005**, *70*, 3336–3338.
7. Li, C.; Li, W.; Wang, J. "Gold(I)-catalyzed arylmethylation of terminal alkynes" *Tetrahedron Lett.* **2009**, *50*, 2533–2535.
8. Biradar, D. P.; Gau, H.-M. "Simple and efficient nickel-catalyzed cross-coupling reaction of alkynylalanes with benzylic and aryl bromides" *Chem. Commun.* **2011**, *47*, 10467–10469.